Microbial Infection and Mechanisms of Intestinal Inflammation

Hannah Margaret Wessel

BSc, MRes

Submitted in fulfilment of the requirements for the Degree of
Doctor of Philosophy

Institute of Infection, Immunity and Inflammation

College of Medical, Veterinary and Life Sciences

University of Glasgow

September 2017

Abstract

The intestinal immune system plays an essential role in maintaining the delicate balance between mounting protective responses against invading pathogens and sustaining tolerance towards self-antigens and the endogenous microbiota. Disturbing this balance leads to intestinal inflammation, such as is seen in inflammatory bowel disease (IBD). IBD is characterised by alterations in the mucosa-associated microbiota, such as the increase in adherent and invasive *Escherichia coli* (AIEC) species in Crohn's disease (CD) patients. Concomitantly, the inflamed mucosa exhibits an elevated rate of apoptosis in IBD, a phenomenon that also accompanies infection with a range of enteric bacterial pathogens. While phagocytosis of apoptotic cells by dendritic cells (DC) is required for self-tolerance in the healthy intestine, there is evidence to suggest that apoptotic cell uptake during infection activates protective T cell responses.

In order to investigate the link between the recognition of apoptotic cells and intestinal inflammation, we used a range of different *in vivo* enteric bacterial infection models. Previously published work had implicated the AIEC strain NRG857c in the induction of chronic intestinal inflammation *in vivo*. We did not, however, find that NRG857c caused any signs of chronic colitis in mice, either by histological examination, or in-depth analysis of both innate and adaptive immune responses in the lamina propria and mesenteric lymph nodes (MLN).

Due to the important role of DC in acquiring apoptotic cell antigen and priming protective T cell responses, we next characterised the expression of apoptotic cell receptors, specifically TIM4, on DC populations in steady state mucosal tissues. We demonstrated that TIM4 expression was enriched on $CD11b^{-}$ $CD103^{+}$ DC, which have previously been shown to cross-present apoptotic cell-derived antigen. However, upon migration in mesenteric lymph, all intestinal DC populations upregulated TIM4, and migratory $CD11b^{+}$ $CD103^{+}$ had the highest frequency of $TIM4^{+}$ cells in the MLN. However, blocking TIM4 did not affect DC migration *in vivo*. We also found that infection with *C. rodentium* elevated the percentage of $TIM4^{+}$ DC in a population-specific manner, but that TIM4 was not essential for the induction of protective T cell responses during infection with either *C. rodentium* or *S.* Typhimurium. We therefore provide a detailed analysis of the intestinal immune response to bacterial infection, focussing specifically on the role of the apoptotic cell receptor TIM4 on intestinal DC populations.

Table of Contents

List of Tables

List of Figures

Acknowledgements

"It's like in the great stories Mr. Frodo, the ones that really mattered. Full of darkness and danger they were, and sometimes you didn't want to know the end, because how could the end be happy? How could the world go back to the way it was when so much bad happened? But in the end, it's only a passing thing, this shadow. Even darkness must pass. A new day will come. And when the sun shines, it will shine out the clearer. Those were the stories that stayed with you, that meant something; even if you were too small to understand why. But I think, Mr. Frodo, I do understand. I know now. Folk in those stories had lots of chances of turning back, only they didn't. Because they were holding on to something." *~ Samwise Gamgee*

These past three years have truly been a great adventure, and as that epic voyage across Middle Earth made by a peculiar but close Fellowhip of friends, my journey has been enriched, supported and made memorable by many uniquely beautiful people along the way. I will struggle to include everyone on paper, but in the end, it is only paper, and the actual memories and friendships carried forward are the truest testament to the impact many have had on my story.

Simon and Dónal, I am so thankful for all your guidance and support throughout the past three years. Thank you for giving me direction when I needed it, for always having an open ear for me when trying to disentangle science, or work through life in general. And thank you for encouraging me to search out my own adventures, even if they brought more questions than answers. I am truly grateful for all your help in the few months leading up to thesis submission, I don't know how I would have finished so quickly without you!

I want to thank Darren and Olwyn for getting me started on this journey in the first place. The rigorous training you gave us in during our MRes year brought its rewards and has stayed with me throughout my PhD, forming a solid basis for the years ahead. Thank you also to the whole Wellcome Trust group of friends, you made settling into life in a new city much easier and I will treasure memories of retreats and evenings in the pub together!

There are a few people I would like to thank especially for their technical help pertaining to the data shown herein (although their value in friendship is equally, if not more, important). Firstly, thank you James for all your help with the *Citrobacter* model, from providing me with strains to troubleshooting when things weren't working as well as hoped! Jen, thank you for letting me partner with you in using the TGFβRKO mice – I will never forget those pinworms!! And Vuk, thank you for looking at TIM4 in the CCR7-gfp

mice, as well as always being ready to chat science with me! Du bist große Klasse! (There's an incentive for you to learn German!)

I'm also incredibly thankful to you, Diane, for making long days in the FACS lab so smooth and, most importantly, fun! I will get those socks finished, I promise! A big thanks also goes to all the wonderful staff at the CRF and JRF. Tony and Joanne, thank you for putting up with me coming late for surgery more often than not, and for all your encouragement and help (especially when the mice just wouldn't flow). Also thank you to Colin for giving me such a friendly welcome to the JRF and helping so wonderfully with all my *Citrobacter* infected mice.

To **all** the Wallies and the Mowlings, both past and present, thank you for being such great companions on this adventure! I was able to learn so much from you all, be it in the way of experiments and thinking about science, or life in general. Much was discussed in both offices that will never reach the outside world (which is maybe a good thing…). Thank you for coming alongside me in my sad times and for encouraging me to be bold in pursuing my next adventure. I have many fond memories of evenings over beer (or wine), movie nights, Level 2 Bakeoff competitions (which I don't think I ended up ever baking in…), cocktail parties and hikes in the hills. I'm especially thankful to you, Allan, for all your advice and encouragement throughout my time in Glasgow. And Mr Frodo, we did it! We actually arrived at the end and live to tell the tale! Thank you for all your support, for listening, for telling me to go home and not take work with me in the holidays. YOU were actually MY Sam!

A big thanks also goes to the Craibs and the Walkers for being my second family here in Glasgow. I am so grateful to you for opening your homes to me and supporting me through some difficult times. And to Sabina, Tom and Hil, Simone and Jess – your friendship has meant to so much to me. Thank you for letting me share life with you. Finally, I want to thank my family, who have been such steadfast companions to me throughout my life. It's hard to find the words, but I love you and thank God for giving you to me.

As Sam said, "Folk in those stories had lots of chances of turning back, only they didn't. Because they were holding on to something."

~ Isaiah 39, 28-31

Author's declaration

I declare that, except where reference is made to the contribution of others, this thesis is the result of my own work and has not been submitted for any other degree at the University of Glasgow or any other institution.

Signature: ..... Printed name: Hannah Margaret Wessel

Abbreviations

ACR	apoptotic cell receptor(s)
ad lib.	*ad libitum*
A/E	attaching and effacing
AhR	aryl hydrocarbon receptor
AIEC	adherent and invasive *E. coli*
BMDC	bone marrow-derived DC
BSA	bovine serum albumin
CD	Crohn's disease
CDP	common DC precursor
CEACAM	carcinoembryonic antigen-related cell adhesion molecule
CFU	colony forming unit(s)
CT	threshold cycle
DAMPs	danger-associated molecular patterns
DAPI	4',6-diamidino-2-phenylindole
DC	dendritic cell(s)
DEAB	Diethylaminobenzaldehyde
DSS	dextran sodium sulphate
DTT	dithiothreitol
EDTA	ethylenediaminetetraacetic acid
EHEC	enterohaemorrhagic *Escherichia coli*
ELISA	enzyme linked immunosorbent assay
EPEC	enteropathogenic *Escherichia coli*
FACS	fluorescence activated cell sorting
FCS	foetal calf serum
Flt3L	Fms like tyrosine kinase 3 ligand
FSC	forward scatter
GALT	gut-associated lymphoid tissue
GAP	goblet cell-associated passage

G-CSF	granulocyte-colony stimulating factor
GF	germ-free
GI	gastrointestinal
GM-CSF	granulocyte macrophage-colony stimulating factor
HBSS	Hanks' Balanced Salt Solution
H&E	Haematoxylin & Eosin stain
HEV	high endothelial venule
hi	high
IBD	inflammatory bowel disease
IDO1	Indoleamine 2,3-Dioxygenase-1
IEC	intestinal epithelial cell(s)
IEL	intraepithelial lymphocyte(s)
Ig	immunoglobulin
IL	interleukin
ILC	innate lymphoid cell(s)
ILF	isolated lymphoid follicle(s)
ILN	inguinal lymph node(s)
int	intermediate
i.p.	intraperitoneal
ISO	isotype control
IVC	individually ventilated cage(s)
LB	Luria broth
LEE	locus of enterocyte effacement
LP	lamina propria
LPS	lipopolysaccharide
lo	low
M cell	microfold cell
MDP	macrophage and DC precursor
MFI	mean fluorescence intensity
MHCII	MHC class II

MLN	mesenteric lymph node(s)
cMLN	colon / caecum-draining lymph node(s)
sMLN	small intestine-draining lymph node(s)
MNP	mononuclear phagocyte(s)
NLR	NOD-like receptor(s)
NKT	natural killer T cell
OVA	ovalbumin
PAMPs	pathogen-associated molecular patterns
PBMC	peripheral blood mononuclear cell(s)
PBS	phosphate buffered saline
pDC	plasmacytoid DC
PFA	paraformaldehyde
p. i.	post-infection
PMA	phorbol 12-myristate 13-acetate
PP	Peyer's patch(es)
PRR	pathogen recognition receptor(s)
PS	phosphatidylserine
qRT-PCR	quantitative real-time PCR
RA	retinoic acid
RALDH	retinaldehyde dehydrogenase
RBC	red blood cell
RNAi	RNA interference
RNA-Seq	RNA sequencing
ROI	region of interest
rpm	revolutions per minute
SCFA	short chain fatty acid(s)
S.D.	standard deviation
SFB	segmented filamentous bacteria
SILT	small isolated lymphoid tissue
SOC	secondary antibody only control

SPI	*Salmonella* pathogenicity island
SPF	specific pathogen-free
SSC	side scatter
T3SS	Type III secretion system
TCR	T cell receptor
TED	trans-epithelial dendrite
TIM	T cell immunoglobulin mucin protein
TNF	tumour necrosis factor
TLR	Toll-like receptor
Treg	regulatory T cell(s)
UC	ulcerative colitis
WT	wildtype

Chapter 1: General Introduction

1.1 The cells and anatomy of the intestinal immune system

Nourishment and defence are two of the body's fundamental functions sustained by the gastrointestinal (GI) tract, which facilitates nutrient and water absorption, and contains the largest proportion of the body's immune cells. Both the anatomical and cellular structure of the intestine ensures these functions are maintained and can adapt to outside changes and challenges.

1.1.2 Anatomy and physiology of the gastrointestinal tract

The GI tract reaches from the stomach, involved in the mechanical and chemical breakdown of food, to the large intestine and rectum, where indigestible foodstuffs are passed out of the system. Along the tract, the structure and function of the intestine changes. The small intestine begins at the pyloric sphincter and is divided into three segments; the duodenum, which is the most proximal, followed by the jejunum, and finally the ileum, which connects the small intestine with the colon at the ileocaecal valve. The presence of villi, finger-like protrusions into the lumen of the small intestine, significantly increases its surface area and provides an essential requirement for its central function – the absorption of nutrients. Connecting the small intestine with the colon is the caecum, which varies in size depending on the organism. Herbivores such as rabbits and mice have a relatively large caecum with a high microbial burden that allows breakdown of cellulose. The human caecum, on the other hand, is much smaller, reflecting a more varied diet. Lastly, the colon allows reabsorption of water and the digestion of dietary fibre by commensal bacteria.

The intestinal epithelium and lamina propria

The regional specialisation of the distinct compartments within the GI tract is reflected by differences in their tissue structure and cellular composition (Mowat and Agace 2014). On the luminal side, the GI tract is lined by a single cell layer of columnar epithelium. This is made up of a variety of different cell types with specialised functions, all of which arise from stem cell precursors situated in the intestinal crypts. Cells are constantly renewed and undergo differentiation as they move as on an "escalator" upwards away from the crypt, before finally being shed at the tip of the villus or intestinal fold into the lumen (Creamer et

al. 1961a, Creamer et al. 1961b, Clarke 1970, Cliffe et al. 2005). In the small intestine, enterocytes facilitate the digestion and uptake of food components through the expression of enzymes and nutrient transporters. Furthermore, the presence of microvilli, forming an apical "brush border", further increases the surface area to ensure maximum absorptive capacity. Microvilli are not present on colonic enterocytes, which allow active reabsorption of water across the membrane.

In the small intestine, specifically the ileum, Paneth cells are located at the base of the crypt. These have important functions in maintaining crypt stem cell survival (Sato et al. 2011), as well as in the production of anti-microbial peptides (Eisenhauer et al. 1992, Salzman et al. 2010). Paneth cells are not present, however, in the healthy colon. Conversely, the concentration of goblet cells in the epithelium is greater in the colon than the small intestine. These are mucus-secreting cells that allow formation of a protective mucus layer, or "glycocalyx", separating the epithelium from the luminal contents. In the small intestine a single thin mucus layer is formed, whilst the glycocalyx is comprised of two layers in the colon, where it serves to prevent commensals from accessing the epithelium (Johansson et al. 2008). A third population of intestinal epithelial cells (IEC) are tuft cells, the function of which has only recently begun to be uncovered. They are a minor secretory cell population in the epithelium of both the small intestine and colon (Sato 2007) and have an important role in initiating Th2 responses to intestinal helminth infections (Gerbe et al. 2016). They expand rapidly upon infection with the helminth *Nippostrongylus brasiliensis*, and secrete IL-25, which stimulates the production of IL-4 and IL-13 by Type 2 innate lymphoid cells (ILC2) (Moro et al. 2010, Neill et al. 2010, Gerbe et al. 2016, Moltke et al. 2016).

Underneath the epithelium is the lamina propria (LP), separated from the former only by a basement membrane. This tissue provides structural support to villi and crypts and contains the extensive blood supply to and from the tissue, which underpins both nutrient transport and leukocyte recruitment. In addition to blood vessels, lymphatic vessels mediate efficient transport of nutrients to the blood, and antigens to secondary lymphoid organs. The LP is filled with leukocytes that maintain a delicate balance between tolerance and defence. The composition of leukocytes found in the LP differs between intestinal compartments (Mowat and Agace 2014), allowing further functional specialisation and adequate responses to be mounted against tissue-specific challenges.

Lymphoid tissues associated with the intestines

As well as in the LP itself, immune interactions also take place within tertiary lymphoid structures that make up the gut-associated lymphoid tissue (GALT). Among these, macroscopically visible structures are present in the small intestine and the caecum, in the form of Peyer's patches (PP) and the caecal patch, respectively, and smaller colonic patches in the colon and rectum. These organised lymphoid structures are characterised by B cell follicles containing germinal centres, flanked by T cell areas. On the luminal side, they are covered by a follicle-associated epithelium, containing microfold cells (M cells), which allow antigen uptake and transfer to underlying antigen-presenting cells (Mabbott et al. 2013). As well as being a site of T cell priming (Smith et al. 2002), an important function of organised lymphoid structures in the intestine is the production of secretory IgA in response to the commensal microbiota (Masahata et al. 2014). Small isolated lymphoid tissues (SILT) are only visible under microscopic examination and are present in both the small intestine and colon. These vary in size with age (Pabst et al. 2005) and include cryptopatches and the larger isolated lymphoid follicles (ILF), which may represent a continuum of maturation states (Mowat and Agace 2014). ILF contain B cell zones and germinal centres and have been implicated in the production of IgA. However, contrary to PP, this is T cell independent (Tsuji et al. 2008). Formation of ILF and their maturation is dependent on the microbiota and Toll-like receptor (TLR) signalling (Bouskra et al. 2008). Furthermore, development of both SILT and the larger GALT such as PP requires lymphotoxin B signalling (Futterer et al. 1998, Pabst et al. 2005) and RORγt^{+} Type 3 ILC (ILC3) (Eberl and Littman 2004).

In the intestine, the main site of antigen presentation and T cell priming are the lymph nodes (LN) that drain the GI tract. Studies in both rats and mice have shown that the tissue compartments of the intestine are drained by distinct LN (Tilney 1971, Carter and Collins 1974, Houston et al. 2016). The principal LN that drain the intestines are found in the mesentery, hence their designation as mesenteric lymph nodes (MLN). These are arranged in a chain, with the proximal and middle nodes draining the jejunum and ileum (hereafter termed small intestine-draining MLN, or sMLN) (Carter and Collins 1974, Houston et al. 2016), whilst the colon is drained by the most distal LN in the chain and a smaller LN associated with the connective tissue below the MLN chain (hereafter colon-draining MLN, or cMLN) (Houston et al. 2016). Furthermore, lymph flow from the distal colon and rectum is directed to the caudal LN, located below the bifurcating aorta (Tilney 1971,

Carter and Collins 1974, Veenbergen et al. 2015). This compartmentalisation of lymphatic drainage has important implications for the tissue-specific nature of immune responses initiated (Houston et al. 2016), thus further maintaining and regulating the differential functions of intestinal tissues.

1.1.2 Innate immunity in the intestine

In the intestine, innate immune cells both maintain tissue homeostasis and serve as a front-line defence to invading pathogens. Mononuclear phagocytes (MNP) constitute an important arm of innate immunity in the intestine. Macrophages and dendritic cells (DC) are the main MNP found in the intestinal LP. They are phagocytic cells capable of sensing pathogen-associated molecular patterns (PAMPs) and presenting antigen to T cells via MHC class II (MHCII) molecules. Due to these similarities, studies in the past have often failed to correctly distinguish macrophages and DC from one another. More in depth study of their phenotype, function and development, however, has highlighted that these distinct cell types indeed possess unique roles in regulating immunity (Cerovic, Bain, et al. 2014).

Macrophages

Intestinal macrophages constitutively produce large amounts of interleukin 10 (IL-10) (Denning et al. 2007, Takada et al. 2010), which is required for the maintenance of tolerance in the LP, partly through IL-10 signalling in macrophages themselves (Murai et al. 2009, Shouval et al. 2014). Furthermore, expression of inhibitory receptors such as CD200R (Snelgrove et al. 2008) further underpins their tolerogenic role in the intestine. Macrophages in most tissues of the body have been shown to be of embryonic origin (Gomez Perdiguero et al. 2015), and to undergo self-renewing proliferation *in situ* (Hashimoto et al. 2013, Yona et al. 2013). However, this is not the case in the intestine. Instead, colonic LP macrophages are constantly replenished from incoming blood monocytes, which lose expression of Ly6C during differentiation and concomitantly upregulate MHC II (Bain et al. 2014). This process is primarily driven by the microbiota (Bain et al. 2014). Mature intestinal macrophages are characterised by expression of CD64 (FcγR1) (Tamoutounour et al. 2012), F4/80 and CD11b, as well as high levels of the fractalkine receptor CX3CR1 (Bain et al. 2013, 2014). Macrophages are tissue resident cells that do not migrate in lymph (Yrlid et al. 2006b, Cerovic et al. 2013), and are therefore not primary inducers of an adaptive immune response (Figure 1. 1). They can, however, mediate the secondary activation of antigen-specific T cells in the LP (Rossini et al. 2014)

(Figure 1. 1) and have been shown to be important for the expansion of intestinal regulatory T cells (Treg) (Denning et al. 2007, Hadis et al. 2011).

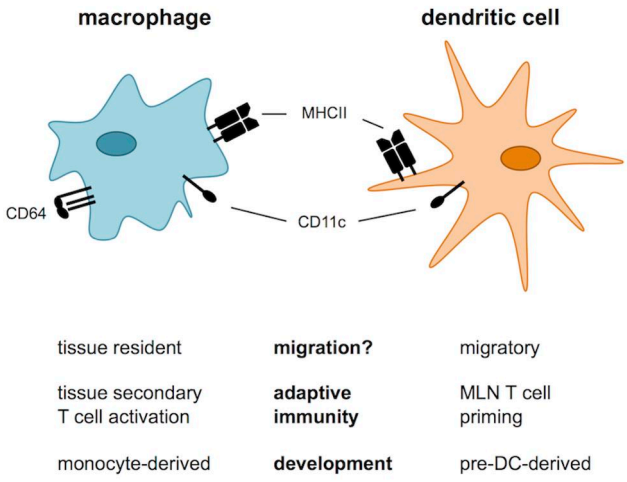

Figure 1. 1: Comparing intestinal macrophages and DC

Both macrophages and DC in the LP express MHCII and CD11c. However, they can be differentiated based on the expression of CD64, which is macrophage-specific. Several other factors that differentially characterise macrophages and DC are listed, including migratory capacity, their impact on adaptive immunity, and their development in the intestine from pre-cursors.

Dendritic cells

Together with MHCII and CD11c, specific conventional DC populations share expression of CD11b and CX3CR1 with intestinal macrophages. This phenotype similarity has led to much of the confusion surrounding the accurate differentiation between these two cell types. Intestinal conventional DC, on the other hand, do not express CD64 or F4/80 (Tamoutounour et al. 2012, Cerovic et al. 2013) (Figure 1. 1). They are developmentally distinct from macrophages, as they are not monocyte-derived, but differentiate from pre-DC that leave the bone marrow and enter the tissue via the blood (Liu et al. 2009). DC sample antigen in the LP and subsequently migrate to the draining LN, where they are responsible for the initial priming of T cell responses (Figure 1. 1). Conventional DC (hereafter referred to simply as "DC") must be further differentiated from plasmacytoid DC (pDC), which in mice are characterised by the expression of B220, and have important functions in anti-viral responses via the production of Type I interferons (Kato et al. 2005). Mainly present in the small intestinal LP (Wendland et al. 2007, Mowat and Agace 2014), pDC do not migrate in mesenteric lymph (Yrlid et al. 2006b). However, they may have an important role in activating intestinal DC by the production of interferon-α (IFNα) after TLR stimulation (Yrlid et al. 2006c).

Polymorphonuclear leukocytes

A second group of innate immune cells in the intestinal LP are polymorphonuclear leukocytes. These include neutrophils and eosinophils, both characterised by the ability to release cytotoxic mediators by degranulation, and have important functions during inflammation. Neutrophils are highly phagocytic cells that possess potent anti-microbial machinery for the killing of internalised bacteria. They are not frequently found in the healthy intestinal LP, and their presence is therefore used as a diagnostic indicator of infection and inflammation. Eosinophils, on the other hand, are abundant in the LP at steady state. Their number is especially high in the small intestine, and decreases along the GI tract (Chu, Jimenez-Saiz, et al. 2014). Lack of eosinophils *in vivo* results in defective IgA secretion, possibly due to defective class-switching in PP (Chu, Beller, et al. 2014). Interestingly, their numbers are not reduced in germ-free (GF) mice (Mishra et al. 1999), indicating that their recruitment and function in the steady state LP is independent of the microbiota.

Innate lymphoid cells

The importance of ILC in controlling tissue homeostasis at mucosal sites is becoming increasingly clear. ILC do not express the T cell receptor (TCR), but develop from common lymphoid progenitors in the bone marrow (Serafini et al. 2015). Their differentiation is dependent on IL-7 and the transcription factors ID2 and NFIL3 (Serafini et al. 2015, Lim et al. 2017). ILC can be classified into three main subsets, based on their differential expression of the transcription factors Tbet (ILC1), GATA3 (ILC2) and RORγt (ILC3). These subsets have different effector functions, which are linked to the expression of cytokines mirroring $CD4^+$ T helper cell responses (see below), such as IFNγ (ILC1), IL-4 and IL-33 (ILC2), as well as IL-17 and IL-22 (ILC3) (Serafini et al. 2015). The production of cytokines by ILC is an important factor in the coordination of early responses against bacterial and helminth pathogens in the intestine (Hoyler et al. 2012, Qiu et al. 2012, Gerbe et al. 2016).

1.1.3 Adaptive immunity: lymphocyte subsets in the intestine

The induction of intestinal adaptive immune responses is mediated in both the MLN and the GALT. Both humoral immunity, based on the production of antibody by B cells, as well as cell-mediated immune responses carried out by effector T cells, have important roles in maintaining intestinal homeostasis in the steady state and during inflammation.

B cells

B cells located in the MLN and the GALT engage in cognate antigen-binding via the B cell receptor, which triggers B cell proliferation and antigen presentation on MHCII molecules, for recognition by $CD4^+$ T cells. This interaction between B cells and T helper cells is required for the formation of a germinal centre (Qi et al. 2008), where antibody class-switching occurs and B cells differentiate into mature plasmablasts. These then migrate into the LP and produce antibody. As previously mentioned, the production of IgA in the intestine constitutes an important defence mechanism that is dependent on the presence of the microbiota (Talham et al. 1999, Kunisawa et al. 2013). Its protective roles include limiting the translocation of bacteria into the LP (Macpherson and Uhr 2004), as well as shaping microbiota composition (Fagarasan et al. 2002).

$CD4^+$ T helper cell subsets

$CD4^+$ T cell responses in the LP are required to coordinate immune interactions and maintain intestinal homeostasis, by the release of pro-inflammatory or regulatory cytokines. $CD4^+$ T cells are primed by DC in the MLN and subsequently home back to the intestine to carry out effector functions. In general, it is thought that this initial priming step is required for skewing $CD4^+$ T cell differentiation into one of four main subsets (Figure 1. 2), depending on the signals received from the DC in the form of cytokines or other mediators. Expression of subset-specific master transcription factors drives the differentiation of $CD4^+$ T cells and their commitment to a certain phenotype and function.

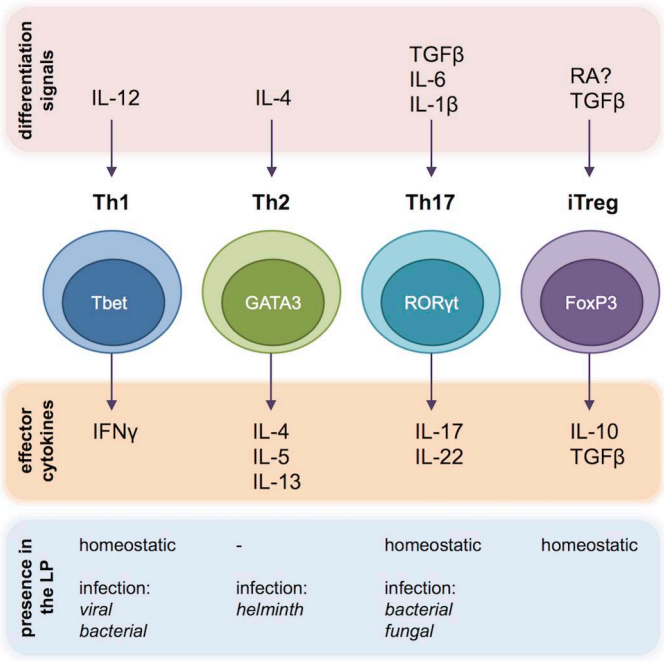

Figure 1. 2: Differentiation and function of LP CD4⁺ subsets

Different signals in the form of specific cytokines and metabolites are required to drive development of CD4⁺ T cell subsets. These display unique effector functions, which are governed by the expression of master transcription factors. The frequency of distinct CD4⁺ T cell subsets in the LP differs between the healthy state and infection, with certain pathogens preferentially eliciting the differentiation of one or more effector T cell subsets.

The Th1 lineage of CD4⁺ T cells is induced by IL-12 signalling (Figure 1. 2) (Macatonia et al. 1995). Expression of the transcription factor Tbet is central to their ability to produce IFNγ, the hallmark feature of these cells (Szabo et al. 2000). Th1 cells are present in the steady state LP throughout the GI tract (Mowat and Agace 2014), but are also readily induced during viral and bacterial infection. In the healthy intestine, IFNγ coordinates cell proliferation and turnover of IEC (Nava et al. 2010). However, it is also a vital mediator in the response against pathogens. IFNγ is required for the expansion of CD4⁺ and CD8⁺ T cells during infection with *S.* Typhimurium and successful clearance of the pathogen (Bao et al. 2000). This is likely due to the induction of IL-12 by IFNγ signalling in MNP (Snijders et al. 1998, Monteleone et al. 1999). IFNγ is also important for the killing of intracellular pathogens phagocytosed by macrophages, as it increases the capacity of these cells to undergo oxidative burst (MacMicking 2012) and initiates transcription of GTPases that are involved in the assembly of intracellular defence machinery such as inflammasomes (Kim et al. 2012).

The transcription factor GATA3 marks Th2 cells, which are rare in the healthy LP, but form an essential part of the defence against intestinal helminths through the production of

Th2-associated cytokines IL-4, IL-5 and IL-13 (Figure 1. 2). Signalling through the IL-4 receptor is vital to the coordination of humoral immunity to helminths, as it induces class switching to IgE in B cells (Yoshida et al. 1990). It also stimulates the production of anti-helminthic mediators such as Arginase-1 and RELMα by macrophages (Nair et al. 2005).

Apart from Th1 cells, a further $CD4^+$ effector T cell type important in the response against invading bacteria is the Th17 cell. Enteric pathogens such as *Citrobacter rodentium* (*C. rodentium)* induce a robust Th17 response (Symonds et al. 2009), which is characterised by the production of IL-17 by $CD4^+$ T cells that express the transcription factor RORγt (Figure 1. 2). Th17 cells are also important mediators of anti-fungal defences (Saijo et al. 2010). IL-17 promotes the haematopoiesis and recruitment of neutrophils into the infected tissue via the upregulation of granulocyte colony stimulating factor (G-CSF) (Ye et al. 2001) and of chemokines on endothelial cells (Griffin et al. 2012). Th17 cells also produce IL-22, which acts on the intestinal epithelium to maintain barrier integrity and production of antimicrobial peptides (Sonnenberg et al. 2011). IL-22 is vital for efficient clearance of bacteria, as *C. rodentium*-infected mice deficient in IL-22 signalling succumb to infection (Zheng et al. 2008). However, these functions are also important in maintaining epithelial homeostasis in the healthy intestine, and it is therefore not surprising that Th17 cells are present in the LP at steady state (Denning et al. 2011). Several cytokines have been implicated in the induction and maintenance of Th17 cells. The combined effects of TGFβ and IL-6 signalling on naïve T cells instructs their differentiation towards a Th17 phenotype (Bettelli et al. 2006, Veldhoen et al. 2006). Furthermore, in the absence of TGFβ, IL-6 and IL-1β can synergistically induce Th17 cell differentiation (Ghoreschi et al. 2010). IL-23, on the other hand, whilst not vital for induction, is required for Th17 maintenance in the tissue (Veldhoen et al. 2006, Stritesky et al. 2008, McGeachy et al. 2009). Th17 induction in the intestine is dependent on the microbiota, specifically the presence of segmented filamentous bacteria (SFB) in mice (Ivanov et al. 2009, Lécuyer et al. 2014), and microbial adherence to the epithelium has been shown to be a vital underlying factor for this (Atarashi et al. 2015). The frequency of Th17 cells is highest in the small intestine and decreases along the GI tract in mice (Denning et al. 2011), which is likely to be linked to the small intestinal colonisation of SFB.

In contrast to these effector $CD4^+$ T helper cell subsets that have been implicated in the clearance of different types of pathogens, $FoxP3^+$ Treg cells support the maintenance of tolerance in the face of dietary antigens and the commensal microbiota. Their regulatory

function is mediated to a large extent by the production of IL-10 and TGFβ (Figure 1. 2) (Bollrath and Powrie 2013). Two main types of Treg cells with different origins have been identified; natural Treg (nTreg) cells are induced in the thymus after recognition of self peptides (Fontenot et al. 2003), while induced Treg (iTreg) cells differentiate in the periphery (Liang et al. 2005) via TGFβ signalling (Chen et al. 2003). In the MLN, Treg cell induction has also been linked to the production of retinoic acid (RA) by DC (Coombes et al. 2007). The frequency of LP Treg cells is higher in the colon than the small intestine at steady state (Denning et al. 2011), in contrast to the pattern identified for Th17 cells. However, evidence suggests this is also linked to the microbiota, specifically to the presence of *Clostridia* species in the colon (Atarashi et al. 2011).

$CD8^+$ T cells

Also present in the intestinal LP are $CD8^+$ T cells, which have a tissue resident phenotype, thus ensuring the mounting of fast and efficient responses upon activation (Sheridan et al. 2014). They produce granzyme B (Masopust et al. 2006), a potent cytotoxic mediator, and constitute an important defence mechanism during viral and bacterial infections (Rose et al. 1998, Bergsbaken and Bevan 2015). These LP resident $CD8^+$ T cells are distinct from $CD8^+$ intraepithelial lymphocytes (IEL). The latter express CD103, which is upregulated in a TGFβ-dependent manner (Sheridan et al. 2014), and act as sentinels guarding the epithelial barrier. IEL frequency is highest in the small intestine, and these decrease to low numbers in the colonic epithelium (Camerini et al. 1993). Furthermore, $CD8^+$ IEL can express either the αβTCR, or the γδTCR, with the latter being mainly present in the small intestine (Camerini et al. 1993). Infection with *Listeria monocytogenes* (*L. monocytogenes*) induces a rapid increase in $CD8^+$ IEL numbers (Sheridan et al. 2014), highlighting their protective role in anti-microbial immune responses.

1.1.4 Control of T cell homing to the intestine

Intestinal T cell responses are initiated in the MLN, after which activated T cells recirculate in the bloodstream and enter the LP via high endothelial venule (HEV)-like structures. In the small intestine, this homing process is mediated by the induction of CCR9 and the α4β7 integrin on T cells during priming in the MLN. Induction of both is dependent on the production of RA by DC (Iwata et al. 2004, Jaensson et al. 2008), which is metabolised from dietary Vitamin A by the retinaldehyde dehydrogenase family of enzymes, specifically RALDH2 (Iwata et al. 2004). The integrin α4β7 interacts with mucosal addressin cell

adhesion molecule-1 (MAdCAM-1) found on the vascular endothelium of venules in the small intestinal LP (Hamann et al. 1994). Furthermore, α4β7 also directs lymphocyte homing to PP (Berlin et al. 1993, Farstad et al. 1997). Integrin α4β7 expression on $CD8^+$ memory T cells is required for their ability to effectively combat rotavirus infection *in vivo* (Rose et al. 1998), indicating that as well as controlling homeostatic homing to the small intestine, it is also required under inflammatory conditions. In fact, this has successfully been targeted therapeutically in Crohn's disease, where treatment with vedolizumab, a monoclonal antibody against α4β7, increased the rate of clinical remission (Sandborn et al. 2013).

Expression of CCL25, the cognate ligand for CCR9, is limited to the small intestinal epithelium under homeostatic conditions (Svensson et al. 2002), and decreases in expression from the duodenum to the ileum (Stenstad et al. 2007). Deficiency in CCR9 *in vivo* decreases the accumulation of effector $CD4^+$ T cells in the small intestinal LP (Stenstad et al. 2006), and is also required for the recruitment of $CD8^+$ IEL to the epithelium (Stenstad et al. 2007). Interestingly, there is some evidence to suggest that, while not involved in T cell migration to the healthy colon, CCR9/CCL25 interactions may play a regulatory role during colitis (Wurbel et al. 2011). CCL25 expression increases in the colonic epithelium after recovery from dextran sodium sulphate (DSS)-induced colitis in mice, and *Ccr9*$^{-/-}$ mice exhibit decreased survival in this model (Wurbel et al. 2011). However, it is as yet unclear if these interactions play an essential role in the recruitment of colonic effector T cells during inflammation.

The mechanisms that govern T cell homing to the colon under homeostatic conditions are as yet unclear. The expression of CCL28, the cognate ligand for the chemokine receptor CCR10, on colonic epithelium (Pan et al. 2000) has sparked investigation into the possibility that CCR10/CCL28 interactions instruct T cell migration to the colon. IgA^+ plasmablasts in the colon are $CCR10^+$ (Kunkel et al. 2003), and experiments tracking plasma cells in the GI tract have shown that $CCR10^+$ IgA^+ plasmablasts are generated in the caecal patch and subsequently migrate to the colon (Masahata et al. 2014). However, it is still unknown if CCR10 expression is required for T cell homing to the colon. A second candidate for the induction of colon-specific migration is the G-protein-coupled receptor GPR15. This has been shown to be expressed on colonic Treg cells and is required on these cells to rescue CD40-mediated colitis in T cell-deficient mice (Kim et al. 2013). Treg cell and $CD44^+$ $CD4^+$ T cell accumulation in the colon is decreased in mixed bone marrow

chimeras of *Gpr15*^{het} with *Gpr15*$^{-/-}$ origin (Nguyen et al. 2014). However, GPR15 expression was not detected in the colon-daining MLN (Houston et al. 2016), which calls into question whether GPR15 is indeed induced during priming. Further investigation will be required to help address how GPR15 mediates accumulation of T cells in the colon, and what other potential molecules are involved in this process.

1.2 Microbiota-immune interactions in the intestine

1.2.1 Structure of the microbiota throughout the gastrointestinal tract

The advent of sophisticated and powerful genomic, transcriptomic and metabolomic techniques in the past decade has been instrumental for the in-depth characterisation of the intestinal microbiota (Turnbaugh et al. 2007). The intestinal microbiota is made up of bacteria, fungi and viruses, and while the latter two components are receiving increasing attention, bacteria have been the focus of the vast majority of studies. Bacterial composition of the microbiota changes throughout the GI tract (Figure 1. 3) (Mowat and Agace 2014, Pereira and Berry 2017). While not a sterile organ, the stomach exhibits a very low microbial burden, owing to its acidic pH (Nardone and Compare 2015). Similarly, bacterial colonisation of the duodenum and jejunum is limited, with mainly facultative anaerobes such as *Lactobacillus* and *Streptococcus* being present (Figure 1. 3) (Zoetendal et al. 2012, Gu et al. 2013). In the descending parts of the GI tract, however, microbial burden and diversity increase. Other facultative anaerobes begin to thrive; *Enterobacteria* such as *Escherichia coli* (*E. coli*) and *Enterococcus*, members of the Firmicutes phylum, are both commensals of the terminal ileum and colon that have also been described as "pathobionts" as they have the potential to cause inflammation after perturbation of the microbiota (Arias and Murray 2012, Ayres et al. 2012). In contrast to facultative anaerobes, obligate anaerobes fail to survive in oxygenated environments. Examples of these are *Clostridium* and *Bacteroides*, which are enriched in the colon (Figure 1. 3) (Mowat and Agace 2014). The shift from predominantly facultative anaerobes in the small intestine to a mixture of facultative and obligate anaerobes in the colon is underpinned by the decreasing oxygen tension as the GI tract descends (He et al. 1999) and reduced flux of intestinal content.

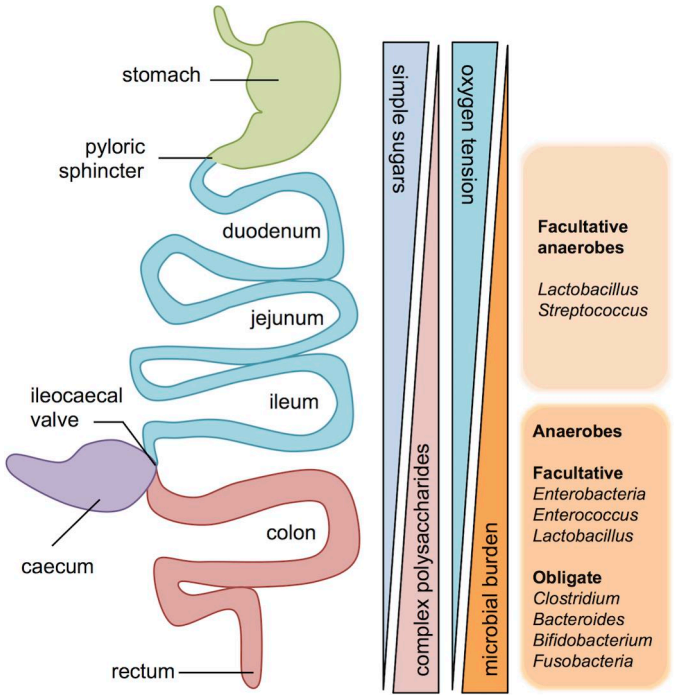

Figure 1. 3: Structure of the gastrointestinal tract and its microbiota

Simplified schematic of the different tissue compartments within the gastrointestinal tract and the accompanying changes in various factors influencing the colonisation of facultative and obligate anaerobes. Microbial burden is highest in the colon, and correlates with a greater availability of complex polysaccharides. On the other hand, higher oxygen tension and the increased levels of simple sugars favour colonisation of the small intestine with a limited number of facultative anaerobes.

Diet itself has an important role in regulating species abundance in the intestine (Faith et al. 2011), and the distribution of nutrients within the tissue is thought to establish ecological niches allowing different bacterial species to thrive (Pereira and Berry 2017). This instigates competition between bacterial species, and is thought to be an important factor driving colonisation resistance of pathogenic species, such as *Salmonella enterica* serovar Typhimurium (*S.* Typhimurium) (Barthel et al. 2003, Deriu et al. 2013). The abundance of simple sugars found in the small intestine is a ready food source for facultative anaerobes (Zoetendal et al. 2012). In the colon, on the other hand, complex polysaccharides and mucins that make up the secreted glycocalyx are the dominant nutrients available for the commensal microbiota. Indeed, the abundance of dietary fibre is an important determinant of species abundance in the colon (Walker et al. 2011), with specific bacteria such as members of *Bacteroides* and *Clostridium* genera being the main metabolisers of fibre *in vivo* (Tannock et al. 2014).

Microbiota composition not only varies between intestinal tissues, but studies have highlighted the importance of differentiating between luminal and mucosa-associated bacterial communities (Eckburg et al. 2005, Lepage et al. 2005, Ringel et al. 2015). Again,

factors such as nutrient availability and oxygen concentration, as well as adhesion and sensitivity to host defence factors play a role in determining bacterial composition of these compartments (Van den Abbeele et al. 2011). As mentioned previously, the mucus layer not only serves to protect the underlying epithelium and LP from translocating commensals, but also acts as a food source. While the inner mucus layer in the colon is normally sterile (Johansson et al. 2008), the outer mucus layer harbours a bacterial community distinct from that found in the lumen (Li et al. 2015). Members of both Bacteroidetes and Firmicutes phyla can be found associated with the mucus layer (Hong et al. 2011, Nava et al. 2011). The ability to degrade mucins is likely to be one factor influencing this (Macfarlane and Gibson 1991), as well as the propensity to adhere to the mucus layer itself (Huang et al. 2011). Very few commensal bacteria penetrate the mucus layer and survive in close proximity to the epithelium. A well-studied example is afforded by SFB (Jepson et al. 1993, Schnupf et al. 2015). Taken together, this spatial regulation of the microbiota is important to maintaining intestinal health, as intestinal inflammation is induced by the ability of enteric pathogens such as *Shigella* and enteroaggregative *E. coli* to penetrate the mucus layer and interact with the underlying epithelium (Harrington et al. 2009).

1.2.2 Microbial antigen acquisition

The commensal microbiota provides a wealth of bacterial-derived antigen, especially in the colon. Both the acquisition of, and the immune responses to, these antigens are tightly controlled in the intestine to prevent inflammation. In order to achieve this, microbiota-derived antigen must be safely sampled without allowing translocation of bacteria across the epithelium. Tight junction integrity is central to ensuring the epithelial barrier is maintained, but also prevents the passive transit of soluble antigen between IEC.

The best documented route of antigen sampling in the mucosa is through M cells in the GALT. These can engage in phagocytosis and transcytosis of both soluble antigen and whole bacteria (Mabbott et al. 2013), functions which are supported by the expression of a range of receptors that allow recognition of bacterial antigen. For example, the M cell-specific protein GP2 binds FimH on bacterial pili, and mediates bacterial uptake (Hase et al. 2009). Interestingly, the expression of GP2 on M cells is higher in the PP compared with the caecal patch, which was accompanied by suppressed M cell maturation in the latter (Kimura et al. 2014). This may allow the exercising of tighter control over antigen sampling

in the face of an elevated microbial burden. Transcytosed antigen is released into basolateral pockets, invaginations of the M cell membrane (Neutra et al. 1987), where it can be taken up by antigen-presenting cells. Indeed, M cells closely interact with MNP situated under the follicle-associated epithelium (Wang et al. 2011), and there is some evidence that MNP can extend dendrites through M cells to sample luminal contents (Lelouard et al. 2012).

As well as M cells, goblet cells have been implicated in the transfer of soluble luminal antigen to underlying MNP (McDole et al. 2012). So-called "goblet cell-associated passages" (GAPs) were first identified in the small intestinal, but not colonic epithelium (McDole et al. 2012). However, antibiotic-treated and GF mice do exhibit the formation of GAPs in the colon, found to be mediated by a MyD88-dependent mechanism (Knoop et al. 2015). Together with the regional differences observed in GP2 expression and differentiation of M cells (Kimura et al. 2014), this further supports the conclusion that antigen uptake, be it active or passive, is tightly controlled in the presence of the microbiota.

In addition to the transcellular carriage of antigen, several reports exist of antigen-presenting cells extending dendrites between epithelial cells, so-called "trans-epithelial dendrites" (TEDs), indicating the possibility of active sampling of the luminal environment. Even though often classified as DC, these $CD11c^+$ (Chieppa et al. 2006), $CX3CR1^+$ (Niess et al. 2005) cells are most likely to instead be LP macrophages, given that these express higher levels of CX3CR1 than DC (Cerovic et al. 2013). On the other hand, some evidence indicates the ability of $CD103^+$ cells to form TEDs in the small intestine, especially after infection with *S.* Typhimurium (Farache et al. 2013), which may indeed point to the ability of DC to undertake similar functions.

1.2.3 Metabolites produced by the microbiota and their impact on intestinal immunity

It is becoming increasingly clear that the ways the microbiota shape intestinal immunity are not limited to the delivery of antigens, but also that the production of immunoregulatory metabolites is important for immune cell survival and function in the intestine. Many of these metabolites are generated as by-products of bacterial fermentation of dietary fibre.

Tryptophan metabolites and the aryl hydrocarbon receptor

An example of these are indoles, tryptophan derivatives that arise from plant product metabolism (Zelante et al. 2013, Jin et al. 2014). Tryptophan metabolism is mainly carried out by the host enzyme Indoleamine 2,3-Dioxygenase-1 (IDO1), which is expressed at high levels in the intestine (Dai and Zhu 2010). However, indoles are found at high concentration in the caecal content of wildtype (WT) mice (Jin et al. 2014), and can be produced by commensal *E. coli* (Domka et al. 2006). This suggests that the microbiota itself can also metabolise tryptophan. Indeed, IDO1 deficiency leads to the increased abundance of tryptophan producing *Lactobacillus* species detected in the stomach (Zelante et al. 2013). Furthermore, deficiency in CARD9, a signalling component of the NOD2 receptor complex recognising intracellular bacterial components, induces a shift in the colonic microbiota and a simultaneous reduction in tryptophan metabolites, which correlates with increased susceptibility to colitis (Lamas et al. 2016). Taken together, these findings admit the possibility that tryptophan metabolism by both the host and the microbiota is interdependent and has profound effects on both.

Indoles constitute ligands for the aryl hydrocarbon receptor (AhR), which has been shown to have an important role in regulating intestinal homeostasis and inflammation in leukocyte populations (Martin et al. 2009, Kiss et al. 2011, Li et al. 2011). *Ahr*$^{-/-}$ mice develop more severe colitis when treated with 3% DSS than WT controls, characterised by enhanced bacterial translocation to the LP (Li et al. 2011). This was due to a decrease in IEL numbers, as AhR signalling was required to maintain their survival in the epithelium (Li et al. 2011). A second way that AhR ligands maintain intestinal barrier integrity is by inducing the production of IL-22. AhR is preferentially expressed in CD4^{+} T cells that have undergone *in vitro* differentiation to a Th17 phenotype, and its ligation induces the production of IL-22 by these cells (Veldhoen et al. 2008). As well as LP Th17 cells, ILC3 produce large amounts of IL-22 that is required for protection against enteric infection (Qiu et al. 2012). As seen in Th17 cells, AhR signalling induces the upregulation of IL-22 in intestinal ILC3 (Qiu et al. 2012). In fact, ILC3 numbers are significantly reduced in both the small intestinal and colonic LP of *Ahr*$^{-/-}$ mice (Kiss et al. 2011), indicating that, as in IEL, AhR signalling sustains ILC3 survival. Consequentially, AhR signalling deficiency leads to lack of isolated lymphoid follicle formation after birth (Kiss et al. 2011), a process that is dependent on ILC3 (Eberl and Littman 2004). Together, these findings highlight the

vital protective role of AhR ligands in maintaining the gut barrier and enabling the acquisition of microbiota-derived antigen in the GALT.

Dietary fibre and short chain fatty acids

The breakdown of dietary fibre by the commensal microbiota generates short chain fatty acids (SCFA), which act both directly on the epithelium to promote integrity of the intestinal barrier, and have important immunoregulatory functions. Acetate is the most abundant SCFA present in luminal content (Cummings et al. 1979), and is produced by most enteric commensals via carbohydrate fermentation (Louis et al. 2014). Distinct pathways operated by different species of bacteria have been described for the production of the other two SCFA, propionate and butyrate (Reichardt et al. 2014). While propionate is predominantly produced by Bacteroidetes (Louis et al. 2014, Reichardt et al. 2014), butyrate is mainly generated by Firmicutes (Louis et al. 2014). Acetate itself can also be converted to butyrate by certain commensal species (Duncan et al. 2002). The composition of the microbiota is therefore a key determinant of the levels of available SCFA at any given time.

The abundance of colonic SCFA contributes to the colonisation resistance of enteric pathogens. For example, propionate has bactericidal properties against *E. coli* and *Salmonella* (Cherrington et al. 1991, Shin et al. 2002), and butyrate negatively regulates expression of virulence factors in *S. enterica* (Gantois et al. 2006). Furthermore, acetate production by *Bifidobacteria* has been shown to impart resistance to enteropathogenic *E. coli*-induced mortality *in vivo* (Fukuda et al. 2011). Thus, in the first instance, SCFA production by the commensal microbiota reduces the ability of pathogenic bacteria to cause inflammation.

However, SCFA also have a substantial impact on the host. One example is the maintenance of epithelial barrier function. Butyrate constitutes one of the primary energy sources for colonocytes (Roediger 1980, Ardawi and Newsholme 1985, Zambell et al. 2003) and thus inhibits the induction of autophagy by IEC (Donohoe et al. 2011). Furthermore, it has been implicated in reducing IEC layer permeability (Kinoshita et al. 2002). SCFA can also act via engagement of G-protein coupled receptors (Brown et al. 2003). Deficiency in GPR43, one of the main SCFA receptors, leads to increased severity of DSS colitis in mice (Maslowski et al. 2009). Furthermore, feeding mice a high fibre diet is protective during the induction of DSS colitis, which is dependent on GPR43 signalling (Macia et al. 2015).

Furthermore, GPR43 was required for the induction of the NLRP3 inflammasome in colonic epithelial cells, a protective response in the face of epithelial cell damage and inflammation (Macia et al. 2015). There is also evidence to suggest that SCFA stimulate the production of antimicrobial peptides from IEC (Schauber et al. 2003, Sunkara et al. 2012).

As well as IEC, it is becoming increasingly clear that SCFA exercise potent regulatory functions on immune cells, both influencing innate responses via myeloid cells, and shaping adaptive immune responses. For example, SCFA treatment of neutrophils reduces the production of pro-inflammatory mediators upon stimulation (Vinolo, Rodrigues, et al. 2011), and SCFA signalling via GPR43 stimulates neutrophil chemotaxis (Vinolo, Ferguson, et al. 2011). Recent work has shown that butyrate treatment decreases the production of pro-inflammatory mediators by intestinal macrophages both *in vitro* and *in vivo* (Chang et al. 2014). Furthermore, this was shown to be independent of G-protein-coupled receptor signalling, but mediated instead via the inhibition of histone deacetylases (Chang et al. 2014). In addition to regulating immune function in the intestinal environment, SCFA can impact immunity on a systemic level by stimulating haematopoiesis of DC precursors (Trompette et al. 2014).

GF mice have reduced Treg cell frequencies in the colonic LP compared with specific pathogen-free (SPF) mice (Smith et al. 2013) and two seminal studies have shown that SCFA are required for the maintenance of colonic Treg cells *in vivo* (Furusawa et al. 2013, Smith et al. 2013). Thus, SCFA produced by members of the microbiota are likely to be important for sustaining Treg cell-mediated tolerance in the colon. Findings by Atarashi et al. (2013) indicate that *Clostridia* species may be one important source of SCFA. They showed that colonisation of GF mice with a mixture of 17 human *Clostridia* strains led to the increased intestinal concentration of SCFA and mediated colonic Treg cell expansion by stimulating the release of TGFβ (Atarashi et al. 2013). Together, these findings indicate that SCFA production by members of the commensal microbiota such as *Clostridia* is required for maintaining the large pool of colonic Treg cells, and as a consequence, immunological tolerance towards the microbiota.

1.3 When things go wrong: mechanisms of intestinal inflammation

1.3.1 Host-microbiota interactions in inflammatory bowel disease

In the healthy gut, the mucosal immune system must maintain a delicate balance between tolerance to food antigens and commensal bacteria, and defence against invading pathogens. Disturbing this balance can lead to the onset of inflammatory bowel disease (IBD), which affects approximately one in 150 people in Europe and is becoming increasingly common around the world (Molodecky et al. 2012). The aetiology of IBD remains unclear, but the current understanding based on a large body of research suggests a role for both an unbalanced intestinal microbiota and a deregulated mucosal immune response in perpetuating a state of relapsing-remitting inflammation of the intestine. IBD is a broad term describing two main diseases; Crohn's disease (CD), which can affect any part of the GI tract and is often characterised by transmural, granulomatous inflammation, and ulcerative colitis (UC), which only involves colonic inflammation and presents as mucosal ulceration. However, the considerable variation in symptoms and clinical characteristics within both CD and UC indicates that these in themselves in fact may represent a spectrum of diseases with potentially different mechanisms of pathogenesis (Cleynen et al. 2015).

Changes in the intestinal microbiota

An increasing body of evidence points towards the microbiota as an underlying, and potentially causative, factor in driving intestinal inflammation in IBD. This is based on studies that have used sequencing approaches to define both the luminal and mucosa-associated microbiota in patients with IBD compared with healthy individuals. In CD, disease phenotype and genotype have been correlated with changes in *Faecalibacterium* and *Escherichia* taxa (Frank et al. 2011), and an overall decrease in Firmicutes, specifically *Clostridia*, has been observed (Gophna et al. 2006, Scanlan et al. 2006, Morgan et al. 2012). Given the importance of *Clostridia* in the production of SCFA and maintenance of Treg cells in the colon (Atarashi et al. 2013), the availability of SCFA may be a contributing factor in IBD pathogenesis. However, it does not seem to be the case that a universal CD signature exists (Frank et al. 2007). Instead, the common factor to be exposed by most studies is a decrease in microbial diversity (Manichanh et al. 2006, Sepehri et al. 2007, Dicksved et al. 2008). It is yet unclear if this state of microbial imbalance, also termed dysbiosis, results in, or is a result of inflammation.

Recently, the fraction of the faecal microbiota that is coated by host IgA has been compared between IBD patients and healthy individuals (Palm et al. 2014). In defence against enteric pathogens, IgA-coating allows recognition by myeloid cells and pathogen neutralisation. However, commensal bacteria are also coated with IgA, albeit with antibody of lower affinity and specificity (Pabst 2012). For example, flagellin-specific IgA-coating helps prevent crossing of the intestinal barrier by commensal bacteria (Cullender et al. 2013). In their seminal work, Palm et al. (2014) showed that the frequency of IgA-coated bacteria was increased in IBD, and were able to identify disease-specific signatures based on the coating of bacterial strains. Moreover, while colonisation of GF mice with these strains was not sufficient to induce colitis, they did exacerbate pathology in DSS colitis (Palm et al. 2014). This indicates that the IBD-associated microbiota is not pathogenic in itself, but is likely to contribute, together with other host susceptibility factors, to on-going inflammation. Interestingly, faecal microbiota transplantation has shown varying levels of success in the treatment of UC (Moayyedi et al. 2015, Rossen et al. 2015), thus further highlighting the need to understand what components of the microbiota or its downstream effects are involved in the disease process.

How disease susceptibility impacts host-microbe interactions

Taken together, these findings indicate that unravelling the interactions between the intestinal microbiota and host susceptibility factors is likely to be important in understanding IBD pathogenesis. Genome-wide association studies (GWAS) have been instrumental in explaining some degree of inherited disease susceptibility in IBD, as well as identifying important pathways in different arms of the immune response as potential drivers of pathogenesis. Indeed, many genetic associations are linked with the host response to microbial infection (Jostins et al. 2012). One extensively studied example is the *NOD2* locus on chromosome 16 (Ogura et al. 2001). NOD2 belongs to the NOD-like family pathogen recognition receptors (PRR) and is involved in the activation of NF-κB and downstream pro-inflammatory pathways (Inohara et al. 2001) upon sensing of intracellular bacteria. The three most common CD-associated variants of the *NOD2* gene are loss-of-function mutations and result in inability to efficiently clear intracellular bacteria (Cooney et al. 2010). Bacterial persistence could also be brought about by defective autophagy. The CD-associated T300A allele variant of autophagy-related gene *ATG16L1*, is impaired in its ability to induce autophagy, and drives enhanced levels of IL-1β production by $CD11c^+$ cells from MLN and $CD11b^+$ cells of the LP (Lassen et al. 2014), indicating that

aberrant caspase activation by this variant in MNP may be one of the factors driving inflammation in CD.

GWAS have also pointed towards the role of many immunological signalling pathways in IBD pathogenesis. For example, IBD-associated loci include regulatory cytokines such as *IL10* (Jostins et al. 2012, Bank et al. 2014). In fact, defective IL-10 signalling leads to early-onset IBD in children (Glocker et al. 2009), indicating that maintenance of a tolerogenic environment in the intestine is essential for the prevention of inflammation during the increasing microbial colonisation in the first few months of life. Another gene with IBD-associated polymorphisms encodes the chemokine receptor CCR6 (Barrett et al. 2008). CCR6 is expressed by Th17 cells (Liu and Rohowsky-Kochan 2008) and its cognate chemokine ligand, CCL20, is elevated in the epithelium of CD patients (Kwon 2002). This suggests that aberrant lymphocyte migration control could contribute to the development of CD. It also points to a role for Th17 cells in the pathogenesis of IBD. Association of CD with *STAT3* polymorphisms (Barrett et al. 2008) further supports this, as STAT3 phosphorylation is induced by IL-6 signalling, one of the factors that induces Th17 cell differentiation (Bettelli et al. 2006). Production of IL-22, required for the maintenance of epithelial barrier integrity (Sonnenberg et al. 2011), is regulated by STAT3 signalling in Th17 cells (Backert et al. 2014), again highlighting the importance of regulating host defence to the commensal microbiota.

Animal models used in the investigation of IBD pathogenesis

Important insights into intestinal immune regulation during inflammation have been uncovered using *in vivo* models. The pivotal role of Treg cells in maintaining intestinal homeostasis was first shown using a model of T cell-dependent colitis (Read et al. 2000), which involves the adoptive transfer of naïve $CD4^+$ T cells to T cell-deficient mice (Leach et al. 1996). Transfer of $CD4^+$ $CD25^+$ T cells, which contain a large proportion of Treg cells, together with naïve $CD4^+$ T cells, inhibited the onset of colitis (Read et al. 2000). On the other hand, the vital protective role of the epithelium is evident from studies using DSS colitis, which involves chemical-induced destruction of the colonic epithelium (Dieleman et al. 1994). In this model, the chemical damage to the intestinal tissue, coupled with translocation of bacteria to the underlying LP, drives inflammation. During DSS colitis, bacterial recognition is vital for the induction of an adequate immune response, and for limiting dissemination of bacteria to the MLN (Fukata 2005). This model has been used extensively to study intestinal immune cell function in the context of inflammation.

In line with the findings from GWAS studies in IBD patients, mice that lack components of disease-associated pathways can also develop spontaneous colitis. Interestingly, in many of these models, the microbiota has an important impact on the initiation or severity of inflammation. For example, *Il10*$^{-/-}$ mice develop colitis only in the presence of the pathobiont *Helicobacter hepaticus* (Kullberg et al. 1998, Sellon et al. 1998). Similarly, treatment of *H. hepaticus*-infected mice with IL-10 receptor blocking antibody induces the onset of caecal and colonic pathology (Kullberg et al. 2006). Another example is provided by *Tnf*$^{\Delta ARE}$ mice that lack AU-rich elements (ARE) at the *Tnf* gene locus (Kontoyiannis et al. 1999). SPF, but not GF *Tnf*$^{\Delta ARE}$, mice develop spontaneous ileitis that is transferrable to GF mice upon transplantation of the microbiota (Schaubeck et al. 2015). More recently described, IEC-specific deletion of ATG16L1 induces transmural ileitis in mice, although in this case it was not transmissible via faecal microbiota transplantation (Tschurtschenthaler et al. 2017). Nevertheless, conventionally housed *Tnf*$^{\Delta ARE}$ and *Atg16l1*$^{\Delta IEC}$ animals exhibit dysbiosis (Schaubeck et al. 2015, Tschurtschenthaler et al. 2017). This highlights the important possibility that, as well as being impacted by the microbiota, intestinal inflammation may also cause alterations in the host microbiota that further perpetuate disease.

1.3.2 Commensal turned rogue: adherent and invasive *E. coli*

The search for a single *bona fide* microbial driver of inflammation for IBD has remained largely unfruitful. However, over the past decade there has been an accumulation of evidence in support of a role for the human gut commensal *E. coli* in CD. Commensal strains of *E. coli* can colonise the intestinal mucus layer due to the availability of mono- and disaccharides, which serve as nutrients (Møller et al. 2003, Miranda et al. 2004). However, *E. coli* is associated with 100% of early and 65% of chronic CD inflammatory lesions (Darfeuille-Michaud et al. 1998) and many of the *E. coli* strains isolated from these CD patients have adhesive and invasive properties (Martin et al. 2004), coining the term "adherent invasive *E. coli*" (AIEC). These can be found in 20-40% CD patient intestinal biopsies compared with 2-4% healthy controls (Darfeuille-Michaud et al. 2004, la Fuente et al. 2014). Their ability to adhere to and invade IEC is thought to be mediated by binding to CEACAM6 (carcinoembyonic antigen related cell adhesion molecule 6), an adhesion molecule that is upregulated in the CD epithelium (Barnich and Darfeuille-Michaud 2007, Carvalho et al. 2009). CD patients with systemic manifestations of inflammation in the form of peripheral spondyloarthritis have elevated levels of faecal IgA-coated *E. coli*

compared with patients with gut-limited disease (Viladomiu et al. 2017). These strains were identified as AIEC based on both genomic and functional analyses (Viladomiu et al. 2017), indicating that an active on-going immune response against AIEC in the gut correlates with systemic disease presentation in CD.

Granulomas are a common histological feature used in the diagnosis of CD and *E. coli* may be one of the driving factors in their development, as a sizeable proportion of granulomas in intestinal sections from CD patients have been shown to contain *E. coli* DNA (Ryan et al. 2004). Accordingly, certain AIEC strains are able to persist and replicate in macrophages *in vitro* and activate the inflammasome (Glasser et al. 2001, la Fuente et al. 2014), as well as induce granuloma-like cell aggregates when cultured with human peripheral blood mononuclear cells (PBMC) (Meconi et al. 2007). Furthermore, antibodies against *E. coli* proteins are found at increased concentrations in the serum of CD patients (van Schaik et al. 2013). It is conceivable that the dysbiosis observed in many CD patients may allow outgrowth of *E. coli* strains in proximity to the mucosal wall. Indeed, antibiotic treatment of mice has been shown to induce the expansion of *E. coli* in mice, indicating that a functional microbiota may be required to control the abundance of this commensal in the intestine (Ayres et al. 2012). This is further supported by the fact that dysbiosis during DSS colitis allows enhanced growth of commensal *E. coli* strains *in vivo* due to their ability to utilise nitrate released during inflammation (Winter et al. 2013). The ability of AIEC to invade IEC and translocate to the underlying LP may enable these strains to act as opportunistic pathogens and contribute to the development of intestinal inflammation and the chronic inflammatory phenotype of CD.

Elucidating dynamics and immunological effects of AIEC colonisation in vivo

Studying the colonisation dynamics and pathogenicity of *E. coli* strains *in vivo* has been carried out mainly in mice with streptomycin pre-treatment, which allows exogenous *E. coli* strains to occupy distinct niches created in the otherwise colonisation-resistant mouse intestine (Meador et al. 2014). A recent study in five different WT mouse strains showed that streptomycin can be used to establish a chronic and persistent colonisation with an AIEC strain isolated from a CD patient, NRG857c O83:H1, that mimics the intestinal inflammation seen in CD (Small et al. 2013). The main site of pathology was the caecum, with transmural fibrosis developing as early as seven days post-infection (p. i.). Furthermore, the pathology was accompanied by an increase in F4/80^{+} cells within the mucosa, likely to be inflammatory macrophages, as well as higher numbers of mucosal

T cells (Small et al. 2013). Concomitantly, NRG857c infection resulted in elevated levels of TNFα, IFNγ and IL-17 in both the caecum and colon (Small et al. 2013). Interestingly, in C57BL/6 mice this T cell-mediated pathology persisted after clearance of AIEC at later stages of the infection (Small et al. 2013), suggesting that the bacteria trigger a permanent shift in the mucosal immune response from tolerance to misdirected defence.

Other studies have employed variations of the DSS colitis model to disrupt the intestinal barrier and allow colonisation of the CD-associated AIEC strain LF82. Flagellated LF82 caused exacerbated inflammation during DSS colitis, whilst this effect was lost with non-flagellated mutants (Carvalho et al. 2008). This implicates flagellin as an important AIEC-derived PAMP recognised by the immune system after epithelial cell injury. Using a humanised mouse model, where the human CEACAM6 adhesin is present on the apical surface intestinal epithelium (Chan and Stanners 2004), Carvalho et al. (2009) showed that colonisation was dependent on expression of type I pili such as FimH on LF82, as the Δ*fimH* mutant was significantly decreased in its ability to colonise and cause intestinal inflammation. Given previous work showing that FimH binds the GP2 receptor on M cells (Hase et al. 2009), this could be one mechanism by which LF82 mediates transcytosis of across the epithelium. Similarly, genomic analysis of the NRG857c strain of AIEC has revealed two amino acid variations in its FimH (N91S, S99N) (Nash et al. 2010) that have been associated with *E. coli* strains isolated from IBD patient tissue (Sepehri et al. 2011). As of yet however, it is unclear what effect these variations may have on bacterial virulence.

Using the streptomycin pre-treatment model of AIEC infection, Small et al. (2013) found that *Rag1*$^{-/-}$ mice developed more severe intestinal inflammation than WT mice (Small et al. 2013). Furthermore, when they selectively depleted CD4^{+} or CD8^{+} T cells in WT animals, they found that absence of CD8^{+} T cells similarly induced a pronounced aggravation of inflammation, while CD4^{+} depletion showed no change in pathology (Small et al. 2013). Given the important role of CD8^{+} IEL in surveillance of the epithelial barrier, this indicates that a defect in the mucosal CD8^{+} T cell compartment may contribute to the persistence of *E. coli* species within the epithelium and LP, thus leading to chronic inflammation.

1.3.3 Bacterial enteric infections

Intestinal inflammation not only occurs with the onset of IBD, but can also be caused by infection with enteric bacterial pathogens. Infectious diarrhoeal-associated mortality is one of the leading causes of death in children globally, with most cases occurring in developing

countries (Black et al. 2010). The most common infectious agents responsible for enteric infections include *Salmonella*, *E. coli*, *Campylobacter* and *Shigella* (Fletcher et al. 2013). The expression of virulence factors such as adhesins and bacterial toxins allow pathogen colonisation, invasion of host cells and the subversion of immune responses. The mechanisms that govern the intestinal immune response to enteric pathogens have been extensively studied using *in vivo* models. Two commonly used examples are infection with *S.* Typhimurium (Barthel et al. 2003) and *C. rodentium* (Higgins et al. 1999, Atarashi et al. 2015).

Salmonella: subverting immunity to establish infection

In humans, *S.* Typhimurium causes a self-limiting gastroenteritis, whilst during infection with a related strain, *S.* Typhi, the pathogen spreads to systemic sites after establishing a seat of infection in the GI tract, and causes typhoid fever. Mice are generally resistant to *S.* Typhimurium-induced intestinal infection, although in genetically susceptible mouse strains *S.* Typhimurium causes systemic disease and mortality, without eliciting colitis (Griffin and McSorley 2011). The resistance to intestinal infection can be overcome by pre-treatment of mice with streptomycin (Barthel et al. 2003), and this model of infection has been widely used to study the intestinal immune response to *S.* Typhimurium.

S. Typhimurium is a Gram-negative, flagellated facultative anaerobe that preferentially colonises the terminal ileum and colon. Its first point of entry is through binding to M cells in PP (Jones et al. 1994, Clark et al. 1994) and the SILT in the small intestine (Halle et al. 2007). The pathogen's ability to successfully colonise and cause inflammation is largely due to the expression of motility genes (Schmitt et al. 2001) and of virulence factors encoded on the *Salmonella* pathogenicity islands (SPI) (Tsolis et al. 1999). Among these virulence factors, one of two Type III secretion systems (T3SS-1, encoded by SPI-1) allows insertion of effector proteins into host cells, and subsequent invasion (Raffatellu et al. 2005), which is important for the induction of inflammation (Zhang et al. 2002). Replication of *S.* Typhimurium within the epithelial cell cytosol leads to the activation of caspase-1 in these cells and subsequent inflammatory cell death. This is followed by extrusion of IEC from the epithelial layer, thus enabling shedding of *S.* Typhimurium in the faeces (Knodler et al. 2010).

In order to maintain infection and allow systemic spread, *S.* Typhimurium effectively subverts innate immune responses. Once it is engulfed by an MNP, the second T3SS,

encoded by SPI-2, is activated and sustains bacterial survival by the inhibition of phagosome maturation (Ochman et al. 1996). Furthermore, as in IEC, *S.* Typhimurium can induce MNP inflammatory cell death, also termed pyroptosis, which relies on the activation of caspase-1. This is mediated by the T3SS protein SipB, which binds to and cleaves caspase-1 (Hersh et al. 1999, van der Velden et al. 2003), but can also be initiated via the activation of the NLRC4 inflammasome (Miao, Leaf, et al. 2010). During infection with *S.* Typhimurium, the host upregulates the production of anti-microbial proteins such as lipocalin-2 and calprotectin, which act to limit the availability of metals such as iron required for bacterial growth (Goetz et al. 2002, Corbin et al. 2008). However, *S.* Typhimurium is able to compete with these host pathways of metal sequestration by expression of its own metal chelating proteins, thus giving it a selective advantage over other bacteria in the intestine and sustaining its rapid growth (Raffatellu et al. 2009, Liu et al. 2012, Behnsen et al. 2014). The uptake of *S.* Typhimurium by DC in the LP, together with cell-free migration in lymph, allows its spread to the MLN (Voedisch et al. 2009). Containment in the MLN is vital for inhibiting further dissemination to the liver and spleen, and the onset of systemic disease (Voedisch et al. 2009).

Citrobacter rodentium: an attaching effacing pathogen

The murine pathogen *C. rodentium* has been used as a model of human disease caused by enteropathogenic and enterohaemorrhagic *E. coli* (EPEC, EHEC). These strains establish infection in the intestine by forming attaching and effacing (A/E) lesions (Frankel and Phillips 2008). The initial site of colonisation by *C. rodentium in vivo* is the caecal patch, after which it establishes infection in the distal colon and rectum by ten days p. i. (Wiles et al. 2004) and causes colitis (Mundy et al. 2005). The infection is self-limiting and is cleared after three to four weeks (Wiles et al. 2004).

Expression of genes encoded by the locus of enterocyte effacement (LEE) (McDaniel et al. 1995), which is shared by *C. rodentium* and both EPEC and EHEC, is required for A/E lesion formation (Jarvis et al. 1995, Frankel and Phillips 2008). The LEE encodes a T3SS that mediates translocation of the bacterial effector Tir, which incorporates into the mammalian membrane and acts as a binding site for the bacterial adhesin intimin (Hartland et al. 1999). Intimin binding results in epithelial cell actin polymerisation and the formation of a pedestal, on top of which the bacteria resides (Frankel and Phillips 2008). Expression of these LEE-encoded virulence factors is essential for the establishment of infection by *Citrobacter* (Schauer and Falkow 1993, Deng et al. 2003). GF mice infected

with *C. rodentium* do not clear the infection naturally as SPF mice do (Kamada et al. 2012), indicating that the microbiota plays an important role in the resolution of infection. Indeed, Kamada et al. (2012) showed that LEE-encoded virulence genes were expressed early during infection, but not during the clearance phase, leading to increased detection of *C. rodentium* in the lumen at later time points. The propensity of members of the commensal microbiota for utilising similar nutrient sources to *C. rodentium* may therefore lead to the outcompeting and clearance of this pathogen *in vivo* (Kamada et al. 2012).

C. rodentium is well-equipped for the subversion of host defences. For example, colonisation of the intestinal epithelium by *C. rodentium* causes the weakening of tight junctions, leading to increased barrier permeability (Guttman, Li, et al. 2006, Guttman, Samji, et al. 2006). Opsonisation of bacteria by components of the complement pathway allows targeted phagocytosis by MNP, and *C. rodentium* effector EspJ has been shown to inhibit complement-mediated uptake (Marches et al. 2008). This pathogen can also inhibit the induction of apoptosis in host cells via its effector proteins NleH and NleB1 (Hemrajani et al. 2010, Pearson et al. 2013), thereby preventing the detachment and shedding of enterocytes, that are required for *C. rodentium* colonisation of the intestine. In particular, NleB1 mediates this via inhibiting Fas ligand-induced activation of caspase-8 (Pearson et al. 2013). This is especially important given the ability of IEL to activate Fas ligand-induced apoptosis (Corazza et al. 2000). *C. rodentium* therefore has a range of virulence factors at its disposal for supporting its growth in the intestine and escaping elimination by the host immune system.

1.3.4 Phases of inflammation based on cellular involvement

The immune response to bacteria is coordinated in phases, with different immune cells playing their part during the acute and chronic stages of the infection (Figure 1. 4). Early acute responses against bacteria are carried out by tissue neutrophils that are recruited by epithelial cell-derived IL-8 (Singer and Sansonetti 2004). Their ability to efficiently phagocytose bacteria and secrete cytotoxic mediators makes them an important component of the innate response. Infection with *S.* Typhimurium causes a robust IL-8 response, presumably orchestrated by sustained interactions with the epithelium (Hobbie et al. 1997, Gewirtz et al. 1999). Neutrophils thus attracted to the epithelial barrier not only combat infection whilst resident in the LP, but can also transmigrate across the epithelium into the lumen, induced by the IEC release of chemoattractant protein hepoxilin A_3

(McCormick et al. 1998, Mrsny et al. 2004). Once on the apical side, neutrophils can further combat the infection via the secretion of cytotoxic mediators and the formation of neutrophil extracellular traps. During infection with *C. rodentium*, neutrophils are recruited via a CXCR2-dependent mechanism, due to the production of CXCL1, 2 and 5 by MNP in the LP (Spehlmann et al. 2009).

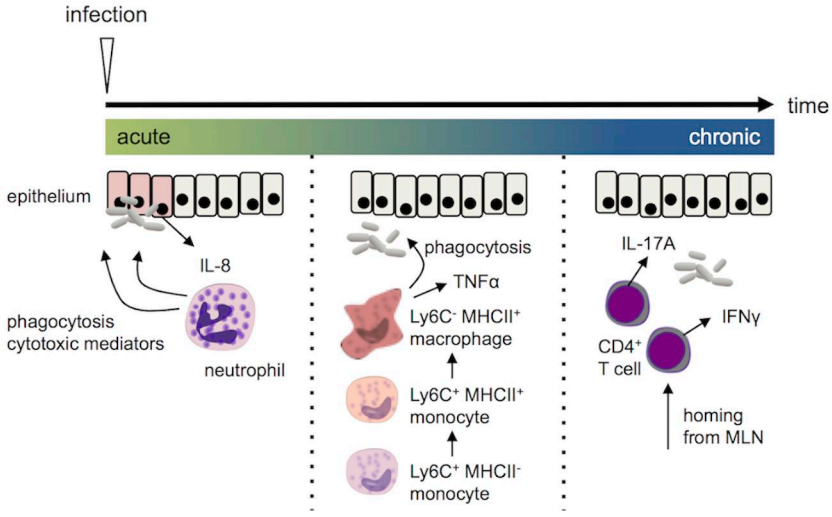

Figure 1. 4: Role of innate and adaptive immune cells during progression of bacterial infection from acute to chronic

Simplified schematic summarising the time-dependent roles of innate and adaptive immune cells in combatting bacterial infection. Epithelial cell-derived IL-8 attracts $Ly6G^+$ neutrophils, which in turn phagocytose bacteria and secrete cytotoxic mediators. As the infection progresses, classical blood $Ly6C^+$ $MHCII^-$ monocytes enter the tissue and differentiate by acquiring MHCII into $Ly6C^-$ $MHCII^+$ pro-inflammatory macrophages. These then engage in phagocytosis and secrete pro-inflammatory cytokines such as TNFα. Finally, an enhanced infiltrate of $CD4^+$ T cells is a marker of the final and chronic stage of infection. These home to the intestine after having been activated by dendritic cells in the MLN and once at the site of infection, secrete pro-inflammatory cytokines such as IFNγ and IL-17A in response to bacterial antigen recognition.

Eosinophils are a second type of granulocyte that has mainly been implicated in Th2-driven diseases such as allergies or parasitic infections. However, recent work by Griseri et al. (2015) suggests that they may be important mediators of chronic intestinal inflammation. This group reported on a granulocyte macrophage colony-stimulating factor (GM-CSF)-dependent mechanism of eosinophil expansion in the LP, which was induced by colitis-driven IL-23. *H. hepaticus* and IL-10R blockade-induced colonic inflammation was significantly associated with eosinophil production of cytotoxic mediators such as eosinophil peroxidase and tumour necrosis factor α (TNFα) (Griseri et al. 2015).

Once a robust acute response to the invading pathogen has been established, monocyte recruitment to the LP and their differentiation to inflammatory macrophages constitute the second important innate response to bacteria in the intestine (Figure 1. 4). DSS colitis

leads to an influx of Ly6C$^+$ monocytes into the LP (Bain et al. 2013), caused by the translocation of commensal bacteria across the damaged barrier. During *C. rodentium* infection, intestinal monocytes are recruited in a CCR2-dependent manner and give rise to macrophages, which produce pro-inflammatory cytokines such as IL-1β via the activation of the inflammasome by *C. rodentium* (Seo et al. 2015). This is required for the activation of ILC3 (Seo et al. 2015), important mediators of pathogen clearance (Qiu et al. 2012). As well as ILC, macrophages help to polarise and maintain intestinal T cell responses during infection via the production of IL-12 (Schreiber et al. 2013) and IL-23 (Aychek et al. 2015).

Following the initial innate response to a pathogen, DC migration to the draining lymph node will initiate the adaptive response in the form of T cell activation and differentiation. Activated T cells home to the site of infection through the upregulation of chemokine receptors, where they orchestrate the final phase of the defence by production of pro-inflammatory cytokines (Figure 1. 4). *C. rodentium* infection elicits an increase in LP Th17 cells (Mangan et al. 2006), while infection with *S.* Typhimurium causes a mixed Th1/Th17 response (Lee et al. 2012). A similar inflammatory T cell response is observed in the chronic intestinal inflammation of patients with IBD, characterised by both Th1 and Th17 infiltration of the inflamed mucosa (Rovedatti et al. 2009, Olsen et al. 2011).

A deeper understanding of the phases of immune activation and the factors that trigger and control each step will be important to both further illuminating the mechanisms of pathogenesis in IBD, and identifying therapeutic targets in the resolution of acute and chronic inflammation.

1.4 Intestinal dendritic cells and their role in anti-bacterial immunity

1.4.1 Development of dendritic cell subsets

In the context of the different phases of the immune response to bacterial infection, DC are at the cross-section of innate and adaptive immunity, as they provide the initial stimulus for T cells to become activated and differentiate into a particular effector phenotype. Originally described by Steinman and Cohen (1973), these professional antigen-presenting cells develop from bone marrow precursors via several rounds of differentiation (Figure 1. 5), and are dependent upon the cytokine Fms-like tyrosine kinase 3 ligand (Flt3L) (Maraskovsky 1996, McKenna et al. 2000, Naik et al. 2007, Waskow et al. 2008). The dynamics of this process have mainly been studied in mice, with some recent insights from

human studies. During haematopoiesis, the common DC precursor (CDP) (Naik et al. 2007, Onai et al. 2007) differentiates from common myeloid progenitors, possibly via an intermediary step of the macrophage and DC precursor (MDP), although conflicting evidence exists for the involvement of this step (Fogg et al. 2006, Sathe et al. 2014, Lee, Breton, et al. 2015). Both pDC and cDC lineages originate from the CDP (Naik et al. 2007, Onai et al. 2013). In cDC development, the CDP further gives rise to pre-cDC (Naik et al. 2007, Breton et al. 2015), which leave the bone marrow and circulate in the blood to lymphoid organs and peripheral tissues (Figure 1. 5) (Diao et al. 2006, Naik et al. 2006, Bogunovic et al. 2009, Ginhoux et al. 2009). Once arrived in the tissue environment, pre-cDC terminally differentiate into tissue cDC subsets.

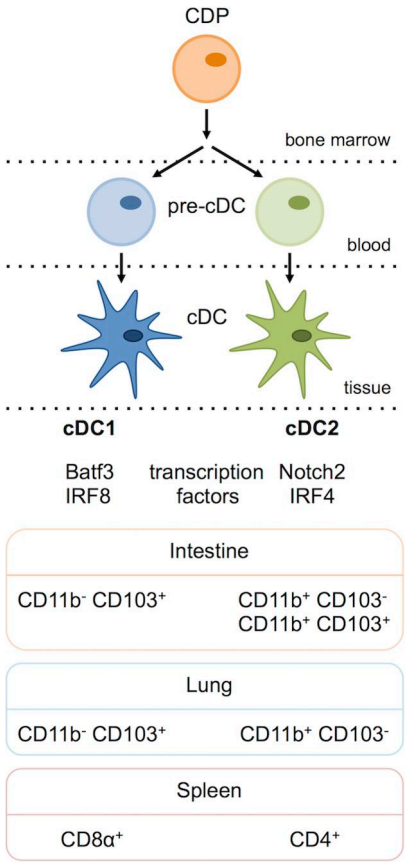

Figure 1. 5: Murine cDC development and lineages

In the bone marrow, the CDP (common DC precursor) gives rise to pre-DC, which are already committed to either the cDC1 or cDC2 lineage. These pre-cDC circulate in the blood to tissues, where they undergo terminal differentiation into tissue cDC. Transcription factors implicated in the development and survival of cDC lineages are detailed, as well as the phenotype of cDC1 and cDC2 in the intestine, lung and spleen, based on their surface marker expression.

Within tissues, a varying number of DC populations can be defined, based on the expression of a range of cell surface markers (Figure 1. 5). In the spleen, CD4 and CD8 define two subsets of DC, while CD11b, SIRPα and CD103 help distinguish two to four

mucosal DC populations at different sites (Guilliams et al. 2014). The observation of some level of functional overlap between DC populations found at distinct tissue sites, together with the increasing evidence for shared transcriptional regulation of their developmental pathways has led to the proposal that DC can be classified into two main subsets, cDC1 and cDC2 (Guilliams et al. 2014). Development of DC precursors into either of these subsets is likely determined during the transition from CDP to pre-cDC, as recent work has discovered the presence of cDC1 and cDC2 committed pre-cDC in the bone marrow of mice (Schlitzer et al. 2015) and in human blood (See et al. 2017).

The cDC1 lineage of DC comprises the CD8α$^+$ DC in the spleen, and CD11b$^-$ CD103$^+$ DC at mucosal sites such as the intestine and lung (Figure 1. 5) (Guilliams et al. 2014). These are characterised by their dependence on the transcription factors Batf3 (Hildner et al. 2008) and IRF8 (Schiavoni et al. 2002, Tamura et al. 2005), and their ability to activate CD8$^+$ T cells by cross-presentation of antigen (Hildner et al. 2008, Cerovic, et al. 2014b). The cDC2 lineage of DC, on the other hand, is made up of CD4$^+$ splenic DC and CD11b$^+$ SIRPα$^+$ DC in peripheral tissues (Guilliams et al. 2014). These are dependent on Notch2 (Satpathy et al. 2013) and IRF4 (Persson et al. 2013b, Schlitzer et al. 2013) signalling, and are functionally heterogeneous, although evidence indicates they may be important for orchestrating CD4$^+$ T cell responses during infection (Satpathy et al. 2013, Schlitzer et al. 2013).

1.4.2 Dendritic cell populations in the intestine

Four murine intestinal populations of migratory DC can be identified based on their differential expression of CD11b and CD103. Among these, CD11b$^-$ CD103$^+$ DC are classed as cDC1, whilst CD11b$^+$ CD103$^-$ and CD11b$^+$ CD103$^+$ DC form part of the cDC2 lineage (Figure 1. 6). The origin of the fourth DC population, which is CD11b$^-$ CD103$^-$, remains unclear. In the human intestine, a similar classification can be achieved based on expression of SIRPα and CD103, with SIRPα$^+$ CD103$^-$ and SIRPα$^+$ CD103$^+$ DC exhibiting a transcriptional profile aligned with murine cDC2, while SIRPα$^-$ CD103$^+$ DC belong to the cDC1 lineage (Watchmaker et al. 2014).

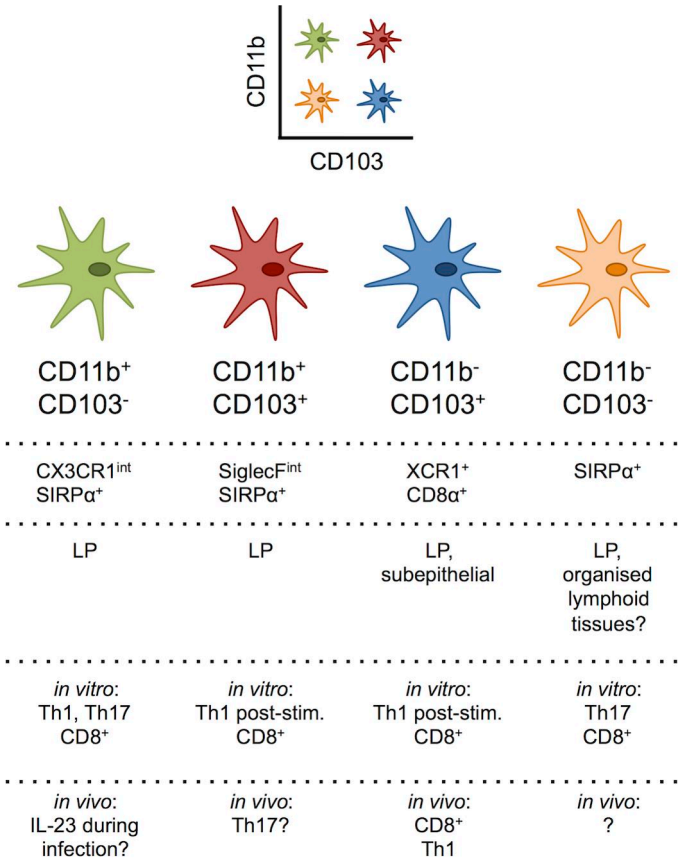

Figure 1. 6: Intestinal DC populations and their functions

Four intestinal DC populations can be identified in the intestine based on the differential expression of CD11b and CD103. The differential expression of additional cell surface markers, as well as their tissue localisation are detailed. Furthermore, intestinal DC populations have been implicated in the induction of different effector T cell responses both *in vitro* and *in vivo*.

The distribution of DC populations changes along the GI tract. For example, CD11b$^+$ CD103$^+$ DC are the most prominent population in the small intestine and sMLN, whilst their frequency in the colon and cMLN is reduced (Houston et al. 2016). On the other hand, CD11b$^-$ CD103$^+$ DC constitute the highest percentage of total DC in the colonic LP and cMLN (Houston et al. 2016). These tissue-specific differences point to both the functional specialisation of intestinal DC populations, and the important role of the tissue environment in conditioning DC differentiation and survival. Indeed, a range of studies has identified population-specific phenotypes and functions both *in vitro* and *in vivo*.

Intestinal CD11b$^+$ CD103$^-$ DC

The role of intestinal CD11b$^+$ CD103$^-$ DC in orchestrating mucosal immune responses has long been overlooked, due to the inaccurate discrimination between DC and macrophage populations in the LP. This is perhaps not surprising, as among all the four intestinal DC

populations, they are the phenotypically most similar to macrophages. For example, together with the shared expression of CD11b, they also express intermediate levels of CX3CR1, which is found at high levels on mature intestinal macrophages (Cerovic et al. 2013). However, they are in fact a *bona fide* DC population, as they migrate in lymph (Cerovic et al. 2013), and constitute one of the four migratory DC populations found in the MLN. Furthermore, they arise from pre-DC and are Flt3L-responsive (Cerovic et al. 2013, Scott et al. 2014a). They also express SIRPα, one of the shared characteristics of the cDC2 lineage (Cerovic, Houston, et al. 2014, Watchmaker et al. 2014). Lymph CD11b$^+$ CD103$^-$ DC are highly potent in their ability to prime antigen-specific CD4$^+$ T cell responses *in vitro*, and can induce the differentiation of IFNγ$^+$ Th1 and IL-17A$^+$ Th17 cells without prior stimulation (Denning et al. 2007, Cerovic et al. 2013). Whether this also translates to the *in vivo* setting still remains to be determined. CD11b$^+$ CD103$^-$ DC have, however, been implicated in the production of IL-23 during infection with *C. rodentium* (Aychek et al. 2015), suggesting that they may have a role in sustaining Th17 responses in the LP, as well as inhibiting excessive Th1-mediated pathology (Aychek et al. 2015). Furthermore, CD11b$^+$ CD103$^-$ DC have also been shown to drive Th2 responses to *Schistosoma mansoni* (*S. mansoni*) eggs in the colon (Mayer et al. 2017). This population of intestinal DC therefore seems to be able to respond to a range of different stimuli, leading to distinct T cell differentiation fates both *in vitro* and *in vivo*.

Intestinal CD11b$^+$ CD103$^+$ DC

The CD11b$^+$ CD103$^+$ population of DC is unique to the intestine, as for example the lung mucosa only contains two main DC populations, CD11b$^-$ CD103$^+$ DC (cDC1) and CD11b$^+$ CD103$^-$ (cDC2) (Desch et al. 2013, Persson et al. 2013a). Intestinal CD11b$^+$ CD103$^+$ DC are SIRPα$^+$ (Cerovic et al. 2014b) and express intermediate levels of SiglecF (Houston et al. 2016). They are developmentally dependent on IRF4 (Persson et al. 2013b, Schlitzer et al. 2013) and Notch2 (Lewis et al. 2011, Satpathy et al. 2013), as well as RA signalling (Klebanoff et al. 2013). Contrary to CD11b$^+$ CD103$^-$ DC, whilst able to drive antigen-specific CD4$^+$ T cell activation *in vitro*, they are less capable of eliciting a T cell-mediated cytokine response (Cerovic et al. 2013). Only after stimulation with TLR ligands do they induce antigen-specific Th1, but not Th17 differentiation *in vitro* (Cerovic et al. 2013). Conversely, IRF4 deficiency decreases the frequency of LP Th17 cells in the steady state, as well as after induction of an immune response (Persson et al. 2013b, Schlitzer et al. 2013). Similarly, DC specific deletion of Notch2 leads to the worsening of colitis and

increased mortality during *C. rodentium* infection (Satpathy et al. 2013). These findings point to a role for CD11b$^+$ CD103$^+$ DC in the induction of Th17 responses *in vivo*. Interestingly, depletion of intestinal CD11b$^+$ CD103$^+$ DC in mice that express diphtheria toxin under control of the human Langerin promoter (huLangerin-DTA mice) does not lead to increased weight loss during *C. rodentium* infection (Welty et al. 2013). A lack of protective responses induced by Notch2 deficiency may therefore also be due to functional defects in CD11b$^+$ CD103$^-$ DC, the other cDC2 population, rather than simply a reduction in CD11b$^+$ CD103$^+$ numbers. Furthermore, while huLangerin-DTA mice also exhibited reduced LP IL-17A$^+$ CD4$^+$ T cells, this was independent of MHCII expression on CD11b$^+$ CD103$^+$ DC (Welty et al. 2013). Given that mesenteric lymph CD11b$^+$ CD103$^+$ DC do not drive Th17 differentiation *in vitro* (Cerovic et al. 2013), the contribution of this population to Th17 responses in the intestine may therefore be independent of T cell activation in the MLN, and further work will be required to fully elucidate their functional role in maintaining Th17 responses *in vivo*. Intriguingly, whilst CD11b$^+$ CD103$^-$ DC were shown to drive Th2 responses in the colon, CD11b$^+$ CD103$^+$ DC were the only population in the small intestine to induce Th2 activation to *S. mansoni* eggs in the small intestine (Mayer et al. 2017). This indicates that tissue environment regulates the differential ability of DC populations to prime protective CD4$^+$ T cell responses *in vivo* and further work will be required to identify tissue-specific factors that are involved in shaping the function of intestinal DC populations.

Intestinal CD11b$^-$ CD103$^+$ DC

As in the spleen, intestinal CD11b$^-$ CD103$^+$ cDC1 express CD8α. Whilst all mesenteric lymph DC populations can induce the antigen-specific proliferation of CD8$^+$ T cells *in vitro*, only CD11b$^-$ CD103$^+$ DC are able to do so *in vivo* (Cerovic et al. 2014b). This unique ability to acquire and process antigen for cross-presentation has also been shown for cDC1 in other tissues, including the lung (Desch et al. 2011) and spleen (Iyoda et al. 2002). Furthermore, they uniquely express the chemokine receptor XCR1 (Cerovic et al. 2014b). Its ligand XCL1 is secreted by CD8$^+$ T cells upon activation by CD8α$^+$ DC (Dorner et al. 2009), and is required for the maintenance of XCR1$^+$ DC and CD8$^+$ T cell populations in the intestine (Ohta et al. 2016). Their ability to undergo cross-presentation *in vivo* is likely due to an enhanced capacity to take up cell-derived antigen. Indeed, CD11b$^-$ CD103$^+$ in the MLN contain cytokeratin inclusions, indicating an increased rate of IEC uptake (Cerovic et al. 2014b). Furthermore, they express high levels of Clec9A (also known as DNGR-1)

(Cerovic et al. 2014b), which allows recognition of damaged cells via binding of actin filaments (Zhang et al. 2012), thus providing a possible explanation for their ability to acquire and present cell-derived antigen.

Batf3 deficiency selectively depletes cDC1, including intestinal CD11b$^-$ CD103$^+$ DC (Hildner et al. 2008, Edelson et al. 2010, Cerovic et al. 2014b), and lack of this population is associated with increased mortality during *Toxoplasma gondii* infection (Mashayekhi et al. 2011). This is mediated by the loss of protective IL-12 production by CD11b$^-$ CD103$^+$ DC (Mashayekhi et al. 2011). On the other hand, they are not required for mounting a protective response against *C. rodentium* (Satpathy et al. 2013). Instead, the production of IL-12 by CD11b$^-$ CD103$^+$ DC is decreased during *C. rodentium* infection due to its negative regulation by IL-23 signalling, which thus prevents the induction of a detrimental Th1 response (Aychek et al. 2015). *In vitro* findings indicate that CD11b$^-$ CD103$^+$ DC can induce the differentiation of Th1 cells, but only after stimulation (Cerovic et al. 2013). Together, these observations provide evidence for a functional role of CD11b$^-$ CD103$^+$ DC in the induction of Th1 responses in the context of infection.

Intestinal CD11b$^-$ CD103$^-$ DC

While the smallest population of DC in the intestine does not express either CD11b or CD103, it does express SIRPα (Cerovic et al. 2013). Much still remains to be clarified as to their origin and function, which are likely to represent a heterogeneous population of cells. CD11b$^-$ CD103$^-$ DC migrate in lymph and can activate antigen-specific CD8$^+$ T cells *in vitro* (Cerovic et al. 2014b). They also induce the differentiation of Th17 cells without the need for prior stimulation (Cerovic et al. 2013). Furthermore, lymph CD11b$^-$ CD103$^-$ DC express co-stimulatory molecules such as CD80 and CD86 (Cerovic et al. 2013). In the light of these findings, they must, therefore, be classed as *bona fide* DC. With respect to their origin, Cerovic et al. (2013) found that CD11b$^-$ CD103$^-$ DC were decreased in *Rorc*$^{-/-}$ mice, which lack intestinal organised lymphoid tissues. It is therefore conceivable that these are primarily present in the GALT, and there contribute to the priming of T cells. A further possibility is that a proportion of these cells represent precursors for cDC2 in the LP, given their expression on SIRPα, but this hypothesis is yet to be tested.

The regulation of T cell homing by intestinal DC populations

As detailed above, the induction of CCR9 and α4β7 on activated T cells in the MLN is dependent on RA production by DC (Iwata et al. 2004). Furthermore, this ability to induce

homing markers seems to be specific to CD103$^+$ DC (Jaensson et al. 2008), which would include both CD11b$^+$ CD103$^+$ and CD11b$^-$ CD103$^+$ DC. Mice that lack either CD11b$^-$ CD103$^+$ DC due to Batf3 deficiency, or CD11b$^+$ CD103$^+$ DC after deletion of IRF4 in CD11c$^+$ cells have normal levels of CCR9 and α4β7 induction in the MLN (Edelson et al. 2010, Persson et al. 2013b). It is therefore likely that a high degree of redundancy exists in the ability to induce homing receptor expression between the two CD103$^+$ populations. More recently, however, it has become clear that all mesenteric lymph DC populations are able to metabolise Vitamin A to produce RA to the same extent and induce CCR9 expression on CD8$^+$ T cells *in vitro* (Cerovic et al. 2013). Further investigation will therefore be required to elucidate the functional role for RA production by CD103$^-$ DC during this process *in vivo*. Moreover, it will also be important to investigate the contribution of stromal cells in the MLN, which have previously been shown to be able to sustain the induction of CCR9 on T cells *in vitro* (Hammerschmidt et al. 2008).

1.4.3 DC migration and antigen presentation

Once a DC has taken up antigen in the intestine, it leaves the LP via lymphatic endothelial vessels and migrates in lymph to the MLN. This process of migration is constitutive and has been studied in several different ways. The first involves the feeding or injection of fluorescent antigen and detection of fluorescent DC in the MLN. While this can be informative, the ability of many antigens to travel cell-free in lymph means that labelled DC in the MLN may not exclusively be made up of migratory populations. Instead, antigen can be taken up by LN resident DC and processed for presentation (Sixt et al. 2005). Recently, the generation of transgenic Kaede mice has provided an elegant way of circumventing this problem (Tomura et al. 2008). These mice ubiquitously express the fluorescent Kaede-green protein, which derives from the stony coral *Trachyphyllia geoffroyi*, and can be photoconverted from a green to red emission state under exposure to violet light (Ando et al. 2002). The Kaede-red state is stable *in vitro* (Ando et al. 2002) and for up to seven days *in vivo*, where it allows tracking of immune cells across tissues (Tomura et al. 2008). Indeed, Houston et al. (2016) successfully used this technique to study the differentiation migration pattern of small intestinal and colonic LP DC to the MLN. A third method involves surgical removal of MLN, and subsequent cannulation of the thoracic duct once lymphatic vessels have reanastomosed (Cerovic et al. 2013). Instead of only tracking cell migration, this technique allows isolation and the carrying out of functional assays on DC that are still in the process of migration, rather than having

arrived in the MLN where their phenotype is likely to change due to the altered tissue environment. It also permits analysis of DC without prior activation during the digestion protocols otherwise necessary for their isolation from tissues.

DC migration is primarily controlled by the upregulation of CCR7 (Förster et al. 1999, Jang et al. 2006). This allows DC to migrate along a chemokine gradient of the CCR7 ligands CCL19 and CCL21, which are expressed in the T cell areas of LN, as well as by the lymphatic endothelium (Gunn et al. 1998, Luther et al. 2000). Furthermore, DC migration to draining LN was shown to be independent on the expression of integrins that can mediate cell-cell contact between leukocytes and the lymphatic endothelium (Lämmermann et al. 2008). CCR7 upregulation is induced upon TLR ligands binding by DC, as well as by the action of pro-inflammatory cytokines such as TNFα (Sallusto et al. 1998, Sozzani et al. 1998). Indeed, *Myd88*$^{-/-}$ mice have significantly lower expression of CCR7 (Hägerbrand et al. 2015), confirming a role for PAMPs in inducing DC migration.

DC enter the MLN via the afferent lymphatics and first accumulate in the subcapsular sinus region before migrating to T cell zones (Girard et al. 2012). There, DC encounter naïve T cells and present antigen in the form of peptide-MHCII or peptide-MHCI complexes recognized by $CD4^+$ and $CD8^+$ T cells, respectively. Antigen-specific activation is controlled by the need for recognition of the peptide-MHC by the TCR. This interaction forms "Signal 1" required for antigen-specific T cell activation and is the central interaction that constitutes the formation of the stable immunological synapse (Huppa and Davis 2003). The second essential signal is provided by costimulatory molecules expressed by DC upon maturation, such as CD80 and CD86. These are upregulated in response to TLR ligands, but also by the binding of CCL19 by DC once they have entered the LN (Marsland et al. 2005). CD80 and CD86 bind CD28 and CTLA-4 on the T cell, further stabilizing the immunological synapse (Brzostek et al. 2016). The resulting signaling cascade initiated in the T cell induces the production of IL-2, which is required for T cell proliferation (Brzostek et al. 2016). Production of cytokines such as IL-6, IL-10 and IL-12 by DC further helps to instruct T cell differentiation. After antigen presentation, DC are thought to remain in the MLN and undergo apoptosis (Chen et al. 2006), as thoracic duct lymph does not normally contain DC (Pugh et al. 1983, Cerovic et al. 2013).

1.4.4 Pathogen sensing by DC

Antigen presenting cells such as macrophages and DC can respond microbial stimuli provided by the microbiota or bacterial infection via the recognition of PAMPs. These encompass a wealth of different molecular components (Fukata and Arditi 2013, Muralidharan and Mandrekar 2013). MNP sense PAMPs via expression of a range of membrane-bound and intracellular PRR (Figure 1. 7), which can be largely grouped into two main families, TLR and NOD-like receptors (NLR) (Fukata and Arditi 2013, Muralidharan and Mandrekar 2013).

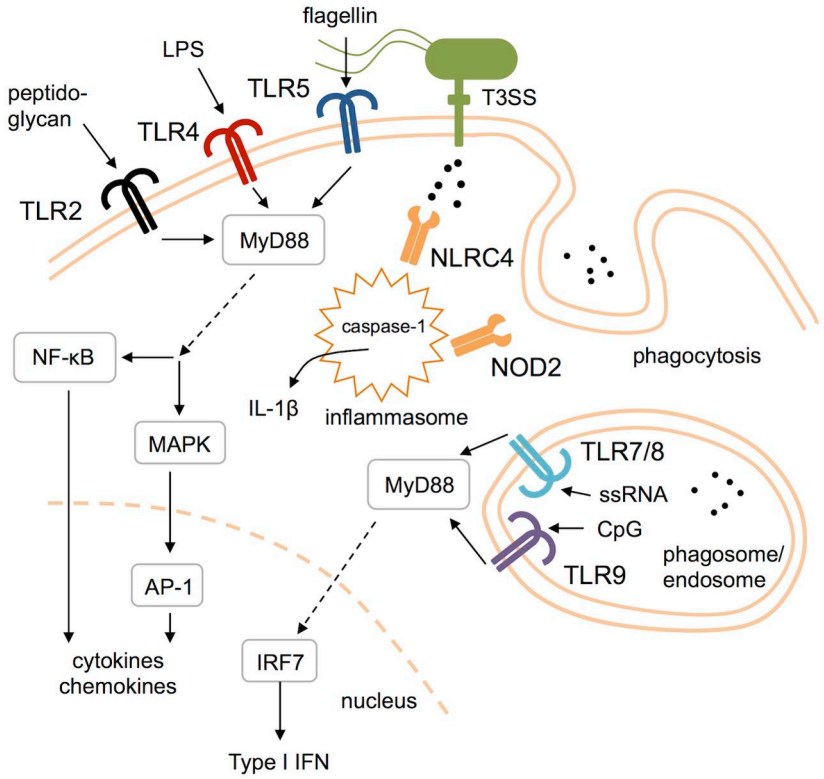

Figure 1. 7: PRR signalling in response to PAMPs

Simplified schematic giving an overview of PRR signalling pathways in antigen-presenting cells. Activation of different extracellular TLR by a range of ligands induces the recruitment of MyD88 and subsequent activation of a signalling cascade leading to the activation of NF-κB and MAP Kinase (MAPK). NF-κB and the MAPK-induce transcription factor AP-1 in turn initiate the transcription of genes encoding pro-inflammatory cytokines and chemokines. TLR located in the membrane of endosome or phagosomes also induce MyD88 signalling, but this leads to the mobilisation of interferon response factor 7 (IRF7) to the nucleus and the subsequent expression of Type I interferons. Cytoplasmic PAMPs, including components of bacterial T3SS, are recognised by a range of NLR, which include NOD2 and NLRC4. These assemble to form the inflammasome, which mediates caspase-1 cleavage. This in turn facilitates the activation of IL-1β.

Extracellular PAMPs include peptidoglycan from Gram-positive bacteria, recognised by TLR2, lipopolysaccharide (LPS) that is bound by TLR4, and flagellin that activates TLR5. Binding of these TLR recruits the master regulator MyD88, together with a range of adapter proteins, and initiates a downstream signalling cascade that leads to the activation

of NF-κB and the MAP-kinase pathway (Figure 1. 7). NF-κB and the MAP-kinase activated transcription factor AP-1 then trigger the transcription of cytokines, chemokines and antimicrobial peptides. Intracellular PAMPs are confined in endosomes generated either through viral infection or in phagosomes after the phagocytosis of bacteria (Figure 1. 7). For example, single stranded viral RNA is recognised by TLR7/8, and bacterial single stranded DNA harbouring CpG motifs is bound by TLR9 (Figure 1. 7). Again, MyD88 is recruited and in this case induces a signalling cascade that leads to the activation of IRF7, which is then able to trigger transcription of Type I interferons.

Intestinal macrophages are hyporesponsive to TLR stimulation (Denning et al. 2007, Smythies et al. 2010). This inert state is not due to a lack of TLR expression, but rather due to negative regulation of downstream signalling (Smythies et al. 2010). This constitutes a vital safety mechanism in the face of the wealth of PAMPs provided by the commensal intestinal microbiota. On the other hand, there has been some debate about the responsiveness of intestinal DC to PAMPs via TLR activation. Intestinal $CD11c^+$ $MHCII^+$ cells have been shown to be hyporesponsive to signalling via a range of TLR (Monteleone et al. 2008), including TLR4 (Uematsu et al. 2006). However, due to the lack of differentiation based on macrophage-specific markers in these studies, it is impossible to determine if these observations hold true for LP DC as well as macrophages. More definitive studies on mesenteric lymph DC have shown that hyporesponsiveness is limited to TLR4 signalling (Cerovic et al. 2009), and further indicate that mesenteric lymph DC populations differ in their ability to respond to TLR stimulation (Yrlid et al. 2006a).

The other main class of PRR comprises the NLR family. These PRR are present in the cytoplasm and their activation results in the formation of the inflammasome (Fukata and Arditi 2013). NOD2 for example recognises muramyldipeptide, a component of the bacterial cell wall, while flagellin and components of bacterial T3SS can activate NLRC4 (Miao et al. 2010b, Fukata and Arditi 2013) (Figure 1. 7). Upon assembly, the inflammasome cleaves pro-caspase-1 to generate active caspase-1, which then goes on to cleave and activate IL-1β (Figure 1. 7) (Gagliani et al. 2014).

NOD signalling in DC and macrophages has been shown to induce autophagy (Cooney et al. 2010, Travassos et al. 2010). This involves the sequestration of cytoplasmic components such as organelles, or bacteria in infected cells, into autophagosomes, which can subsequently be degraded (Levine and Kroemer 2008). Furthermore, this leads to the upregulation of MHCII and antigen presentation on DC (Cooney et al. 2010), providing a

further example of the ability of PAMPs to induce DC maturation. During infection with *S.* Typhimurium, the expression of NOD1 in DC, another NLR, was required to control systemic spread of the pathogen (Le Bourhis et al. 2009). Furthermore, activation of the NLRC4 inflammasome by *S.* Typhimurium induces pyroptosis in macrophages and the subsequent release of intracellular bacteria, which are then effectively phagocytosed and killed by neutrophils (Miao et al. 2010a). Thus, NLR signalling in DC and macrophages is a vital mechanism by which these cells are able to respond to intracellular pathogens, both by the production of IL-1β and the elimination of cytoplasmic bacteria by autophagy or pyroptosis.

1.5 Importance of apoptotic cell uptake in regulating intestinal immunity

1.5.1 Apoptosis at steady state and during intestinal inflammation

Early experiments investigating the rate of epithelial turnover in the GI tract showed that IEC rapidly migrate upwards from the intestinal crypt and are shed within a matter of days (Creamer, Shorter, and Bamforth 1961a, 1961b, Clarke 1970). Later work demonstrated that apoptosis occurs in the epithelial layer throughout the GI tract, but that this is mainly confined to IEC at the tips of villi or equivalent superficial positions in the colonic crypt structure (Hall et al. 1994, Strater et al. 1995). This was accompanied by extrusion of apoptotic cells from the epithelial cell layer (Strater et al. 1995). More recent work has confirmed the presence of cleaved caspase-3 in shedding IEC (Bullen et al. 2006). However, these appear to be in the early stages of apoptosis, due to the lack of evidence for late stage apoptotic cell bodies higher up in the crypts (Bullen et al. 2006). There is still some debate about whether apoptosis precedes shedding, or if shedding and the resulting loss of cell adhesion instead initiate cell death via anoikis in IEC. *In vitro* data indicate that apoptotic epithelial cells in a monolayer signal to neighbouring cells via S1P to induce actin rearrangements to facilitate cell extrusion (Rosenblatt et al. 2001, Gu et al. 2011). However, this process was caspase independent (Rosenblatt et al. 2001), and recent work has highlighted that overcrowding in the epithelial layer can also lead to the extrusion of live cells that is dependent on similar signalling pathways as previously described for apoptotic cells (Eisenhoffer et al. 2012). Taken together, therefore, it is possible that a range of mechanisms exists to ensure the efficient turnover of the intestinal epithelium.

Regulation of cell death during enteric bacterial infections

IEC cell death is also a phenomenon observed in infections with a range of bacterial pathogens such as EHEC, *Helicobacter pylori* and *Shigella* (Moss et al. 1996, Zychlinsky et al. 1996, Barnett Foster et al. 2000). Host defences rely on the elimination of infected cells to prevent bacterial spread and loss of barrier integrity. For example, epithelial cells infected with *Salmonella enterica* serovar Dublin or enteroinvasive *E. coli* undergo delayed apoptosis dependent on the action of TNFα and nitric oxygen synthase (Kim et al. 1998). Paesold et al. (2002) further showed that this delayed cell death response to *S.* Dublin was dependent on virulence factors encoded by SPI-2. Similarly, EHEC and *C. rodentium* can induce apoptosis via the effector protein EspF (Torchinsky et al. 2009, Zhao et al. 2013), which causes mitochondrial dysfunction (Nougayrède and Donnenberg 2004, Nagai et al. 2005). *Shigella flexneri* also induces necrosis-like cell death in non-myeloid cells via disruption of mitochondrial function (Carneiro et al. 2009). Interestingly, the increased exposure of phosphatidylethanolamine during EHEC-induced apoptosis may support bacterial adhesion (Barnett Foster et al. 2000), which indicates that pathogens can exploit the host cell death mechanisms intended for defence.

On the other hand, the control of IEC cell death during infection is also crucial for the pathogen (Kim et al. 2010). Bacteria must inhibit the induction of apoptosis during the early stages of infection to allow colonisation and immune evasion. *S.* Typhimurium, for example, can activate caspase-3 during the early stages of IEC infection without inducing apoptosis (Srikanth et al. 2010). Instead, it exploits this as a means of activating the T3SS effector protein SipA (Srikanth et al. 2010). A second *S.* Typhimurium effector, SopB, inhibits IEC apoptosis by sustaining cell survival signalling within the cell (Knodler et al. 2005, Kum et al. 2011). EPEC is also equipped with several strategies to subvert host cell apoptosis; for instance, it can antagonises death receptor signalling by expression of the effector NleB1 (Pearson et al. 2013). A second effector protein, NleH, directly interferes with the host cell pro-apoptotic protein Bax inhibitor-1, thus preventing caspase-3 cleavage and stalling apoptosis (Hemrajani et al. 2010). During bacterial infection, therefore, a constant state of antagonism exists between pathogenic survival strategies and host defences in regulating apoptosis in the intestine.

Apoptosis in IBD

As well as acute infectious gastroenteritis, chronic inflammation of the intestinal mucosa has been associated with increased levels of apoptosis. The epithelium of affected mucosa

has a higher frequency of apoptotic enterocytes in both CD (Di Sabatino et al. 2003) and UC (Iwamoto et al. 1996, Hagiwara et al. 2002) patients compared with healthy controls. Furthermore, proteomic analysis of IEC from IBD patients revealed an increase in potential pro-apoptotic mediators (Shkoda et al. 2007). However, the interplay between factors governing this increased frequency of apoptosis in IBD is yet unclear, although they are likely to be made up of genetic susceptibility, dysregulated recognition and clearance of bacteria by phagocytes, and perturbations of the microbiota.

One indication of a possible role for host genetics comes from the finding that polymorphisms in the XBP1 gene are associated with IBD (Kaser et al. 2008). This transcription factor plays an important role in regulating the response to ER stress (Calfon et al. 2002), and XBP1 deletion caused Paneth cell apoptosis *in vivo* (Kaser et al. 2008). Furthermore, IEC cell death in this model is linked to NF-κB signalling and can be ameliorated by the induction of autophagy (Adolph et al. 2013). However, the loss of both ER stress pathways and autophagy in the intestinal epithelium has a compounded detrimental effect, causing severe CD-like ileitis *in vivo*, which is dependent on the microbiota (Adolph et al. 2013). Given that genetic variation in the autophagy-related ATG16L1 gene are also associated with IBD, these findings indicate that increased apoptosis in IBD may stem from a dysregulation in IEC autophagy and ER stress response mechanisms.

A second important factor involved in the induction of apoptosis during inflammation is TNFα. This pro-inflammatory cytokine is increased in the mucosa of IBD patients (Murch et al. 1993, Breese et al. 1994). TNFα signalling induces NF-κB nuclear localisation and this is required for the induction of a pro-survival response (Beg and Baltimore 1996, Van Antwerp et al. 1996). Whilst this protective mechanism occurs in most tissues, treatment with TNFα induces rapid and wide-spread apoptosis in the intestinal epithelium (Piguet et al. 1999). Conversely, anti-TNFα therapy in CD patients effectively decreases IEC apoptosis (Zeissig 2004), thus providing a potential mechanism for its effectiveness. A similar effect was also observed in a murine model of chronic ileitis (Marini et al. 2003). Furthermore, polymorphisms in genes linked with apoptosis, including caspase-9 and Fas ligand, are predictive of a treatment response to the TNFα-targeting monoclonal antibody infliximab in IBD (Hlavaty et al. 2005). Thus, TNFα-mediated apoptosis is likely to constitute a fundamental driving factor in IBD-associated pathology.

1.5.2 Innate recognition of apoptotic cells

Macrophages and DC in the LP can recognise and take up apoptotic cells or cell-derived antigen. This is mediated by the expression of various apoptotic cell receptors (ACR), and enabled by the phagocytic nature of these cells. Given the rapid turnover of IEC and extrusion of cells from the epithelial layer before showing signs of the late stages of apoptosis, there has been some debate over the ability of macrophages in particular to acquire IEC-derived antigen. Early studies identified sub-epithelial macrophages intimately associated with the epithelium and apoptotic cells (Han et al. 1993, Iwanaga et al. 1993, Shibahara et al. 1995). However, later work using more sophisticated staining techniques was not able to show the same; instead, CD68 staining was concentrated in the LP and did not associate with shedding IEC (Bullen et al. 2006). Nonetheless, cytokeratin inclusions have been found both in LP macrophages (Nagashima et al. 1996) and DC (Huang et al. 2000, Cerovic et al. 2014b), indicating that these cells nonetheless do succeed in phagocytosing epithelial cell-derived antigen.

One of the principal and most well studied signals that is recognised by MNP on apoptotic cells is phosphatidylserine (PS). This lipid component of the cell membrane is associated with the inner membrane leaflet in live cells, but becomes externalised upon induction of apoptosis (Fadok et al. 1992, Leventis and Grinstein 2010). Recognition of PS by MNP can be facilitated by a range of PS receptors (PSR). Among these, some receptors directly mediate binding to PS, whereas others require the presence of an adapter molecule. An example for the latter is given by the TAM receptor family. This is made up of three distinct receptors, Tyro3, Axl and MerTK, which all mediate uptake of apoptotic cells via the recognition of PS by adapter molecules Gas6 or Protein S (Lemke 2013). Upon adapter binding, TAM receptors dimerise, allowing phosphorylation of their intracellular tyrosine kinase domains, and the activation of signalling cascades that result in the rearrangement of the actin cytoskeleton and phagocytosis (Lemke 2013). TAM receptor signalling also serves to activate immunosuppressive pathways in the phagocyte upon activation. For example, Gas6 binding in bone marrow-derived DC (BMDC) inhibited the inflammatory response downstream of TLR9 induction, and this was shown to be due to the mobilisation of SOCS1 and SOCS3, important negative regulators of TLR signalling (Rothlin et al. 2007). Expression of TAM receptors on intestinal MNP is variable. For example, MerTK is expressed on colonic LP macrophages (Bain et al. 2014), but not mesenteric lymph DC (Cerovic et al. 2014b). Furthermore, Axl expression in BMDC is low at steady state, but is

increased upon TLR stimulation (Rothlin et al. 2007). Together, these findings indicate that differential regulation of TAM receptor expression on MNP populations may be important for coordinating the downstream response to apoptotic cells.

A further example of a PSR is given by members of the T cell immunoglobulin and mucin (TIM) domain family of proteins. TIM1, TIM3 and TIM4 are conserved between humans and mice, with genes clustering together on human chromosome 5q33.2, within a region that has been linked with allergy and asthma (Marsh et al. 1994, McIntire et al. 2001). These three proteins have been shown to have PS binding ability (Kobayashi et al. 2007, Freeman et al. 2010), with TIM1 and TIM4 mediating uptake of apoptotic cells by macrophages (Kobayashi et al. 2007). High expression of TIM4 has been documented on peritoneal macrophages (Kobayashi et al. 2007), and facilitates their homeostatic function of apoptotic cell clearance *in vivo* (Wong et al. 2010).

In addition to PSR, scavenger receptors mediate the sampling of apoptotic cell antigen via recognition of other cellular components that are accessible in dying or damaged cells. These components are also referred to as danger-associated molecular patterns (DAMPs), and resemble PAMPs in their ability to induce pro-inflammatory signalling in MNP. CD205 (also known as DEC205) is a member of the mannose receptor family that allows recognition of apoptotic cells by binding keratins (Cao et al. 2016). These are intermediate filaments that have been implicated as having an important role in regulating colonic epithelial cell differentiation (Lahdeniemi et al. 2017). Furthermore, activated caspases induce keratin cleavage during apoptosis (Caulin et al. 1997), which may in turn lead to keratin exposure during later stages of apoptosis. CD205 can localise to the endosome (Chatterjee et al. 2012), and recognises apoptotic cell components after a conformational change due to low pH (Cao et al. 2015). In cells undergoing apoptosis the cytoplasm becomes acidified (Matsuyama et al. 2000), which may in turn lower the environmental pH due to leakage from the dying cell, and allow CD205 binding. Initially, CD205 was described as a DC-specific marker (Kraal et al. 1986, Pack et al. 2008), but has subsequently also been described on intestinal macrophages (Kamada et al. 2009).

1.5.3 Role of apoptotic cell-derived antigen in driving intestinal T cell responses

Apoptotic cell uptake can have opposing effects on downstream T cell-mediated immunity (Green et al. 2009). Firstly, it allows the processing of self peptides and thus constitutes an important mechanism for the induction of tolerance (Steinman et al. 2000). Over the past

two decades, the cellular and molecular determinants for this process have become increasingly clear. As mentioned in an earlier section, cDC1 are characterised by their ability to cross-present antigen to $CD8^+$ T cells (Guilliams et al. 2014). As well as being an important defence mechanism during viral infection (Hildner et al. 2008), cross-presentation allows the expansion of $CD8^+$ T cells in response to self-antigen associated with apoptotic cells (Liu et al. 2002). However, subsequent deletion of antigen-specific $CD8^+$ T cells leads to the induction of tolerance (Liu et al. 2002). In a different study, the cross-presentation of apoptotic cell-derived antigen by $CD8\alpha^+$ DC induced activation of $CD8^+$ T cells which in themselves were found to mediate regulatory functions, although this was not linked to the production of immunosuppressive cytokines such as IL-10 or TGFβ (Ferguson et al. 2002). In the intestine, tolerance induction to cross-presented self-antigen mainly occurs in the MLN, as depletion of PP via administration of lymphotoxin-β receptor antibody does not abolish tolerance to luminal OVA, contrary to simultaneous depletion of MLN and PP (Chung et al. 2005). Similarly, Worbs et al. (2006) showed that the induction of oral tolerance was CCR7-dependent and that it was abrogated in mesenteric lymphadenectomised mice. Accordingly, $CD11b^-$ $CD103^+$ lymph DC that have been able to acquire epithelial cell-derived antigen drive antigen-specific expansion of MLN $CD8^+$ T cells *in vivo* (Cerovic et al. 2014b).

The phagocytosis of apoptotic cells *in vitro* induces production of immunosuppressive cytokines by antigen-presenting cells, including IL-10 and TGFβ (Fadok et al. 1998, Lucas et al. 2003, Chung et al. 2007, Perruche et al. 2008, Torchinsky et al. 2009). Furthermore, ingestion of apoptotic cells by antigen-presenting cells decreases expression of CD86, resulting in a decreased capacity to induce antigen-specific $CD4^+$ T cell activation, despite prior stimulation with LPS (Stuart et al. 2002). Macrophages increase the production of RA after apoptotic cell uptake (Sarang et al. 2014). In line with the importance of TGFβ and possibly RA in Treg cell differentiation (Chen et al. 2003, Coombes et al. 2007), antigen-presenting cells that have taken up apoptotic cells can induce Treg cell responses *in vitro* (Torchinsky et al. 2009). *In vivo*, the systemic infusion of apoptotic cells expanded the Treg cell population in the spleen (Maeda et al. 2005, Kleinclauss et al. 2006). Furthermore, presentation of tissue-derived antigen by $Langerin^+$ dermal DC mediates Treg cell differentiation *in vivo* via the production of active TGFβ (Azukizawa et al. 2011). Therefore, the induction of Treg cell responses is a second important mechanism by which

the phagocytosis of apoptotic cells could facilitate tolerance to self-antigen. However, the exact mechanisms that govern this process in the intestine still remain to be established.

In addition to the induction of tolerance, apoptotic cell uptake can also mediate the activation of pro-inflammatory processes (Green et al. 2009), including the differentiation of effector T cell responses. This occurs primarily due to the stimulation of antigen-presenting cells by TLR ligands that are present in the phagocytosed material (Torchinsky et al. 2009). Indeed, stimulation of TLR signalling in macrophages that have ingested apoptotic cell material changes their cytokine expression profile from TGFβ alone to include pro-inflammatory TNFα and IL-12 (Lucas et al. 2003). Similarly, *in vitro* phagocytosis of apoptotic cells infected with *E. coli* stimulates both IL-6 and TGFβ production by antigen-presenting cells, which in turn leads to the differentiation of Th17 cells (Torchinsky et al. 2009). In addition, antigen-presenting cells that have been loaded with virus-infected apoptotic fibroblasts can induce IFNγ responses by $CD8^+$ T cells *in vitro* (Arrode et al. 2000). The downstream effect of apoptotic cell uptake by DC and macrophages is therefore highly dependent on the immunogenic state of the dying cell, thus tailoring the adaptive response to distinguish between self-antigens and infection.

1.6 The phosphatidylserine receptor TIM4

1.6.1 TIM4 structure

Sharing a similar structure with the other TIM molecules, TIM4 is made up of an immunoglobulin (Ig) V-like domain, a mucin-like domain containing N-linked and O-linked glycosylation sites, and a transmembrane domain with a cytoplasmic tail (Freeman et al. 2010) (Figure 1. 8). PS binding is mediated by the PS-binding pocket located in the IgV domain (Santiago et al. 2007). Within this binding pocket, TIM4 has a metal ion coordination site, which facilitates Ca^{2+}-dependent ligand binding (Santiago et al. 2007). Furthermore, the presence of four further PS-binding residues, which engage in weaker interactions with the ligand, could allow TIM4 to differentiate between differential levels of PS exposure based on ligand density in the binding pocket (Tietjen et al. 2014). The IgV domain also contains an RGD motif (Kuchroo et al. 2003) that is removed from the PS binding pocket but predicted to be accessible to potential binding by integrins (Flannagan et al. 2014). The large number of O-linked glycosylation sites found on the extracellular mucin-like domain mediates the potential for extensive glycosylation of TIM4. Moreover,

the presence of an additional N-glycosylation site facilitates even further possible diversification of the glycosylation pattern exhibited by TIM4. This could mediate specific cell-cell interactions which rely on the recognition of glycolipids, a process that is vital during leukocyte trafficking (Wright and Cooper 2014). Contrary to other members of the TIM family, TIM4 does not contain a tyrosine kinase phosphorylation site in its cytoplasmic tail (Freeman et al. 2010), and was found not to mediate intracellular signalling (Park et al. 2009). However, subsequent work has shown that this domain is important for initiating phagocytosis of apoptotic cells, as removal abrogates this function (Wong et al. 2010).

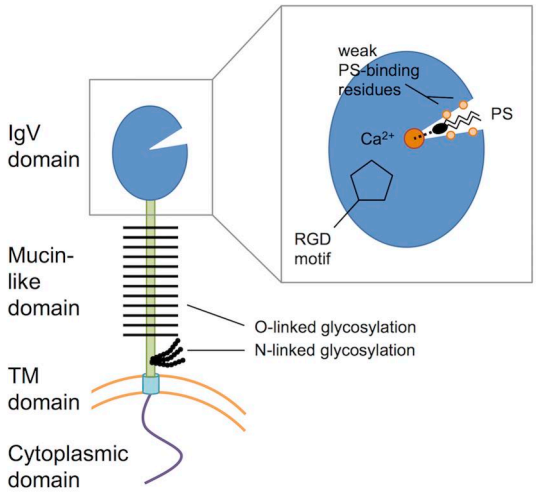

Figure 1. 8: TIM4 domain structure

Simplified schematic showing the domain structure of the murine TIM4 molecule. Its immunoglobulin V (IgV) domain contains a PS (phosphatidylserine)-binding pocket with a Ca^{2+}-dependent coordination site and four residues that mediate additional, but weaker, PS binding. The IgV domain also contains an RGD motif located at a position removed from the PS-binding pocket. A mucin-like domain containing numerous O-linked glycosylation sites and one N-linked glycosylation site connects the IgV domain with the cell membrane, where it is anchored by a transmembrane (TM) domain. Within the cell, TIM4 extends a cytoplasmic tail that lacks a tyrosine kinase phosphorylation site.

1.6.2 TIM4 expression pattern in tissues and on cells

The first study to characterise murine TIM4, originally given the name SMUCKLER (spleen, mucin-containing, knockout of lymphotoxin) showed that TIM4 was highly expressed in lymphoid tissue such as the spleen, LN and PP in mice (Shakhov et al. 2004). The enrichment of TIM4 in peripheral lymphoid tissue has since then been confirmed by additional studies in mice (Meyers et al. 2005, Miyanishi et al. 2007) and humans (Kobayashi et al. 2007, Uhlen et al. 2015). $TIM4^+$ cells were mainly found in the subcapsular sinus area in the LN and the subepithelial dome in the PP, with some penetrating into T cell areas (Shakhov et al. 2004). Subsequently, this has also been shown

in the mediastinal LN (Albacker et al. 2013). Mice deficient in lymphotoxin signalling exhibit defective lymphoid organ development, and have a dramatic decreased expression of TIM4 in both spleen and MLN (Shakhov et al. 2004). These findings first highlighted a possible role for TIM4 in the induction of immune responses in lymphoid tissue.

Whilst TIM1 and TIM3 were first described as mainly expressed by T cells (McIntire et al. 2001, Khademi et al. 2004, Meyers et al. 2005), TIM4 was shown to be restricted to antigen-presenting cells (Meyers et al. 2005). Since then it has become clear that TIM4 is found on macrophages and DC in a range of different tissues. For example, resident peritoneal macrophages express high levels of TIM4 (Kobayashi et al. 2007, Miyanishi et al. 2007, Nishi et al. 2014, Thornley et al. 2014), as do $CD169^+$ subcapsular macrophages in skin-draining LN (Thornley et al. 2014) and medullary macrophages in mediastinal LN (Albacker et al. 2013). Furthermore, TIM4 is expressed by resident DC in the mediastinal LN, as well as both $CD11b^+$ $CD103^-$ and $CD11b^-$ $CD103^+$ subsets of migratory DC (Albacker et al. 2013). Recently, TIM4 was shown to be present on a small population of $CD103^+$ $CD207^+$ dermal DC (Zhang et al. 2016) and Yang et al. (2007) demonstrated that $TIM4^+$ $CD11c^+$ cells could be detected in the small intestinal LP.

It is still unclear what factors mediate transcriptional control of TIM4 expression. However, several studies indicate that TLR signalling could be involved in its regulation. For example, bone marrow-derived mast cells can upregulate expression upon stimulation with flagellin (Li et al. 2014). Furthermore, human PBMC-derived macrophages and murine BMDC increase TIM4 upon culture with LPS (Rodriguez-Manzanet et al. 2008, Xu et al. 2013), and $CD11c^+$ PBMC upregulate TIM4 when stimulated with Staphylococcal enterotoxin B (Liu et al. 2007). TIM4 is also increased on splenic $CD11c^+$ cells upon LPS and CD40L stimulation (Mizui et al. 2008). In liver tissue TIM4 expression is elevated during ischemia-reperfusion injury, possibly due to a concomitant elevation in PS levels, and there TIM4 was shown to be expressed by infiltrating $CD11b^+$ $F4/80^{lo}$ cells (Ji et al. 2014). This indicates that both TLR ligands in the form of PAMPs or DAMPs, as well as possibly the increased density of exposed PS itself, can modulate TIM4 expression. Intriguingly, there is also some evidence for the ability of RA to elevate TIM4 expression on bone marrow-derived macrophages (Sarang et al. 2014).

1.6.3 TIM4 function *in vitro* and *in vivo*

Phosphatidylserine binding and uptake of apoptotic cells

The first definitive description of a functional role for TIM4 was made by Miyanishi et al. (2007), who showed that TIM4 acted as a *bona fide* PSR and mediated the uptake of apoptotic cells. This was confirmed around the same time by another group that further demonstrated the same for TIM1 (Kobayashi et al. 2007). At resting state, TIM4 distribution in the cell membrane of peritoneal macrophages is diffuse, but upon culturing with apoptotic thymocytes, punctate clusters becomes visible at the intersection between macrophages and apoptotic cells (Wong et al. 2010). While the molecular mechanisms that govern TIM4-mediated phagocytosis upon PS binding have yet to be fully elucidated, there is evidence to suggest that it acts in concert with other PSR and integrins. It was thought initially that TIM4 simply acts as a tethering receptor and requires the additional action of integrins or other PSR to facilitate phagocytosis. These conclusions were based on the observation that TIM4 on its own bound PS-bearing apoptotic cells without engulfing them (Toda et al. 2012, Nishi et al. 2014). Instead, phagocytosis was induced upon additional expression of MerTK (Nishi et al. 2014) or αvβ3 integrin (Toda et al. 2012). Subsequent work showed, however, that TIM4 actively participates in phagocytosis, and confirmed that it does indeed associate with integrins, specifically the β1 subunit, during this process (Flannagan et al. 2014). Furthermore, integrin binding was required for the uptake of apoptotic cells by TIM4, and this was accompanied by the activation of integrin signalling components (Flannagan et al. 2014). Interestingly, blocking TIM4 abrogated tyrosine kinase phosphorylation of MerTK during phagocytosis of apoptotic cells, further indicating that TIM4 can act synergistically with other PSR (Toda et al. 2012).

Phagocytosis of apoptotic cells is followed by formation of a double-membraned vesicle termed the phagosome (Kinchen and Ravichandran 2008). A series of acidification steps then lead to the degradation of phagosomal cargo, components of which can subsequently be loaded onto MHC molecules for antigen presentation (Kinchen and Ravichandran 2008). Autophagy and phagocytosis share some signalling components, and indeed, phagocytosis of TLR ligand-bearing particles induces engagement of autophagy pathways, including the recruitment of autophagosome marker LC3 (Sanjuan et al. 2007). This has also been shown to be an important pathway governing the clearance of apoptotic cells (Martinez et al. 2011). This could be initiated by the presence of DAMPs on dying cells, as well as possible TLR stimulation by PAMPs if apoptosis was induced due to infection.

Intriguingly, LC3-associated phagocytosis by macrophages was dependent on TIM4 (Martinez et al. 2009), highlighting this as an intracellular pathway initiated by TIM4-mediated apoptotic cell uptake.

TIM4 has been implicated in the clearance of dying cells by resident peritoneal macrophages *in vivo* (Rodriguez-Manzanet et al. 2010, Wong et al. 2010), and *Timd4*$^{-/-}$ mice exhibit higher cellularity in the peritoneal cavity, although the frequency of leukocytes among these was not assessed (Wong et al. 2010). However, *Timd4*$^{-/-}$ peritoneal macrophages produced higher levels of TNFα than their WT counterparts at resting state, but were unable to respond by increasing this after stimulation with LPS, indicating that deletion of TIM4 fundamentally changes their ability to adequately respond to environmental stimuli (Wong et al. 2010). Moreover, overexpression of TIM4 on macrophages *in vivo* increased the rate of survival during LPS-induced endotoxic shock by negatively regulating NF-κB signalling and the resulting production of pro-inflammatory cytokines by peritoneal macrophages (Xu et al. 2016). Liver macrophages from *Timd4*$^{-/-}$ mice do not upregulate the expression of chemokines to the same level as WT macrophages during hepatic ischemia-reperfusion injury, providing evidence for the TIM4-mediated clearance of apoptotic cells during sterile inflammation having the potential to stimulate leukocyte recruitment to the site of injury (Ji et al. 2014). As well as being externalised on dying cells, PS can be found on the surface of vesicles released by cells infected with *L. monocytogenes* (Czuczman et al. 2014). Uptake of these by macrophages mediated by TIM4 has been shown to facilitate *L. monocytogenes* spread (Czuczman et al. 2014). Thus, TIM4 may play an important role in determining the course of bacterial infections *in vivo* with bacteria using either apoptotic cells or cellular debris as Trojan horses to mediate spread to phagocytes, and possibly subsequent systemic dissemination via migratory DC.

Several studies have highlighted that TIM4 may mediate immune tolerance by controlling the pool of antigen-specific T cells (Albacker et al. 2010, 2013). The number of activated T cells increases dramatically at the induction of an adaptive immune response, but then undergoes a phase of contraction, mediated by apoptosis (Kaech and Wherry 2007). Blocking TIM4 *in vivo* during viral infection increased the percentage of antigen-specific CD8^{+} T cells in the spleen. Conversely, mice that overexpressed TIM4 in MHCII^{+} cells exhibited a decreased level of secondary antigen-specific T cell activation after subcutaneous immunisation (Albacker et al. 2010). This was not, however, due to the

enhanced activation of Treg cells in these mice (Albacker et al. 2010). The recognition and engulfment of Jurkat cells by macrophages is controlled by the level of PS exposed, with macrophages being able to mediate phagocytosis even at lower levels of PS than normally present on apoptotic cells (Borisenko et al. 2003). Low-level PS is transiently exposed on activated T cells (Fischer et al. 2006) and it is therefore possible that TIM4-overexpressing cells are able to recognise and engulf T cells that have just undergone activation, decreasing the resulting memory pool (Albacker et al. 2010). In a similar set of experiments, mice immunised intranasally with antigen exhibited reduced tolerance and an elevated number of antigen-specific T cells in mediastinal LN when TIM4 was blocked *in vivo* (Albacker et al. 2013). In these mice antigen-specific T cells could be detected in close proximity to, or within $TIM4^+$ cells in the LN medulla, and depletion of $F4/80^+$ macrophages reduced the induction of tolerance (Albacker et al. 2013). Based on these findings, the intriguing possibility presents itself that TIM4-mediated clearance of antigen-specific T cells is an important mechanism driving tolerance.

TIM4 as a co-stimulatory or inhibitory molecule during T cell priming

There have been several conflicting reports of TIM4 directly binding T cells and mediating either co-stimulatory or inhibitory effects on proliferation. As well as binding PS, TIM4 can interact with TIM1 *in vitro* (Meyers et al. 2005, Wilker et al. 2007). This binding required both the IgV domain and the glycosylated mucin-like domain (Wilker et al. 2007). TIM4-Ig fusion protein was able to increase T cell proliferation and differentiation *in vitro* (Rodriguez-Manzanet et al. 2008), and induced T cell hyperproliferation during immunisation *in vivo*, which was attributed to its ability to engage TIM1 on the surface of activated T cells (Meyers et al. 2005). Furthermore, treatment of T cells with TIM4-Ig induced TIM1 phosphorylation *in vitro* (Rodriguez-Manzanet et al. 2008), which had previously been noted after TIM1 crosslinking on T cells (Binne et al. 2007). Interestingly, contrary to the indication that TIM4 may be important in decreasing the activated T cell pool by clearance of activated or apoptotic T cells (Albacker et al. 2010, 2013), TIM4-Ig treatment upregulates anti-apoptotic machinery in T cells and decreases cell death (Rodriguez-Manzanet et al. 2008). On the other hand, TIM4-Ig has also been shown to inhibit naïve $CD4^+$ T cell activation, but this was not mediated by TIM1 (Mizui et al. 2008, Cao et al. 2011). However, when T cells were first stimulated and treated with TIM4-Ig 12 h later, the inhibitory response was abrogated (Mizui et al. 2008). It is likely, therefore, that TIM4-mediated interactions with T cells will be context and ligand-dependent, thus

allowing the differential control at various phases of the T cell response. *Timd4*$^{-/-}$ animals exhibit normal lymphocyte subset frequencies in the thymus, spleen and peripheral LN (Rodriguez-Manzanet et al. 2010), indicating that loss of TIM4 signalling does not induce T cell hyperproliferation at the steady state. However, in *Timd4*$^{-/-}$ animals immunised with peptide plus adjuvant, splenic and LN T and B cells exhibited increased production of effector cytokines or antibodies, respectively (Rodriguez-Manzanet et al. 2010), indicating that TIM4 interaction with T cells may be more important during the initiation of antigen-specific responses.

Blocking TIM4 in several different systems has been shown to have an effect on the downstream differentiation fate of CD4^{+} T cells. Co-culture of BMDC with naïve T cells in the presence of both αCD3 and αTIM4 antibodies without the addition of conditioning factors increases TGFβ concentration in culture supernatants (Yeung et al. 2013). Furthermore, blocking TIM4 increased the percentage of FoxP3^{+} Treg cells generated in the presence of TGFβ (Yeung et al. 2013). A similar increase in Treg cell frequencies upon systemic αTIM4 administration was seen *in vivo* during a model of skin allograft transplantation (Yeung et al. 2013). These findings suggest that TIM4 may negatively regulate the differentiation of Treg cells in the periphery.

It has also been reported that TIM4 may act to skew T cell responses towards a Th2 phenotype. Conditioning of small intestinal LP CD11c^{+} cells with Staphylococcal enterotoxin B stimulates Th2 differentiation in an antigen-specific manner (Yang et al. 2007). However, this was abrogated by treatment with either αTIM4 or αTIM1 antibody (Yang et al. 2007). This study showed a similar effect in a food allergy model, where mice were sensitised intraperitoneally with OVA and Staphylococcal enterotoxin B before oral re-challenge seven and 14 days later. Mice that had received αTIM4 at the point of sensitisation exhibited reduced serum and tissue levels of IL-4 (Yang et al. 2007). This was also the case for TIM1 blockade, indicating that these effects could be mediated by TIM4-TIM1 interactions (Yang et al. 2007).

Whilst the above discussed findings suggest that TIM4 on antigen-presenting cells inhibits regulatory T cell responses (Yeung et al. 2013) and can instead induce Th2 differentiation upon prior conditioning with Staphylococcal enterotoxin B (Yang et al. 2007), further evidence points to its ability to inhibit Th17 differentiation (Cao et al. 2011). This was shown *in vitro* after culture of naïve T cells under Th17 polarising conditions (Cao et al.

2011). However, this was not accompanied by a decrease in STAT3 phosphorylation, a central transcription factor governing Th17 fate (Cao et al. 2011). Given the range of systems employed across these studies, as well as the difficulty in accounting for differences in cell culture conditions, drawing an overall conclusion about the role of TIM4 in T cell differentiation is challenging. Interestingly, opposing effects on the activation and skewing of effector T cell responses have been documented during the use of two different αTIM1 blocking antibodies (Xiao et al. 2007). Whilst one antibody caused strong activation and induction of Th1 and Th17 responses, the other did not and instead induced a robust Th2 response (Xiao et al. 2007). Upon further investigation, this was shown to be due to a higher avidity for TIM1 exhibited by the activating antibody (Xiao et al. 2007). Thus, the use of different antibody clones and concentrations may have a marked effect on the outcome of studies employing TIM4 blockade. Further work *in vivo* employing clearly defined models will be required to shed more light on the molecular and cellular mechanisms involved in TIM4-mediated effects on T cells.

1.7 Main aims and hypotheses

The induction of immune responses to the microbiota and bacterial pathogens is tightly regulated in the intestine. DC are important players in facilitating this control due to their ability to integrate signals from the tissue environment and sampled antigen in order to instruct the mounting of adequate T cell responses. A great amount of progress has been made over the past two decades in furthering our understanding of the molecular and cellular mechanisms that govern these processes. However, unanswered questions remain, especially with regard to the functional specialisation of DC populations in the intestine and its determining factors. We therefore sought to begin addressing these questions with a particular focus on the mechanisms that drive intestinal inflammation.

Given the important contribution of the microbiota to the pathogenesis of IBD, we first sought to establish the role of AIEC in driving intestinal inflammation *in vivo*. Previous work had indicated that the ileal clinical AIEC isolate NRG857c was able to cause chronic colitis in mice (Small et al. 2013). We therefore hypothesised that infection with NRG857c would lead to intestinal pathology characterised by the elevated infiltration of myeloid and T cells into the LP and an increased frequency of activated T cells in the MLN.

Both the chronic intestinal inflammation that characterises IBD and infection with enteric bacterial pathogens such as *C. rodentium* are associated with increased levels of apoptosis.

Furthermore, the uptake of apoptotic cells is important for priming of protective T cell responses both in the healthy intestines and during inflammation. Our second main aim was to characterise the expression of ACR on DC populations across different tissues, with a special focus on TIM4. Among DC populations, the cDC1 lineage has been implicated in the acquisition and cross-presentation of apoptotic cell-derived antigen. We therefore hypothesised that expression of ACR such as TIM4 would be enriched on cDC1. Furthermore, we set out to test the hypothesis that TIM4 expression on DC populations was tissue-specific, and could therefore be differentially regulated by environmental factors. In order to begin to shed light on how the uptake of apoptotic cells might affect DC function, we also aimed to determine if $TIM4^+$ and $TIM4^-$ DC exhibited altered functional profiles.

Whilst there have been a number of *in vitro* studies investigating what factors induce expression of TIM4 on various cell populations, not much is known about how these findings translate into the *in vivo* setting. As part of our third aim, we hypothesised that TIM4 expression is regulated either by cytokine signalling, or by microbial stimulation mediated by the microbiota or bacterial infection. TIM4 has been linked to the induction of Th2 responses (Yang et al. 2007), and we therefore first characterised TIM4 expression in IL-4-deficient mice. Given the importance of TGFβR signalling on DC in maintaining intestinal homeostasis (Ramalingam et al. 2012), we next hypothesised that TIM4 expression is TGFβR-dependent and tested this in transgenic mice lacking TGFβR specifically on $CD11c^+$ cells. TIM4 is upregulated on cells after TLR stimulation (Xu et al. 2013, Li et al. 2014). We thus hypothesised that an intact microbiota was required to stimulate TIM4 expression in the healthy intestine, and that infection would lead to its upregulation *in vivo*.

Our final aim was to determine the functional role of TIM4 on DC in the healthy and inflamed intestine. We hypothesised that blocking TIM4 would interfere with different DC-specific functions, including migration and antigen presentation, in ways that would be important for the development of protective immune responses against intestinal pathogens. To this end, we tracked DC migration to the MLN in Kaede mice, and analysed the induction of T cell responses both *in vitro*, and *in vivo* during bacterial infection, after blocking TIM4. These investigations will form the basis for future work determining the role of TIM4 on intestinal DC populations both in the LP and the MLN, and what

functional implications this has for the regulation of intestinal T cell responses to apoptotic cell antigen.

Chapter 2: Materials and Methods

2.1 Mice and *in vivo* procedures

2.1.1 Mice

C57BL/6 and CD1 mice were purchased from Harlan or Charles River Laboratories and maintained in individually ventilated cages (IVC) prior to infection. OT-II mice were either bred under specific pathogen-free conditions at the Veterinary Research Facility or Central Research Facility, Glasgow. CD11c-cre *Tfbr1*$^{fl/fl}$ *Rag1*$^{-/-}$, Kaede, *Cx3cr1*$^{+/gfp}$, Ly5.1, OT-I, KN2 and KN2het mice were bred under specific pathogen-free conditions at the Central Research Facility, Glasgow. *Ccr7*$^{gfp/gfp}$ mice were bred and maintained under specific pathogen-free conditions at the Universtätsklinikum, Aachen. Animals fed on AhR ligand deficient chow or infected with *C. rodentium* were a mixture of C57BL/6 and *Rorc*$^{+/gfp}$ mice bred under specific pathogen-free conditions at the Veterinary Research Facility, Glasgow. All protocols were approved by the local ethical committee and conducted under licenses issued by the UK Home Office.

2.1.2 Mouse surgical procedures

Kaede photoconversion

Kaede mice were anaesthetised by continuous inhalation of isoflurane (Abbott Animal Health). After laparotomy, either the caecum or proximal colon was exposed and kept moist with saline, whilst shielding all other abdominal organs from light using black card or aluminium foil. The tissue was photoconverted using two low power violet light sources (395 nm, Amazon) for 6 min (caecum) or 10 min (proximal colon) in total. After replacing the tissue, the muscle layer was closed by suture and the skin held together with surgical clips. Mice were maintained in IVC for 24-48 h until tissue harvest.

Thoracic duct cannulation

Male 6-8 week old mice were anaesthetised by continuous inhalation of isoflurane (Abbot Animal Health). After laparotomy, mesenteric lymphadenectomy was performed by blunt dissection. The muscle layer was sutured, followed by closing the skin with surgical clips, and the animals usually maintained in IVC for at least six weeks before thoracic duct cannulation to allow the mesenteric lymph vessels to reanastomose. Mice then underwent a

second surgical procedure after receiving 200 µl olive oil by gavage to visualise the lymphatics, which involved insertion of a polyurethane cannula (2 Fr, Linton Instrumentation) into the thoracic duct. The cannula was held in place by securing it with super glue (Loctite), and the muscle layer sutured. To avoid biting and severing of the cannula, this was fed through a wire tube attached to a harness worn by the mouse. Lymph was collected on ice in 1 ml sterile PBS supplemented with 20 U/ml heparin sodium (Wockhardt) for 16-24 h after surgery.

2.1.3 *In vivo* antibiotic treatment

Mice were given a cocktail of five antibiotics in their drinking water, supplemented with saccharin tablets (10/500 ml) to encourage drinking. The following antibiotics were used: ampicillin (1 mg/ml), neomycin (1 mg/ml), gentamicin (1 mg/ml), metronidazole (1 mg/ml) and vancomycin (0.5 mg/ml). Control animals received water supplemented only with saccharin. Mice were kept on oral antibiotics for seven days, during which both groups were weighed daily and received additional baby food mixed with drinking water to ensure adequate hydration.

2.1.4 *In vivo* blocking of TIM4

Mice were given i.p. injections of 200 µg αTIM4 (RMT4-53, BioXCell) or Rat IgG2a isotype control (2A3, BioXCell). Treatment time points and frequency varied with experiments. For assessing DC migration, Kaede mice were treated 24 h prior to photoconversion of the proximal colon. For infection experiments, mice were treated either 24 h before infection with *S.* Typhimurium, or four and six days after infection with *C. rodentium*.

2.2 Bacterial infections

2.2.1 Bacterial strains and culture

Overnight cultures of NRG857c were grown in Luria broth (LB) at 37°C, 180 rpm. After 1:1000 dilution in LB the next day and growth until an OD_{600} of 0.8 was reached, cells were centrifuged at 5000 ×g, 4°C, for 10 min and resuspended in sterile PBS.

Bioluminescent wildtype *C. rodentium* strain ICC16842 (Petty et al. 2010) was kindly provided by Dr Andrew Roe and Dr James Connolly at the University of Glasgow. It was

generated by inserting the plasmid p16S::lux encoding the lux operon of *Photorhabdus luminescens* and an erythromycin resistance gene. The plasmid is permissive at 30°C and stable integration into the bacterial chromosome at the 16S locus by site-specific recombination was achieved upon temperature shift to 42°C, according to the method described by Riedel et al. (2007) . For *in vivo* infections, *C. rodentium* was grown overnight in LB at 37°C, 180 rpm. The following day, the culture was diluted 1:100 in fresh LB and grown until an OD_{600} of 0.75 had been reached. Cells were then centrifuged at 5000 × g, 4°C, for 10 min and resuspended in sterile PBS.

The wildtype *S.* Typhimurium strain SL1344 was used for *in vivo* infections.
S. Typhimurium was incubated in LB overnight at 37°C, 180 rpm. The following day, cultures were diluted 1:10 in LB and grown incubated without agitation at 37°C to simulate an anaerobic environment until an OD_{600} of 0.70 was reached. Cells were centrifuged at 5000 × g, 4°C, for 10 min and resuspended in sterile PBS.

2.2.2 Mouse infections

Bacterial infections were carried out in male and female 6-14 week old mice. Animals within each experimental group were co-housed where possible. For NRG857c and *S.* Typhimurium infections, mice were treated orally by gavage with 20 mg streptomycin sulphate (Sigma) in sterile H_2O 24 h before infection. Mice were infected with between 6×10^8 and 7×10^9 colony forming units (CFU) NRG857c or 6×10^8 CFU *S.* Typhimurium by gavage. Control animals received streptomycin followed by sterile PBS 24 h later. Serial dilutions of the inoculum were plated on LB agar to determine the actual infective dose for each experiment. Mouse weights were monitored on a regular basis. At appropriate time points, mice were killed and tissues harvested. For DSS experiments, mice were given 0.5% DSS in their drinking water for two days prior to and two days post-infection with NRG857c. For experiments with AhR ligand deficient diet, mice were fed on AIN-76A chow (Special Diet Services) for a week prior to NRG857c infection and for the entirety of the experimental period thereafter.

For *C. rodentium* infections, mice received between 1-3 × 10^9 CFU *C. rodentium*, or sterile PBS by gavage. Serial dilutions of the inoculum were plated on LB agar containing 500 μg/ml erythromycin (Sigma) to determine infective dose for each experiment. At appropriate time points, mice were killed and tissues harvested for analysis.

2.2.3 Bacterial quantification from faeces and tissues

Faeces were collected throughout the period of infection and / or at the time of tissue harvest. After weighing, samples were homogenised in an appropriate volume of PBS to achieve a 10% w/v dilution and samples centrifuged at 9,000 revolutions per minute (rpm) for 10 s to sediment debris. Serial dilutions of the supernatants were plated out on chloramphenicol (34 μg/ml, Sigma) and ampicillin (100 μg/ml, Sigma) containing LB agar to select for NRG857c, or LB agar supplemented with 500 μg/ml erythromycin to select for *C. rodentium*, and incubated overnight at 37°C before quantification of CFU.

Tissues were harvested in 2 ml sterile PBS, weighed, and kept on ice until further processing. Intestinal tissues were placed in 5 ml 5 mM DTT (Sigma) to remove the mucus layer and incubated at room temperature for 15 min, 5 min of which were under rotation at 300 rpm. Tissues were then placed in 2 ml of fresh PBS and the mucus fraction combined with the initial collection fraction. Serial dilutions were performed of this pooled suspension for all infected samples and dilutions plated out on chloramphenicol (34 μg/ml) and ampicillin (100 μg/ml) containing LB agar. Tissues were homogenised using a tissue homogeniser (Benchmark, D1000) and serial dilutions of homogenates plated out on LB agar as above. Tissues homogenates from control animals were plated out without prior dilution. After incubation of plates at 37°C overnight, the number of CFU per gram of tissue were determined.

2.2.4 Bioluminescent imaging and analysis

Colons and caeca from mice infected with bioluminescent *C. rodentium* were harvested and luminescence measured using an IVIS Spectrum In Vivo Imaging System (Caliper Life Sciences). Images were analysed using Living Image software (Caliper Life Sciences). Firstly, the scale of luminescence measured in average radiance (photons/s/cm^2/sr) was standardised across images. Subsequently, a region of interest (ROI) was specified for each sample to coincide with the rectum. The total flux (photons/s) was calculated for each ROI and then normalised to remove background luminescence by subtracting the mean PBS total flux from each sample.

2.3 Histology and immunofluorescence staining

For immunofluorescence, tissues were taken under terminal anaesthesia, formed into Swiss rolls in O.C.T. medium (Tissue-Tek®, VWR) and snap-frozen in isopentane on dry ice

before storing at -80°C. Tissues were cut in 8 µm sections and fixed using 1% methanol-free paraformaldehyde (PFA) for 10 min. Sections were blocked for 15 min with 5% bovine serum albumin (BSA, Sigma Aldrich), followed by washing in PBS and a 15 min block each with avidin and biotin blocking solutions (Vector). Tissues were stained for 1.5 h in the dark at room temperature with primary antibodies in 5% BSA. Primary antibodies used were anti-O83 (1:50, rabbit polyclonal anti-serum, Oxford Biosystems / Statens Serum Institut), anti-EpCAM (1:200, G8.8, AF647-conjugated, Biolegend) or isotype control Rat IgG2a, κ (RTK2758, AF647-conjugated, Biolegend). Subsequently sections were washed in PBS and incubated with a goat-anti-rabbit AF488-conjugated secondary antibody in 5% BSA (1:200, Life Technologies) for 30 min at room temperature in the dark. As a control for non-specific secondary antibody binding, additional sections were treated with secondary antibody only without previous incubation with anti-O83 serum (secondary antibody only control, SOC). All sections were washed with PBS and nuclei stained with DAPI before mounting.

Tissue samples for histology were either kept in 10% buffered formalin for at least 24 h prior to dehydrating and paraffin embedding, or embedded in O.C.T. medium and snap-frozen before cryosectioning and fixing in ice-cold acetone/ethanol (75/25%). Paraffin and O.C.T. embedded sections were then stained with haematoxylin and eosin (H&E) for histological assessment.

Fluorescence images were captured using an EVOS FL Auto epifluorescence microscope and H&E section images were taken using an Olympus BX41 System Microscope.

2.4 Cell isolation

2.4.1 Murine intestinal tissues

Faeces and remaining fat from intestines were removed, tissues opened longitudinally and washed in Hanks' Balanced Salt Solution (HBSS, Life Technologies) supplemented with 2% heat-inactivated foetal calf serum (FCS). PP were removed from the small intestine. Tissues were then cut into 0.5 cm segments and kept in HBSS / 2% FCS on ice until incubation in HBSS / 2 mM EDTA at 37°C under agitation for 2 × 20 min (small intestine) or 2 × 15 min (caecum, colon) to remove the mucus and epithelial cell layers. Between incubations intestines were washed in pre-warmed HBSS. Small intestines were digested in complete media (RPMI 1640 media supplemented with 100 U/ml penicillin and 100 µg/ml

streptomycin, 2 mM L-Glutamine, 50 µM 2-mercaptoethanol, and 5-10% FCS) supplemented with Collagenase VIII (1 mg/ml, Sigma) for 20 min at 37°C under agitation. Colons from *Ccr7*$^{gfp/gfp}$ mice were digested using the small intestinal protocol. Otherwise, colons and caeca were digested in complete media and Collagenase V (0.85 mg/ml, Sigma), Collagenase D (1.25 mg/ml, Roche), Dispase (1 mg/ml, Gibco) and DNase (30 µg/ml, Roche) for 20-30 min at 37°C under agitation. After tissue digestion, cells were passed through a 40 µm cell sieve (colon, caecum), or both 100 µm and 40 µm cell sieves (small intestine), washed twice with FACS buffer (PBS supplemented with 2% FCS and 2 mM EDTA), and resuspended in FACS buffer for counting and antibody staining for flow cytometry analysis.

2.4.2 Human colonic tissue

Human colonic resection tissue was collected in sterile PBS. The mucosa was carefully dissected from the underlying muscularis externa and cut into 0.5 cm segments. These were then placed in pre-warmed HBSS / 2 mM EDTA and incubated at 37°C for 3 × 15 min under agitation to wash away mucus and the epithelial cell layer. Between incubations, tissues were washed in pre-warmed HBSS. After the final wash, tissues were digested in complete media (RPMI 1640 media supplemented with 100 U/ml penicillin and 100 µg/ml streptomycin, 2 mM L-Glutamine, 50 µM 2-mercaptoethanol, and 10% FCS) supplemented with Collagenase VIII (1 mg/ml, Sigma), Collagenase D (1.25 mg/ml, Sigma), Dispase (1 mg/ml, Gibco) and DNaseI (0.03 mg/ml, Sigma) for 40 min at 37°C under agitation. Cells were then passed through a 100 µm and 40 µm sieve prior to being washed and resuspended in FACS buffer ready for counting and antibody staining for flow cytometry.

2.4.3 Peyer's patches

PP were carefully dissected out from the surrounding tissue and collected in HBSS / 2% FCS on ice. They were then transferred into 1 ml complete media supplemented with Collagenase VIII (1 mg/ml, Sigma) and digested at 37°C under agitation for 15 min. Subsequently, PP were passed through a 40 µm sieve and washed and resuspended in FACS buffer for counting and antibody staining for flow cytometry.

2.4.4 Lymph nodes

Lymph nodes were collected on ice in 1 ml serum-free RPMI 1640 media supplemented with 100 U/ml penicillin and 100 µg/ml streptomycin, 2 mM L-Glutamine, 50 µM 2-mercaptoethanol. This was followed by incubation for 40 min at 37°C under agitation in serum-free RPMI media as above, supplemented with Liberase (0.4 U/ml, Roche) and DNase (50 µg/ml, Roche). After enzymatic digestion, tissues were passed through a 40 µm cell sieve, washed with FACS buffer and centrifuged at 400 ×g, 4°C, for 5 min. Cells were resuspended in FACS buffer and counted before antibody staining for flow cytometry analysis.

2.4.5 Spleens

Spleens were passed through a 40 µm cell sieve and washed with FACS buffer. Cells were resuspended in 5 ml red blood cell (RBC) lysis buffer (Sigma Aldrich) and incubated for 5 min on ice. Then cells were washed with FACS buffer, resuspended and counted before antibody staining for flow cytometry analysis.

2.4.6 Lungs

Lungs were dissected without prior perfusion and cut finely into segments smaller than 0.5 cm. The tissue was transferred into bijoux containing 3 ml complete media supplemented with Collagenase V (0.425 mg/ml, Sigma Aldrich), Collagenase D (0.625 mg/ml, Roche) and Dispase (1 mg/ml, Gibco). Tissues were incubated for 40 min at 37°C under agitation, and shaken vigorously by hand every 5 min. The cell suspension was then passed first through a 100 µm sieve, then a 40 µm sieve and washed with FACS buffer. The pellets were resuspended in 4 ml RBC lysis buffer (Sigma Aldrich) and incubated on ice for 5 min before washing in FACS buffer. After resuspending for counting, cells were stained with antibodies for flow cytometry analysis.

2.4.7 Bone marrow

Bone marrow isolation was carried out by removing all muscle and fat from the tibia and femur separately, followed by carefully cutting an opening on either end of the bones. Four bones were placed in a 0.5 ml eppendorf tube, after punching a hole in the bottom of the tube using a 21 gauge needle. The 0.5 ml eppendorf tube containing the bones was then placed in a 1.5 ml eppendorf tube and spun at 5000 ×g for 30 s, allowing the bone marrow

to collect in the 1.5 ml eppendorf tube. Cells were resuspended in 5 ml RBC lysis buffer (Sigma Aldrich) and incubated for 5 min before washing in FACS buffer and resuspending for counting and staining with antibodies for flow cytometry analysis.

2.5 Flow cytometry and FACS

2.5.1 Cell stimulation for intracellular cytokine staining

Between 2-5 × 10^6 cells were incubated in 500 µl complete media supplemented with 1:500 of a cell stimulation cocktail including protein transport inhibitors (eBioscience) at 37°C for 4 h. Cells were then washed and resuspended in FACS buffer, ready for surface marker staining with antibodies for flow cytometry.

2.5.2 FACS antibody staining and sample acquisition

All anti-mouse antibodies were used at a concentration of 1:200 in FACS buffer. The following fluorochrome-conjugated antibodies were used: CCR6 (29-2L17), CCR9 (CW-1.2), CD3 (MEL-14, 17A2), CD4 (GK1.5), CD8α (53-6.7), CD11b (M1/70), CD11c (N418), CD19 (6D5), CD25 (PC61), CD44 (IM7), CD45 (30-F11), CD64 (X54-5/7.1), CD135 (A2F10), CD205 (NLDC-145), IL-17A (TC11-18H10.1), Ly6G (1A8), MHCII (M5/114.15.2), NK1.1 (PK136), TIM1 (RMT1-4) and TIM4 (RMT4-54) from Biolegend, CD8α (53-6.7), FOXP3 (FJK-16s), Ly6C (HK1.4), MHCII (M5/114.15.2) and TIM4 (RMT4-54) from eBioscience, and SiglecF (E50-2440) and IFNγ (XMG1.2) from BD Biosciences. The following fluorochrome-conjugated anti-human antibodies were used at a concentration of 1:40 in FACS buffer: CD3 (UCHT1), CD11c (Bu15), CD14 (HCD14), CD16 (3G8), CD19 (HIB19), CD56 (5.1H11), CD64 (10.1), CD123 (6H6), HLA-DR (L243), SIRPα (SE5A5) and TIM4 (9F4) from Biolegend, CD103 (B-Ly5) from eBioscience, and CD45 (HI30) from BD Biosciences. Viability staining was performed using 7AAD viability dye (1:10, Biolegend) in FACS buffer, or eFluor780 fixable viability dye (1:10, eBioscience) in PBS. Blocking of F_c receptors was carried out for 5 min at 4°C before surface staining using anti-mouse CD16/32 (1:200, 93) or Human TruStain FcX (1:40) from Biolegend.

Staining of intracellular proteins such as cytokines or transcription factors was carried out using the FOXP3/Transcription Factor staining kit following manufacturer's instructions (eBioscience). Briefly, cells were fixed in 300-500 µl Fix/Perm buffer for 2-3 h or overnight

at 4°C before washing and resuspending in 1× Permeabilisation buffer. Cells were then incubated with antibodies against intracellular proteins in 1× Permeabilisation buffer for 1 h at room temperature. Subsequently, they were washed in 1× Permeabilisation buffer and then FACS buffer ready for analysis.

Samples were acquired in FACS buffer on an LSR II, an LSR Fortessa, a FACSAria IIu or FACSAria III (BD Biosciences) for analysis. For FACS sorting on a FACSAria IIu or III, cells were resuspended in complete medium containing 10% FCS. If cells were to be used for *in vitro* co-culture, they were sorted into complete medium containing 10% FCS. For RNA isolation, cells were sorted into 500 µl RLT buffer from the RNeasy Micro kit (Qiagen) and stored at -80°C prior to use.

2.5.3 Aldefluor assay

RALDH enzyme activity was determined using the Aldefluor assay (Stemcell Technologies), according to manufacturer's specifications. Briefly, 1-2 × 10^6 cells were resuspended in 1 ml Aldefluor assay buffer. For each sample, half the cells were treated with Aldefluor reagent only, and half the cells were treated with Aldefluor reagent and an inhibitor, DEAB (Diethylaminobenzaldehyde). Samples were incubated as such at 37°C for 45 min. Cells were then centrifuged to remove the supernatant and resuspended in Aldefluor assay buffer ready for staining with antibodies for flow cytometry analysis.

2.6 Gene expression analysis

2.6.1 RNA extraction and reverse transcription

For RNA extraction, samples were thawed and processed using the RNeasy Micro kit (Qiagen) according to the supplier's specifications. RNA was eluted in 14 µl of RNAse-free water and kept on ice prior to reverse transcription using the High Capacity RNA-to-cDNA kit (Applied Biosciences) according to supplier's specifications. Samples were kept at 4°C prior to quantitative real-time PCR (qRT-PCR).

2.6.2 Quantitative real-time PCR (qRT-PCR)

The primer sets used for qRT-PCR are listed in Table 1. PCR reactions were carried out in 384-well qPCR plates (Starlab) and with a reaction volume of 10 µl, using SYBR Green PerfeCTa Fastmix ROX (Quanta Biosciences). Primers were used at a final concentration

of 3 µM. Per reaction, 2-3 µl cDNA was added as template. Melt curves and threshold cycle (CT) values for each sample and primer set were determined on a Quantstudio Flex Real-time PCR machine (ThermoFisher).

Table 1: List of qRT-PCR primers used

Gene	Forward primer sequence (5'3')	Reverse primer sequence (5'3')
Ccr7	ATTGCTGCTGAGGGAAGAG	ACTTTTGGCTGTCGTTTTGG
Il1b	CGCTCAGGGTCACAAGAAAC	GAGGCAAGGAGGAAAACACA
Aldh1a2	TGTAATCCAGCCACAGGAGAGCAA	ACGTCCTCTTTCAGACGCATCCAT
Itgb8	GGGTGTGGAAACGTGACAAGCAAT	TCTGTGGTTCTCACACTGGCAACT

2.7 *In vitro* OT-II and OT-I MLN cell co-culture with DC

To establish the ability of various DC populations to drive antigen-specific T cell responses *in vitro*, FACS sorted DC were either kept at 4°C without antigen loading, or pulsed with either 2 mg/ml soluble ovalbumin (OVA) protein (Lorne Laboratories) in complete medium containing 10% FCS for 2 h at 37°C, or 3 µg/ml 323-339 ovalbumin peptide (Invivogen) for 30 min at 37°C. After pulsing, DC were washed twice with 3 ml complete medium containing 10% FCS and resuspended in the appropriate volume for co-culture. OVA-specific OT-II and OT-I cells were isolated from the MLN of OT-II and OT-I mice by mechanical dissociation using a 40 µm cell sieve, and washed with PBS. Prior to co-culture with DC, 200,000 OT-II and OT-I cells per well were labelled with 5 µM CFSE (eBioscience) for 1 min, immediately quenched and washed with 3 ml complete media containing 10% FCS. Depending on the experiment, 4,000-12,500 DC were co-cultured with 200,000 OT-II or OT-I cells per well for 3-6 days in complete medium containing 10% FCS. For *in vitro* TIM4 blocking experiments, 5µg/ml purified αTIM4 antibody (RMT4-54, Biolegend) or Rat IgG2a (RTK2758, Biolegend) were added to co-cultures. Finally, OT-II and OT-I cells were stained with antibodies in FACS buffer for analysis by flow cytometry.

2.8 Statistical analysis

If data were found to be normally distributed using a D'Agostino & Pearson omnibus normality test or a Shapiro-Wilk normality test, a parametric t test was employed for statistical analysis. If this was not the case, nonparametric tests were used for comparison

testing, such as a Mann-Whitney test or Kruskal-Wallis test. A Dunn's post-test was employed to correct for multiple comparisons. Statistical significance was defined as $p < 0.05$.

Chapter 3: Colonisation and host response to adherent and invasive *Escherichia coli*

3.1 Aims and hypotheses

It is not understood if persistent colonisation with pathobionts such as AIEC in WT mice can lead to intestinal inflammation. This is important because bacterial persistence, in particular of *E. coli* species, have been described as causative factors in human IBD. Such an *in vivo* model would therefore be useful in studying the cellular mechanisms that contribute to the pathogenesis of IBD.

To address this, we took advantage of a recently described model system of chronic intestinal inflammation that is induced by infection with a strain of AIEC, NRG857c (Small et al. 2013). This ileal CD patient isolate induced fibrosis and other signs of chronic caecal and colonic pathology, in five different WT mouse strains. This was accompanied by T cell infiltrate and elevated cytokine production in these tissues between three and nine weeks post infection (p. i.) (Small et al. 2013). To test this in our hands, we set out to analyse the cellular host response to long-term infection (3-9 weeks) with NRG857c. We chose this time frame based on the previously reported ability of NRG857c to drive chronic inflammation (Small et al. 2013). Given the different phases of infection characterised by the influx of different immune cells, we assessed the involvement of both innate and adaptive immune cells in the intestine and draining LN.

We aimed to pinpoint which phases of the immune response were active after six and nine weeks of infection. This would then allow us to use this model to elucidate the cellular and molecular mechanisms driving chronic inflammation and relate them to human disease by applying our findings to work with IBD patient samples.

3.2 Results

3.2.1 NRG857c infection causes long-term colonisation of the caecum and colon and can be found associated with the intestinal epithelium

Previous observations suggest that NRG857c causes caecal and colonic pathology in wildtype (WT) mouse strains, including C57BL/6 and CD1 mice (Small et al. 2013). We began focussing our investigations on the C57BL/6 strain due to the wide availability of genetically modified variants on this background that could be of use for future mechanistic studies. Mice were treated with streptomycin 24 h before orally infecting with NRG857c or treating with PBS (Figure 3. 1a). Shedding of bacteria into the faeces was assessed throughout as a measure of colonisation. Colony forming units (CFU) were quantified after culturing faecal extracts on LB agar supplemented with chloramphenicol and ampicillin to select for NRG857c, as it carries resistance to both antibiotics, unlike other intestinal bacteria. Shedding was variable between mice, but could be detected up to nine weeks p. i. (Figure 3. 1b). To determine which part of the intestine is preferentially colonised by NRG857c, tissues were homogenised seven days p. i. and homogenates serially diluted and plated on selective LB agar. The same was performed for the mucus fraction of the intestines, isolated by incubating the tissues in 5mM dithiothreitol (DTT) prior to homogenisation as described previously (Martin et al. 2004), to break disulphide bonds between mucin molecules and allow solubilisation of the mucus. NRG857c was found to most heavily colonise the caecum, followed by the colon (Figure 3. 1c). Comparable total numbers of bacteria could be recovered from mucus and tissue fractions (Figure 3. 1d). These findings led us to focus on the caecal and colonic tissues for further characterisation of longer term NRG857c interaction with the host.

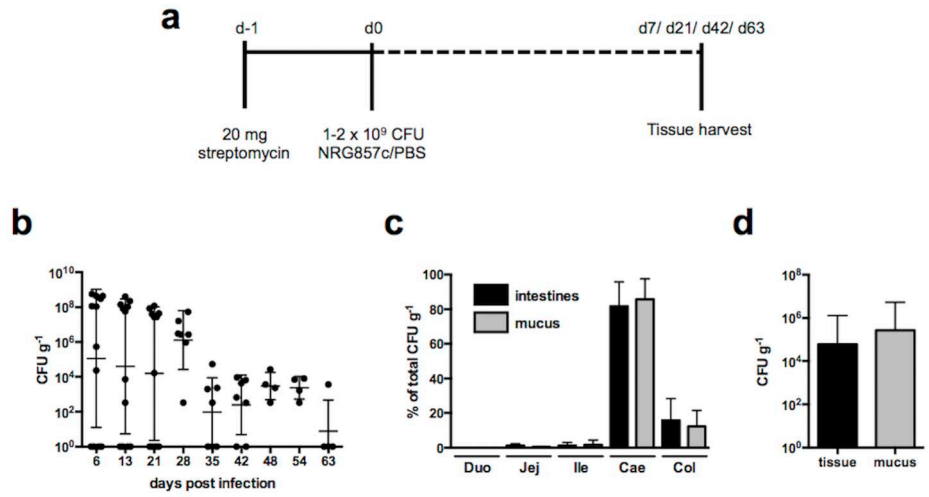

Figure 3. 1: NRG857c infection leads to long-term persistence in the intestines

(a) Mice were infected with 1-2 × 10^9 CFU NRG857c by gavage 24 h after treatment with 20 mg streptomycin orally. **(b)** Faecal shedding of NRG857c was monitored over nine weeks and CFU g^{-1} determined by selective growth on LB agar supplemented with chloramphenicol and ampicillin. **(c, d)** NRG857c burden in tissues and mucus seven days p. i. was determined; soluble mucus fractions were collected after incubating tissues in 5mM DTT; CFU g^{-1} of tissue were determined by growth on selective LB agar. **(c)** CFU g^{-1} per tissue type as percentage of total number of CFU recovered per entire intestine. **(d)** Total additive CFU g^{-1} recovered from tissue and mucus fractions of all intestinal tissue types. Error bars represent S.D. with n = 4-12 **(b)** and n = 4 **(c, d)**. Abbr.: Duo = duodenum, Jej = jejunum, Ile = ileum, Cae = caecum, Col = colon

Previous work demonstrated the ability of NRG857c to adhere to and invade human IEC *in vitro* (Eaves-Pyles et al. 2008). Furthermore, AIEC have been shown to induce granuloma-like aggregates of macrophages *in vitro* (Meconi et al. 2007). To determine if these observations were similarly maintained during long-term infection of mice with NRG857c *in vivo*, we stained colon sections from mice six and nine weeks p. i. for immunofluorescence analysis. NRG587c localisation in caecal crypts four weeks p. i. has been previously successfully described using identification of O83, the LPS O antigen produced by NRG857c (Small et al. 2013). When colonic sections were co-stained for O83 and EpCAM to identify epithelial cells, $O83^+$ rod-shaped bacteria could be found in aggregates in the lumen, and associated with the epithelial cell layer at six but not nine weeks p. i. (Figure 3. 2). No $O83^+$ bacteria were found within the LP, suggesting that NRG857c colonises at the mucosal surface without breaching the epithelial barrier.

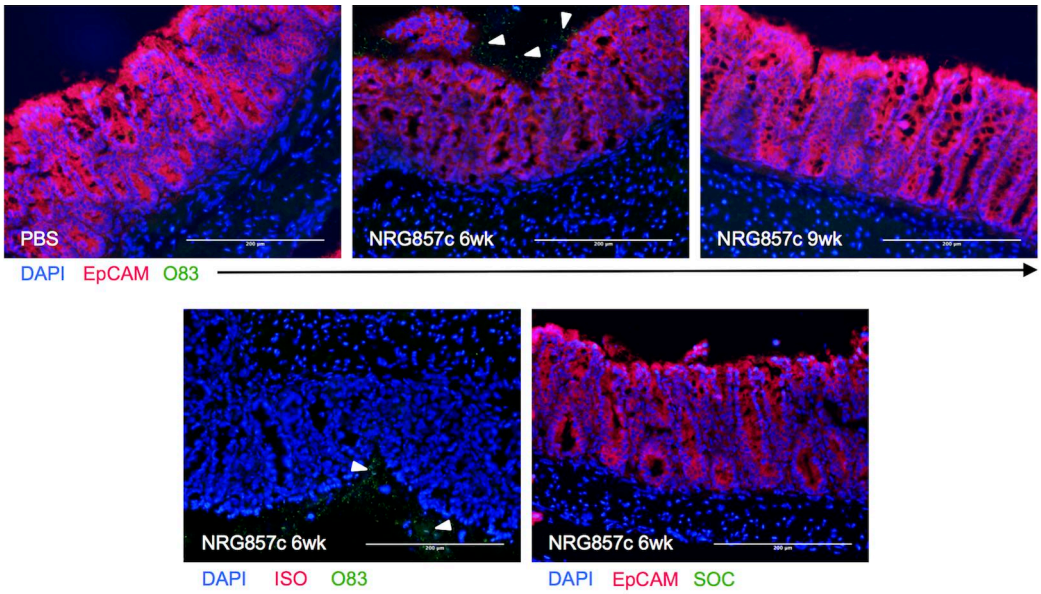

Figure 3. 2: NRG857c is found in the lumen and associated with the epithelium of the colon at 6 weeks p. i.

C57BL/6 mice were given 20 mg streptomycin by gavage followed 24 h later by oral infection with 1-3 × 10^9 NRG857c or PBS. Immunofluorescence staining of colonic tissue six weeks (6wk) and nine weeks (9wk) p. i. with NRG857c and from uninfected animals (PBS). Frozen colonic tissue sections were stained with AF647-conjugated anti-EpCAM antibody (epithelial cells, red) or isotype control (ISO) and polyclonal rabbit anti-O83 serum followed by an AF488-conjugated goat-anti-rabbit secondary antibody (bacteria, green). An additional control included a section incubated with no anti-O83 serum and subsequent staining with AF488-conjugated secondary antibody (secondary antibody only control, SOC). All sections were stained with DAPI (nuclei, blue). White arrows denote green $O83^+$ bacteria. Scale bars represent 200 μm.

3.2.2 NRG857c infection causes no overt intestinal pathology

Having demonstrated that NRG857c can colonise the colon and caecum long-term, we next aimed to determine if it drives pathology at the site of colonisation. Diarrhoea and weight loss are common symptoms of colonic inflammation in mice. However, we observed neither diarrhoea, nor changes in weight, over nine weeks p. i. (Figure 3. 3a). A further indication of pathology is colon shortening, but this also did not occur in infected mice compared to uninfected controls three or six weeks p. i. (Figure 3. 3b). *Salmonella* Typhimurium causes a severe acute infection in mice and caecal shrinking. However, we did not observe any changes in caecal appearance after infection with NRG857c (data not shown).

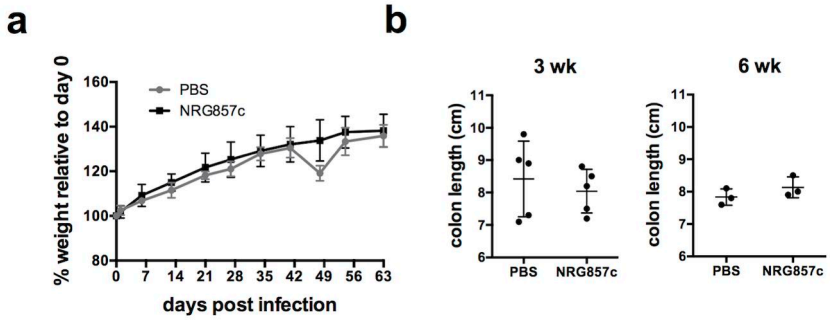

Figure 3. 3: NRG857c infection does not cause weight loss or colon shortening

C57BL/6 mice were treated with 20 mg streptomycin by gavage 24 h before oral infection with 1-2 × 10^9 CFU NRG857c or PBS. **(a)** Percentage weight changes over nine weeks relative to pre-infection weight at day 0; **(b)** colon lengths at three (3wk) and six (6wk) weeks p. i. compared with PBS-treated controls; Error bars represent S.D.; n = 4-12 **(a)** and n = 3-5 **(b)**.

Histological indications of intestinal inflammation include crypt elongation, goblet cell hyperplasia, a damaged epithelial cell layer, mucosal thickening, and cellular infiltrate into the LP. However, we were unable to detect any of these consistently in ileal, caecal or colonic tissue sections from infected mice compared with uninfected controls at various time points during the course of infection with NRG857c (Figure 3. 4).

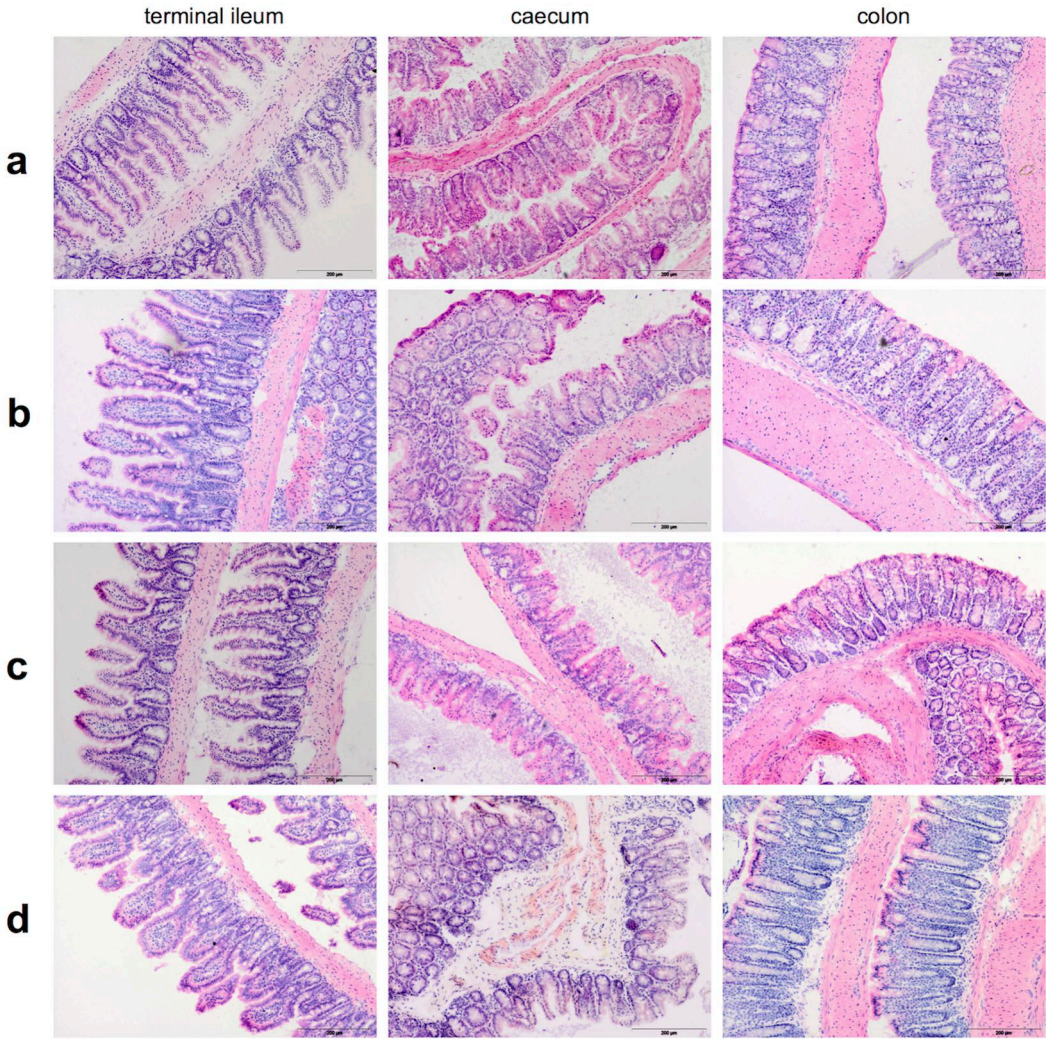

Figure 3. 4: NRG857c infection causes no overt intestinal pathology.

C57BL/6 mice were treated with 20 mg streptomycin by gavage 24 h before oral infection with 1-2 × 10^9 CFU NRG857c or PBS. Terminal ileum, caecum and colon were harvested from PBS-treated **(a)** and infected mice at three **(b)**, six **(c)** or nine **(d)** weeks p. i. and paraffin or OCT embedded tissue sections stained with H&E. Images were taken at 10x magnification and scale bars represent 200 µm.

3.2.3 NRG857c infection has no effect on innate cell influx to the intestinal LP

Even though no clear histological evidence of inflammation could be found, changes might be happening on the cellular level that are too subtle to be observed in sections. We therefore sought to define the changes in immune cell populations during infection with NRG857c by flow cytometry. Bacterial infection in the intestine induces a robust early neutrophil influx (Spehlmann et al. 2009). As NRG857c could still be detected associated with the epithelium at six weeks, increased neutrophils in the LP would be a good indication of an active infective process as opposed to non-symptomatic colonisation. Neutrophils were defined as CD45$^+$, CD11b$^+$, Ly6G$^+$ cells. However, we did not observe any changes in neutrophil frequencies or absolute numbers at six or nine weeks p. i. (Figure 3. 5).

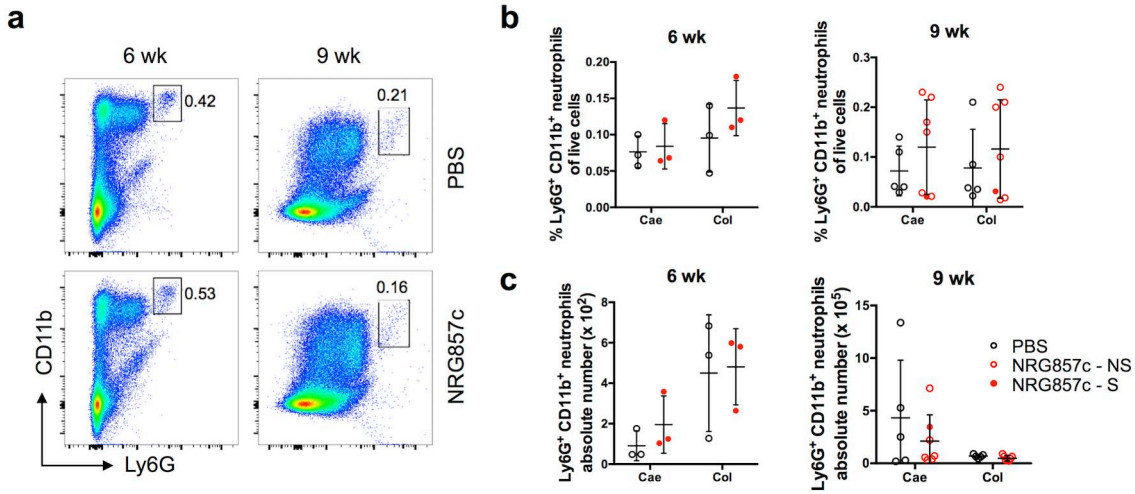

Figure 3. 5: Long-term NRG857c infection has no effect on Ly6G$^+$ neutrophil frequencies and numbers in the caecum and colon

C57BL/6 mice were treated with 20 mg streptomycin by gavage 24 h before oral infection with 1-2 × 10^9 CFU NRG857c or PBS. Tissues from infected (NRG857c) and uninfected (PBS) animals were collected at six (6wk) or nine (9wk) weeks p. i. and cells from colonic and caecal LP were analysed by flow cytometry.
(a) Representative plots of colonic tissue gated on single, live, CD45$^+$, CD11b$^+$, Ly6G$^+$ cells. Data are shown as **(b)** the percentage of Ly6G$^+$ CD11b$^+$ neutrophils among live cells and **(c)** their absolute number. Error bars represent S.D.; 9wk: data representative of two pooled experiments. Abbr.: Cae = caecum, Col = colon, NS = non-shedder, S = shedder

Recent findings have implicated eosinophils as important effectors of chronic colitis through production of TNFα and eosinophil peroxidase (Griseri et al. 2015). We therefore investigated if our model caused an influx of eosinophils into the colonic or caecal LP. Eosinophilia would be an indication of cellular changes that could lead to chronic inflammation. We quantified the percentages of live cells and absolute numbers of SSC^{hi} $CD11b^{+}$ $Ly6G^{-}$ granulocytes in the LP, most of which are likely to be eosinophils. However, we did not see any changes occurring during infection with NRG857c six or nine weeks p. i. (Figure 3. 6).

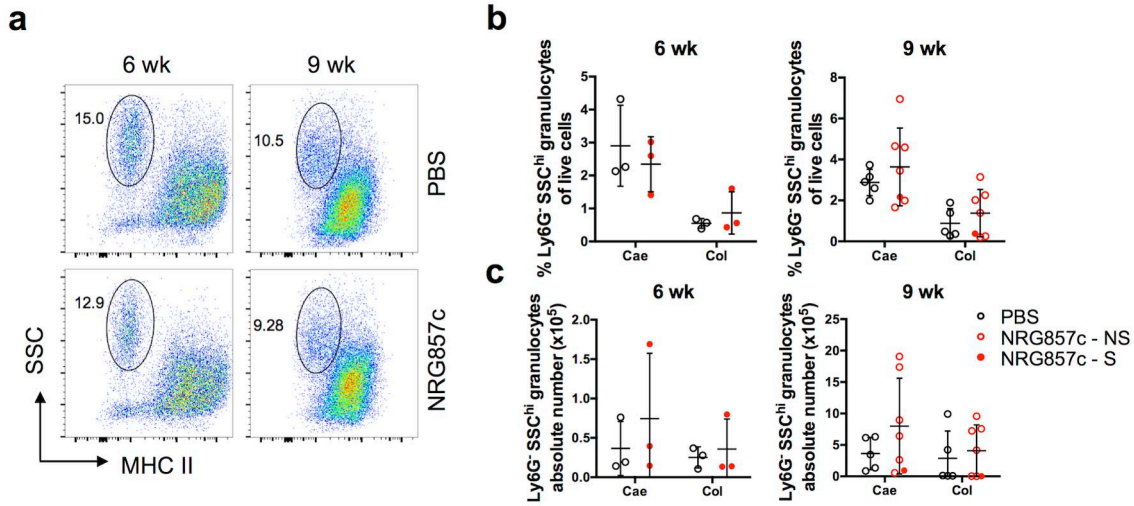

Figure 3. 6: Long-term NRG857c infection has no effect on SSC^{hi} $Ly6G^{-}$ granulocyte frequencies and numbers in the caecum and colon

C57BL/6 mice were treated with 20 mg streptomycin by gavage 24 h before oral infection with 1-2 × 10^9 CFU NRG857c or PBS. Tissues from infected (NRG857c) and uninfected (PBS) animals were collected at six (6wk) or nine (9wk) weeks p. i. and cells from colonic and caecal LP were analysed by flow cytometry.
(a) Representative plots of colonic tissue gated on single, live, $CD45^{+}$, ($CD11b^{+}$), $Ly6G^{-}$, SSC^{hi} cells. Data are shown as **(b)** the percentage of SSC^{hi} $Ly6G^{-}$ cells among live cells **(c)** their absolute cell number. Error bars represent S.D.; 9wk: data representative of two pooled experiments. Abbr.: Cae = caecum, Col = colon, NS = non-shedder, S = shedder

Intestinal macrophages and inflammatory monocytes are further innate cell populations that play an important role in homeostasis and pathogen recognition in the LP. During long-term NRG857c infection however, we saw no significant changes in the frequencies or absolute numbers of monocyte populations, nor in mature macrophages (Figure 3. 7).

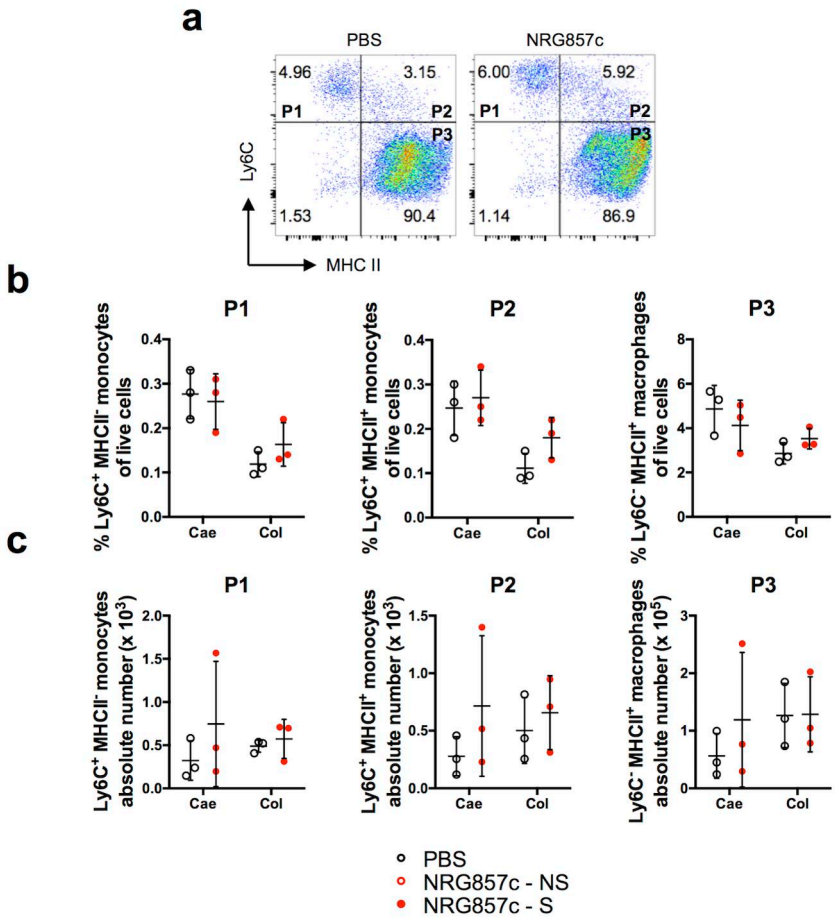

Figure 3. 7: NRG857c infection has no effect on monocyte and macrophage populations in the caecum and colon at 6 weeks

C57BL/6 mice were treated with 20 mg streptomycin by gavage 24 h before oral infection with 1-2 × 10^9 CFU NRG857c or PBS. Tissues from infected (NRG857c) and uninfected (PBS) animals were collected at six weeks p. i. and cells from colonic and caecal LP were analysed by flow cytometry. **(a)** Representative plots of colonic tissue gated on single, live, $CD45^+$, $CD11b^+$, $CD64^+$ cells. Data are shown as **(b)** the percentage of monocyte and macrophage populations among live cells and **(c)** their absolute cell number. Error bars represent S.D.; open circles: controls, closed red circles: NRG857c shedders; Abbr.: P1 = $Ly6C^+$ $MHCII^-$ monocytes, P2 = $Ly6C^+$ $MHCII^+$ monocytes, P3 = $Ly6C^-$ $MHCII^+$ macrophages.

3.2.4 Caecal dendritic cells migrate to the first colon-draining lymph node

As we saw no change in the innate responses in the LP of infected mice, we next sought to characterise the T cell response in the draining MLN. Recent work from our laboratory showed that distinct LN in the MLN chain separately drain the small intestine and colon (Houston et al. 2016). The first node in the chain, often the most prominent, drains the colon, together with a second smaller lymph node off the MLN chain (cMLN1 and cMLN2, respectively) (Figure 3. 8). The remainder of the MLN drain the small intestine (sMLN) (Figure 3. 8). Drainage of the caecum was not included as part of the original investigation, but owing to the high colonisation burden of NRG857c in the caecum, this information is essential for accurately characterising the tissue-specific T cell response to the bacteria. The caecum's anatomical proximity to the cMLN1 (Figure 3. 8) would make this the most likely node involved.

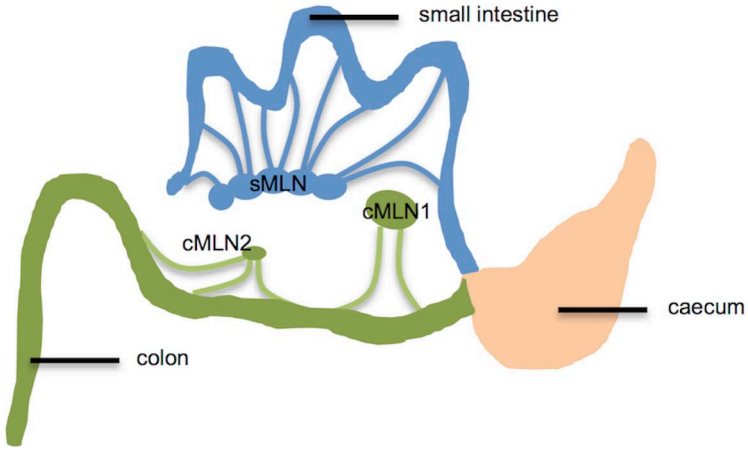

Figure 3. 8: Distinct mesenteric lymph nodes drain the small intestine and the colon.

The MLN chain is comprised of separate lymph nodes that drain different murine intestinal tissues. The first node (from right to left) drains the colon, together with a small node found off the main MLN chain, while the other lymph nodes drain the small intestine. Schematic based on findings by Houston et al. (2016).

To test this hypothesis, we used Kaede mice which ubiquitously express the photoconvertable Kaede protein, allowing us to track migration of cells over time *in vivo* (Tomura et al. 2008). In these mice, violet light stably photoconverts the Kaede protein from green to red. When we surgically exposed the caecum of these mice to violet light and assessed the percentage of Kaede-red^{+} DC in the cMLN1, cMLN2 and sMLN, we could find these only in the cMLN1, confirming this as the major site of caecal dendritic cell migration (Figure 3. 9).

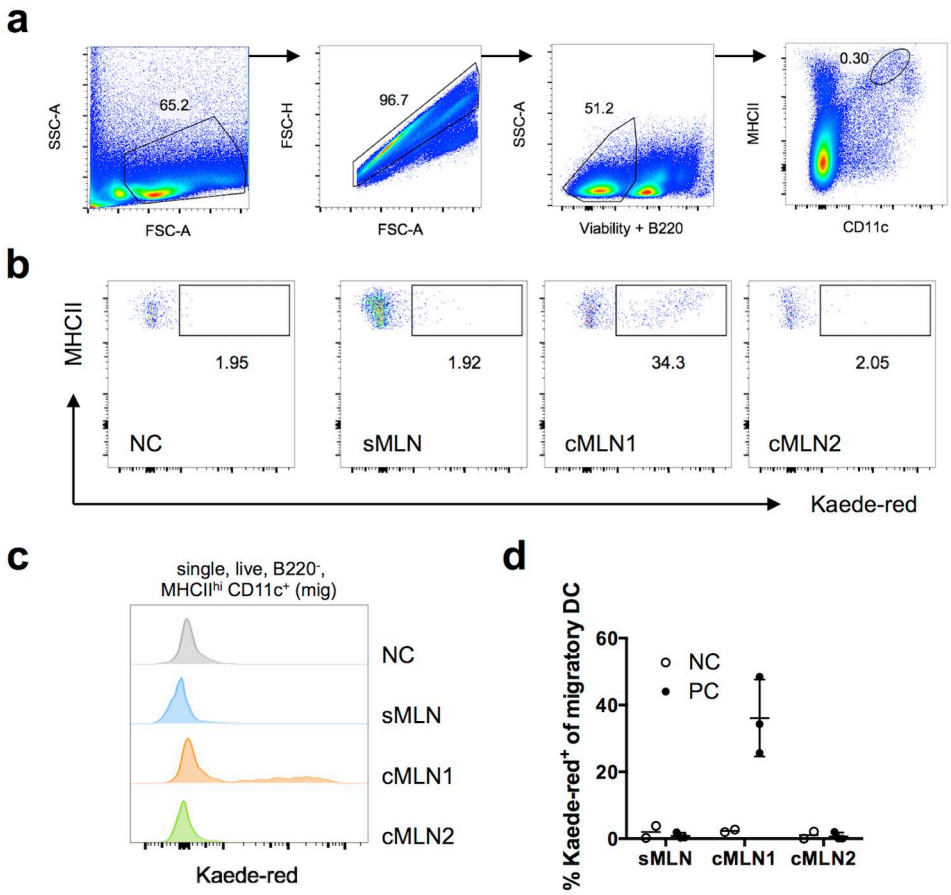

Figure 3. 9: The cMLN1 is the major site of caecal dendritic cell migration.

The caeca of Kaede mice were photoconverted using violet light after laparotomy and the presence of Kaede-red$^+$ dendritic cells in small intestinal MLN (sMLN) and the two colon-draining lymph nodes cMLN1 and cMLN2 was assessed by flow cytometry 24 h later. **(a)** Representative gating strategy of migratory DC; **(b, c)** representative plots and histogram showing Kaede-red$^+$ migratory dendritic cells in cMLN1 of a photoconverted mouse, but not in the sMLN, cMLN2 or cMLN1 of a nonconverted (NC) control; **(d)** percentage Kaede-red$^+$ cells of migratory DC in sampled photoconverted (PC) MLN compared with NC controls. Overall PC samples $p < 0.05$ (Kruskall-Wallis test) with $n = 3$. Error bars represent S.D.

We concluded therefore that the cMLN1 drains both the proximal colon and the caecum (Figure 3. 10) (Houston et al. 2016). Based on these findings, we decided to focus our characterisation on T cells in only the cMLN1 and cMLN2 (from now collectively termed "cMLN") to avoid diluting any colon/caecum-specific effect.

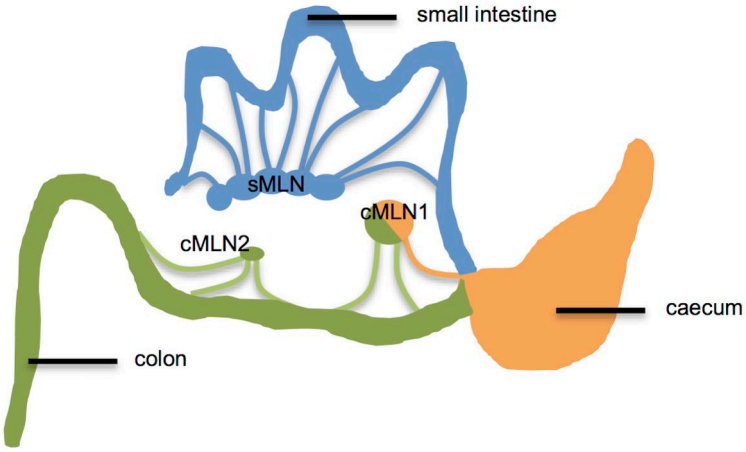

Figure 3. 10: Mapping dendritic cell migration from the three murine intestinal tissues to distinct MLN.

The now complete picture of the DC migration pattern from the three intestinal compartments; the sMLN drain only the small intestine and the cMLN2 only the colon, whilst the cMLN1 constitutes the shared destination of both caecal and colonic DC.

3.2.5 NRG857c infection has no effect on $CD4^+$ T cell activation or expression of chemokine receptors in the colon-draining MLN

We saw no changes in the overall frequencies of $CD4^+$ or $CD8^+$ T cells in the cMLN (Figure 3. 11a) six or nine weeks after NRG857c infection. $CD4^+$ T cell populations in the LN can be defined by their expression of CD62L (naïve), CD44 (recently activated) and CD25 (ready to undergo proliferation). During an on-going immune response, the percentage of $CD62L^+$ $CD44^-$ naïve T cells would be expected to decrease, and a corresponding increase in activated $CD44^+$ $CD62L^-$ T cells should be observed. This was not the case; no changes in the frequency of $CD44^+$ $CD62L^-$ or $CD25^+$ $CD4^+$ T cells were observed six or nine weeks p. i. with NRG857c (Figure 3. 11b).

NRG857c infection also did not induce increased expression of CCR9 on $CD44^+$ $CD4^+$ T cells (Figure 3. 11c), suggesting that infection had no effect on the gut-homing potential of activated T cells. We used CCR6 as a surrogate marker for Th17 cells in the cMLN, and could detect no changes in the frequencies of $CCR6^+$ $CD44^+$ $CD4^+$ T cells p. i. with NRG857c (Figure 3. 11c)

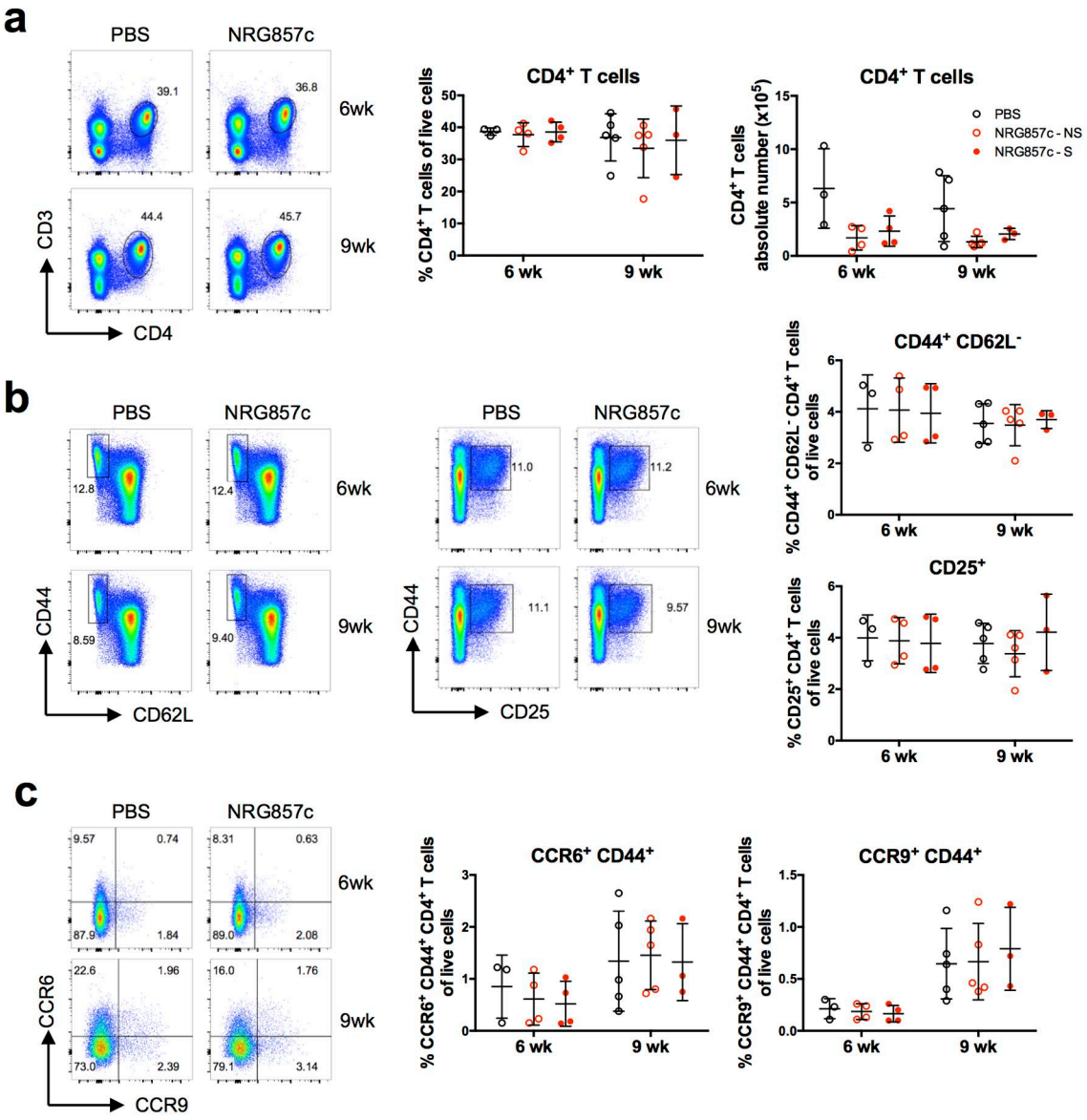

Figure 3. 11: NRG857c infection has no effect on CD4⁺ T cell activation or expression of specific chemokine receptors in the cMLN.

C57BL/6 mice were treated with 20 mg streptomycin by gavage 24 h before oral infection with 1-3 × 10^9 CFU NRG857c or PBS. Tissues from infected (NRG857c) and uninfected (PBS) animals were collected at six (6wk) or nine (9wk) weeks p. i. and CD4⁺ T cells from the cMLN were analysed by flow cytometry; **(a)** percentage among live cells and absolute cell number of live CD4⁺ CD3⁺ T cells gated on single, live, CD45⁺ cells. **(b)** CD44⁺ CD62L⁻ CD4⁺ T cells and CD25⁺ CD4⁺ T cells as percentage among live cells; gated on single, live, CD45⁺, CD3⁺, CD4⁺ cells. **(c)** Expression of CCR6 and CCR9 on CD44⁺ T cells; gated on single, live, CD45⁺, CD3⁺, CD4⁺, CD44⁺ cells. Error bars represent S.D.; data pooled from two independent experiments for both six and nine week time points with n = 3-4 in control and infected groups. Abbr.: NS = non-shedders, S = shedders

3.2.6 Long-term NRG857c infection has no effect on CD4⁺ or CD8⁺ T cell frequencies and numbers in the caecum and colon

Even though in our hands no signs of elevated innate responses to NRG857c were seen in the LP during long-term infection, the nature of the immune response might have changed to a T cell-mediated adaptive response at the chosen time points. The frequencies and total numbers of CD4⁺ and CD8⁺ T cells infiltrating the LP were therefore determined at six and nine weeks p. i. with NRG857c and compared with PBS-treated controls. However, contrary to the earlier published work (Small et al. 2013), we were unable to find evidence of an elevated T cell response in the colons or caeca of these animals (Figure 3. 12). Taken together, these findings suggest that NRG857c colonisation is asymptomatic in our hands and that it is unable on its own to establish a persistent and chronic infection in the intestine of C57BL6 mice.

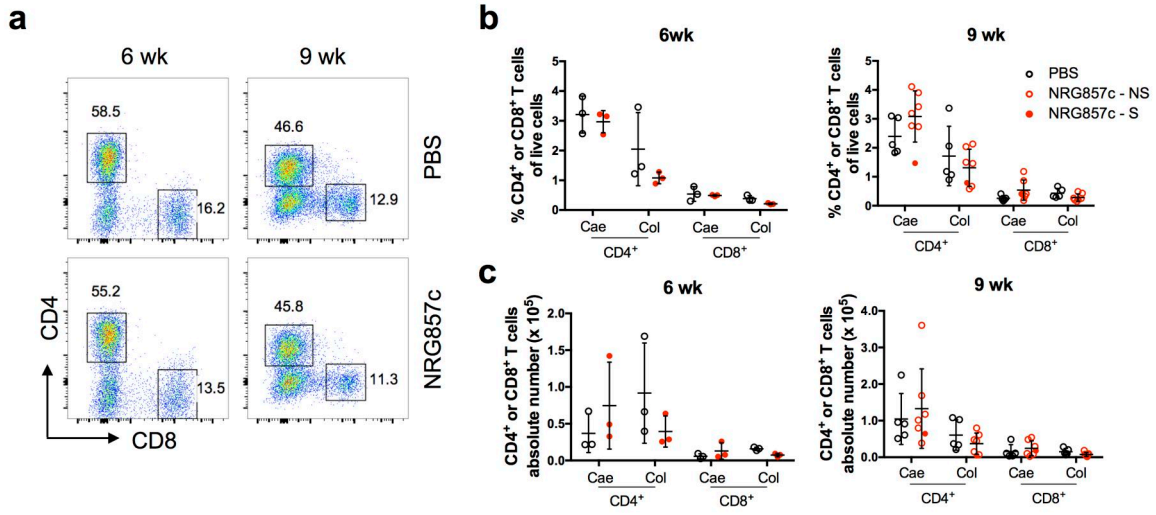

Figure 3. 12: Long-term NRG857c infection has no effect on CD4⁺ or CD8⁺ T cell frequencies and numbers in the caecum and colon.

C57BL/6 mice were treated with 20 mg streptomycin by gavage 24 h before oral infection with 1-2 × 10^9 CFU NRG857c or PBS. Tissues from infected (NRG857c) and uninfected (PBS) animals were collected at six (6wk) and nine weeks (9wk) p. i. and T cells from colonic and caecal LP were analysed by flow cytometry. **(a)** Representative plots of colonic tissue gated on single, live, CD45⁺ CD3⁺ cells. Data are shown as **(b)** the percentage of CD4⁺ and CD8⁺ cells among live cells and **(c)** their absolute cell number. Error bars represent S.D.; 9wk: data from two pooled experiments; Abbr.: Cae = caecum, Col = colon, NS = non-shedder, S = shedder

3.2.7 NRG857c does not cause changes in tissue innate or adaptive responses in out-bred CD1 mouse strain

The immune response to a pathogen can be genetically determined and has been shown to vary in different mouse strains. Indeed, Small et al. (2013) found that NRG857c-associated pathology manifested itself in both histological changes and a robust increase in pro-inflammatory cytokine production in both colonic and caecal tissue in C57BL/6 and CD1 mice (Small et al. 2013). The latter is an out-bred mouse strain that is most commonly used in toxicology and oncology. As we were unable to detect any consistent signs of pathology in infected C57BL/6 mice, we sought to define the response to NRG857c in CD1 mice in an attempt to explore the aspect of genetic susceptibility to disease. The infection was further carried out in male and female mice separately, to identify any gender-specific differences.

The time point for analysis was chosen to be three weeks, as this was the time frame that was shown to induce tissue inflammation in CD1 mice in the original report by Small et al. (2013). No evidence of consistent neutrophilia as part of an early, acute response to NRG857c was found in either males or females (Figure 3. 13).

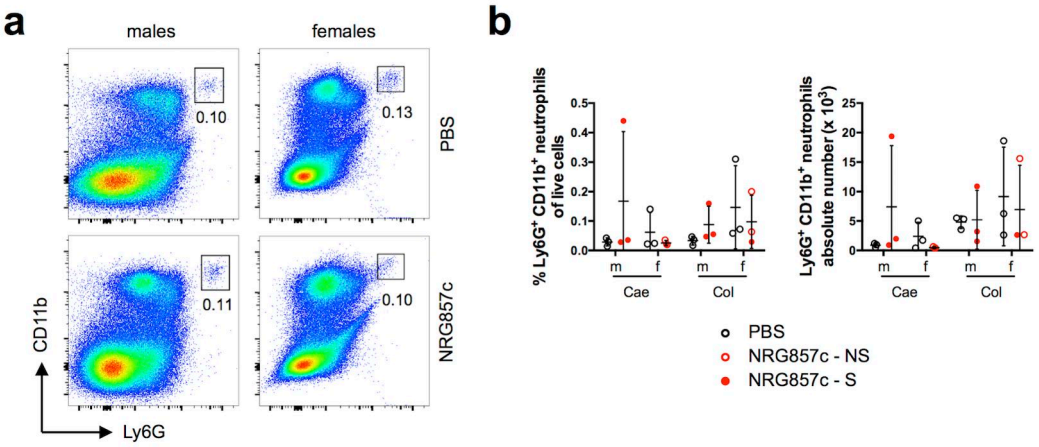

Figure 3. 13: NRG857c does not cause changes in tissue neutrophil frequencies in out-bred CD1 mouse strain.

Male and female CD1 mice were treated with 20 mg streptomycin by gavage 24 h before oral infection with 2-3 × 10^9 CFU NRG857c or PBS. Tissues from infected (NRG857c) and uninfected (PBS) animals were collected at three weeks p. i. and cells from colonic and caecal LP were analysed by flow cytometry. **(a)** Representative plots of $Ly6G^+$ $CD11b^+$ colonic neutrophils gated on single, live, $CD45^+$ cells. **(b)** Data are shown as the percentage of $Ly6G^+$ $CD11b^+$ among live cells, and their absolute cell number. Open circles: PBS-treated, closed red circles: NRG857c shedders, open red circles: NRG857c non-shedders. Error bars represent S.D.; Abbr.: m = males, f = females, Cae = caecum, Col = colon.

We next quantified the incoming monocyte populations in these mice. No significant changes in monocyte influx were observed in female mice (Figure 3. 14). Males displayed a trend towards increased Ly6C$^+$ MHCII$^-$ monocyte numbers and decreased Ly6C$^-$ MHCII$^+$ mature macrophage numbers (Figure 3. 14), although more biological repeats would be required to determine statistical significance.

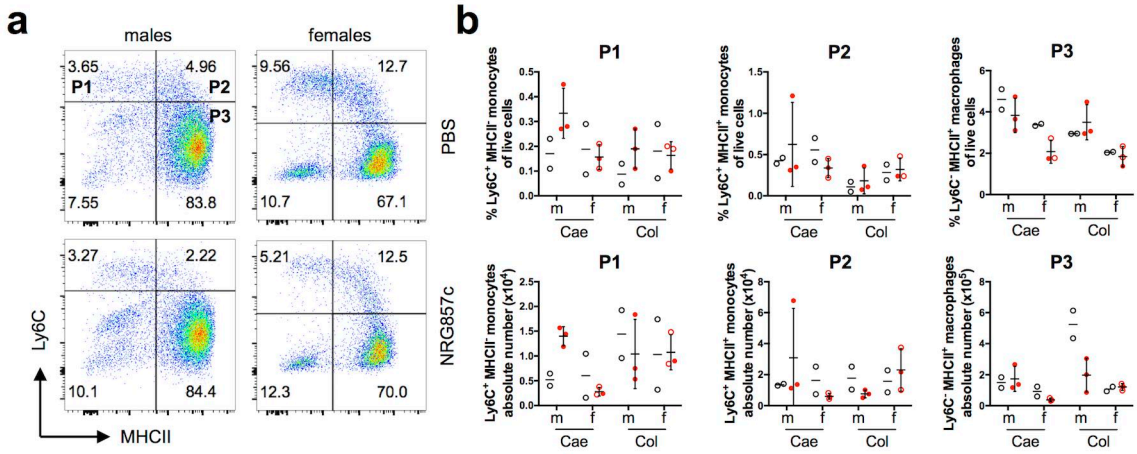

Figure 3. 14: NRG857c may cause changes in tissue monocyte and macrophage frequencies in male CD1 mice.

Male and female CD1 mice were treated with 20 mg streptomycin by gavage 24 h before oral infection with 2-3 × 10^9 CFU NRG857c or PBS. Tissues from infected (NRG857c) and uninfected (PBS) animals were collected at three weeks p. i. and cells from colonic and caecal LP were analysed by flow cytometry. **(a)** Representative plots showing colonic monocytes and macrophages gated on single, live, CD45$^+$, CD11b$^+$, Ly6G$^-$, SSC^{lo} cells. Data are shown as **(b)** the percentage of monocyte and macrophage populations among live cells and **(c)** their absolute cell number. Open circles: PBS-treated, closed red circles: NRG857c shedders, open red circles: NRG857c non-shedders. Error bars represent S.D.; Abbr.: m = males, f = females, Cae = caecum, Col = colon, P1 = Ly6C$^+$ MHCII$^-$ monocytes, P2 = Ly6C$^+$ MHCII$^+$ monocytes, P3 = Ly6C$^-$ MHCII$^+$ macrophages.

Finally, no indication of an enhanced adaptive T cell response was seen in these mice, as $CD4^+$ and $CD8^+$ T cell frequencies and numbers in the colonic and caecal LP remained unchanged three weeks p. i. with NRG857c (Figure 3. 15).

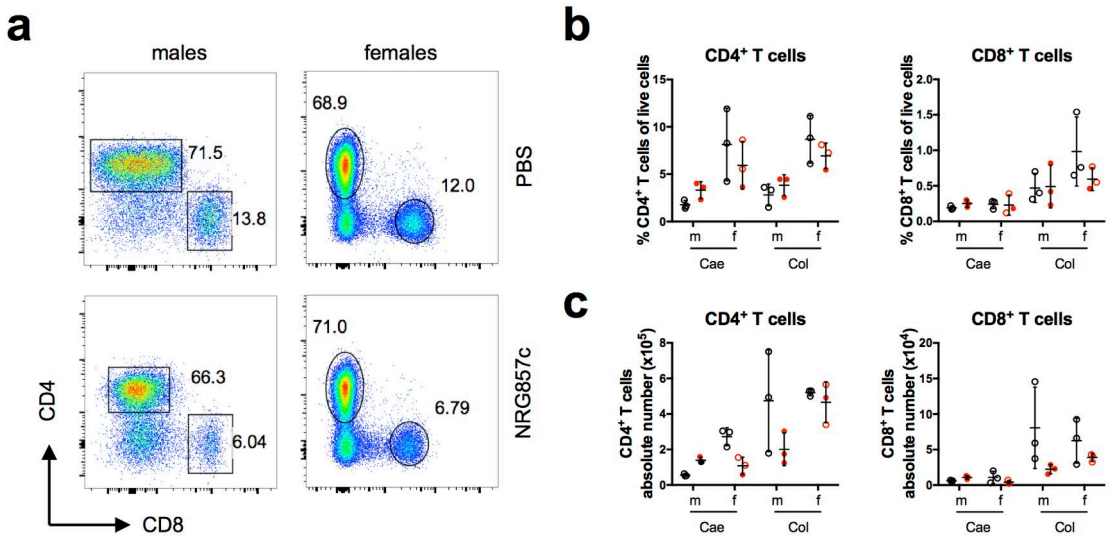

Figure 3. 15: NRG857c does not cause changes in tissue T cell frequencies in out-bred CD1 mouse strain.

Male and female CD1 mice were treated with 20 mg streptomycin by gavage 24 h before oral infection with 2-3 × 10^9 CFU NRG857c or PBS. Tissues from infected (NRG857c) and uninfected (PBS) animals were collected at three weeks p. i. and cells from colonic and caecal LP were analysed by flow cytometry. **(a)** Representative plots showing $CD4^+$ and $CD8^+$ T cells from colonic LP gated on single, live, $CD45^+$, $CD3^+$ cells. Data are shown as **(b)** the percentage of $CD4^+$ and $CD8^+$ T cells among live cells and **(c)** their absolute cell number. Open circles: PBS-treated, closed red circles: NRG857c shedders, open red circles: NRG857c non-shedders; Error bars represent S.D.; Abbr.: m = males, f = females, Cae = caecum, Col = colon.

3.2.8 Treatment with 0.5% DSS does not enhance NRG857c ability to drive cellular influx to the colonic or caecal LP

Previous models investigating the role of AIEC in driving colonic inflammation used an alternative strain, LF82 (Carvalho et al. 2008, 2009). This group found that infection with LF82 aggravated inflammation when mice were treated with 2% DSS treatment to induce colonic epithelial cell injury (Carvalho et al. 2008). As NRG857c could be detected associated with the colonic epithelium in our model, we hypothesised that low-level DSS treatment concomitantly to infection might be enough to break down the barrier and allow NRG857c to cross and induce chronic inflammation. The experimental regimen we used is depicted in Figure 3. 16a. Briefly, male and female C57BL/6 mice were given 0.5% DSS in their drinking water for 24 h before streptomycin treatment and subsequent infection with 2 × 10^9 CFU NRG857c or gavage with PBS for controls. Mice were kept on DSS for a further two days p. i. and then put on standard drinking water.

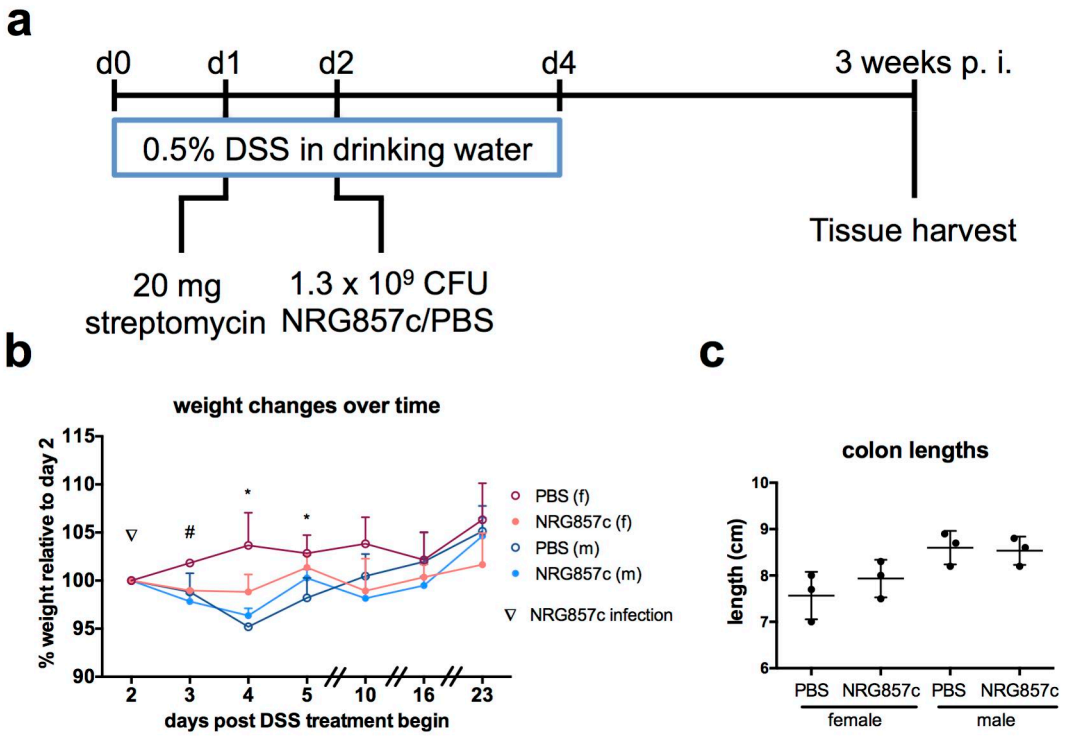

Figure 3. 16: DSS treatment may enhance the ability of NRG857c to induce weight loss in female but not male mice.

(**a**) Male and female C57BL/6 mice were given 0.5% DSS in their drinking water for five days, beginning a day before treatment with 20 mg streptomycin by gavage and subsequent oral infection with 1×10^9 NRG857c or PBS 24 h later. Weights were monitored at regular intervals throughout the experimental period and colons harvested at three weeks p. i. for analysis. (**b**) Percentage weight changes over three weeks relative to pre-infection weight on day 2. (**c**) Colon lengths three weeks p. i.; error bars represent S.D.; statistical analysis was carried out using a Kruskal-Wallis test with a Dunn's test for multiple comparisons; # $p < 0.05$ between female PBS-treated and male NRG857c infected animals, * $p < 0.05$ between female and male PBS-treated animals. Abbr.: f = female, m = male.

We monitored weight over the course of infection, as DSS treatment is known to induce weight loss and we hypothesised that additional infection with NRG857c would aggravate this. We found that within the control group, male mice had lost weight during by 4-5 days of treatment, whereas females had not (Figure 3. 16b). On the other hand, there was no difference in weight loss between infected and control animals, regardless of gender. We also did not observe any differences in colon lengths between infected and control mice three weeks p. i. (Figure 3. 16c).

To determine if concurrent DSS treatment with infection induced mucosal inflammation, colonic LP cells were analysed three weeks p. i. by flow cytometry. No significant increase in CD11b$^+$ Ly6G$^+$ neutrophils was detected in males or females infected with NRG857c (Figure 3. 17a).

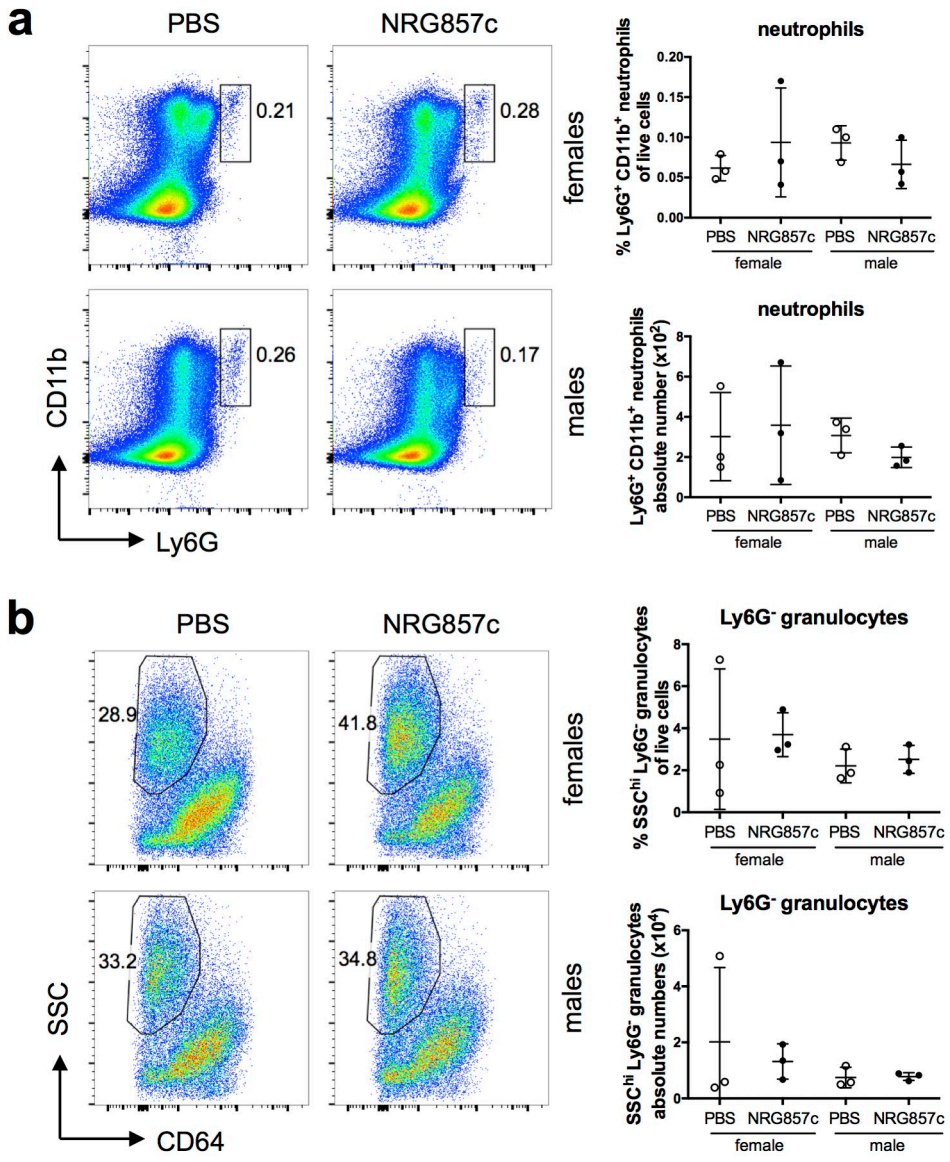

Figure 3. 17: DSS treatment does not enhance the ability of NRG857c to induce granulocyte influx into colonic lamina propria.

Male and female C57BL/6 mice were given 0.5% DSS in their drinking water for five days, beginning a day before treatment with 20 mg streptomycin by gavage and subsequent oral infection with 1×10^9 NRG857c or PBS 24 h later. Colons were harvested for analysis three weeks p. i. (p. i.) and LP cells analysed by flow cytometry. **(a)** Representative plots showing colonic Ly6G$^+$ CD11b$^+$ neutrophils gated on single, live, CD45$^+$ cells; data shown as the percentage of Ly6G$^+$ CD11b$^+$ among live cells and their absolute cell number. **(b)** Representative plots showing colonic SSC^{hi} granulocytes gated on single, live, CD45$^+$, CD11b$^+$, Ly6G$^-$, CD11c$^{(lo\text{-}int)}$ cells. Data are shown as the percentage of SSC^{hi} Ly6G$^-$ cells among live cells, and as their absolute cell number. Error bars represent S.D.

Furthermore, when analysing CD11b^{+} SSC^{hi} Ly6G^{-} granulocytes, a population that is mainly constituted by eosinophils, no change was found between experimental groups (Figure 3. 17b). We further hypothesised that infection with NRG857c would enhance the influx of monocytes to the LP that had been observed during DSS colitis previously (Bain et al. 2013). However, this was not the case, as no changes in monocyte or macrophage frequencies were noted between infected and control animals of either gender (Figure 3. 18).

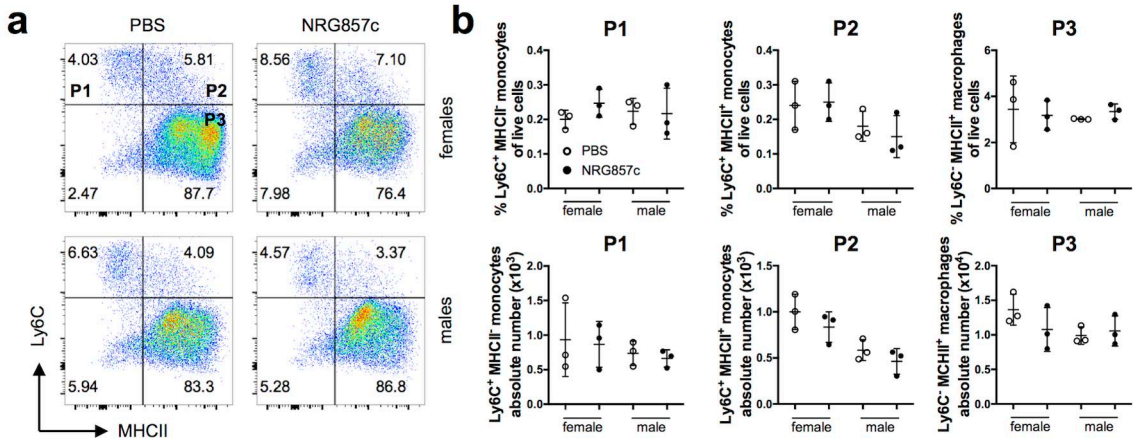

Figure 3. 18: DSS treatment together with NRG857c infection does not change monocyte and macrophage population frequencies in the colonic lamina propria.

Male and female C57BL/6 mice were given 0.5% DSS in their drinking water for five days, beginning a day before treatment with 20 mg streptomycin by gavage and subsequent oral infection with 1×10^9 NRG857c or PBS 24 h later. Colons harvested for analysis three weeks p. i. (p. i.) and colonic LP cells analysed by flow cytometry. **(a)** Representative plots showing colonic monocyte and macrophage populations gated on single, live, CD45^{+}, CD11b^{+}, CD64^{+}, CD11c$^{(lo\text{-}int)}$, SSC^{lo} cells. **(b)** Data are shown as the percentage of monocyte and macrophage populations among live cells, and as their absolute cell number. Error bars represent S.D.; Abbr.: P1 = Ly6C^{+} MHCII^{-} monocytes, P2 = Ly6C^{+} MHCII^{+} monocytes, P3 = Ly6C^{-} MHCII^{+} macrophages.

Finally, CD4⁺ and CD8⁺ T cell frequencies and absolute numbers remained unaltered in the colons of animals infected with NRG857c relative to PBS-treated mice three weeks p. i. (Figure 3. 19).

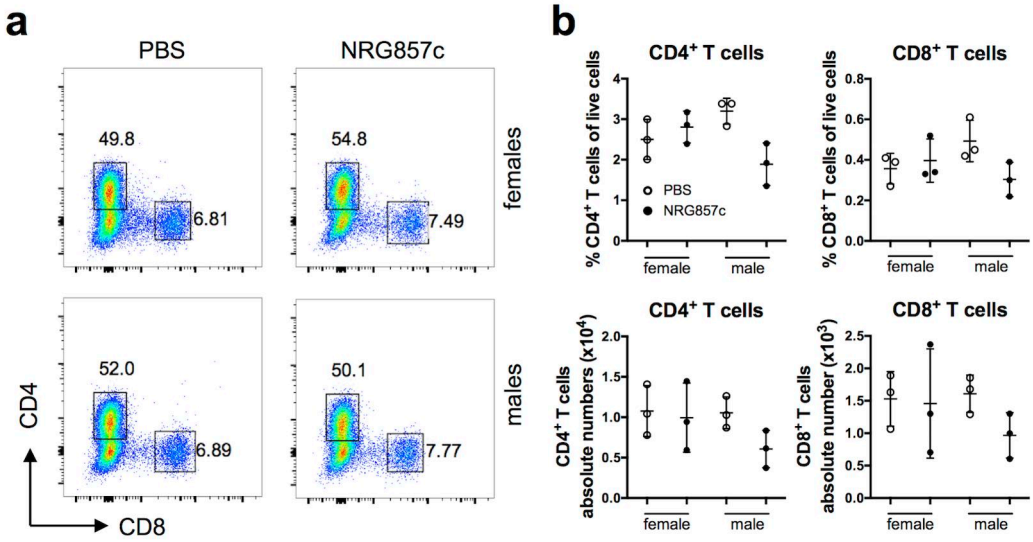

Figure 3. 19: DSS treatment does not enhance the ability of NRG857c to induce T cell influx to colon.

Male and female C57BL/6 mice were given 0.5% DSS in their drinking water for five days, beginning a day before treatment with 20 mg streptomycin by gavage and subsequent oral infection with 1×10^9 NRG857c or PBS 24 h later. Colons harvested for analysis three weeks p. i. (p. i.) and colonic LP cells analysed by flow cytometry. **(a)** Representative plots showing colonic CD4⁺ and CD8⁺ T cells gated on single, live, CD45⁺, CD3⁺ cells. **(b)** Data are shown as the percentage of T cell populations among live cells, and as their absolute cell number. Error bars represent S.D.

3.2.9 Lack of aryl hydrocarbon ligands does not enhance the ability of NRG857c to induce intestinal inflammation

Dietary metabolites such as tryptophan derivatives are important for maintaining survival of IEL in the intestinal epithelium (Li et al. 2011). These play a vital role in immune surveillance and defence against bacterial pathogens (Edelblum et al. 2015). We set out to test the hypothesis that feeding mice an AhR ligand-deficient diet would affect the IEL compartment sufficiently to allow increased translocation of NRG857c to the LP after infection and lead to persistent inflammation. Mice were fed an AhR ligand-deficient diet (AIN-76A) for a week. Animals were then administered streptomycin 24 h prior to treatment with NRG857c or PBS (Figure 3. 20a). All animals were kept on the diet for the entirety of the experimental period. Weights remained unchanged between PBS-treated and infected groups (Figure 3. 20b) and we did not observe any colon shortening three weeks p. i. with NRG857c (Figure 3. 20c).

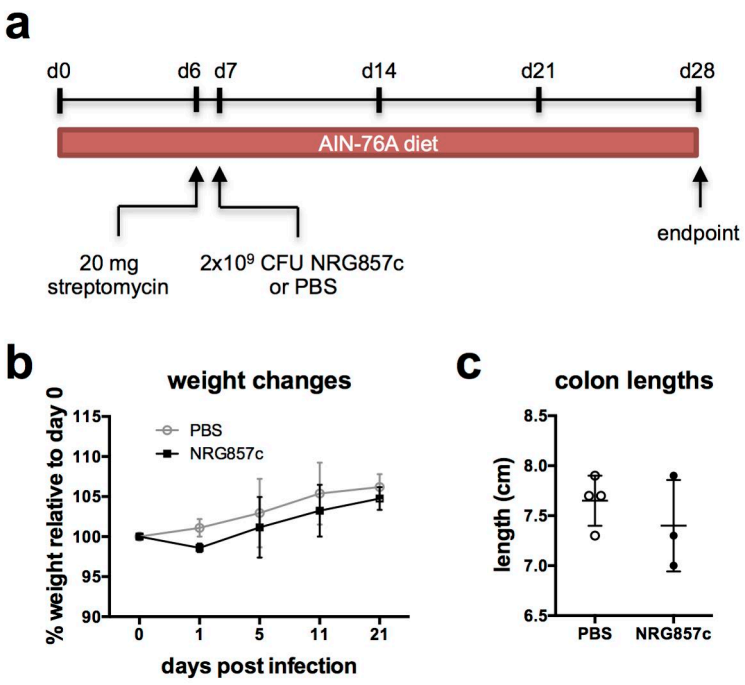

Figure 3. 20: Lack of AhR ligands does not enhance the ability of NRG857c to induce weight loss or colonic shortening.

(a) Mice were fed *ad lib.* on an AhR ligand-deficient diet (AIN-76A) for a week before treatment with 20 mg streptomycin and subsequent oral gavage with 1×10^9 CFU NRG857c or PBS 24 h later. Mice were kept on the AIN-76A diet for the duration of the experiment and their weights monitored at regular intervals before colons were harvested three weeks p. i.. **(b)** Percentage weight changes over three weeks relative to pre-infection weight. **(c)** Colon lengths compared between NRG857c infected and PBS-treated mice at three weeks p. i.. Error bars represent S.D.; both groups contain data pooled from male and female mice representative of one experiment with n = 3-4.

The frequencies of Ly6G$^+$ neutrophils (Figure 3. 21a) and SSC^{hi} Ly6G$^-$ granulocytes (Figure 3. 21b) were unchanged in the colonic LP of infected mice compared with controls at three weeks.

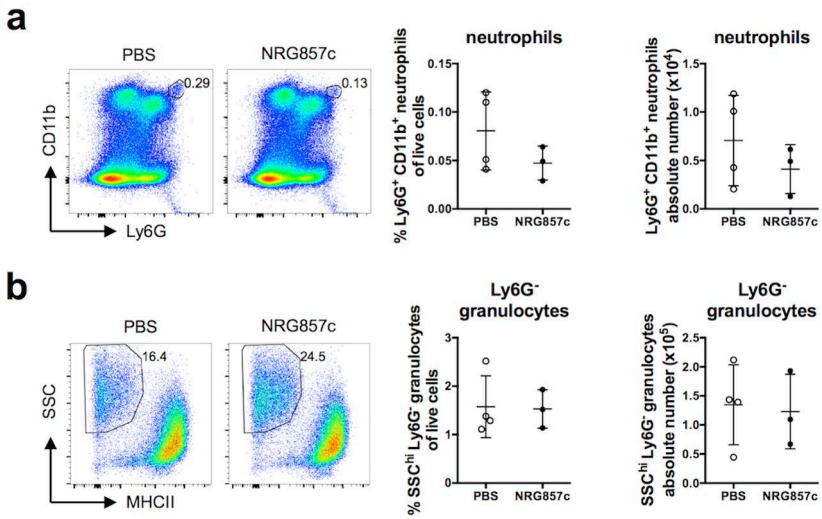

Figure 3. 21: Lack of AhR ligands does not enhance the ability of NRG857c to induce granulocyte influx into the colonic LP

Mice were fed *ad lib.* on an AhR ligand-deficient diet (AIN-76A) for a week before treatment with 20 mg streptomycin and subsequent oral gavage with 1×10^9 CFU NRG857c or PBS 24 h later. Mice were kept on the AIN-76A diet for the duration of the experiment. Colons were harvested three weeks p. i. and LP cells were analysed by flow cytometry for frequencies of immune cell populations. **(a)** Representative plots showing Ly6G$^+$ CD11b$^+$ neutrophils gated on single, live, CD45$^+$ cells; data are shown as the percentage of Ly6G$^+$ CD11b$^+$ cell among live cells, and as their absolute cell number. **(b)** Representative plots showing SSC^{hi} granulocytes gated on single, live, CD45$^+$, CD11b$^+$, Ly6G$^-$ cells; data are shown as the percentage SSC^{hi} Ly6G$^-$ cells among live cells, and as their absolute cell number. Error bars represent S.D.; both groups contain data pooled from male and female mice representative of one experiment with n = 3-4.

Lack of dietary AhR ligands also had no effect on the ability of NRG857c to drive monocyte influx into the LP, and we found no significant change in the frequency of mature macrophages in infected mice (Figure 3. 22a). Finally, CD4$^+$ and CD8$^+$ T cell frequencies and absolute numbers were not affected in the colonic LP of NRG857c-treated mice (Figure 3. 22b), similar to the observations made in infected mice given a standard diet (Figure 3. 12). Unfortunately, we did not assess if lack of AhR ligands reduced the frequency of IEL in our hands, which would have been important to confirm that the diet was indeed inducing a change in the epithelial compartment.

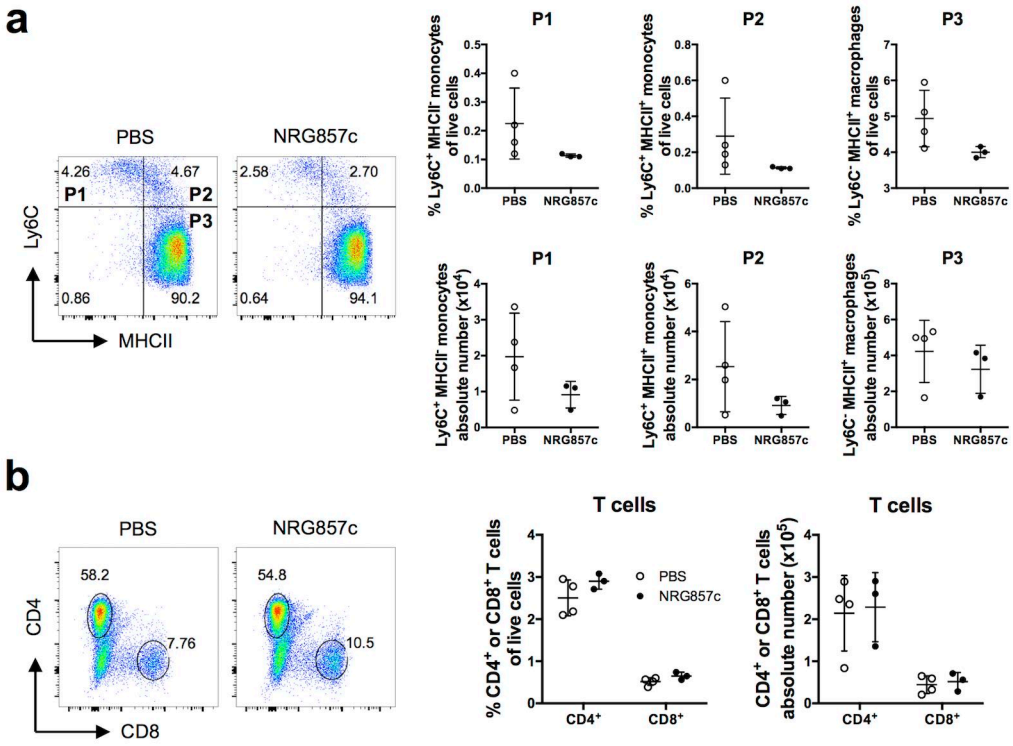

Figure 3. 22: Lack of AhR ligands does not enhance the ability of NRG857c to change colonic monocyte, macrophage or T cell frequencies.

Mice were fed *ad lib.* on an AhR ligand-deficient diet (AIN-76A) for a week before treatment with 20 mg streptomycin and subsequent oral gavage with 1×10^9 CFU NRG857c or PBS 24 h later. Mice were kept on the AIN-76A diet for the duration of the experiment. Colons were harvested three weeks p. i. and LP cells were analysed by flow cytometry for frequencies of immune cell populations. **(a)** Representative plots showing monocyte and macrophage populations gated on single, live, $CD45^+$, $CD11b^+$, $Ly6G^-$, SSC^{lo}, $CD11c^{(lo\text{-}int)}$, $CD64^+$ cells; data are shown as percentage of live cells and absolute numbers. **(b)** Representative plots showing $CD4^+$ and $CD8^+$ T cells gated on single, live, $CD45^+$, $CD3^+$ cells; data are shown as percentage of live cells and absolute numbers. Error bars represent S.D.; both groups contain data pooled from male and female mice representative of one experiment with n = 3-4.

3.3 Discussion

To investigate microbiota-specific immunity during chronic intestinal inflammation we aimed to use a previously published model, in which mice were infected with the CD-associated AIEC strain NRG857c. Our results show that NRG857c colonises the murine colon and caecum. It persists and is shed by infected mice for up to nine weeks. However, we could find no evidence of intestinal inflammation following long-term NRG857c infection in two different WT mouse strains. This was also not the case when animals were treated in parallel with 0.5% DSS, or when fed an AhR ligand-deficient diet. These results are conflicting with the previously published report that suggested a single oral dose of NRG857c post-streptomycin treatment is sufficient induce chronic, fibrosing inflammation of the caeca of five different WT mouse strains (Small et al. 2013). In our hands, even infection of CD1 mice, which were among those exhibiting the most severe pathology in the published study, did not result in intestinal inflammation. At six weeks p. i. we detected bacteria likely to be NRG857c associated with the colonic epithelium. However, we did not observe any bacteria in the LP and crypts, as had previously been described (Small et al. 2013).

The disparities between the previous work and our observations could stem from variability introduced by technical issues. For example, the age of mice used in our investigations ranged from between seven and 14 weeks and infective doses between experiments were variable. However, to control for the latter, data points were analysed separately for shedders and non-shedders where possible. Unfortunately, the number of data points available was not sufficient in some cases to allow for statistical analysis, and where intra-group variability was high (as for example for $Ly6G^+$ neutrophil frequencies), more experimental repeats would have added to the conclusiveness of the observed outcome. A further confounding factor may have been the use of the anti-helminthic agent fenbendazole in administered chow to counteract infection with pinworm that is common in our animal facility. To date little is known about the effects of this drug on gut immunity or the microbiota. However, it is unlikely to have an inhibitory effect on NRG857c pathogenicity, as we saw no intestinal inflammation in infected mice held on AhR ligand-deficient diet, which does not contain fenbendazole.

Some of our experiments were carried out using male and some with female mice, whilst in the paper by Small et al. (2013) only female mice were used. Work from other groups suggests sex-linked differences in the gut microbiota can impact on the pathogenesis of

autoimmune disease (Markle et al. 2013, Yurkovetskiy et al. 2013). However, we did not see any significant differences in the ability of NRG857c to drive disease in CD1 mice of either sex, suggesting that in that strain of mice at least, gender does not play a detectable role in determining NRG857c colonisation and pathogenicity.

Intestinal bacterial infections take different courses dependent on the infecting organism in question. For example, *S.* Typhimurium causes acute and severe gastroenteritis in streptomycin pre-treated mice within 48 hours of infection (Barthel et al. 2003). *C. rodentium* infection on the other hand, reaches its peak 9-10 days p. i. (Wiles et al. 2004), manifesting as colonic pathology similar to that seen in human EHEC infections, after which it is cleared naturally by the host (Wiles et al. 2006). The time points that were chosen in this study were three, six and nine weeks p. i., in order to assess the level of inflammation after long-term infection. However, as seen for enteric infections mentioned above, immune responses and bacterial load can change within a matter of days. This could have led to the oversight of cellular infiltrate into the LP, for example, due to sampling at the wrong point within the course of infection. This could be circumvented in future studies by the use of an *in vivo* endoscopy system to allow more frequent rectal and colonic pathology scoring.

In their characterisation of the NRG857c infection model, Small et al. (2013) showed increased immune cell influx into the caecal LP at three weeks p. i., constituted by more F4/80$^+$ macrophages and CD3$^+$ T cells in immunostained sections. However, we could not detect any significant changes in LP macrophage or T cell populations between infected and PBS-treated animals at this time point by flow cytometry. Even though this is already a more sensitive read-out for changes in immune cell populations compard with immunohistochemistry, we could have added greater depth to our analyses by assessing changes in T helper subsets and the cytokines they produce. Indeed, colonic explants from infected C57BL/6 mice produced more IL-17 and IFNγ *ex vivo* than control tissue in previous reports (Small et al. 2013), although this could not be replicated conclusively in our hands (data not shown). This implicates NRG857c in induction of Th1/Th17-driven pathology. The outlined infection experiments could therefore be repeated in the future to determine if the percentage of IL-17$^+$/IFNγ$^+$ or RORγt$^+$/T-bet$^+$ CD4$^+$ T cells changes in the colonic LP. Furthermore, recently activated CD4$^+$ T cells upregulate expression of CD69 and CD44, and an on-going T cell mediated tissue immune response would be expected to increase the frequency of CD69$^+$ CD44$^+$ CD4$^+$ T cells. Monocyte and macrophage

populations are also likely to be changed not only in total cell number, but also in expression of cytokines and other regulatory mediators. Differentiated intestinal macrophages are tolerogenic and characterised by production of the regulatory cytokine IL-10 (Bain et al. 2013). However, upon induction of colitis, they upregulate expression of pro-inflammatory mediators such as IL-6 and IL-1β (Bain et al. 2013). Analysing macrophage cytokine expression could have therefore also been a more sensitive readout for NRG857c-induced mucosal changes.

Bacterial infection causes antigen-specific $CD4^+$ T cell expansion in the draining LN (McSorley et al. 2002). To accurately quantify tissue-specific T cell responses, we first had to identify which MLN drained the caecum, which is one of the main sites of inflammation in many models of bacterial infection *in vivo*, including that reportedly caused by NRG857c (Small et al. 2013). We were able to confirm that the first cMLN in the chain (cMLN1) is the only MLN to drain the caecum, by tracking DC migration over 24 h in Kaede mice. However, we could not detect any evidence of $CD4^+$ T cell expansion in the cMLN1 at six or nine weeks p. i., and no increase in activation or intestinal homing receptors. The MLN T cell response was not characterised by Small et al. (2013) in their original description of the model, and our results provide evidence against on-going bacterial-induced antigen presentation and $CD4^+$ T cell activation in the draining LN.

Treatment of animals with low concentrations of DSS concomitant to infection did not have any enhancing effect on the ability of NRG857c to induce mucosal inflammation. However, this experiment was only performed once and may require some optimisation. For example, the percentage of DSS could be too low to have an effect, and the period of administration may have been too short. Administration of low-level DSS throughout the course of infection for example may have greater potential to cause sufficient colonic epithelial damage to allow NRG857c translocation. AhR ligand deficiency also had no effect on cellular recruitment to the LP following infection with NRG857c. However, $CD8^+$ IEL frequencies were not analysed in these mice, which would have been an important control to help understand if the diet was having the effect that had been previously reported (Li et al. 2011).

Apart from issues with experimental design, there may be fundamental biologically relevant reasons for NRG857c not causing intestinal pathology in our hands. One of them may be the difference in microbiota between animal facilities and suppliers. To begin to explore this possibility, experiments were carried out with mice supplied from both Harlan

and Charles River, but no differences were observed between batches. Nonetheless, even though streptomycin treatment is likely to cause a comparable reduction in species diversity in all animals regardless of original microbiota composition, it is conceivable that certain resistant species present in our animals could inhibit NRG857c virulence. Comparison of the faecal microbiota in our animal facility and that of the original report by Small et al. (2013) would be required to confirm this.

A further biological reason could be intrinsic to NRG857c itself. Virulence factors identified in the genome of NRG857c include a Type VI secretion system and long polar fimbriae components (Nash et al. 2010), which may be important factors governing its ability to persist and drive inflammation in the human terminal ileum. However, it may lack the necessary virulence factors required to establish infection in the murine colon. In fact, AIEC strain LF82 was shown to induce colitis in mice that expressed human CEACAMs (Carvalho et al. 2009) but not in WT mice, suggesting that this strain is adapted to express adhesins that specifically allow colonisation of the human mucosa. A similar principle may apply to NRG857c. One of the reasons that enteric pathogens such as *S.* Typhimurium and *C. rodentium* effectively establish an acute infection is that expression of a T3SS allows direct interaction with IEC and efficient translocation of bacterial effector proteins into the cell. This is not the case for NRG857c (Nash et al. 2010), which may be another reason for its inability to cause a strong inflammatory response.

Based on our findings we conclude that this model is not suitable for investigating the cellular and molecular mechanisms governing the intestinal immune response to chronic bacterial infection. While able to colonise long-term, NRG857c does not cause tissue pathology or any induction of innate or adaptive immunity in the intestine. Since its original description by Small et al. (2013) this model has only been used in two papers, one follow-up study from the same laboratory (McPhee et al. 2014), and one independent study (Cieza et al. 2015). Both focus on bacterial colonisation rather than the immune response to NRG857c. However, while the infection regime is maintained in the follow-up publication, mice that only had low-level colonisation or had cleared NRG857c were excluded from that study's analysis (McPhee et al. 2014). This points to a significant degree of variability in their hands and corroborates our findings. Despite the fact that this strain does not breach the epithelial barrier in our hands, it may, however, provide a useful model system to elucidate the molecular determinants leading to bacterial colonisation and

adhesion in the intestine. Insights from such experiments would represent important contributions to understanding the pathogenesis of IBD in humans.

Chapter 4: Expression of apoptotic cell receptors in the intestine

4.1 Aims and hypotheses

Bacterial infection in the intestine causes apoptosis (Moss et al. 1996, Zychlinsky et al. 1996, Barnett Foster et al. 2000), and recognition of apoptotic cells is an important factor regulating the outcome of T cell responses (Torchinsky et al. 2009). DC are likely to be key players in this process, as they convey tissue- and antigen-specific information to the T cell during its priming phase in the LN, thereby directing its differentiation. All intestinal DC subsets migrate in lymph (Cerovic et al. 2013) and can cross-present antigen to $CD8^+$ T cells *in vitro* (Cerovic, Houston, et al. 2014). However, only $CD11b^-$ $CD103^+$ DC can cross-prime $CD8^+$ T cell responses *in vivo*, which is thought to be due to their unique ability to acquire cell-derived antigen (Cerovic, Houston, et al. 2014). Thus, the repertoire of ACR expressed by DC may differ between populations. TIM4 is a PSR with expression restricted to antigen-presenting cells (Meyers et al. 2005). However, little is known about its tissue and population-specific expression on DC. We therefore set out to answer three questions. First, is TIM4 expression restricted to one particular population of DC, potentially the $CD11b^-$ $CD103^+$ DC. Second, does the tissue environment shape the expression of TIM4 on DC, indicating how recognition of apoptosis may affect downstream tissue-specific T cell responses. This led us to our third aim, to investigate the function of TIM4 on DC in different tissues. We aimed to determine which cells $TIM4^+$ DC might be interacting with through receptor-ligand interactions, and to understand how $TIM4^+$ DC differed from $TIM4^-$ DC in their maturation state and ability to prime antigen-specific T cell responses.

4.2 Results

4.2.1 TIM4 is expressed on a small population of colonic CD11b$^-$ CD103$^+$ DC and on intestinal macrophages

To determine if TIM4 is preferentially expressed by a certain DC population in the LP we analysed TIM4 expression on DC isolated from small intestinal and colonic LP, as well as from PP by flow cytometry (Figure 4. 1, Figure 4. 2). TIM4 expression on all small intestinal LP DC was low (Figure 4. 2), whilst in the colon about 10% of CD103$^+$ CD11b$^-$ DC expressed TIM4 (Figure 4. 2). Interestingly, of the PP CD11b$^+$ CD103$^+$ DC, which are the least abundant subset in the PP, more cells expressed TIM4 compared with the small intestinal and colonic LP (Figure 4. 2).

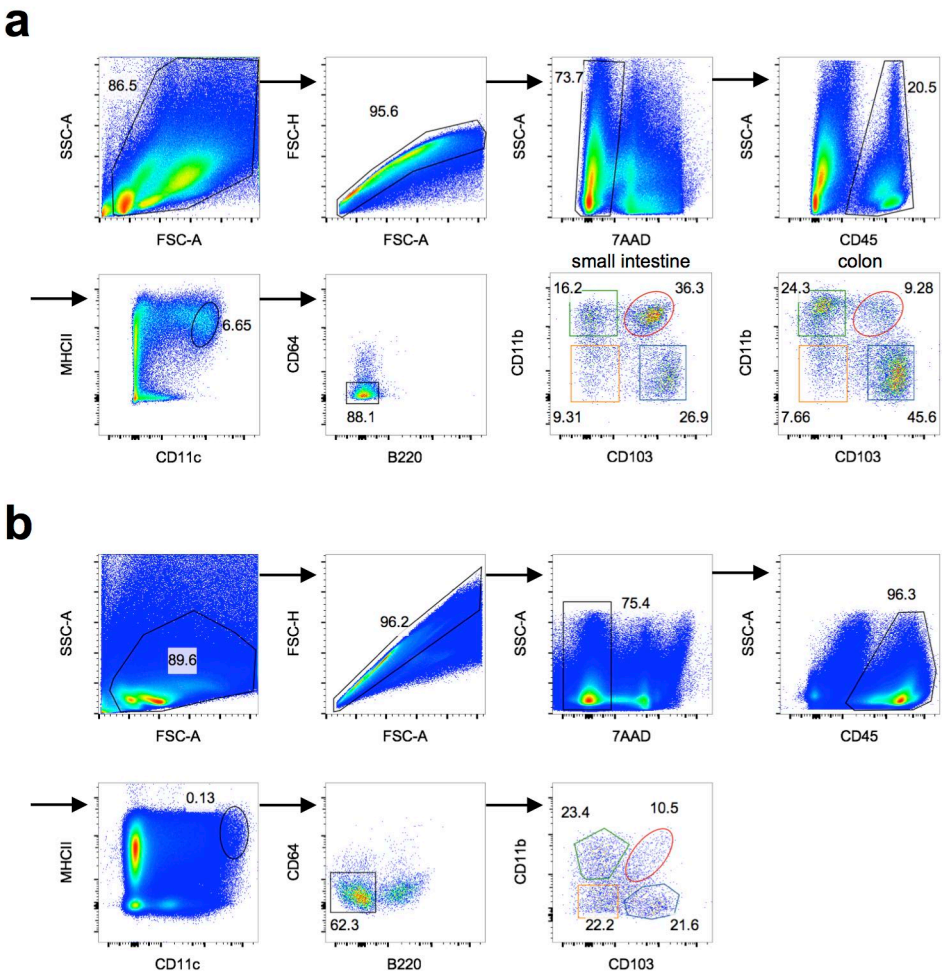

Figure 4. 1: Gating strategy for intestinal DC populations

(a) Small intestinal and colonic DC are gated as single, live, CD45$^+$, MHCII$^+$ CD11c$^+$ cells, with further exclusion of macrophages (CD64$^-$) and B cells and plasmacytoid DC (pDC, B220$^-$). **(b)** Peyer's patch (PP) DC are gated as single, live, CD45$^+$, MHCII$^+$ CD11c^{hi}, and CD64$^-$ B220$^-$ cells to exclude macrophages, and B cells and pDC. In all intestinal tissues, four DC populations are defined based on the expression of CD11b and CD103.

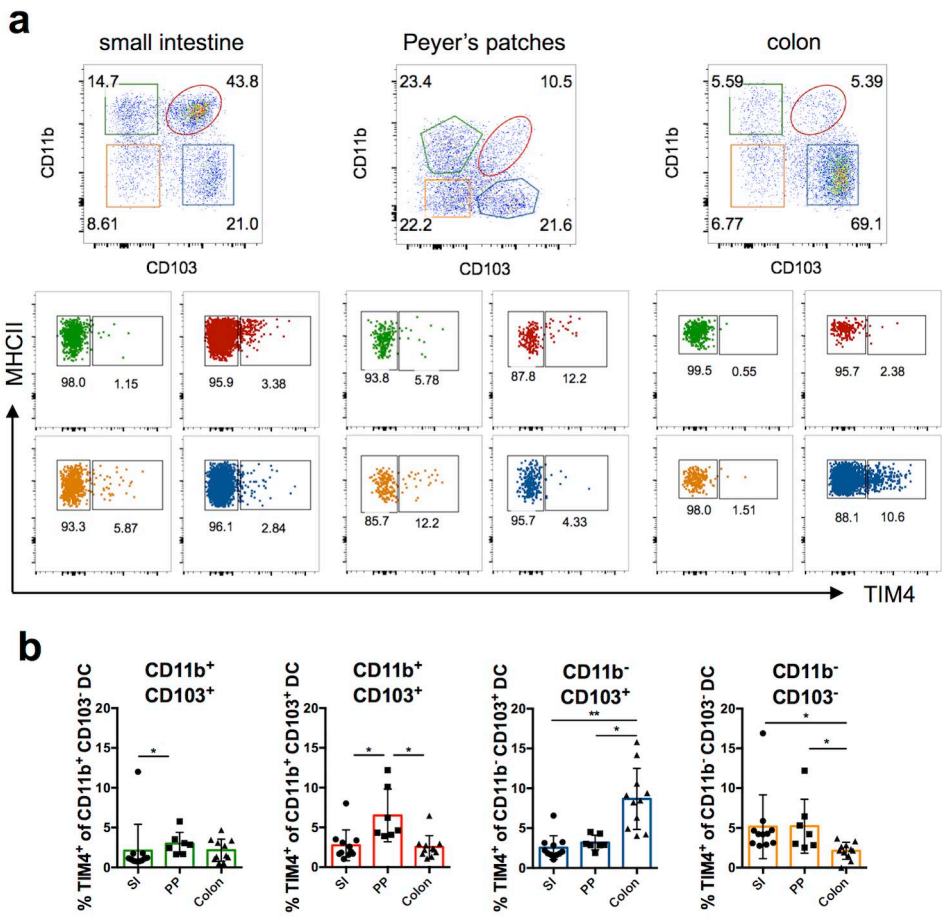

Figure 4. 2: TIM4 is mainly expressed by colonic CD11b$^-$ CD103$^+$ DC

Intestinal tissues from C57BL/6 male mice were collected and LP cells analysed by flow cytometry. **(a)** Representative plots for small intestinal (SI), PP and colonic DC gated on single, live, CD45$^+$, MHCII$^+$, CD11c$^+$, CD64$^-$, B220$^-$ cells. Four DC populations can be defined based on expression of CD11b and CD103: CD11b$^+$ CD103$^-$ (green), CD11b$^+$ CD103$^+$ (red), CD11b$^-$ CD103$^+$ (blue) and CD11b$^-$ CD103$^-$ (orange). **(b)** Data are shown as the percentage of TIM4$^+$ cells among DC populations. Error bars represent S.D.; statistical analysis performed using a Kruskal-Wallis test with a Dunn's post-test for multiple comparisons. * $p < 0.05$, ** $p < 0.001$.

As macrophages differentiate from incoming monocytes, they upregulate MHCII and CX3CR1 (Bain et al. 2013) (Figure 4. 3a). We found that about 15% of colonic CX3CR1^{hi} macrophages expressed TIM4 (Figure 4. 3b). Interestingly, CX3CR1^{hi} macrophages in the small intestine showed a trend to higher expression levels of TIM4 compared with the colon, although this did not reach statistical significance (Figure 4. 3b).

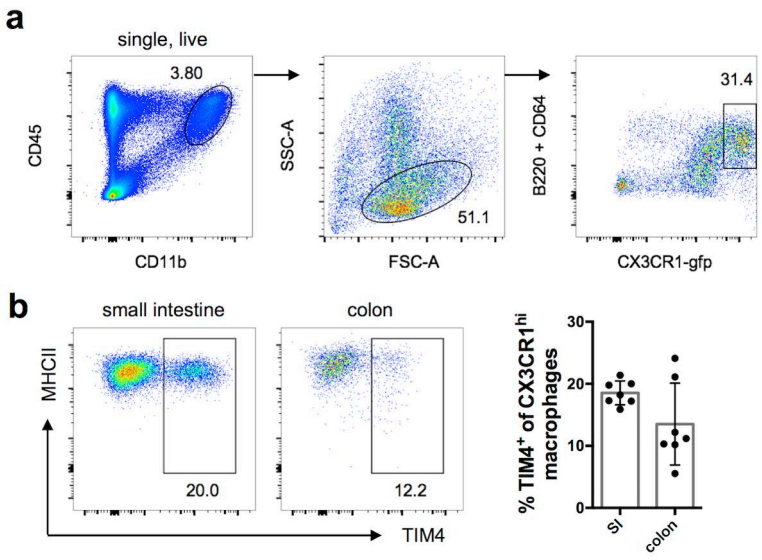

Figure 4. 3: TIM4 is expressed on CX3CR1^{hi} macrophages in both the small intestine and colon

Intestinal tissues from *Cx3cr1*$^{+/gfp}$ mice were collected and LP cells analysed by flow cytometry. **(a)** Representative plots of colonic tissue are shown illustrating the gating strategy for CD11b+ CD64+ CX3CR1^{hi} macrophages. **(b)** Representative plots of TIM4 staining on small intestinal and colonic macrophage populations, and summary data shown as the percentage of TIM4+ cells within CX3CR1^{hi} macrophages of the small intestine (SI) and colon. Error bars represent S.D.; statistical analysis performed within populations between tissues using an unpaired t test.

4.2.2 TIM4 is mainly expressed on human colonic macrophages

We used tissue obtained from human surgical colonic resections to determine if the expression pattern of TIM4 observed in the murine intestine was equivalent to that found in the healthy human colon. Human colonic DC were defined with help of a lineage gate to exclude major cell populations such as T and B cells, NK cells, granulocytes and monocytes (CD3, CD19, CD56, CD14, CD16). Furthermore, DC were classed as CD64^{-} and CD123^{-} to exclude macrophages and pDC (Figure 4. 4). As in the murine gut, human colonic DC can be grouped into four distinct subsets based on their expression of SIRPα and CD103 (Watchmaker et al. 2014) (Figure 4. 4).

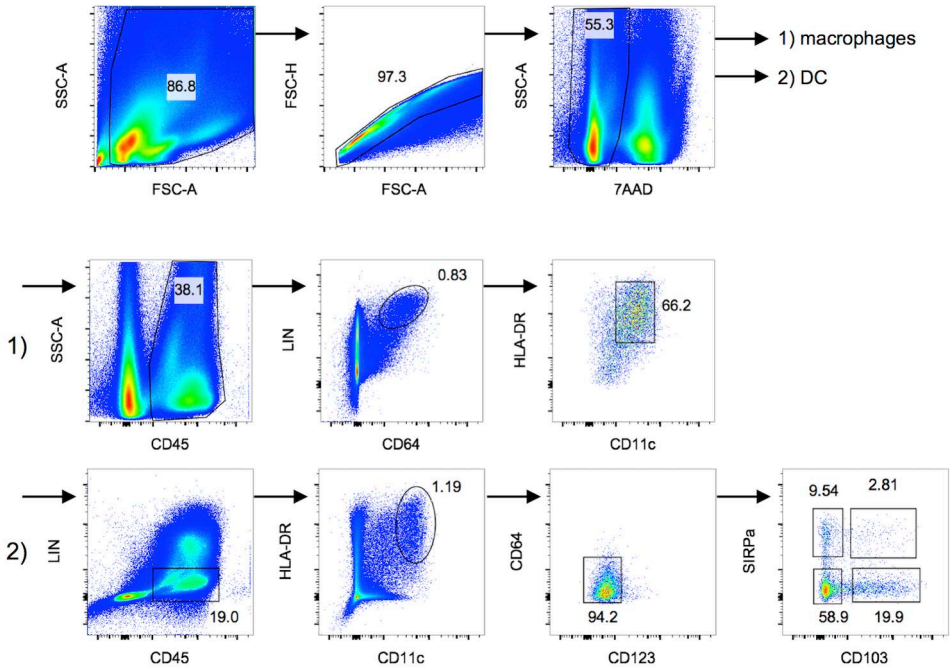

Figure 4. 4: Human colonic macrophage and DC gating strategies

Healthy mucosa from the margins of human colonic resection tissue was digested and LP cells analysed by flow cytometry. Representative plots show gating strategy for 1) colonic macrophages gated as single, live, $CD45^+$, LIN^+ (CD3, CD19, CD56, CD14, CD16), $CD64^+$, HLA-DR^+, $CD11c^{int}$ cells and 2) DC gated as single, live, $CD45^+$, LIN^-, HLA-DR^+, $CD11c^+$, $CD64^-$, $CD123^-$ cells. Four DC populations can be defined on the basis of their expression of SIRPα and CD103.

Macrophages on the other hand were defined as LIN^+ ($CD14^+$) $CD64^+$ HLA-DR^+ (Figure 4. 4) and about 25% expressed TIM4 (Figure 4. 5). We could not, however, detect TIM4 expression on SIRPα^- $CD103^+$ DC, the human counterparts of the murine $CD11b^-$ $CD103^+$ DC, or any of the other human colonic DC subsets (Figure 4. 5).

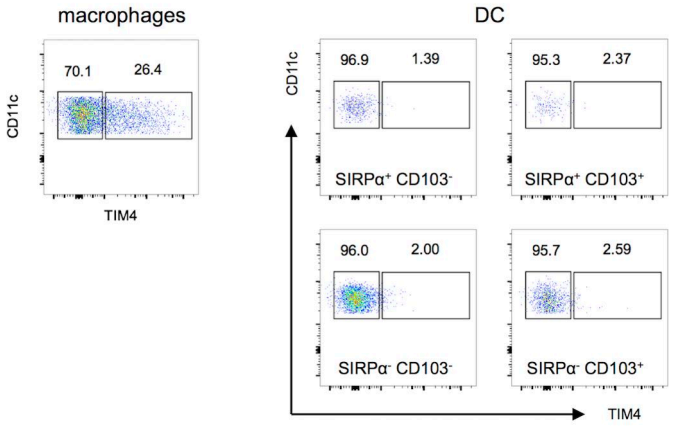

Figure 4. 5: TIM4 is mainly expressed by human colonic macrophages

Healthy mucosa from the margins of human colonic resection tissue was digested and LP cells analysed by flow cytometry. Representative plots show TIM4 expression on colonic macrophages and DC populations.

4.2.3 Expression of apoptotic cell receptor CD205 is higher in the colon compared with the small intestine

Having observed that for specific DC and macrophage populations, TIM4 expression was higher in the colon than it was in the small intestine, we examined if this also held true for another ACR, CD205. We analysed its expression on total colonic macrophages ($CD11b^+$ $CD64^+$ $MHCII^+$ cells) and DC (Figure 4. 6a). Interestingly, we found that CD205 expression was higher on DC than on macrophages, both in the small intestine and the colon (Figure 4. 6b).

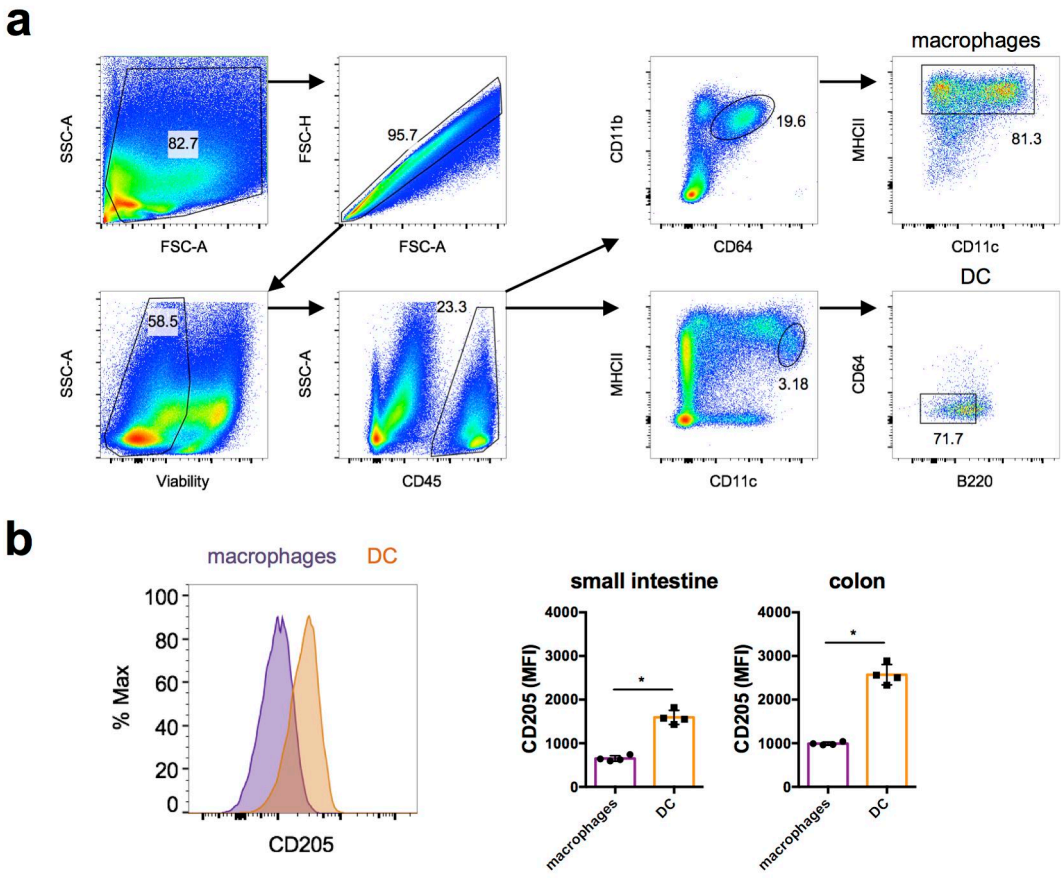

Figure 4. 6: CD205 expression is higher on DC than on macrophages in both the murine colon and small intestine.

Small intestinal and colonic tissues from C57BL/6 male mice were harvested and CD205 expression on LP cell populations analysed by flow cytometry. **(a)** Macrophages were gated as single, live, $CD45^+$ $CD11b^+$, $CD64^+$, $MHCII^+$ cells; DC were gated as single, live, $CD45^+$, $MHCII^+$, $CD11c^{hi}$, $CD64^-$ $B220^-$ cells. **(b)** CD205 expression is higher on DC (orange) than on macrophages (purple) in both the small intestine and colon as assessed by mean fluorescence intensity (MFI). Error bars represent S.D.; statistical analysis was performed using a Mann-Whitney test. * $p < 0.05$.

CD205 levels on all DC populations was highest in the colon, although expression followed the same pattern in the small intestine and the PP, with CD11b$^-$ CD103$^+$ DC exhibiting the highest levels, followed by CD11b$^+$ CD103$^+$ DC (Figure 4. 7). This provides further evidence for the expression of ACR being highest on CD11b$^-$ CD103$^+$ DC in the intestine.

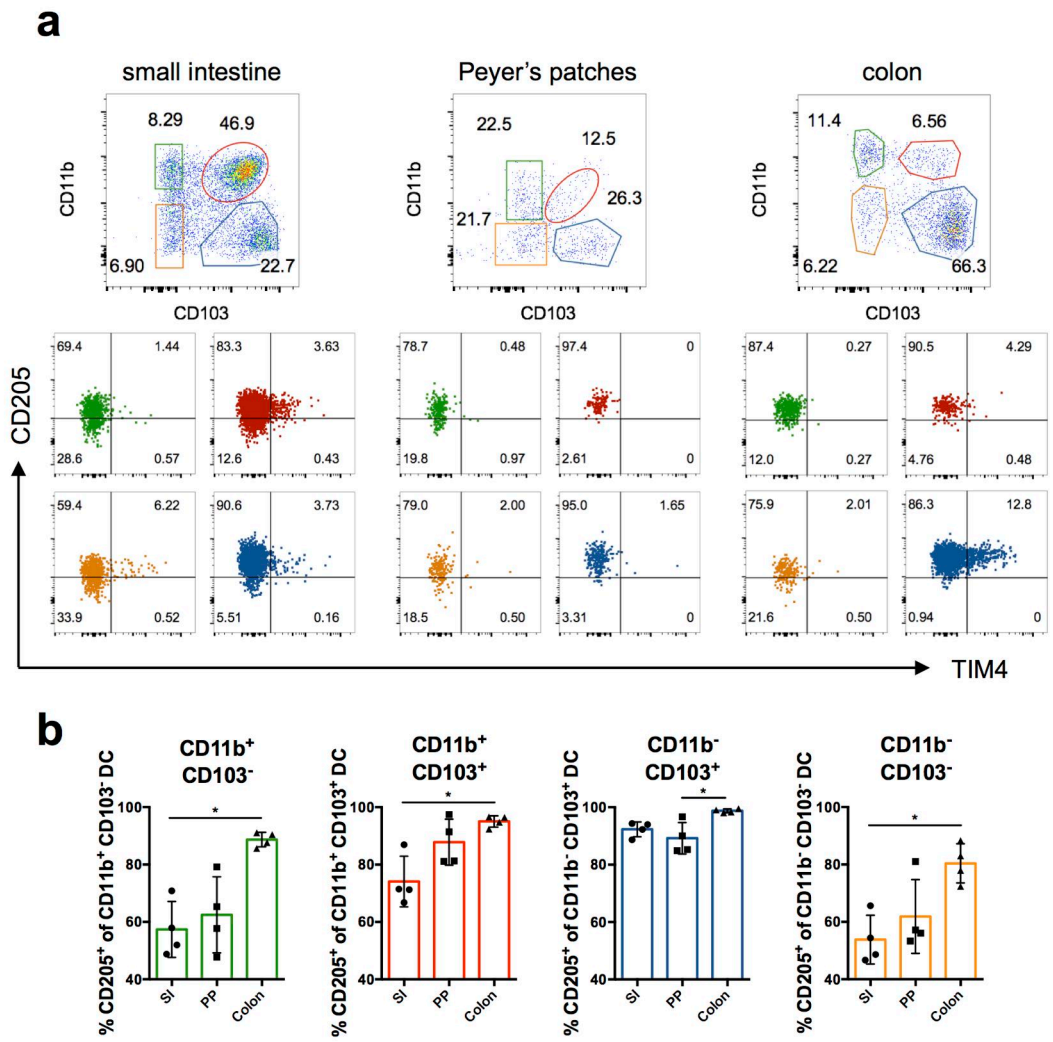

Figure 4. 7: CD205 expression is highest on colonic CD11b$^-$ CD103$^+$ DC

Small intestines (SI), PP and colons from C57BL/6 male mice were harvested and CD205 expression on DC populations analysed by flow cytometry. **(a)** Representative plots of CD205 and TIM4 expression on small intestinal, PP and colonic DC populations gated on single, live, CD45$^+$, MHCII$^+$, CD11c$^+$, CD64$^-$, B220$^-$ cells. Four DC populations can be defined based on expression of CD11b and CD103: CD11b$^+$ CD103$^-$ (green), CD11b$^+$ CD103$^+$ (red), CD11b$^-$ CD103$^+$ (blue) and CD11b$^-$ CD103$^-$ (orange). **(b)** Data are shown as percentage CD205$^+$ cells of DC populations. Error bars represent S.D.; statistical analysis carried out using a Kruskal-Wallis test and Dunn's post-test for multiple comparisons. * $p < 0.05$.

4.2.4 Lung CD103$^+$ DC, but not splenic CD8α$^+$ DC, highly express TIM4

CD103$^+$ CD11b$^-$ DC are also found in the lung mucosa, and are thought to be the mucosal counterparts of splenic CD8α$^+$ DC (Figure 4. 8), as all these subsets are dependent on the transcription factors IRF8 and BATF3 and can cross-present antigen to CD8$^+$ T cells (Edelson et al. 2010).

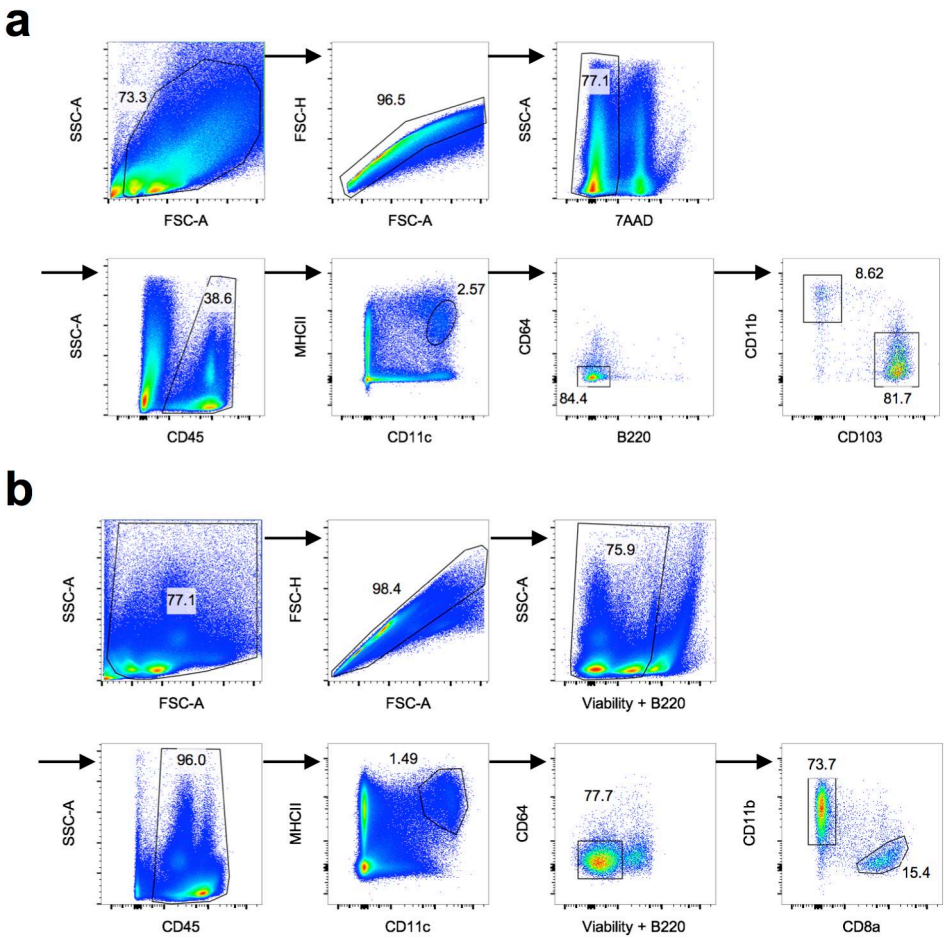

Figure 4. 8: Gating strategies for lung and splenic DC subsets

Lungs and spleens from C57BL/6 mice were harvested and cells analysed by flow cytometry.
(a) Representative gating strategy for lung DC, gated as single, live, CD45$^+$, MHCII$^+$, CD11c$^+$, CD64$^-$, B220$^-$ cells. Two lung DC subsets can be differentiated based on exclusive expression of either CD11b or CD103.
(b) Representative gating strategy for splenic DC, gated as single, live, CD45$^+$, MHCII$^+$, CD11c$^+$, CD64$^-$, B220$^-$ cells. Two splenic DC subsets can be differentiated based on exclusive expression of either CD11b or CD8α.

Strikingly, virtually all lung CD103$^+$ CD11b$^-$ DC were TIM4$^+$, whilst TIM4 expression was low on lung CD11b$^+$ CD103$^-$ DC (Figure 4. 9a). In the spleen only a small percentage of CD8α$^+$ DC expressed TIM4, similar to the splenic CD11b$^+$ DC (Figure 4. 9b). These results indicate that TIM4 expression on DC may be affected locally by tissue-specific factors and signals, as opposed to being determined early in cellular differentiation.

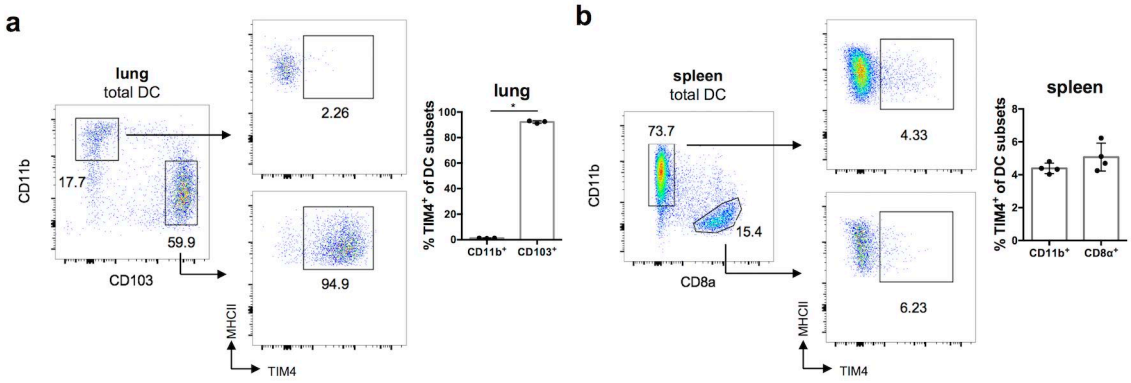

Figure 4. 9: Lung CD103$^+$ DC highly express TIM4

Lungs and spleens from C57BL/6 male mice were harvested and cells analysed by flow cytometry. **(a)** Lung and **(b)** splenic DC gated on single, live, CD45$^+$, MHCII$^+$, CD11c$^+$, CD64$^-$, (F4/80$^-$), B220$^-$ cells. Data are shown as percentage of TIM4$^+$ cells among DC populations. Error bars represent S.D.; statistical analysis performed using a paired t test. * $p < 0.0001$.

4.2.5 TIM4 expression on bone marrow pre-DC is low

Tissue DC differentiate from pre-DC which egress the bone marrow and travel in the blood stream to lymphoid and peripheral tissue sites, where they fully develop into resident DC subsets (Ginhoux et al. 2009, Liu et al. 2009).We hypothesised that if, as our previous results would suggest, TIM4 expression is regulated in a tissue- and population-specific manner, bone marrow pre-DC would not express TIM4. This was indeed the case; when we analysed isolated bone marrow MHCII$^-$ CCR9$^-$ CD135$^+$ CD11c$^+$ pre-DC (Figure 4. 10a), only a very small percentage stained positive for TIM4 (Figure 4. 10b).

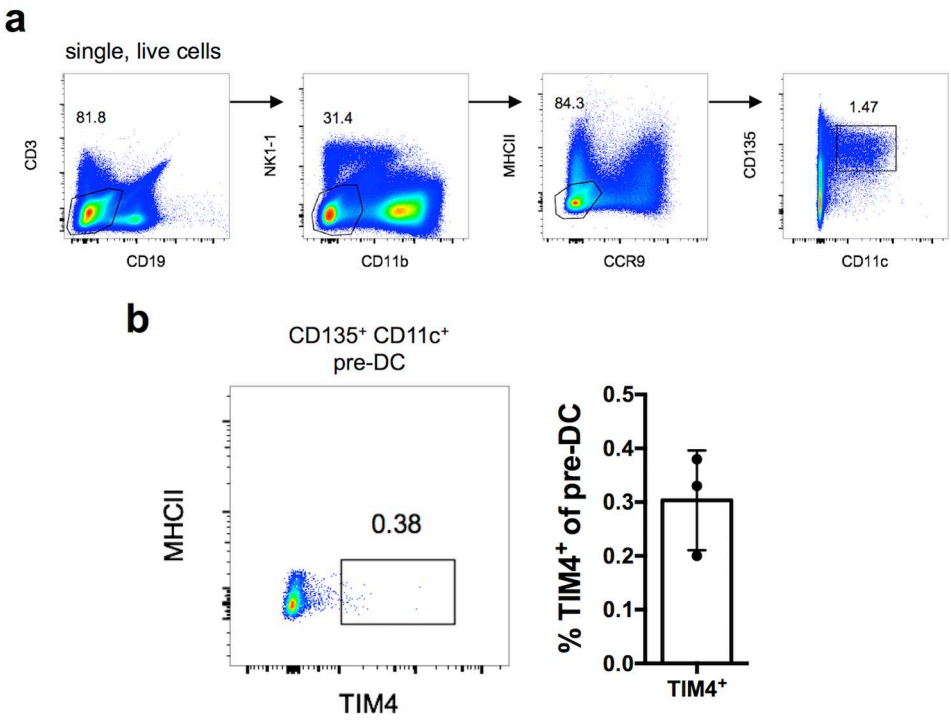

Figure 4. 10: TIM4 is expressed by very few bone marrow pre-DC

Bone marrow from C57BL/6 male mice was harvested and cells analysed by flow cytometry. **(a)** Representative gating strategy for pre-DC as single, live, CD3$^-$, CD19$^-$, NK1.1$^-$, CD11b$^-$, MHII$^-$, CCR9$^-$, CD135$^+$, CD11c$^+$ cells. **(b)** TIM4 expression is low on bone marrow pre-DC. Data represented as percentage TIM4$^+$ cells of pre-DC. Error bars represent S.D.

4.2.6 TIM4 is upregulated on DC migrating in lymph

We hypothesised that a DC looses TIM4 expression after taking up apoptotic cell-derived antigen in the intestine and migrating in lymph to the MLN. There it dies after antigen presentation to T cells, which then leave in the efferent lymph to enter back into circulation via the thoracic duct (Figure 4. 11a). In order to collect and study the phenotype of migratory lymph DC, we performed thoracic duct cannulation on mice that had previously undergone lymphadenectomy of the small intestinal (sMLNx) or colonic (cMLNx)

draining MLN specifically (Figure 4. 11b, c). This allowed us to differentiate between small intestinal and colonic DC that had taken up antigen and received signals to initiate migration (Figure 4. 11).

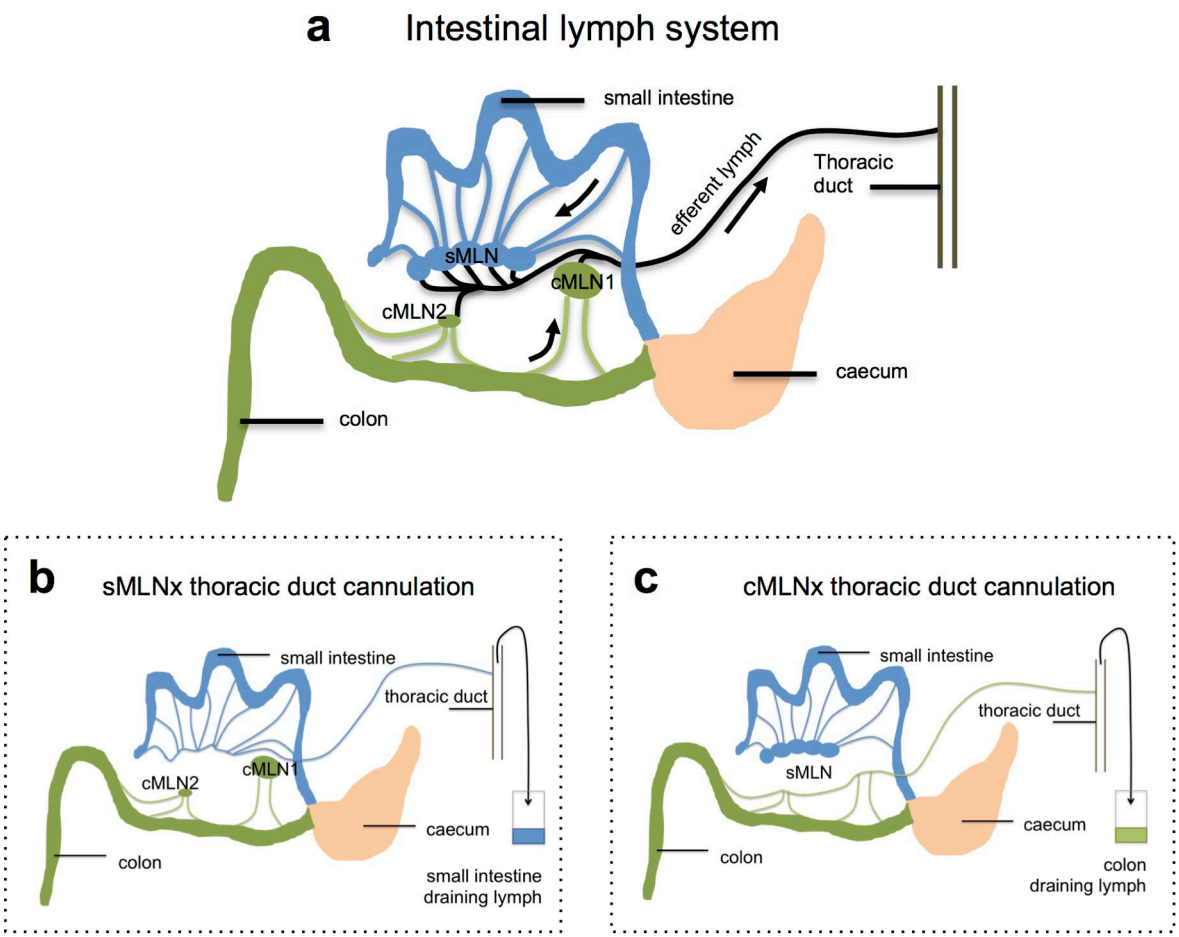

Figure 4. 11: Thoracic duct cannulation procedure overview

(a) Schematic detailing the anatomical localisation of small intestine and colon-draining MLN, and the direction of lymph flow to and from the nodes. After exiting the MLN, efferent lymph collects in the thoracic duct. In preparation for thoracic duct cannulation, mice undergo mesenteric lymphadenectomy six weeks beforehand, where either the small intestine (sMLNx, **b**) or colon-draining (cMLNx, **c**) lymph nodes are removed. During the recovery phase, lymph vessels reanastomose (**b**, **c**). After thoracic duct cannulation of these mice, collected efferent lymph will contain DC that have migrated from either the small intestine (blue, **b**) or colon (green, **c**).

Previous work in the laboratory led to production of an RNA-Sequencing (RNA-Seq) data set comparing DC from small intestinal LP and MLNx lymph (Dr Vuk Cerovic, Dr Lotta Utriainen, John Cole). When interrogated for the expression levels of *Timd4* (TIM4), a 3-4 fold increase in abundance was found in lymph compared with the LP in $CD11b^{+}$ $CD103^{-}$, $CD11b^{+}$ $CD103^{+}$ and $CD11b^{-}$ $CD103^{+}$ DC (unpublished, data not shown), contrary to our original hypothesis. We therefore sought to establish if this translated to the protein level, and if the colon-specific expression pattern we had previously observed also held true in lymph. We observed an increased percentage of $TIM4^{+}$ DC in both

sMLNx and cMLNx lymph compared with the LP (Figure 4. 2, Figure 4. 12). Furthermore, there was indeed a trend towards a higher percentage of TIM4$^+$ DC migrating from the colon than the small intestine, although this did not reach statistical significance (Figure 4. 12b). This trend also applied to the four DC subsets (Figure 4. 12b), which mirror those seen in the LP of the corresponding tissues (Figure 4. 12a), although increased numbers would be required to reach a statistically relevant conclusion.

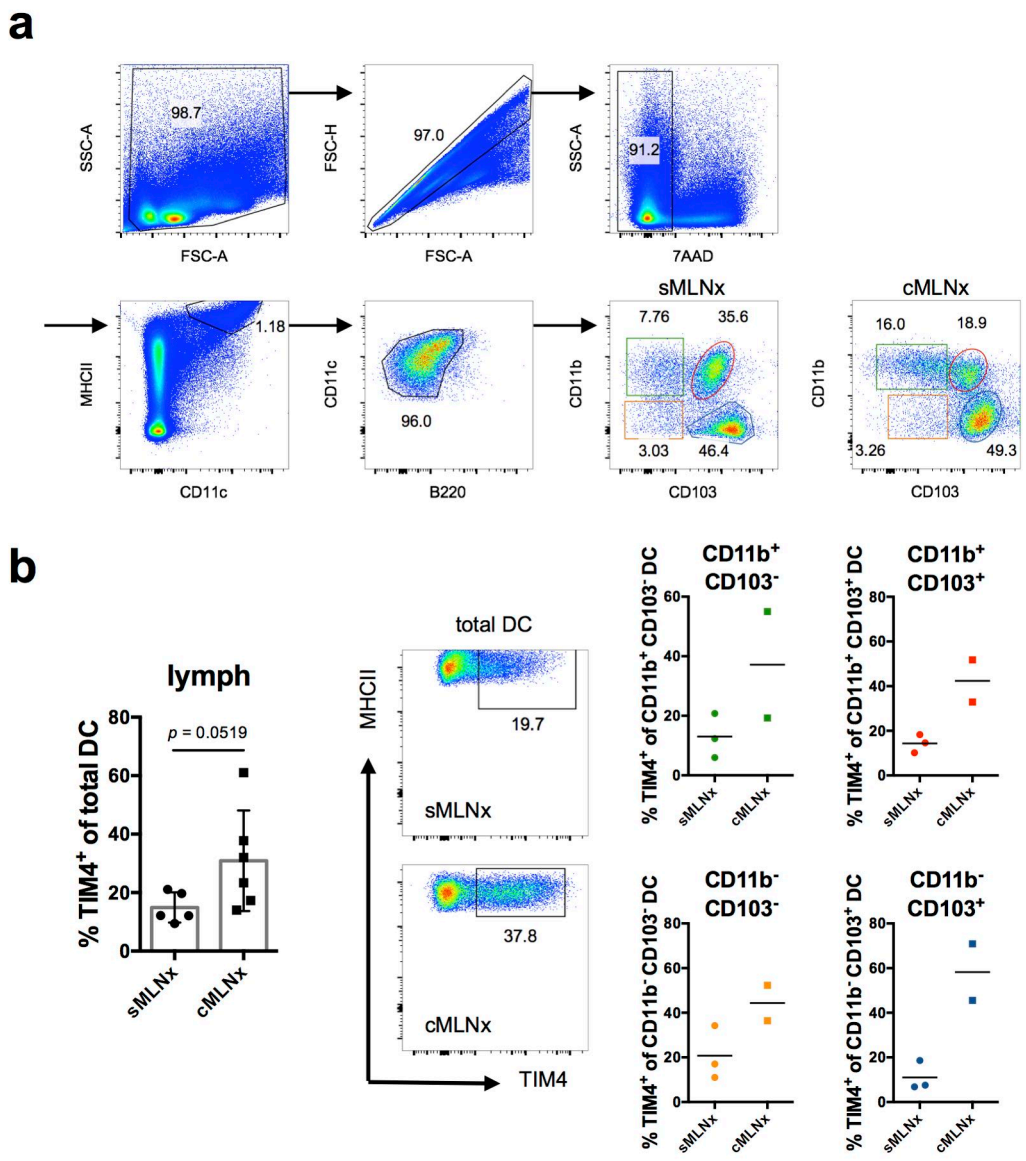

Figure 4. 12: A greater percentage of DC are TIM4$^+$ in cMLNx compared with sMLNx lymph

Lymph was collected from sMLNx and cMLNx mice after thoracic duct cannulation and cells analysed by flow cytometry. **(a)** Representative gating strategy for lymph DC populations gated as single, live, MHCII$^+$, CD11c$^+$, B220$^-$ cells. **(b)** Data are shown as the percentage of TIM4$^+$ total DC or DC population in cMLNx compared with sMLNx lymph. Error bars represent S.D.; statistical analysis for total DC was carried out using a Mann-Whitney test.

4.2.7 TIM4 is expressed on migratory and resident DC in mesenteric and peripheral lymph nodes

The findings that TIM4 was upregulated on DC subsets migrating in lymph compared to the LP suggested to us that it might be involved in the maturation process undergone by DC in preparation for antigen presentation in the lymph node. We therefore determined the percentage of DC that were TIM4$^+$ in the MLN that drain the small intestine (sMLN), and colon (cMLN), as well as the inguinal lymph nodes (ILN). Migratory DC in the LN present higher levels of MHCII on their surface than resident DC (Figure 4. 13a) (Houston et al. 2016), which was used to distinguish the two populations. Whilst TIM4 expression hardly differed between resident and migratory DC in the MLN, the cMLN contained a higher frequency of TIM4$^+$ DC among both resident and migratory populations compared with the sMLN (Figure 4. 13b). Interestingly, the proportion of migratory TIM4$^+$ DC was highest in the ILN (Figure 4. 13b).

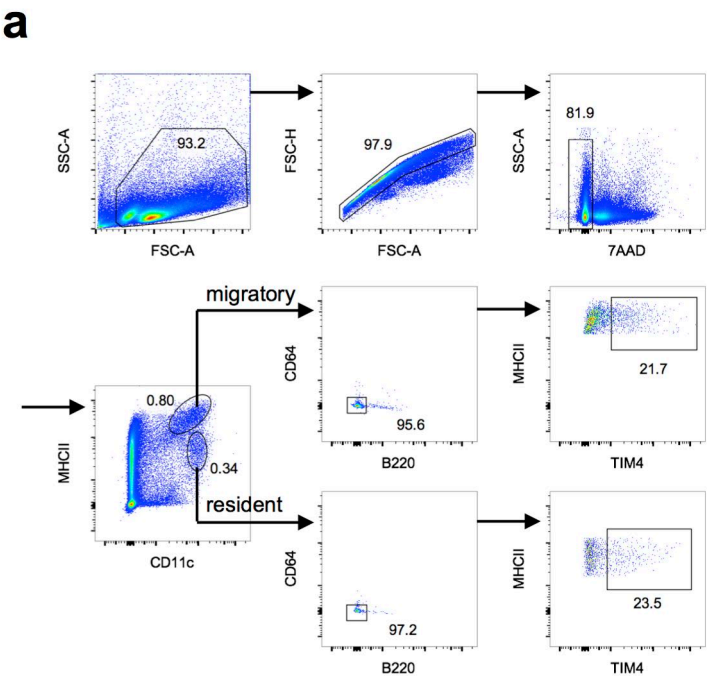

Figure 4.13 continued on next page

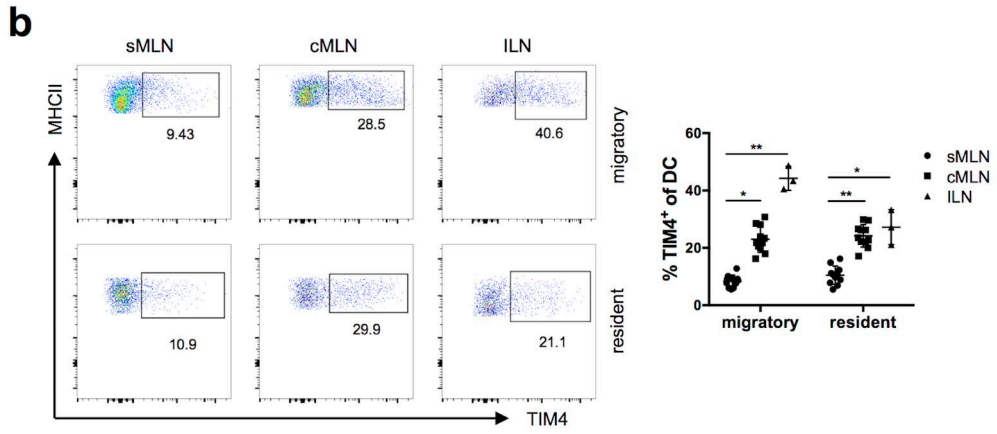

Figure 4. 13: More migratory and resident DC in the cMLN are TIM4$^+$ compared with the sMLN

Small intestine (sMLN) and colon-draining (cMLN) MLN and inguinal lymph nodes (ILN) were harvested from C57BL/6 mice and cells analysed by flow cytometry. **(a)** Representative plots showing gating strategy for DC gated on single, live cells. The level of MHCII expression helps distinguish between migratory and resident DC. DC are defined as CD64$^-$ (F4/80$^-$), B220$^-$ cells. **(b)** Representative plots are shown of the expression of TIM4 on migratory and resident DC in sMLN, cMLN and ILN. The percentage of TIM4$^+$ cells among migratory and resident DC is higher in the cMLN compared with the sMLN, and ILN migratory DC have the highest TIM4 expression of all. Error bars represent S.D.; statistical analysis performed within migratory and resident populations using a Kruskal-Wallis test with a Dunn's post-test for multiple comparisons. * $p < 0.01$, ** $p < 0.001$.

We compared the different migratory DC populations in the sMLN and cMLN for their levels of TIM4 expression and found that the increase in proportion of TIM4$^+$ DC in the cMLN compared with the sMLN was true for all subsets but the CD11b$^-$ CD103$^-$ DC (Figure 4. 14a, b). Strikingly, CD11b$^+$ CD103$^+$ DC in both the sMLN and cMLN had the highest proportion of TIM4$^+$ cells, with 20% and 50% expressing TIM4 in the respective tissues (Figure 4. 14b).

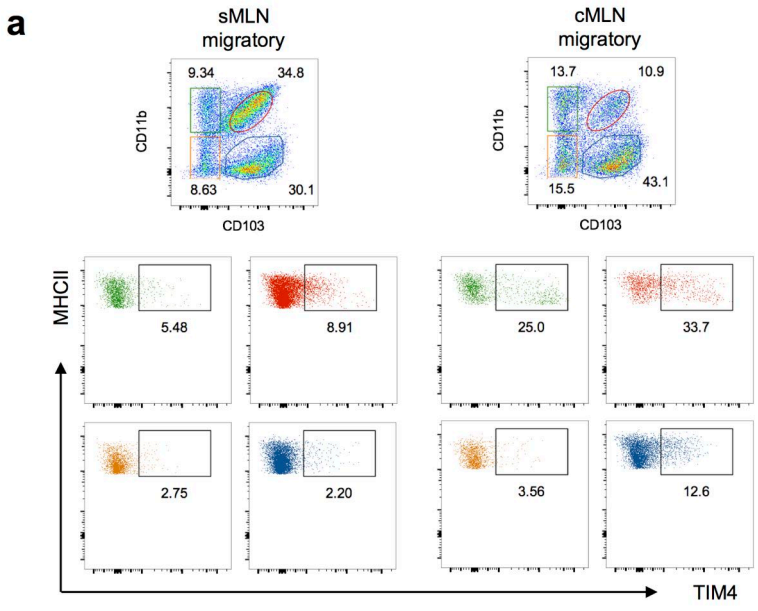

Figure 4.14 continued on next page

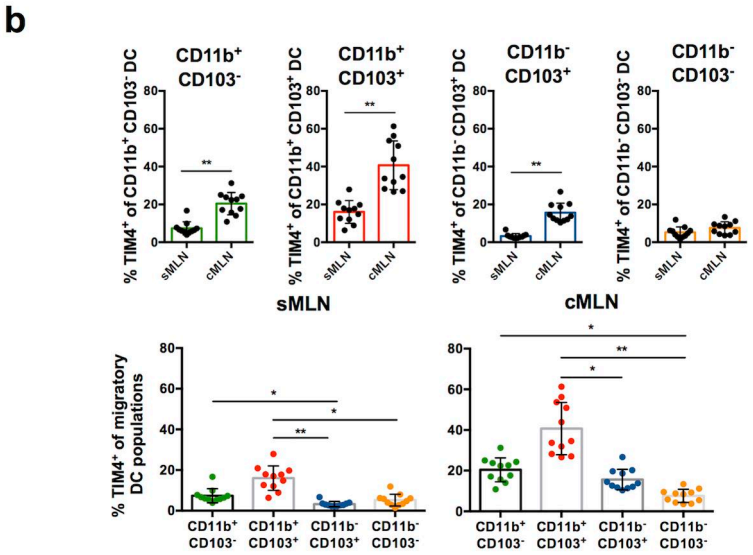

Figure 4. 14: CD11b$^+$ CD103$^+$ DC have the highest percentage of TIM4$^+$ cells in both sMLN and cMLN

Small intestine (sMLN) and colon-draining (cMLN) MLN were harvested from C57BL/6 mice and cells analysed by flow cytometry. **(a)** Representative plots showing migratory DC populations and their expression of TIM4 in sMLN and cMLN gated on single, live, CD45+, MHCII^{hi}, CD11c+, CD64-, B220- cells. Four DC populations can be defined based on expression of CD11b and CD103: CD11b$^+$ CD103$^-$ (green), CD11b$^+$ CD103$^+$ (red), CD11b$^-$ CD103$^+$ (blue) and CD11b$^-$ CD103$^-$ (orange). **(b)** Percentage of TIM4$^+$ cells among migratory DC populations of sMLN and cMLN. Error bars represent S.D.; statistical analyses performed using (top row) a Mann-Whitney test, or (bottom row) a Kruskal-Wallis test with a Dunn's post-test for multiple comparisons. * $p < 0.05$, ** $p < 0.0001$.

Mapping the changes in TIM4 expression with the path of migration for small intestinal and colonic tissues helps identify two main patterns. First, the percentage of TIM4$^+$ cells increases for all DC populations with migration to the MLN (Figure 4. 15a). Second, once arrived in the cMLN, migratory colonic DC exhibit a population-specific pattern of TIM4 expression, where the percentage of TIM4$^+$ cells is only further increased for CD11b$^+$ CD103$^-$ and CD11b$^+$ CD103$^+$ DC in the cMLN (Figure 4. 15b). Conversely, proportions of TIM4-expressing CD11b$^-$ CD103$^+$ and CD11b$^-$ CD103$^-$ DC decrease, albeit to levels higher than those found in the LP (Figure 4. 15b).

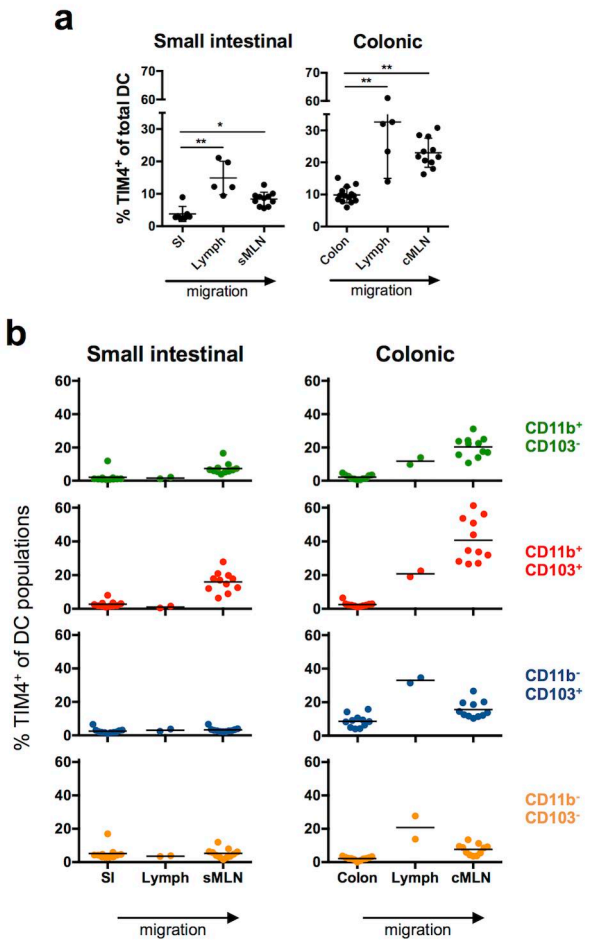

Figure 4. 15: Mapping TIM4 expression with DC migration

(a) TIM4 expression on total DC increases with migration and remains high in the MLN for both small intestinal (SI) and colonic DC. Data are shown as the percentage of $TIM4^+$ cells among total DC in small intestinal and colonic associated tissues. **(b)** Summary of TIM4 expression changes on DC populations in small intestinal and colonic associated tissues. Data are shown as the percentage of $TIM4^+$ cells within the DC populations. Error bars represent S.D.; statistical analysis was carried out using a Kruskal-Wallis test, and a Dunn's post-test for multiple comparisons. * $p < 0.05$, * $p < 0.001$.

4.2.8 TIM1 is preferentially expressed on colonic $CD45^-$ and $CD45^+$ populations in intestinal but not lymphoid tissue

Having observed that the expression of TIM4 on DC is not limited to the intestine, but increases in lymph, we hypothesised that TIM4 may be acting in a capacity other than purely as an apoptotic cell receptor. Previous work has demonstrated that TIM4 is the natural ligand for TIM1 (Meyers et al. 2005), also a member of the TIM family of proteins that acts as a PS receptor (Kobayashi et al. 2007). We first analysed TIM1 expression on the $CD45^-$ cell compartment of the intestines, which is comprised of IEC, stromal cells and endothelial cells. Interestingly, a greater percentage of colonic $CD45^-$ cells expressed TIM1 when compared with the small intestine (Figure 4. 16).

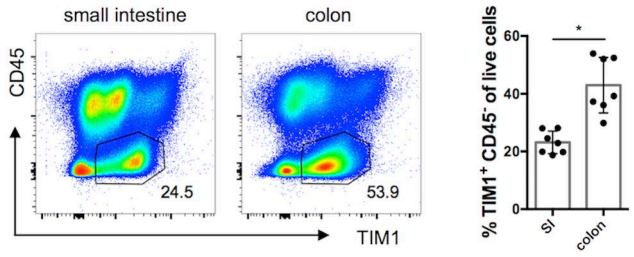

Figure 4. 16: TIM1 expression on CD45$^-$ cells is higher in the colon than the small intestine

Small intestinal (SI) and colonic tissues were harvested from *Cx3cr1*$^{+/gfp}$ mice and cells analysed by flow cytometry. Representative plots show CD45$^-$ TIM1$^+$ cells gated on single, live cells. Data are shown as the percentage of CD45$^-$ TIM1$^+$ cells of live cells. Error bars represent S.D.; statistical analysis was performed using a Mann-Whitney test. * $p < 0.001$.

Furthermore, we found that 80% of mature CX3CR1^{hi} macrophages expressed TIM1 in both the small intestine and the colon (Figure 4. 17).

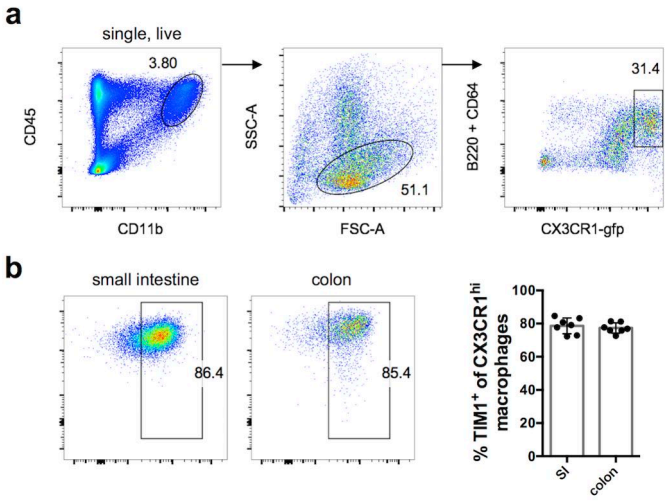

Figure 4. 17: TIM1 is highly expressed on CX3CR1^{hi} macrophages in the intestine

Intestinal tissues from *Cx3cr1*$^{+/gfp}$ mice were collected and LP cells analysed by flow cytometry. **(a)** Representative plots of colonic tissue are shown illustrating the gating strategy for CD11b$^+$ CD64$^+$ CX3CR1^{hi} macrophages. **(b)** Representative plots of TIM1 staining on small intestinal and colonic macrophage populations, and summary data shown as the percentage of TIM1$^+$ cells within CX3CR1^{hi} macrophages of the small intestine (SI) and colon. Error bars represent S.D.; statistical analysis was performed using a Mann-Whitney test.

In lymph, the expression of TIM1 on migrating cells was much lower than that seen on macrophages in the LP. Lymph cells that made up the total TIM1$^+$ populations were MHCII$^+$ B220$^+$ B cells (40%), CD8$^+$ T cells (15-25%) and B220$^-$ CD8$^-$ lymphocytes (20-30%), most likely to be mainly CD4$^+$ T cells (Figure 4. 18a). Interestingly, within the TIM1$^+$ CD8$^+$ T cell compartment, a distinct population of CD103^{int} cells could be identified (Figure 4. 18a). Overall, TIM1$^+$ cells only corresponded to ≤ 0.5% of either lymph B cells or

CD8⁺ T cells (Figure 4. 18b). There was no significant difference in TIM1 expression on lymphocyte populations between sMLNx and cMLNx lymph (Figure 4. 18).

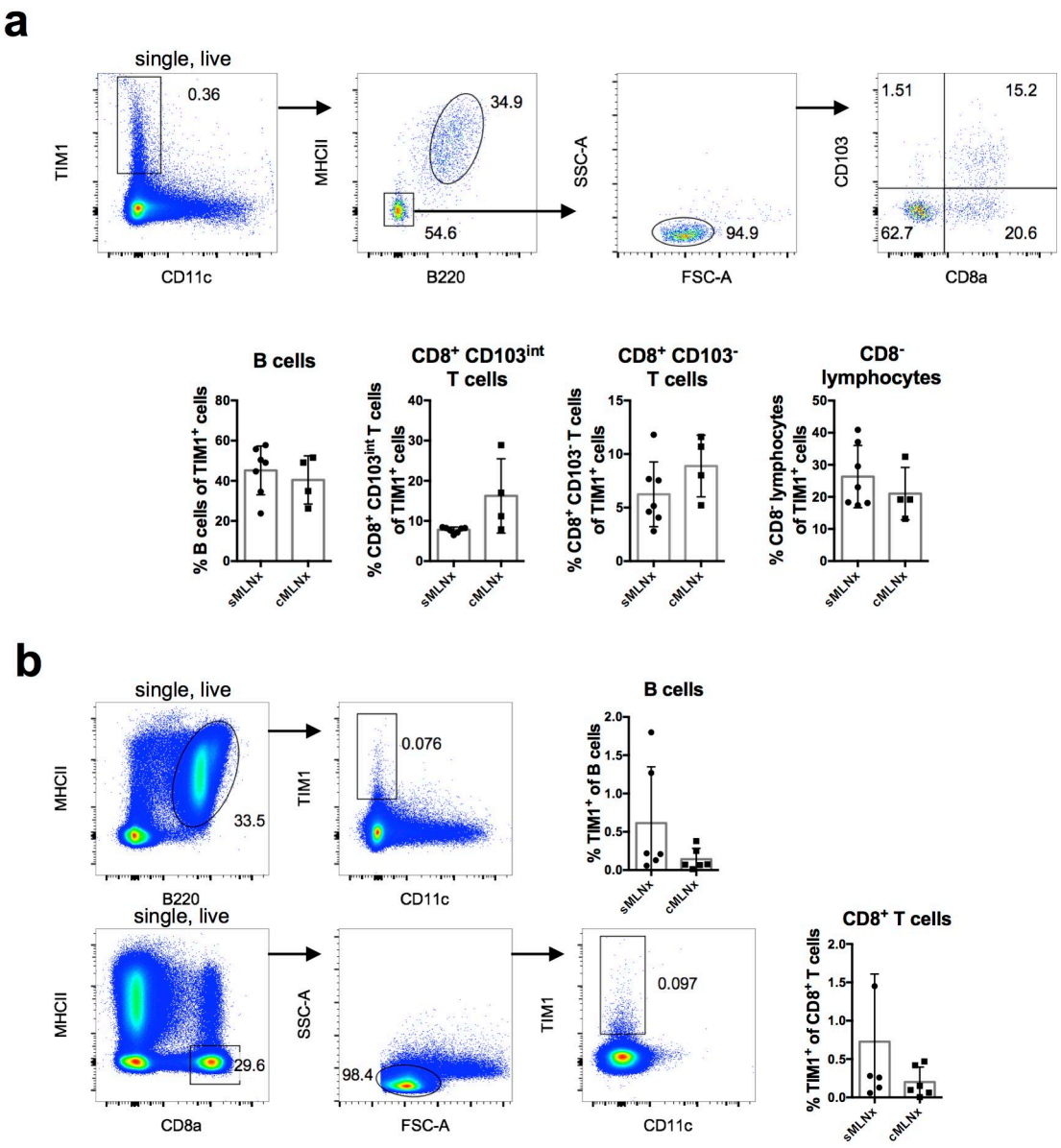

Figure 4. 18: TIM1 is expressed on a small subset of B cells and CD8⁺ T cells in lymph

Lymph was collected after thoracic duct cannulation of sMLNx and cMLNx animals and the expression of TIM1 on lymphocyte populations analysed by flow cytometry. **(a)** Total TIM1⁺ cells were gated on single, live cells. The TIM1⁺ population was made up of MHCII⁺ B220⁺ B cells, and CD8⁺ and CD8⁻ lymphocytes. The CD8⁺ lymphocytes could be further separated into CD103^int and CD103⁻ populations. **(b)** B cells were gated as single, live, MHCII⁺ B220⁺ cells. CD8⁺ T cells were gated as single, live, MHCII⁻, CD8α⁺, SSC^lo, FSC^lo cells. Data are represented as percentage of TIM1⁺ cells among lymphocyte populations. Error bars represent S.D.; statistical analysis was carried out using a Mann-Whitney test.

In the MLN, the majority of TIM1⁺ cells were MHCII⁺ B220⁺ B cells (Figure 4. 19a). TIM1 staining on CD8⁺ T cells could not be detected in the MLN (Figure 4. 19a). Overall, only about 2% of B cells expressed TIM1 in both sMLN and cMLN (Figure 4. 19b).

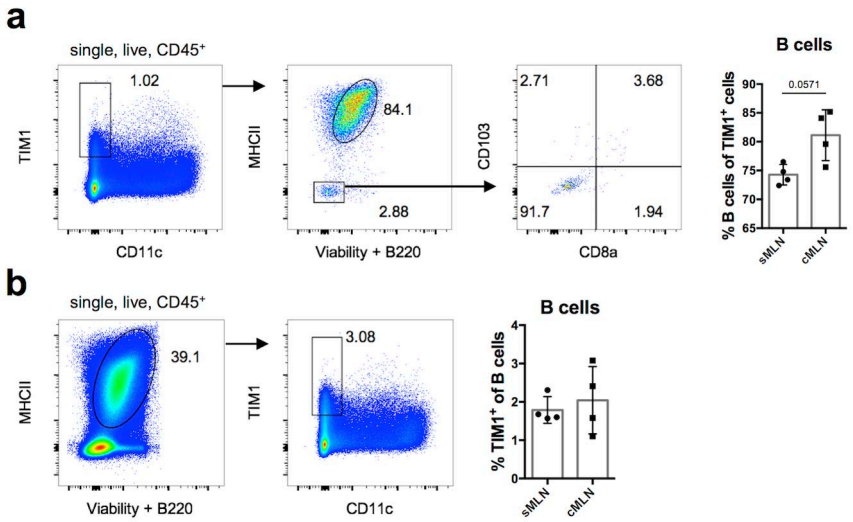

Figure 4. 19: TIM1 is mainly expressed on B cells in the MLN

Small intestinal (sMLN) and colonic (cMLN) draining MLN were harvested from C57BL/6 mice and cell populations analysed by flow cytometry. **(a)** TIM1$^+$ CD11c$^-$ cells were gated on single, live, CD45$^+$ cells. These were comprised of mainly B220$^+$ MHCII$^+$ B cells, and a small population of CD8α$^-$ CD103$^-$ cells. **(b)** B cells were gated as single, live, CD45$^+$, MHCII$^+$, B220$^+$ cells. Data are represented as percentage of B cells among TIM1$^+$ cells **(a)**, and TIM1$^+$ cells among B cells **(b)**. Error bars represent S.D.; statistical analysis was carried out using a Mann-Whitney test.

4.2.9 TIM4 expression on colonic DC may correspond with a migratory signature

Given that a significant proportion of DC upregulate TIM4 when they migrate, we sought to establish if this could in fact be used as a marker of colonic CD11b$^-$ CD103$^+$ DC that had taken up antigen and were just ready to begin migration to the cMLN. One important step in this process is the upregulation of CCR7 (Förster et al. 1999). To begin to answer this question, we FACS-sorted TIM4$^+$ and TIM4$^-$ colonic CD11b$^-$ CD103$^+$ DC (Figure 4. 20a, b) and measured mRNA levels of *Ccr7* by quantitative real-time PCR (qRT-PCR). In accordance with our hypothesis, we found that TIM4$^+$ DC expressed higher levels of *Ccr7* than TIM4$^-$ DC (Figure 4. 20c). Interestingly, *Il1b* mRNA levels were also higher in TIM4$^+$ CD11b$^-$ CD103$^+$ DC compared with their TIM4$^-$ counterparts, thereby implicating the inflammasome pathway as preferentially upregulated in these cells (Figure 4. 20c).

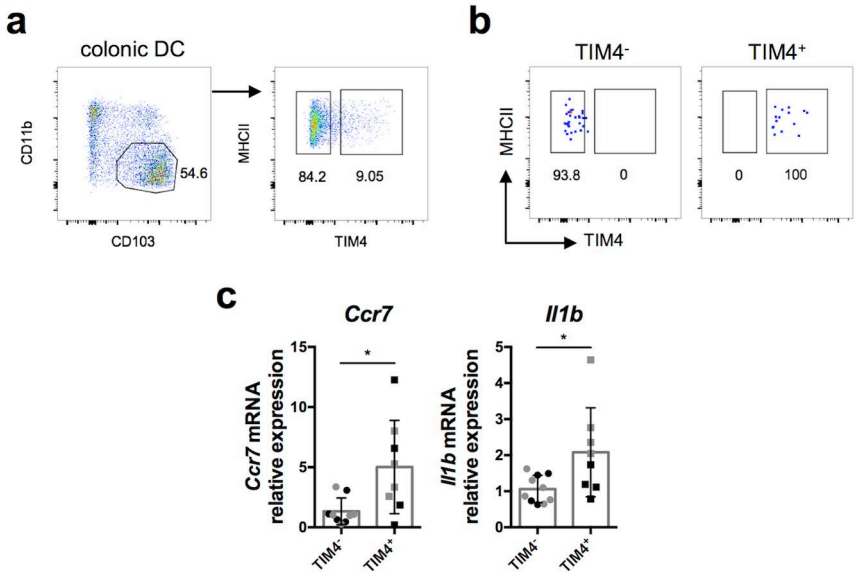

Figure 4. 20: Colonic TIM4$^+$ CD11b$^-$ CD103$^+$ DC express more *Ccr7* and *Il1b* mRNA than their TIM4$^-$ counterparts

Colons were harvested from C57BL/6 mice and TIM4$^+$ and TIM4$^-$ CD11b$^-$ CD103$^+$ DC FACS sorted for analysis of *Ccr7* and *Il1b* mRNA levels by quantitative real-time PCR (qRT-PCR). **(a)** Representative plots showing pre-sort gating strategy of TIM4$^+$ and TIM4- CD11b$^-$ CD103$^+$ DC gated on single, live, CD45$^+$, MHCII$^+$, CD11c$^+$, CD64$^-$, B220$^-$ cells. **(b)** Representative plots showing sort purity of TIM4$^+$ and TIM4$^-$ populations. **(c)** The levels of *Ccr7* and *Il1b* mRNA are higher in TIM4$^+$ CD11b$^-$ CD103$^+$ DC compared with their TIM4$^-$ counterparts. Data are represented as normalised to expression of housekeeping gene TATA-binding protein (ΔCt), and relative to the mean ΔCt value of the TIM4$^-$ population. Data pooled from two experiments (grey and black symbols). Error bars represent S.D.; statistical analysis was carried out using an unpaired t test. * $p < 0.05$.

We analysed the colonic LP of *Ccr7*$^{gfp/gfp}$ knockout/knockin mice, in which both copies of the *Ccr7* gene has been replaced by *gfp*, by flow cytometry to confirm the protein levels of CCR7 on TIM4$^+$ and TIM4$^-$ colonic DC. The experimental procedures for this analysis were kindly carried out by Dr Vuk Cerovic at the Universitätsklinikum Aachen. Indeed, as previously found on an mRNA level, TIM4$^+$ DC had a trend towards higher proportion of gfp$^+$ cells than TIM$^-$ DC, therefore pointing towards increased expression of CCR7 (Figure 4. 21a). Furthermore, the same trend was observed for all colonic DC populations, except for CD11b$^+$ CD103$^-$ DC (Figure 4. 21b). The low percentage of TIM4$^+$ cells in all but CD11b$^-$ CD103$^+$ DC, however, indicates the need for caution when interpreting these data (Figure 4. 21b). Not all CCR7$^+$ cells were TIM4$^+$, which corresponds to the fact that not all migrating lymph DC express TIM4. However, the reverse was also true in that not all TIM4$^+$ cells expressed CCR7. This suggests that TIM4 is not a straightforward marker for migrating cells in the LP, but is likely to have a broader spectrum of functionality.

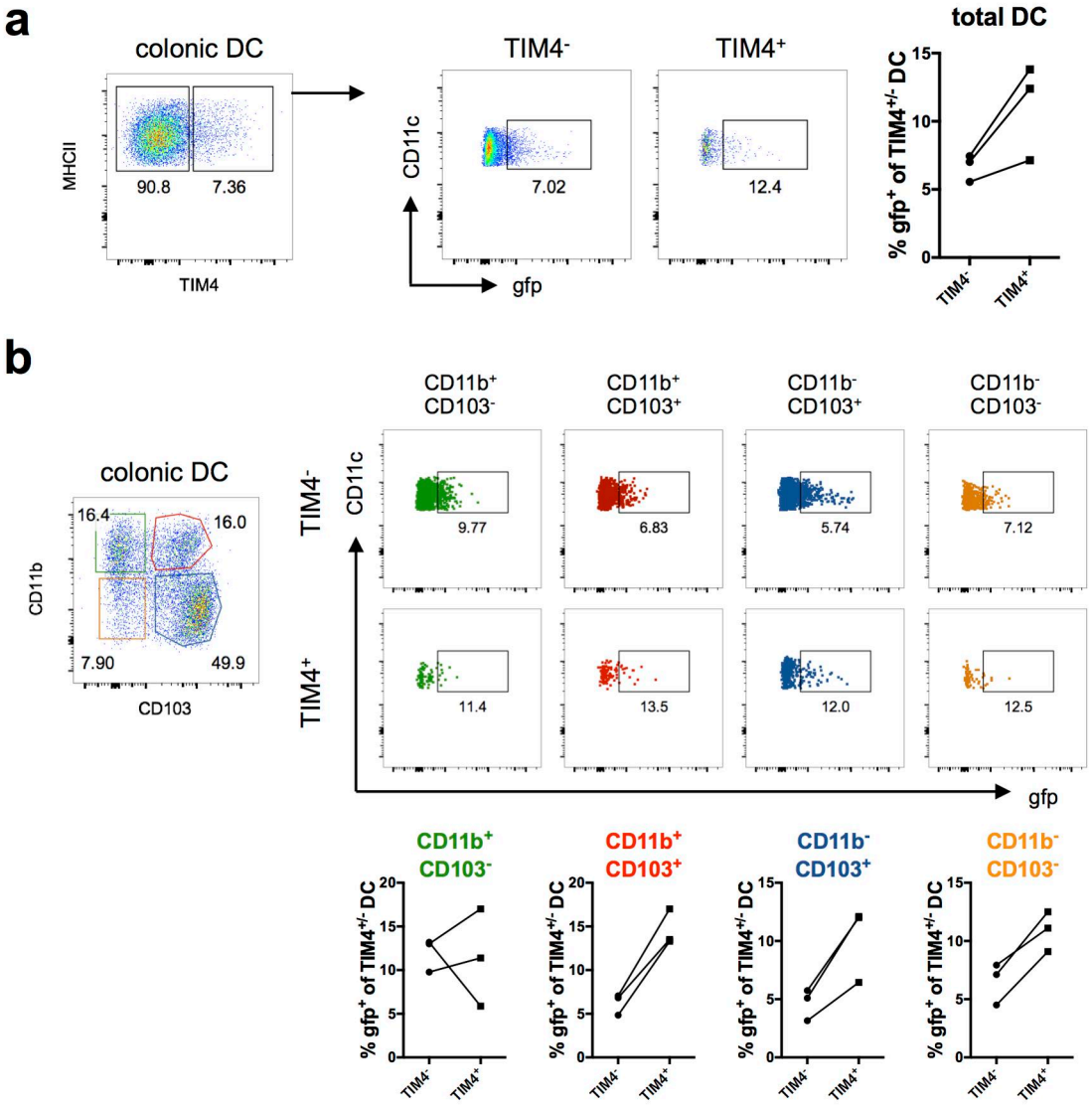

Figure 4. 21: Colonic TIM4⁺ DC may comprise a higher percentage of CCR7-gfp⁺ cells than TIM4⁻ DC

Colonic tissues were harvested from *Ccr7*$^{gfp/gfp}$ knockout/knockin mice and LP cells analysed by flow cytometry. **(a)** Representative plots and summary data showing GFP expression in TIM4⁻ and TIM4⁺ total colonic DC gated on single, live, CD45⁺, MHCII⁺, CD11c⁺, CD64⁻ cells. **(b)** Representative plots and summary data showing GFP expression in TIM4⁻ and TIM4⁺ cells of DC populations gated on single, live, CD45⁺, MHCII⁺, CD11c⁺ CD64⁻ cells. Data are represented as the percentage of GFP⁺ cells among TIM4⁺/TIM4⁻ populations. Statistical analysis was carried out using a Wilcoxon matched-pairs signed rank test.

To better understand the link between TIM4 expression on DC and migration to the MLN, we photoconverted the colons of Kaede mice and determined the percentage of Kaede-red⁺ migratory DC in the cMLN 24 h and 48 h post-switching. We observed a trend towards a greater percentage of Kaede-red⁺ cells within the TIM4⁺ population compared with the TIM4⁻ population of migratory DC at both 24 h and 48 h after colon photoconversion (Figure 4. 22a, b). However, when we analysed DC in the colonic LP at these time points, we also saw that more TIM4⁺ DC were Kaede-red⁺ compared with TIM4⁻ DC, even though the overall frequency of Kaede-red⁺ DC decreased, as expected (Figure 4. 22c).

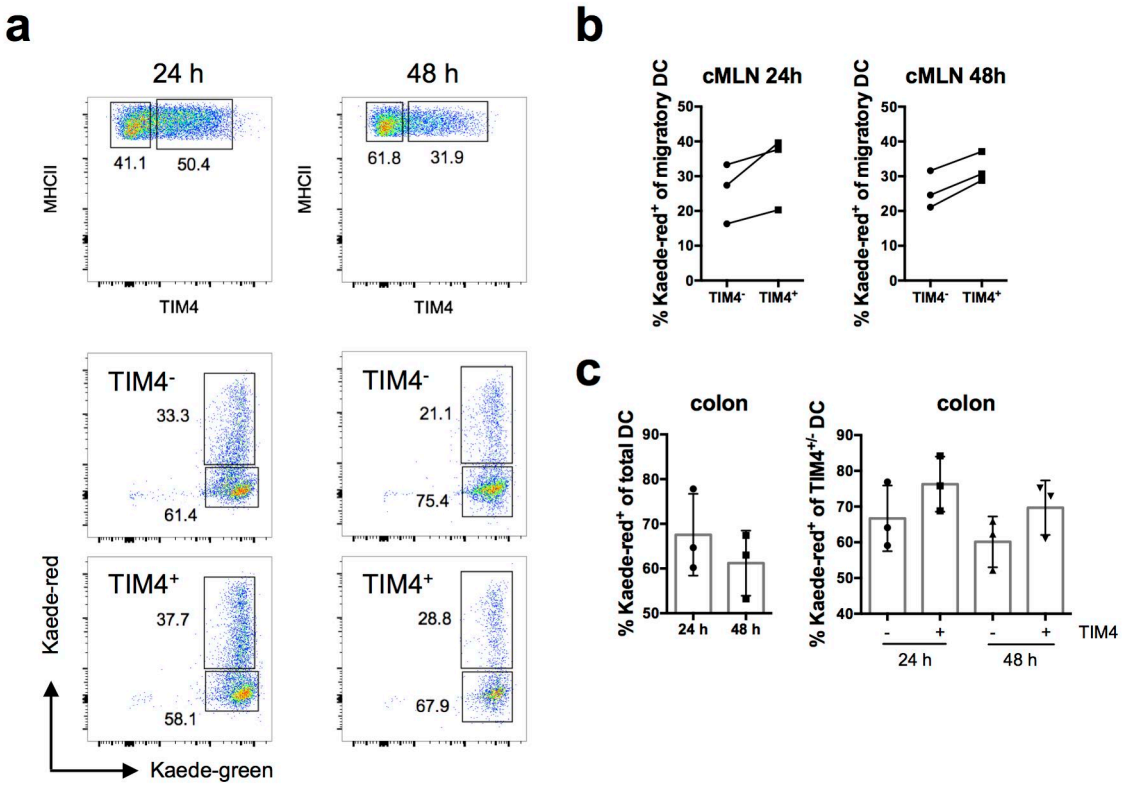

Figure 4. 22: cMLN TIM4$^+$ DC may comprise a higher percentage of Kaede-red$^+$ migratory DC compared with TIM4$^-$ DC

The proximal colons of Kaede mice were photoconverted after surgical laparotomy using violet light and the proximal colons and cMLN harvested at 24 h and 48 h timepoints. **(a)** Total cMLN DC gated on single, live, CD45$^+$, MHCII^{hi}, CD11c$^+$, CD64$^-$, B220$^-$ cells. Representative plots showing TIM4 expression on total cMLN DC and the percentage of Kaede-red$^+$ cells among TIM4$^-$ and TIM4$^+$ DC at 24 h and 48 h post-photoconversion. **(b)** The percentage of Kaede-red$^+$ DC among TIM4$^+$ DC and TIM4$^-$ DC in the cMLN. **(c)** Summary plots showing the percentage of Kaede-red$^+$ cells among total DC, and TIM4$^-$ and TIM4$^+$ DC, in the colonic LP 24 h and 48 h post-photoconversion. Error bars represent S.D.; statistical analysis carried out using a Wilcoxon matched-pairs signed rank test **(b)**, and a Mann-Whitney test or a Kruskal-Wallis test with a Dunn's post-test for multiple comparisons **(c)**.

4.2.10 TIM4$^+$ and TIM4$^-$ MLN DC have different RA-producing capacity and *Aldh1a2* mRNA expression levels

Having found that TIM4 expression may correlate with a migratory signature in colonic LP and cMLN, we next aimed to determine whether TIM4$^+$ and TIM4$^-$ DC differed functionally after arrival in the MLN. The ability of migratory CD103$^+$ DC to induce gut-homing T cells in the MLN through the production of RA has been extensively studied (Iwata et al. 2004, Coombes et al. 2007, Jaensson et al. 2008). Recent work from our laboratory has shown that DC from the small intestinal LP and sMLN have greater activity of RALDH (*Aldh1a2*), the enzyme required for metabolism of vitamin A to RA, than colonic and cMLN DC (Houston et al. 2016). However, it is conceivable that cMLN DC still require the ability to produce RA, albeit at reduced levels. Given that MLN CD11b$^+$ CD103$^+$ DC have the highest frequency of TIM4$^+$ cells compared with the other DC populations (Figure 4. 14b), we assessed the RALDH activity of sMLN and cMLN CD11b$^+$ CD103$^+$ DC. Consistent with previously published work, we found a trend towards higher RA producing capacity in sMLN migratory DC compared with the cMLN (Figure 4. 23a, b). Interestingly, in the sMLN TIM4$^+$ CD11b$^+$ CD103$^+$ DC had a greater proportion of RALDH$^+$ cells than TIM4$^-$ DC (Figure 4. 23c). The same trend was not, however, observed in the cMLN. Furthermore, the number of TIM4$^+$ RALDH$^+$ DC in the sMLN is very small (Figure 4. 23c), so it is difficult to draw a valid conclusion from this observation. Finally, when we determined the mRNA levels of *Aldh1a2* in FACS-sorted TIM4$^+$ and TIM4$^-$ total CD11b$^+$ migratory sMLN and cMLN DC by qRT-PCR, we did not find a difference in *Aldh1a2* expression (Figure 4. 23d).

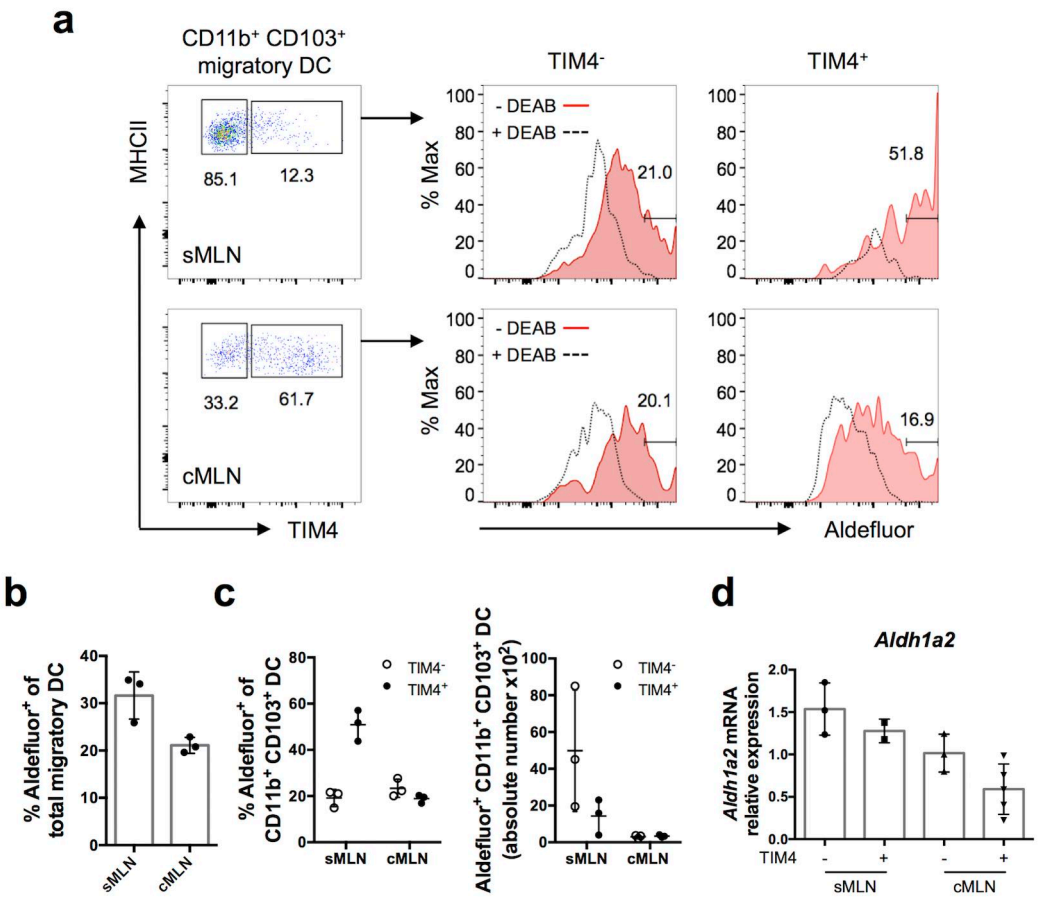

Figure 4. 23: TIM4$^+$ and TIM4$^-$ MLN DC have different *Aldh1a2* mRNA expression levels and retinoic acid producing capacity

(a-c) Small intestine (sMLN) and colon (cMLN) draining MLN were harvested from C57BL/6 mice and subjected to the Aldefluor assay to detect RALDH activity before staining with antibodies to surface markers and analysis by flow cytometry. **(a)** Representative plots show TIM4 expression levels on CD11b+ CD103+ migratory MLN DC (gated on single, live, MHCII$^+$, CD11c$^+$, CD64$^-$, B220$^-$ cells) and the levels of RALDH activity (corresponding to Aldefluor fluorescence intensity) exhibited by TIM4$^-$ and TIM4$^+$ populations. DEAB-treated cells served as an internal negative control for each sample, allowing the positive gate to be determined and background staining to be disregarded. **(b)** Percentage of RALDH$^+$ cells among total migratory DC compared between the sMLN and cMLN. **(c)** Data are shown as percentage of RALDH$^+$ cells among the TIM4$^+$ and TIM4$^-$ subsets of CD11b$^+$ CD103$_+$ migratory MLN DC and their absolute cell number. **(c)** sMLN and cMLN cells were harvested from C57BL/6 mice and single, live, CD45$^+$, MHCII$^+$, CD11c$^+$, CD64$^-$, B220$^-$, total CD11b$^+$ migratory DC were FACS-sorted and *Aldh1a2* mRNA expression levels determined by qRT-PCR. Data are shown as normalised to expression of the housekeeping gene *Tbp* (ΔCt) and relative to the mean ΔCt value of the TIM4$^-$ DC population of either sMLN or cMLN. Data are representative of two separate experiments. Error bars represent S.D.; statistical analysis was performed using a Mann-Whitney test within each tissue group **(b)**, or a Kruskal-Wallis test and a Dunn's post-test for multiple comparisons **(c)**

4.2.11 TIM4 expression on DC does not influence their ability to prime antigen-specific CD4$^+$ T cell responses *in vitro*

We next aimed to determine if this potential difference in RALDH expression had any functional impact on induction of CCR9 on T cells. We also aimed to test the hypothesis that TIM4$^+$ migratory DC in the MLN were more mature and able to drive antigen-specific T cell responses than TIM4$^-$ DC. We FACS-purified TIM4$^+$ and TIM4$^-$ subsets of MLN migratory total CD11b$^+$ and CD103$^+$ CD11b$^-$ DC (Figure 4. 24), pulsed them with ovalbumin (OVA) 323-339 peptide and co-cultured them with CFSE-labelled OT-II MLN cells for five days before analysis of T cell proliferation, CCR9 and cytokine expression by flow cytometry.

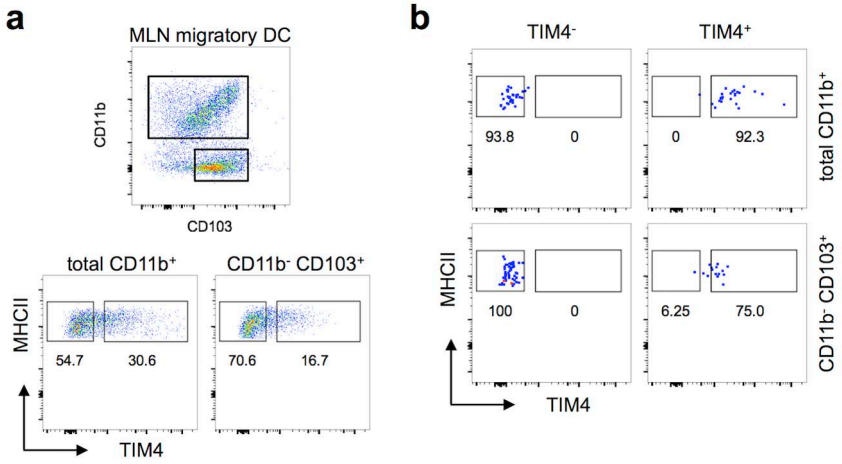

Figure 4. 24: FACS sort gating for MLN DC co-cultured with OT-II MLN cells

Total MLN were harvested from C57BL/6 mice and migratory DC populations FACS sorted for co-culture with OT-II MLN cells. **(a)** Cells were gated as single, live, CD45$^+$, MHCII$^+$ CD11c$^+$, CD64$^-$, B220$^-$; populations sorted were TIM4$^-$ and TIM4$^+$ cells within total CD11b$^+$ DC and CD103$^+$ CD11b$^-$ DC populations.
(b) Representative plots showing sort purity of MLN DC populations.

However, no significant differences were observed in the ability of TIM4$^-$ and TIM4$^+$ DC to drive antigen-specific CD4$^+$ T cell expansion (Figure 4. 25a), or differentiation into Th1 (Figure 4. 25b), Th17 (Figure 4. 25c) or Treg cells (Figure 4. 25d). The levels of CCR9 detected at this time point were too low to allow us to make any valid conclusions (data not shown).

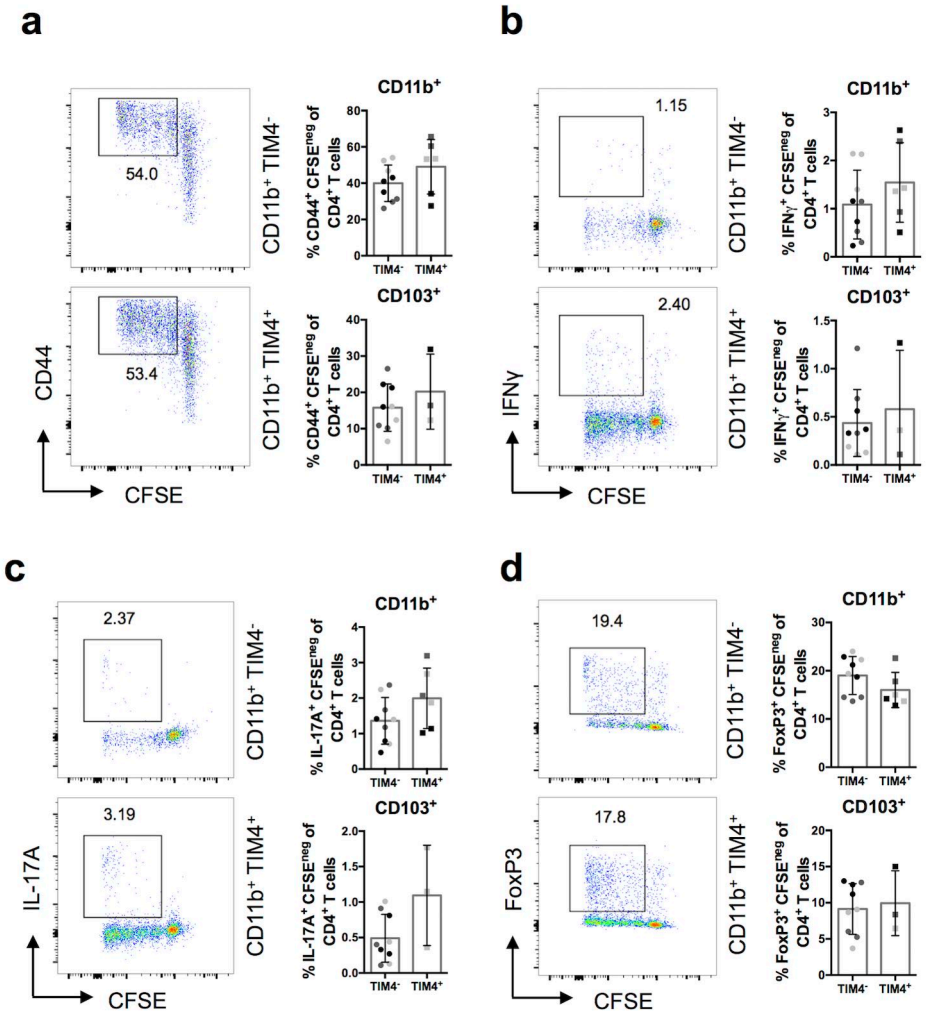

Figure 4. 25: TIM4$^-$ and TIM4$^+$ MLN DC can induce antigen-specific T cell responses with equivalent efficiency *in vitro*

Total MLN were harvested from C57BL/6 mice and migratory DC populations FACS sorted for co-culture with OT-II MLN cells. For this, 4,000 DC were pulsed with 3 µg/ml ovalbumin (OVA) 323-339 peptide for 30 min, and co-cultured with 200,000 CFSE-labelled OT-II total MLN cells. After five days, these were harvested and analysed by flow cytometry. Representative plots for CD11b$^+$ TIM4$^{+/-}$ subsets and summary data shown as percentages of CD44$^+$ CFSE$^-$ **(a)**, IFNγ$^+$ CFSE$^-$ **(b)**, IL-17A$^+$ CFSE$^-$ **(c)** and FoxP3$^+$ CFSE$^-$ **(d)** cells among single, live, CD3$^+$, CD4$^+$ T cells are shown. Symbols of the same shade of grey represent technical replicates from DC sorted from the same MLN. Error bars represent S.D.

4.2.12 TIM4$^-$ and TIM4$^+$ lymph DC can induce specific T cell responses to *in vivo* acquired antigen with equivalent efficiency

We could not determine any difference in the ability of TIM4$^-$ and TIM4$^+$ MLN DC to drive antigen-specific T cell responses *in vitro*. This may point to the fact that TIM4 on DC is important in controlling antigen acquisition and processing rather than priming itself. In order to investigate this, we performed thoracic duct cannulation of MLNx mice that had been gavaged with 10 mg OVA immediately prior to surgery (Figure 4. 26a). TIM4$^+$ and TIM4$^-$ cells among total lymph DC were then FACS sorted and co-cultured with OT-II MLN cells for six days before analysis of T cell proliferation by flow cytometry (Figure 4. 26a, b). We could detect low-level antigen-specific proliferation at this time point in both groups to the same extent (Figure 4. 26c), suggesting that TIM4 expression does not play a role in antigen acquisition or processing in this system.

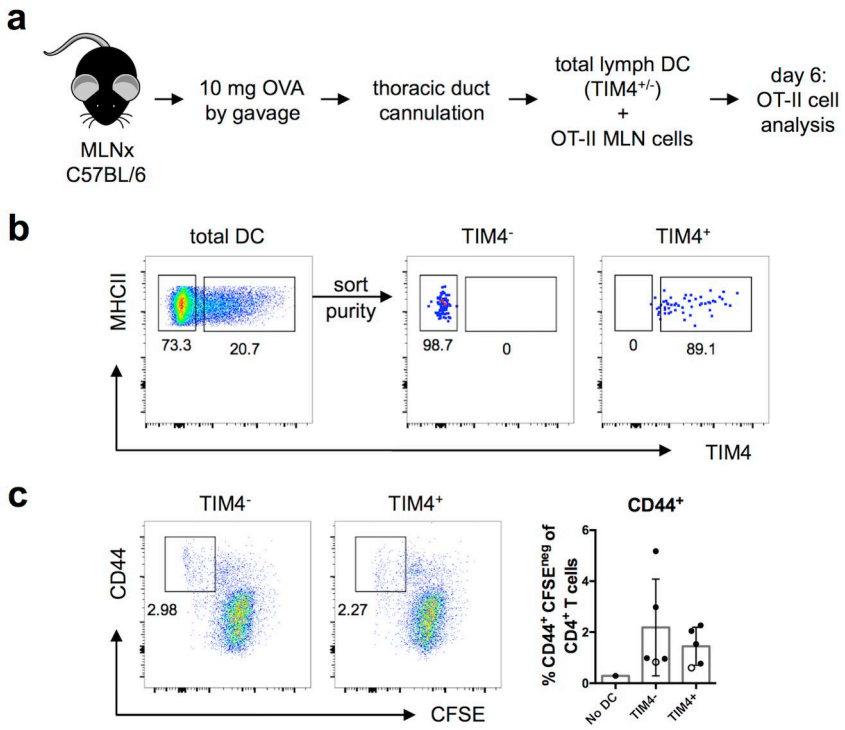

Figure 4. 26: TIM4$^-$ and TIM4$^+$ lymph DC can induce specific T cell responses to *in vivo* acquired antigen with equivalent efficiency

(a) MLNx mice were fed with 10 mg OVA protein by gavage before undergoing thoracic duct cannulation. TIM4$^+$ and TIM4$^-$ DC were FACS sorted from collected lymph and 12,500 DC co-cultured with 200,000 CFSE-labelled OT-II total MLN cells. After six days, these were harvested and analysed by flow cytometry. **(b)** Representative plots showing sort gating for TIM4$^-$ and TIM4$^+$ DC (gated on single, live, CD45$^+$, MHCII$^+$, CD11c$^+$, CD64$^-$, B220$^-$ cells), and sort purity for TIM4$^-$ and TIM4$^+$ DC. **(c)** Representative plots showing CD44$^+$ CFSE$^-$ divided CD4$^+$ CD3$^+$ OT-II cells after six days of co-culture with lymph DC. Data represented as percentage of CD44$^+$ CFSE$^-$ cells of live, CD3$^+$, CD4$^+$ OT-II T cells; one well with no added DC served as negative control for non-specific proliferation. Closed circles represent technical replicates using lymph collected from one mouse. Error bars represent S.D.

4.3 Discussion

The recognition and phagocytosis of apoptotic cells by DC is likely to play an important part in determining the outcome of downstream tissue-specific T cell responses. Given the different transcriptional profiles of DC subsets and their specialised functions in priming adaptive immunity (Watchmaker et al. 2014), we hypothesised that the expression of certain ACR is subset-specific. In particular, due to the unique ability of both intestinal and lung CD11b$^-$ CD103$^+$ DC to acquire and cross-present cell-derived antigen *in vivo* (Desch et al. 2011, Cerovic et al. 2014b), we aimed to establish if this subset indeed expressed higher levels of ACR than other DC subsets. Our results show that the PSR TIM4 is most highly expressed on colonic and lung CD11b$^-$ CD103$^+$ DC compared with the other DC populations found in those tissues. In fact, while only about 10% of colonic CD11b$^-$ CD103$^+$ DC expressed TIM4, this was much higher on lung DC, where up to 90% were TIM4$^+$. Expression of another ACR, CD205, was also highest on small intestinal and colonic CD11b$^-$ CD103$^+$ DC. Previous work has shown that CD11b$^-$ CD103$^+$ lymph DC also uniquely express Clec9A (DNGR-1) (Cerovic et al. 2014b), a mannose receptor that enables DC to recognise actin filaments on damaged cells (Zhang et al. 2012). Interestingly, SIRPα^- (OX41$^-$) CD4$^-$ DC in rat lymph and MLN have been shown to contain apoptotic cell inclusions and epithelial cell derived cytokeratins (Huang et al. 2000), similarly to the CD11b$^-$ CD103$^+$ DC in mouse lymph (Cerovic et al. 2014b), further supporting the hypothesis that this is indeed the main subset of DC responsible for carrying IEC derived apoptotic cell antigen to the MLN. However, recent findings also implicate CD11b$^+$ CD103$^-$ DC in the sampling of apoptotic IEC derived antigen through recognition of PS via the glycoprotein CD300a and thereby suppressing Treg cell maintenance in the colon (Nakahashi-Oda et al. 2015). These observations suggest that a range of ACR on different DC subsets may be important in fine-tuning downstream T cell responses. One possible reason for the enhanced specialisation of CD11b$^-$ CD103$^+$ DC in this regard may be their tissue localisation. The molecule CD103 (integrin αE) binds E-Cadherin found on IEC (Cepek et al. 1994). As well as on DC, CD103 is found on IEL, where it may mediate retention of the cells in the epithelial layer (Schon et al. 1999), although some evidence indicates it may instead be important in IEL recruitment (Sheridan et al. 2014). DC maintain expression of CD103 upon migration in lymph. Its role in retaining DC in proximity to the epithelium therefore remains unclear. Nevertheless, investigation of the tissue distribution of XCR1, a chemokine receptor expressed by CD11b$^-$ CD103$^+$ DC

(Cerovic et al. 2014b), showed that XCR1$^+$ cells indeed reside in the small intestinal villous LP under the epithelium (Becker et al. 2014).

In the human intestine, SIRPα$^-$ CD103$^+$ DC are transcriptionally and functionally most similar to murine CD11b$^-$ CD103$^+$ DC (Watchmaker et al. 2014). Unlike in the mouse intestine, however, human colonic SIRPα$^-$ CD103$^+$ DC did not express TIM4. CD11c$^+$ PBMC from healthy donors have been shown to upregulate TIM4 upon stimulation with staphylococcal enterotoxin B (Liu et al. 2007). However, little is otherwise known about which cells express TIM4 in humans. While we could not detect TIM4 on human colonic DC, we found that about 25% colonic CD64$^+$ macrophages express TIM4 in the healthy human colon. This was also the case in the murine intestine, where about 10-20% of mature CX3CR1^{hi} macrophages were TIM4$^+$. With differentiation, macrophages in the gut upregulate cell machinery required for the specialised function they fulfil in the intestine (Schridde et al. 2017). These include genes associated with phagocytosis, such as TAM receptors and the scavenger receptor CD36 (Schridde et al. 2017). In keeping with this pattern, Schridde et al. (2017) also found that TIM4 expression increased on macrophages both in the colon and small intestine with differentiation, with the highest expression being on CX3CR1^{hi} macrophages. TIM4 expression has also been found on peritoneal macrophages, where it is thought to be a marker of the tissue resident macrophage population (Rosas et al. 2014) and mediates the efficient clearance of apoptotic cells (Wong et al. 2010). These findings indicate that TIM4 expression on mature macrophages helps underpin their homeostatic functions in the tissue. We further analysed the expression of another PSR in the same family of TIM proteins, TIM1, and were able to show that an even higher proportion of CX3CR1^{hi} macrophages in the intestinal LP (80%) express this protein. The ACR CD205, however, did not follow this same pattern, as its expression on intestinal macrophages was lower than that on DC. This is in line with CD205 first being described as a DC- and epithelial cell-specific marker (Kraal et al. 1986).

Together, these findings confirm that, at barrier sites such as the intestinal LP and the lung, TIM4 is upregulated mainly on cell populations that are specialised in taking up and processing apoptotic cell derived antigen, such as mature intestinal macrophages and CD11b$^-$ CD103$^+$ DC. The differential expression pattern of various ACR on antigen-presenting cell populations in the intestinal LP is likely to not simply be a result of redundancy, but also allow cells to fine-tune the downstream response elicited by the encountered apoptotic cell material.

We hypothesised that TIM4 expression would decrease on DC once antigen had been taken up and migration had been initiated. To our surprise however, we found that 20-30% of DC upregulated TIM4 upon migration in mesenteric lymph. Furthermore, once in the MLN, expression on all migratory DC remained higher than that in observed in the LP. It would have been interesting to compare these findings to the mediastinal LN, to elucidate whether expression of TIM4 on lung CD11b^{-} CD103^{+} DC changes or remains high after migration in lymph. In the MLN, CD11b^{+} CD103^{+} migratory DC had the highest frequency of TIM4^{+} cells (up to 50%). Interestingly, this was also the main subset of DC in the PP to express TIM4, even though expression was not as high as in the MLN. Previous work has shown CD11b^{+} CD103^{+} DC to be developmentally dependent on the transcription factors IRF4 (Persson et al. 2013b) and Notch2 (Satpathy et al. 2013), as well as requiring signalling through the GM-CSF receptor (Bogunovic et al. 2009). Recently, TGFβ signalling has been similarly implicated as important for differentiation of CD11b^{+} CD103^{+} DC (Bain and Montgomery et al. *in press*). This population of DC is thought to be unique to the intestine, as it is not present in the murine lung or spleen. Mice that lack IRF4 signalling in CD11c^{+} cells have a decreased ability to mount Th17 responses in the small intestine and MLN, which may not only be due to the reduced number of CD11b^{+} CD103^{+} present, but also a reduction in their ability to produce IL-6 (Persson et al. 2013b). CD11b^{+} CD103^{+} DC express SIRPα and are reduced in number in *Sirpa*$^{-/-}$ mice, which also have diminished Th17 responses to infection with *C. rodentium* (Scott et al. 2014b). SIRPα recognises CD47 on live cells, which functions as a "don't eat me" signal by negatively regulating phagocytosis (Okazawa et al. 2005). Furthermore, interactions between CD47 on T cells and SIRPα on DC may indeed be important in regulating the activation and maturation of both cell types (Latour et al. 2001). Interestingly, CD11b^{+} CD103^{+} DC are not potent inducers of IL-17 production from CD4^{+} T cells *in vitro*, but induce IFNγ secretion by CD8^{+} T cells after stimulation (Cerovic et al. 2013). Recently, CD11b^{+} CD103^{+} DC have further been implicated in the induction of Th2 responses in the small intestinal LP against *S. mansoni* eggs (Mayer et al. 2017).

Together, these findings indicate that CD11b^{+} CD103^{+} DC are efficient inducers of a range of different T cell responses, depending on the antigen and stimulus. Given the increased expression of TIM4 on these cells in the MLN, the site of T cell priming, suggests that this molecule may have a role in supporting these functions. This could take place through the sampling of cell-free antigen that is carried to the MLN in lymph in the form of exosomes

(Srinivasan et al. 2016). TIM4 has been shown to bind PS exposed on exosomes *in vitro* (Miyanishi et al. 2007), which may allow cells to engulf and process exosome-associated antigen for presentation. The fact that TIM4 is also expressed on resident LN DC supports this idea. However, a second possible explanation for the expression of TIM4 on $CD11b^+$ $CD103^+$ DC in the MLN is that it may enable these cells to take up antigen from dying DC that have previously arrived and carry antigen. Apoptosis of DC is required to maintain immunological tolerance, as ablation of apoptosis in $CD11c^+$ cells led to enhanced antigen-specific proliferation of $CD4^+$ and $CD8^+$ T cells *in vitro*, and enhanced autoimmunity *in vivo*, though without affecting the number of Treg cells in these mice (Chen et al. 2006). There is some evidence that injecting apoptotic bone marrow derived DC (BMDC) either systemically or locally into mice leads to increased production of TGFβ by the engulfing viable DC and enhanced Treg cell induction (Kushwah et al. 2009, Notley et al. 2015). Previous stimulation of the BMDC with LPS abolishes this response and instead leads to production of IL-6 (Notley et al. 2015). However, these findings should be interpreted with caution, given the fact that bone marrow cell differentiation with GM-CSF yields a mixture of macrophages and DC (Helft et al. 2015), and that the method of identifying DC *in vivo* used in these investigations was not rigorous enough to be sure of a DC-specific effect. However, they indicate that recognition of apoptotic cell material in the LN may be an important way of regulating T cell differentiation. TIM4-mediated uptake of previously-activated apoptotic DC by $CD11b^+$ $CD103^+$ DC may constitute one mechanism that contributes to their reported ability to drive IL-6 induced Th17 differentiation (Persson et al. 2013b), given that uptake of infected apoptotic cells by DC indeed stimulates production of IL-6 (Torchinsky et al. 2009). Furthermore, recent work on colonic LP DC suggests that functional specialisation of DC subsets allows fine-tuning and balancing of T cell responses to bacterial pathogens (Aychek et al. 2015). In this case, IL-23 produced by $CX3CR1^+$ macrophages and $CD11b^+$ DC was required to dampen down IL-12 production by $CD11b^-$ $CD103^+$ DC during infection with *C. rodentium*, that otherwise led to an inappropriately strong IFNγ-mediated response (Aychek et al. 2015). It is plausible that such an example of cellular crosstalk may also be in place in the MLN, where T cell differentiation is first initiated. There it may be important in limiting IFNγ responses induced by IL-12-secreting $CD11b^-$ $CD103^+$ DC, and instead skewing T cells towards protective Th17 or Treg responses. This could be one reason why TIM4 expression on $CD11b^-$ $CD103^+$ DC is lower than on $CD11b^+$ $CD103^+$ in the MLN. Treg cell differentiation is reported to be supported by the production of RA by $CD103^+$ DC (Coombes et al. 2007).

We compared TIM4$^+$ and TIM4$^-$ CD11b$^+$ CD103$^+$ DC from the sMLN and cMLN for their capacity to metabolise vitamin A to RA and found that in the sMLN, TIM4$^+$ cells indeed had greater RALDH activity than TIM4$^-$ DC. However, due to the low proportion of TIM4$^+$ DC in the sMLN, these results must be interpreted with caution. Moreover, the same trend was not observed in cMLN DC, or in the mRNA expression level of *Aldh1a2* of total CD11b$^+$ DC in the MLN.

Our second hypothesis was that TIM4 expression is tissue-specific. Indeed, not only did we find that TIM4 expression on DC subsets is tissue-dependent, but we also observed that the level of expression differed across tissues. For example, 80% of CD11b$^-$ CD103$^+$ DC in the lung were TIM4$^+$, whereas the same subset in the colon had only 10% TIM4$^+$ cells. This was reduced even further in the small intestine, where staining was minimal, as reported previously (Hilligan et al. 2016). Comparison of TIM4 expression on migratory DC across the sMLN, cMLN and ILN revealed a similar pattern, with sMLN DC exhibiting the lowest proportion of TIM4$^+$ cells (10%), followed by the cMLN (25%), and finally the ILN (45%). When comparing DC between the small intestine and colon, one caveat to these results is the use of two enzymatic digestion protocols, which could differentially affect the retention of TIM4 on the cell surface. However, this can not explain the marked difference in expression observed between colonic and lung CD11b$^-$ CD103$^+$ DC, nor between lymph nodes, suggesting that this variation is indeed tissue-specific. The tissue environment plays a crucial part in determining the eventual differentiated phenotype incoming precursor cells will adopt after arrival. Elegant work in macrophages has illustrated the profound epigenetic imprinting effect elicited by tissue factors (Lavin et al. 2014). In DC development, two separate stages of transcriptomic imprinting are thought to occur before they display the subset and tissue-specific differences observed in fully differentiated tissue DC. The first takes place in the bone marrow during transition of the common DC precursor (CDP) to a pre-DC (Schlitzer et al. 2015). After tissue seeding of pre-DC, tissue derived factors then constitute the second signal that shapes DC subset phenotype. For example, expression and activation of the chemotactic receptor EBI2 is required for development and function of the splenic CD4$^+$ DC (Gatto et al. 2013). We demonstrated that bone marrow pre-DC only exhibit very low levels of TIM4 on their surface. This confirms that, rather than being part of the first subset-specific imprinting event in the bone marrow, TIM4 expression is regulated during differentiation and DC encounter with specific stimuli in the tissue. The three main tissues that exhibited high expression of TIM4 on DC in our investigation were the lung, the cMLN and the ILN. One factor that could be

a common stimulus regulating TIM4 on DC at these sites could be TGFβ. Schridde et al. (2017) have demonstrated the importance of TGFβ signalling on colonic macrophages for their differentiation. Furthermore, tissue resident lung macrophages are able to induce Treg cells at steady state via a TGFβ-dependent mechanism (Soroosh et al. 2013), suggesting a role for this mediator in governing lung homeostasis. TGFβ is also required for Langerhans cell retention in the epidermis (Borkowski et al. 1996, Kel et al. 2010) and *in vitro* studies have further shown a role for TGFβ1 in inducing expression of the TAM receptor Axl on Langerhans cells and GM-CSF generated BMDC (Bauer et al. 2012). However, to date there is no evidence for a similar enhancing effect of TGFβ on TIM4 transcription.

The marked increase in $TIM4^+$ DC in the colonic compared with the small intestinal associated tissues is worth exploring further. This pattern could be observed in the LP, lymph and the distinct MLN draining these tissues. We also found the colon to contain a greater proportion of $CD205^+$ DC than the small intestine. Furthermore, we established that TIM1 is expressed more highly on colonic $CD45^-$ cells than on those of the small intestine. This population is comprised of IEC, endothelial cells and stromal cell subsets, and further work is required to accurately differentiate between these with regard to TIM1 expression. However, TIM1 has previously been described on the epithelium in the kidney (Ichimura et al. 1998), which may therefore also be the case in the intestine. Overall, our observations indicate that transcription of both TIM1 and TIM4 may be governed by similar tissue-specific factors. Nevertheless, the fact that macrophage expression of TIM4 did not follow the same trend, but if anything was decreased in the colon compared with the small intestine, illustrates that cell-specific programmes can override the impact of tissue factors. While we were able to detect TIM4 staining on human colonic macrophages, we did not investigate expression in small intestinal tissue, and it would be interesting to determine if the pattern there is similar to that in the mouse.

One of the most important environmental factors in the colon is the microbiota. Work in GF mice has revealed a role for microbiota derived PAMPs in regulating IEC turnover, as both proliferation and apoptosis are synergistically induced via a TLR2-dependent mechanism in the small intestine (Hormann et al. 2014). Several authors have reported the ability of PAMPs such as flagellin (Li et al. 2014) or staphylococcal enterotoxin B (Liu et al. 2007, Yang et al. 2007) to upregulate TIM4 expression on immune cells, implicating the microbiota as a likely factor driving TIM4 expression in the colon. GF mice have been

shown to lack expression of the TAM receptor adapter protein Gas6 on oral mucosal epithelial cells (Nassar et al. 2017). However, little is known about the expression of other ACR, including TIM4, in the intestine of GF mice. Given the role for PAMPs in TIM4 transcriptional regulation, it is possible that the increased expression on DC in the colon and cMLN constitutes a protective mechanism in allowing DC to be ready to deal more efficiently with apoptosis during bacterial infection. This being the case, one would expect to see enhanced TIM4 expression during *in vivo* infection with enteric pathogens, and in the mucosa of IBD patients. Some evidence suggests that adjuvant-induced colitis increases TIM4 expression on colonic $CD11c^+$ cells (Li et al. 2016). However, more work is needed to determine if the same holds true in bacterial infections and in human disease.

Our final aim was to better understand the functional role TIM4 was playing on DC in different tissues. We showed that *Il1b* mRNA expression was greater in $TIM4^+$ $CD11b^-$ $CD103^+$ DC than in their $TIM4^-$ counterparts. However, this would need to be repeated, as the difference seen was only present in one of the two pooled experiments. If correct, this would indicate that TIM4-mediated phagocytosis might lead to activation of the inflammasome pathway in DC. On the other hand, recently published work has shown that DC from the small intestinal LP do not respond with enhanced transcription of *Il1b* after phagocytosis of apoptotic cells (Cummings et al. 2016). Instead, in BMDC this leads to production of TGFβ (Torchinsky et al. 2009). Uptake of apoptotic cells during bacterial infection has been shown to also induce the production of IL-6 (Torchinsky et al. 2009), and comparison between $TIM4^+$ and $TIM4^-$ DC in the colonic LP under those circumstances might therefore be more informative.

We also found that colonic $TIM4^+$ $CD11b^-$ $CD103^+$ DC have a greater expression of *Ccr7* mRNA. The observed trend towards a greater percentage of $CCR7^+$ cells when using $Ccr7^{gfp/gfp}$ mice further supports this and may indicate that TIM4 expression correlates with a migratory signature in colonic DC. Moreover, when we photoconverted the proximal colon in Kaede mice, we found that $TIM4^+$ DC in the cMLN contained a greater percentage of Kaede-red^+ cells than did $TIM4^-$ DC, indicating that $TIM4^+$ DC may be more efficient at migrating than $TIM4^-$ DC. The number of biological repeats per time point in this experiment would need to be increased, however, as the difference recorded was only small and did not reach statistical significance. Of note, we saw a similar trend in the colonic LP with $TIM4^+$ DC having a higher proportion of photoconverted cells than $TIM4^-$. Hence, the observations made in the cMLN may also be due to a difference originating in the LP

before migration, possibly based on the tissue localisation of TIM4$^+$ cells, and must therefore be interpreted with caution.

The upregulation of TIM4 on DC in lymph does, however, suggest that it is part of a molecular signature initiated upon migration. A possible explanation may be that it serves as a marker of mature DC that are ready to present antigen. It would have been worthwhile to assess the levels of co-stimulatory markers such as CD80, CD40 and CD86 on TIM4$^+$ and TIM4$^-$ DC to help test this hypothesis. We were, however, not able to show an increased propensity of MLN TIM4$^+$ DC to induce antigen-specific T cell responses *in vitro* at steady state. TLR stimulation of DC is important in this process and activation of lymph DC with bacterial lipoprotein has been shown to increase production of IFNγ by CD4$^+$ and CD8$^+$ T cells *in vitro* (Cerovic et al. 2013). We did not include this in our investigation, however, which, together with the absence of conditioning cytokines such as TGFβ, IL-6 or IL-12 may explain the low yield of IFNγ$^+$ and IL-17A$^+$ CD4$^+$ T cells generated in our co-cultures. In the future, it would also be of interest to compare the ability of TIM4$^+$ and TIM4$^-$ CD11b$^-$ CD103$^+$ DC to cross-present antigen to CD8$^+$ T cells and to ascertain if TIM4 expression is required to help capture self-antigen in the gut. In IFABP-tOVA 232-4 mice, OVA is constitutively expressed under control of the fatty acid binding protein promoter in small intestinal epithelial cells (Vezys et al. 2000). These mice were successfully used to first show the subset specificity of cross-presentation in mesenteric lymph DC (Cerovic et al. 2014b). Yet lack of TIM4 expression in the small intestine limits the usefulness of this model in determining its role on CD11b$^-$ CD103$^+$ mediated priming of CD8$^+$ T cells.

TIM4 on DC in lymph and MLN might also be engaging in homotypic interactions with TIM1 on lymphocytes, thereby acting as a co-stimulatory molecule. TIM1 expression has been described previously on activated CD4$^+$ T cells (Umetsu et al. 2005). Using immunisation with peptide antigen in complete Freund's adjuvant Meyers et al. (2005) were able to show that blocking TIM1 *in vivo* reduced T cell activation, while administration of TIM4-Ig had the opposite effect by inducing T cell hyperproliferation. Moreover, proliferation induced by TIM1 ligation on T cells is polyclonal and occurs in the absence of TCR engagement (Mariat et al. 2009). It is, however, dependent on co-stimulation by mature DC (Mariat et al. 2009).These data suggest that TIM4-TIM1 interactions between DC and T cells may be important in sustaining CD4$^+$ T cell responses. When we sought to identify populations of lymphocytes in the MLN and lymph that

express TIM1, we found it mainly on a small population of B cells (0.5-2%). TIM1 identifies regulatory B cells (Ding et al. 2011) and is required for their induction and maintenance (Yeung et al. 2015). Therefore, rather than facilitating interactions with DC, it is more likely that TIM1 is functioning in its main capacity as a PSR on B cells, with the uptake of apoptotic cells stimulating differentiation into a regulatory phenotype (Yeung et al. 2015). Our antibody panel was not comprehensive enough to allow accurate identification of $CD4^+$ T cells, although a small population of $B220^-$ $CD8^-$ lymphocytes was found to express TIM1. As well as B cells and $B220^-$ $CD8^-$ cells, we could also detect two populations of $TIM1^+$ $CD8^+$ T cells in lymph, differentiated based on expression levels of CD103. However, unlike DC, due to the ability of T cells to egress LN via the efferent lymph, it is impossible to ascertain the origin of these cells. Given the very small percentage of non-B cell lymphocytes that expresses TIM1 compared with the much higher percentage of DC that express TIM4 in lymph and the MLN, it is unlikely that homotypic interactions between the two play a significant role at steady state. However, this proportion a may increase during inflammation, and future investigations should take this into account.

Finally, TIM4 on DC may be acting to facilitate migration directly. The TIM4 molecule is made up of a large mucin domain containing O-linked glycosylation sites, and a V-type Ig domain. In *Drosophila melanogaster* mutation in the glycosylating enzyme PGANT3 led to decreased cell adhesion and resulting wing malformation (Zhang et al. 2008), suggesting a role for these structures in interactions between cells and the extracellular matrix. This is supported by the fact that TIM4 binding to glycosylation-deficient cells *in vitro* is reduced (Wilker et al. 2007). Furthermore, the Ig domain of TIM4 binds $CD4^+$ and $CD8^+$ splenocytes *in vitro* in a calcium-dependent manner, thus establishing similarity with C-type lectins (Wilker et al. 2007). Intriguingly, TIM4 exhibits similarity in domain structure with the cell adhesion molecule MAdCAM1, and contains an RGD peptide motif in its Ig domain, which is required for facilitating integrin binding (Newham et al. 1997). Moreover, TIM4 has been shown to co-localise with integrins during phagocytic uptake of PS-bearing targets (Flannagan et al. 2014), although further investigation is needed to establish if direct binding takes place. TIM1 has been shown to act as a ligand for P-selectin, and mediate T cell recruitment to sites of inflammation *in vivo* (Angiari and Constantin 2014). Taken together, it is plausible that TIM4 may be interacting with the lymphatic endothelium via integrins and other glycosylated proteins on their surface, thus directly facilitating DC migration.

We have succeeded in extensively characterising the expression of TIM4 on DC subsets in a range of different tissues and compared it with that of other ACR. As a result, we show that TIM4 expression is both population- and tissue-dependent. Our findings also indicate that it may correlate with a migratory signature on DC. However, while we carried out initial investigations into how TIM4 might bestow subset- and tissue-specific functions on DC, we were unable to describe any functional differences between $TIM4^{+}$ and $TIM4^{-}$ DC. Exploring the factors that regulate TIM4 expression, and determining the role of TIM4 in intestinal inflammation may therefore help to deepen our understanding of its function on DC.

Chapter 5: Factors that regulate TIM4 expression

5.1 Aims and hypotheses

Expression of TIM4 on DC is both population- and tissue-dependent. Our investigations showed that it is expressed mainly by CD11b$^-$ CD103$^+$ DC in the colon and the lung, but is upregulated upon migration in lymph by all DC subsets in the intestine. Once in the MLN, CD11b$^+$ CD103$^+$ migratory DC are the dominant TIM4 expressing population. We also showed that DC had greater TIM4 expression in tissues associated with the colon compared with the small intestine. These findings led us to propose two hypotheses relating to the expression of TIM4.

The first is that TIM4 expression on DC is controlled by specific cytokines present in the tissue environment. Previous work has suggested a role for STAT6 in regulating TIM4 expression on DC (Yang et al. 2016), implicating IL-4 as a potential regulatory factor. Consistent with this, polymorphisms in the TIMD4 gene and promoter locus have been linked to asthma (Cai et al. 2009, Zhao et al. 2011) and there is some evidence for a role of TIM4 on DC in inducing Th2 cell differentiation (Liu et al. 2007, Yang et al. 2007). A second possible factor regulating TIM4 expression is TGFβ, an important mediator of colonic macrophage differentiation (Schridde et al. 2017). Interestingly, TGFβ1 has previously been shown to induce expression of another ACR, Axl, on BMDC (Bauer et al. 2012). This cytokine also has important regulatory functions in the lung (Soroosh et al. 2013) and the skin (Borkowski et al. 1996, Kel et al. 2010). Given that the expression of TIM4 on DC was highest in the lung, cMLN and ILN, we investigated whether TGFβR signalling on DC is important for inducing the expression of TIM4 on these cells.

The observation that TIM4 expression was higher on colonic compared with small intestinal DC led us to formulate our second hypothesis, that TIM4 expression was regulated by the microbiota. *In vitro* studies have indeed confirmed a role for PAMPs in upregulating TIM4 on various immune cells (Liu et al. 2007, Li et al. 2014). However, no studies to date have investigated the role of the microbiota in shaping its expression *in vivo*. We therefore used two approaches to begin to answer this question; in the first instance we depleted the microbiota using oral antibiotics to determine if this would reduce TIM4 expression on colonic DC. Our second approach was to establish if infection with the enteric bacterial pathogen *C. rodentium* would augment TIM4 expression on DC.

Answering these questions will be vital to understanding the role of TIM4 on DC and how it impacts their function during inflammation.

5.2 Results

5.2.1 TIM4 expression on DC is not altered in IL-4-deficient mice

In order to determine if IL-4 functions as a factor regulating TIM4 expression *in vivo*, we used KN2 mice, in which both copies of the *Il4* gene have been replaced by the gene encoding human CD2 (Mohrs et al. 2005). KN2het mice served as a control, which retain a functioning copy of the *Il4* gene and are therefore IL-4 sufficient. We first determined if IL-4-deficient animals had an altered distribution of DC subsets in the colonic LP or cMLN and found no significant changes in either tissue compartment (Figure 5. 1).

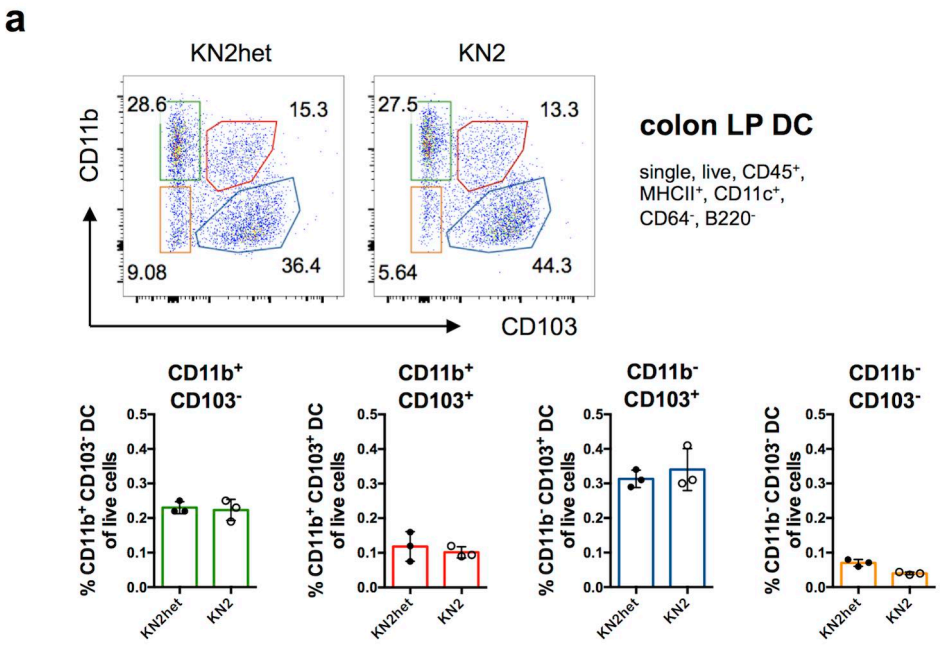

Figure 5.1 continued on next page

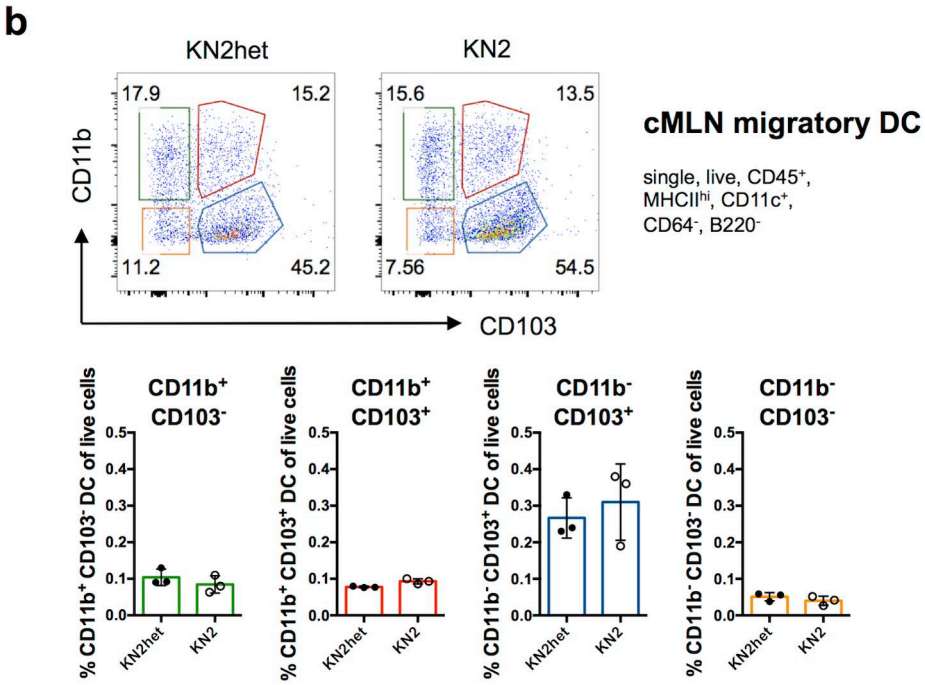

Figure 5. 1: IL-4 deficiency does not change the distribution of colonic or cMLN DC populations

Colons and cMLN from KN2het and KN2 mice were harvested and cells analysed by flow cytometry. **(a)** Representative plots showing colonic DC subsets in KN2het and KN2 mice gated on single, live, $CD45^+$, $MHCII^+$, $CD11c^+$, $B220^-$, $CD64^-$ cells. Summary data are shown as percentage of DC subsets among live cells. **(b)** Representative plots showing migratory cMLN DC subsets in KN2het and KN2 mice gated on single, live, $CD45^+$, $MHCII^{hi}$, $CD11c^+$, $B220^-$, $CD64^-$ cells. Summary data are shown as percentage of migratory DC subsets among live cells. Error bars represent S.D.; statistical analysis carried out using a Mann-Whitney test.

Next, we compared TIM4 expression on total DC and macrophages in the colonic LP between KN2 and KN2het mice. We could not detect any significant differences in TIM4 expression on total DC (Figure 5. 2a) or macrophages (Figure 5. 2b) in the colonic LP, although there was a trend towards increased expression on both cell populations in IL-4-deficient animals.

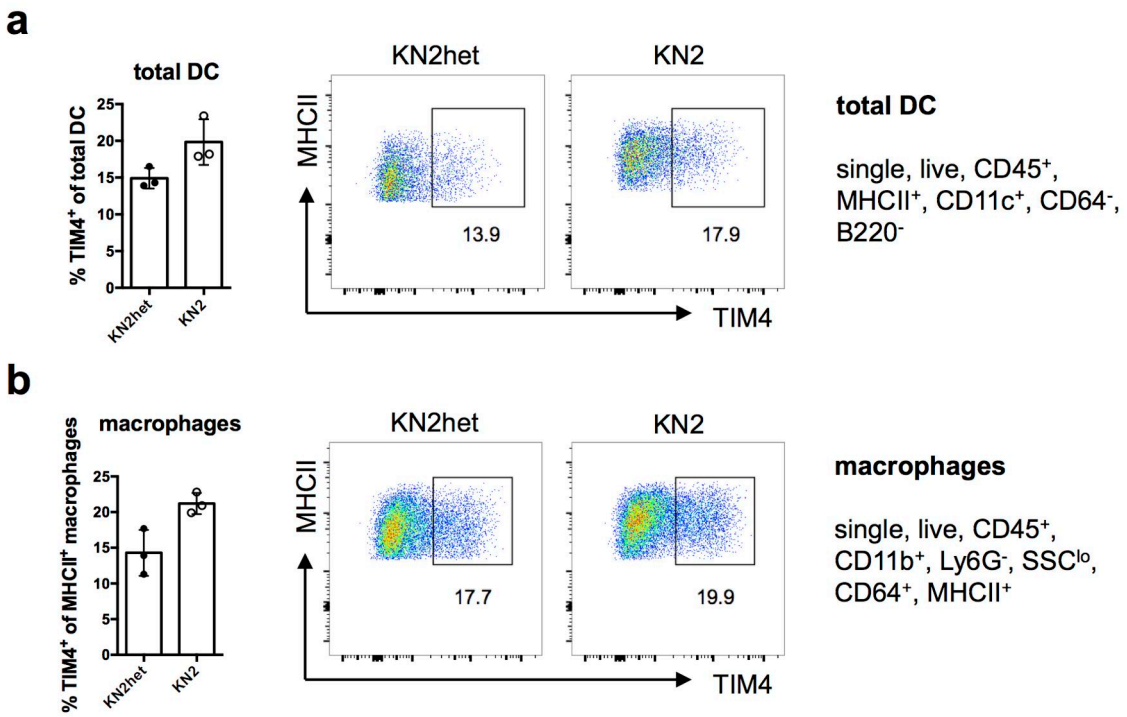

Figure 5. 2: IL-4 deficiency does not reduce expression of TIM4 on colonic DC or macrophages

Colons from KN2het and KN2 mice were harvested and LP cells analysed by flow cytometry. **(a)** Representative plots showing TIM4 expression on total colonic LP DC of KN2het and KN2 mice, and summary data shown as percentage of $TIM4^+$ cells among total colonic DC. DC gated on single, live, $CD45^+$, $MHCII^+$, $CD11c^+$, $CD64^-$, $B220^-$ cells. **(b)** Representative plots showing TIM4 expression on colonic macrophages of KN2het and KN2 mice, and summary data shown as percentage of $TIM4^+$ cells among total colonic macrophages, gated on single, live, $CD45^+$, $CD11b^+$, $Ly6G^-$, SSC^{lo}, $CD64^+$, $MHCII^+$ cells. Error bars represent S.D.; statistical analysis using a Mann-Whitney test.

Moreover, there were no significant DC population-specific changes in TIM4 expression in KN2 compared with KN2het mice (Figure 5. 3).

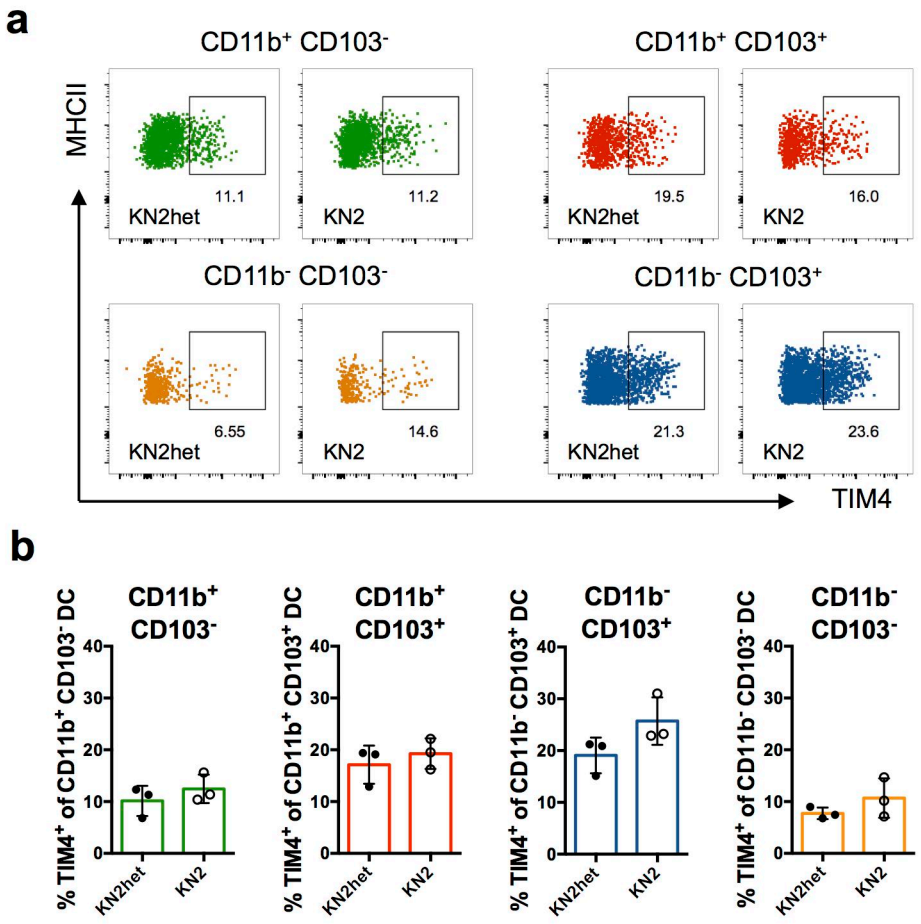

Figure 5. 3: IL-4 deficiency does not change TIM4 expression on colonic DC populations

Colons from KN2het and KN2 mice were harvested and LP cells analysed by flow cytometry. **(a)** Representative plots showing TIM4 staining on DC populations gated on single, live, $CD45^+$, $MHCII^+$, $CD11c^+$, $CD64^-$, $B220^-$ cells. **(b)** Summary data shown as percentage of $TIM4^+$ cells among DC subsets. Error bars represent S.D.; statistical analysis carried out using a Mann-Whitney test.

In the cMLN, TIM4 expression on both total migratory and resident populations of DC was independent of IL-4 (Figure 5. 4), as was its expression on the four migratory DC populations (Figure 5. 5).

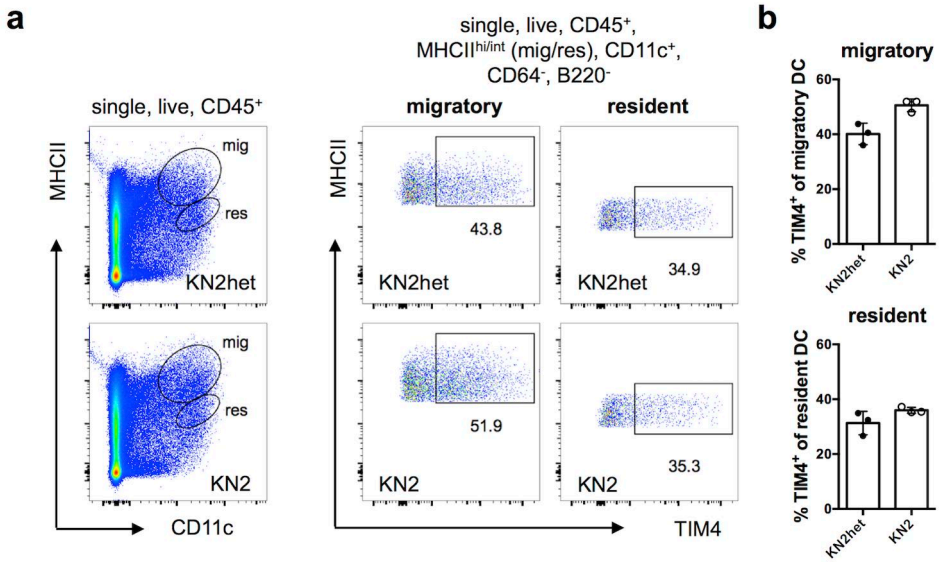

Figure 5. 4: IL-4 deficiency does not change the expression of TIM4 on cMLN migratory and resident DC populations

The cMLN from KN2het and KN2 mice were harvested and cells analysed by flow cytometry. **(a)** Representative plots showing migratory (mig) and resident (res) populations, and TIM4 staining on these, gated on single, live, $CD45^+$, $MHCII^{hi/int}$, $CD11c^+$, $CD64^-$, $B220^-$ cells. **(b)** Summary data shown as percentage of $TIM4^+$ cells among migratory and resident DC populations. Error bars represent S.D.; statistical analysis carried out using a Mann-Whitney test.

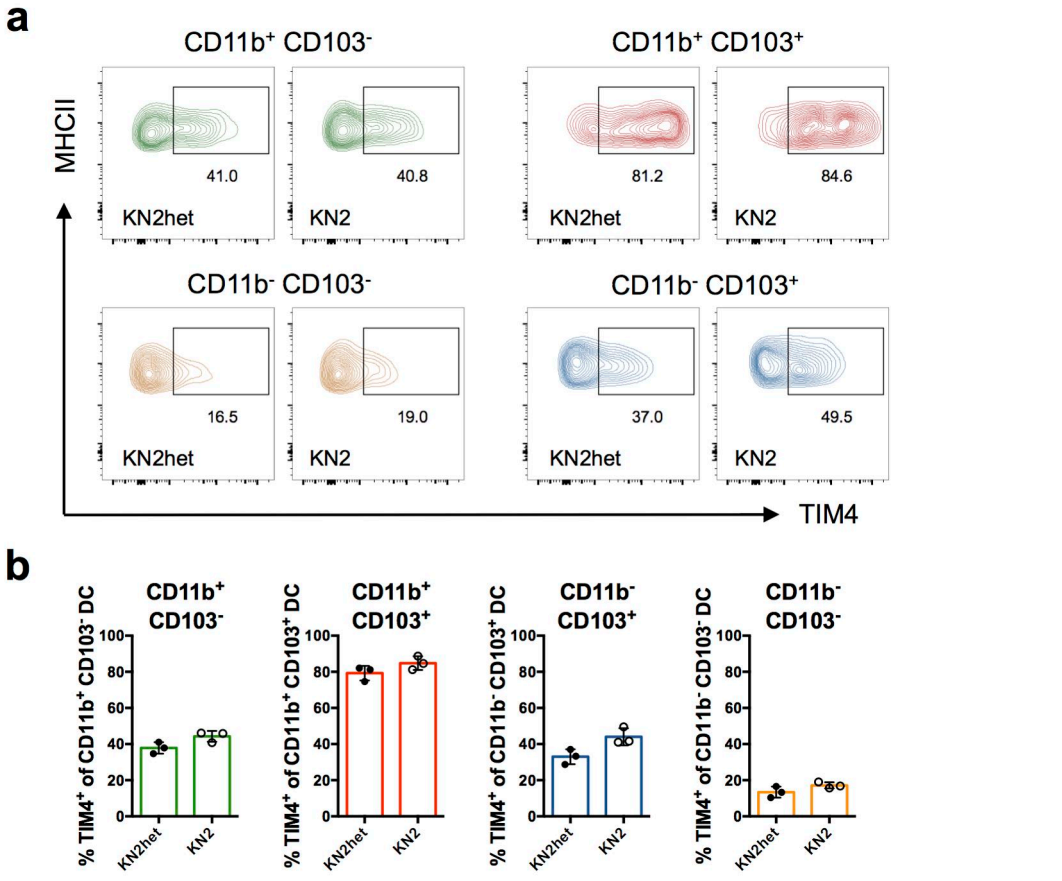

Figure 5. 5: IL-4 deficiency has no effect on the expression of TIM4 on migratory DC populations in the cMLN

The cMLN from KN2het and KN2 mice were harvested and cells analysed by flow cytometry.
(a) Representative plots showing TIM4 expression on migratory DC populations in KN2het and KN2 mice gated on single, live, $CD45^+$, $MHCII^+$, $CD11c^+$, $CD64^-$, $B220^-$ cells. **(b)** Summary data shown as percentage of $TIM4^+$ cells among migratory DC subsets. Error bars represent S.D.; statistical analysis carried out using a Mann-Whitney test.

As observed in the colon, lung DC subset frequencies were unchanged in KN2 mice (Figure 5. 6a), and expression of TIM4 on both CD11b$^+$ and CD103$^+$ DC did not differ significantly between IL-4-deficient and sufficient mice (Figure 5. 6b, c).

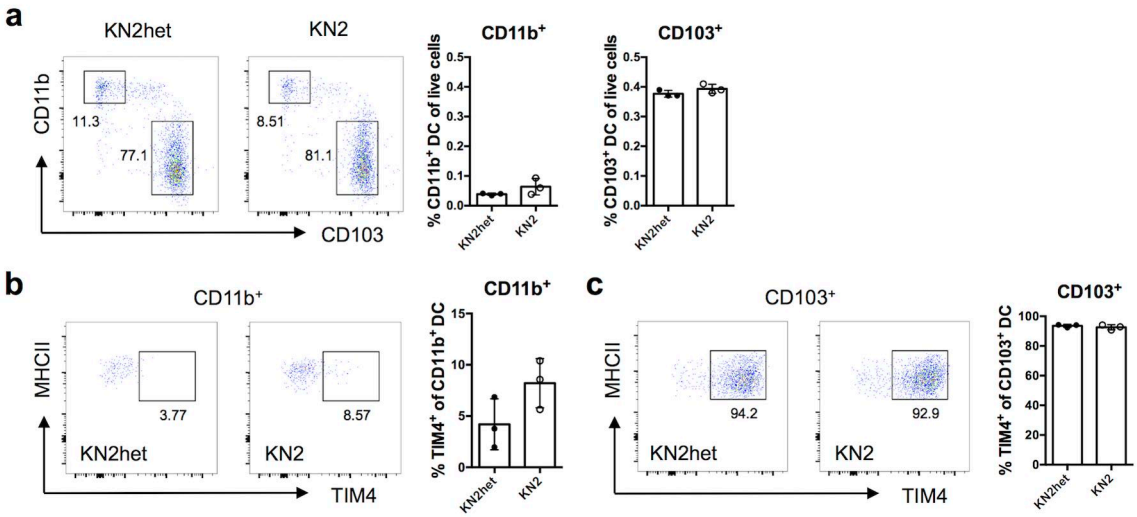

Figure 5. 6: IL-4 deficiency does not affect the distribution of lung DC subsets, or their TIM4 expression

Lung from KN2het and KN2 mice were harvested and cells analysed by flow cytometry. **(a)** Representative plots showing lung DC subsets gated on single, live, CD45$^+$, MHCII$^+$, CD11c$^+$, CD64$^-$, B220$^-$ cells. Summary data are shown as percentage of DC subsets among live cells. **(b)** Representative plots showing TIM4 expression on lung DC subsets. Summary data are shown as the percentage of TIM4$^+$ cells among DC subsets. Error bars represent S.D.; statistical analysis carried out using a Mann-Whitney test.

5.2.2 Lack of TGFβ signalling induces tissue-specific changes in TIM4 expression on DC

After not having found any evidence that TIM4 expression on colonic or lung DC is dependent on IL-4, we next sought to establish if TGFβR signalling was required to allow DC to express TIM4 *in vivo*. To do this, we used CD11c-Cre *Tgfbr1*$^{fl/fl}$ mice (Kel et al. 2010) that had been backcrossed onto a *Rag1*$^{-/-}$ background to stop the development of multi-organ inflammation that otherwise developed due to the activation of Cre recombinase in a small subset of CD11c$^+$ T cells (Bain and Montgomery et al., *personal communication*). The CD11c-Cre not only targets DC, which express high levels of CD11c, but also macrophages, and these mice have been used previously to describe the role of TGFβ in the development of colonic macrophages (Schridde et al. 2017). This system therefore allowed us to examine the need for TGFβR signalling on both DC and macrophages in the LP. TGFβ is one of the factors involved in driving the development of CD11b$^+$ CD103$^+$ DC in the small intestine, and CD11c-Cre *Tgfbr1*$^{fl/fl}$ *Rag1*$^{-/-}$ mice also have a decreased percentage of colonic and lung CD11b$^-$ CD103$^+$ DC compared with Cre$^-$ littermate controls (Bain and

Montgomery et al., *in press*). We were able to replicate these findings for the colon (Figure 5. 7a), but not the lung (Figure 5. 7b) when comparing the frequency of DC subsets between Cre$^+$ and Cre$^-$ littermate controls.

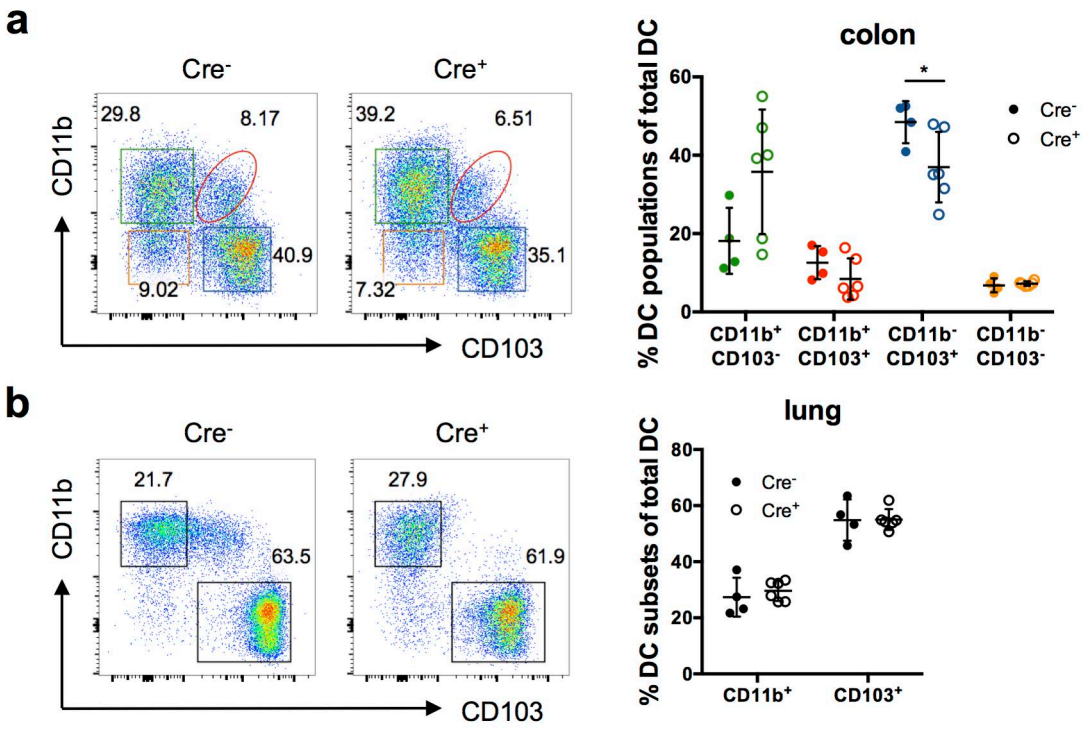

Figure 5. 7: Lack of TGFβR significantly changes the distribution of DC populations in the colon, but not the lung

Colons and lungs from CD11c-Cre *Tgfbr1*$^{fl/fl}$ *Rag1*$^{-/-}$ mice were harvested and cells analysed by flow cytometry. **(a)** Representative plots of colonic DC subsets in Cre$^+$ and Cre$^-$ mice gated on single, live, CD45$^+$, MHCII$^+$, CD11c$^+$, CD64$^-$, B220$^-$ cells. Summary data are shown as the percentage of DC populations among total LP DC. **(b)** Representative plots of lung DC subsets in Cre$^+$ and Cre$^-$ mice gated on single, live, CD45$^+$, MHCII$^+$, CD11c$^+$, CD64$^-$, B220$^-$ cells. Summary data are shown as the percentage of DC subset among total lung DC. Error bars represent S.D.; statistical analysis was carried out for each subset using a Mann-Whitney test between Cre$^+$ and Cre$^-$ groups. * p = 0.0381

However, TIM4 expression was not altered in mice that had lost the ability to mediate TGFβ signalling in total colonic LP DC (Figure 5. 8a) or Ly6C$^-$ MHCII$^+$ macrophages (Figure 5. 8b).

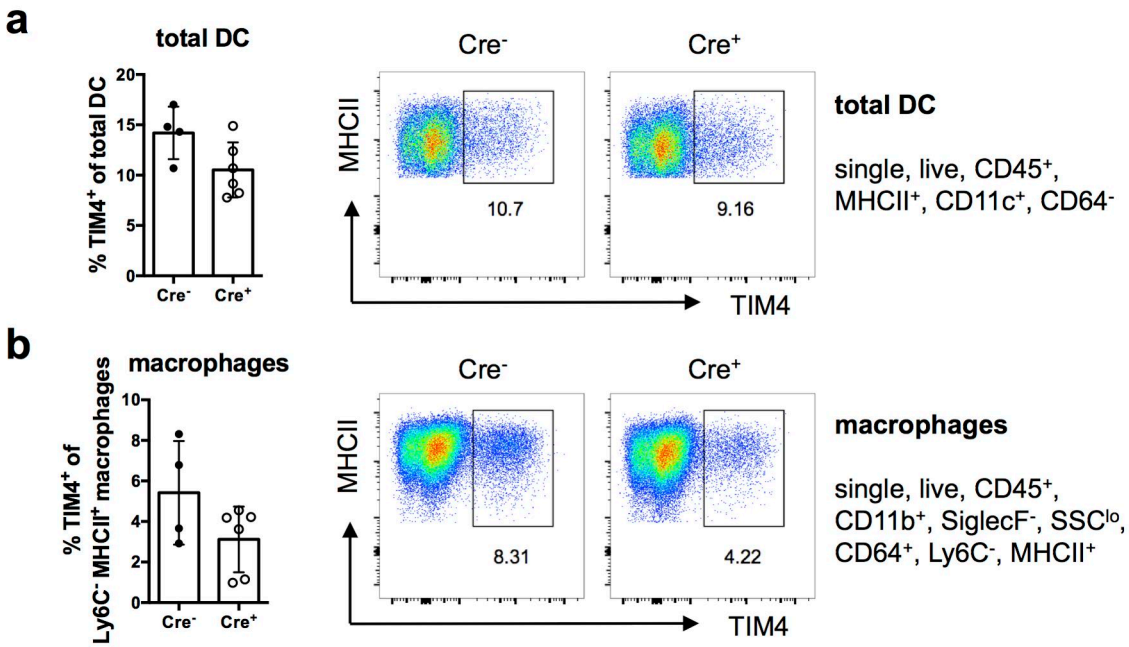

Figure 5. 8: Lack of TGFβR does not significantly change TIM4 expression on colonic macrophages or total DC

Colons from CD11c-Cre *Tgfbr1*$^{fl/fl}$ *Rag1*$^{-/-}$ mice were harvested and LP cells analysed by flow cytometry. **(a)** Representative plots and summary data showing percentage of TIM4$^+$ cells among total LP DC, gated on single, live, CD45$^+$, MHCII$^+$, CD11c$^+$, CD64$^-$ cells. **(b)** Representative plots and summary data showing percentage of TIM4$^+$ cells among colonic macrophages, gated on single, live, CD45$^+$, CD11b$^+$, (SiglecF$^-$), SSC^{lo}, CD64$^+$, Ly6C$^-$, MHCII$^+$ cells. Error bars represent S.D.; statistical analysis was carried out using a Mann-Whitney test.

Interestingly however, the percentage of TIM4$^+$ cells among colonic CD11b$^+$ CD103$^+$ DC was lower in TGFβR1-deficient mice compared with littermate controls (Figure 5. 9).

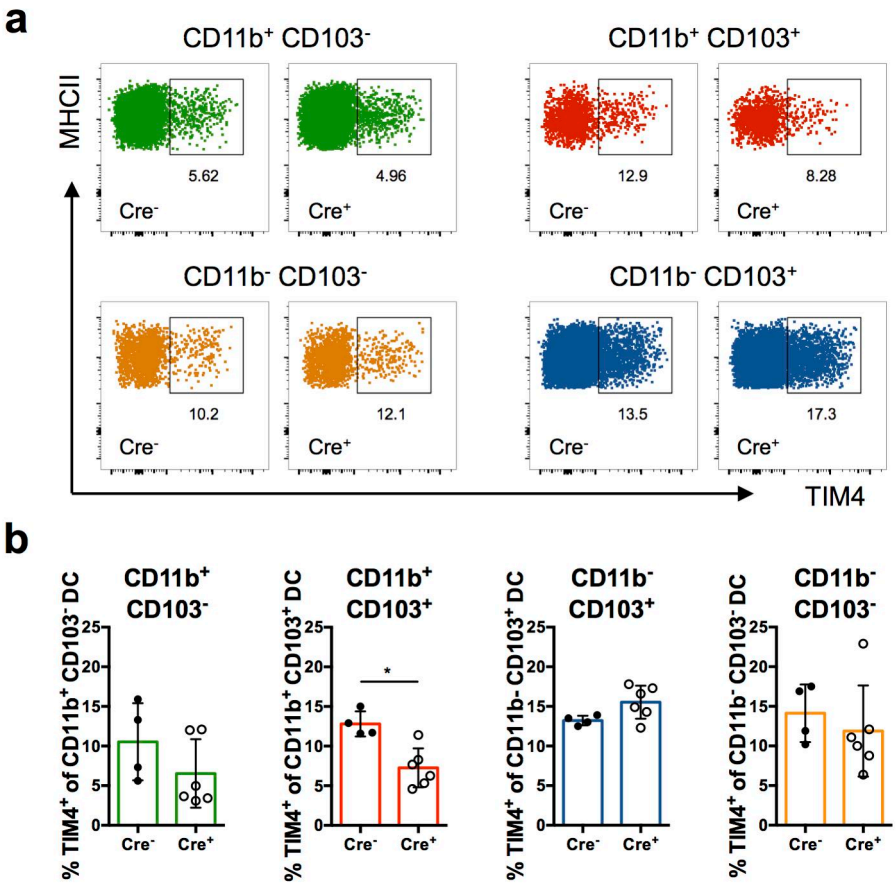

Figure 5. 9: Lack of TGFβR reduces TIM4 expression on colonic CD11b$^+$ CD103$^+$ DC

Colons from CD11c-Cre *Tgfbr1*$^{fl/fl}$ *Rag1*$^{-/-}$ mice were harvested and LP cells analysed by flow cytometry. **(a)** Representative plots showing TIM4 expression on colonic LP DC populations gated on single, live, CD45$^+$, MHCII$^+$, CD11c$^+$, CD64$^-$ cells. **(b)** Summary data shown as percentage of TIM4$^+$ cells among colonic LP DC populations. Error bars represent S.D.; statistical analysis carried out using a Mann-Whitney test. * p = 0.0095.

Whilst TIM4 expression on CD11b$^+$ DC did not change significantly in the lung (Figure 5. 10a), Cre$^+$ mice had a higher percentage of CD103$^+$ DC expressing TIM4 (Figure 5. 10b), contrary to the pattern observed in the colonic LP.

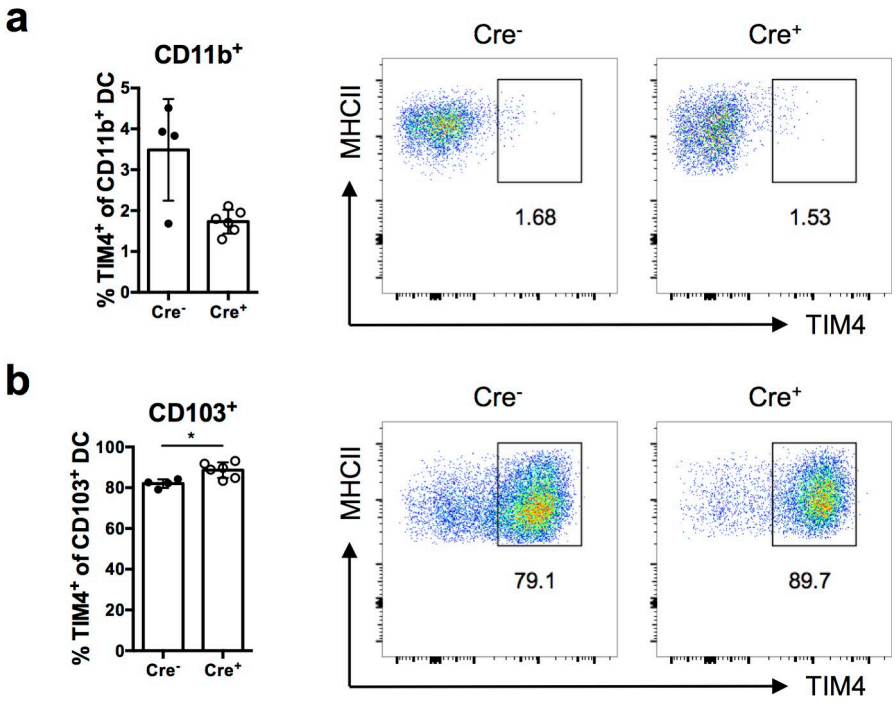

Figure 5. 10: Lack of TGFβR increases expression of TIM4 on lung CD103$^+$ DC

Lungs from CD11c-Cre *Tgfbr1*$^{fl/fl}$ *Rag1*$^{-/-}$ mice were harvested and cells analysed by flow cytometry. Representative plots and summary data showing percentage of TIM4$^+$ cells among **(a)** CD11b$^+$ and **(b)** CD103$^+$ lung DC subsets in Cre$^+$ and Cre$^-$ animals. DC gated on single, live, CD45$^+$, MHCII$^+$, CD11c$^+$, CD64$^-$ cells. Error bars represent S.D.; statistical analysis carried out using a Mann-Whitney test. * p = 0.019.

5.2.3 Antibiotic treatment does not change TIM4 expression on DC

After investigating the role of IL-4 and TGFβ in regulating TIM4 expression on DC, our second aim was to determine if its expression was dependent on the microbiota. We orally treated C57BL/6 mice with a cocktail of five antibiotics (ampicillin, gentamicin, neomycin, metronidazole and vancomycin) by supplementing these in the drinking water, and analysed DC from the colonic LP and cMLN after seven days of treatment. The frequency of the four DC populations in the colon (Figure 5. 11a) or the cMLN (Figure 5. 11b) did not change significantly between antibiotic-treated and control mice.

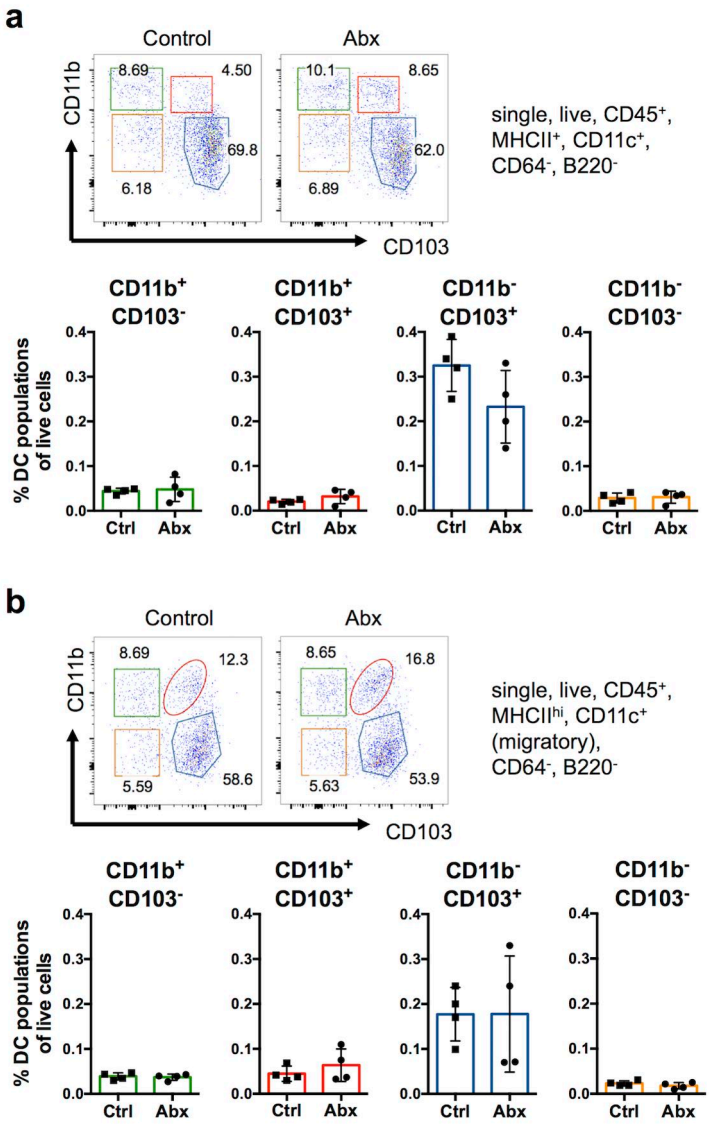

Figure 5. 11: The distribution of colonic and cMLN DC populations does not change after antibiotic treatment

C57BL/6 mice were given drinking water supplemented with five antibiotics and saccharin (Abx), or saccharin alone (Ctrl), for seven days. After this, colons and cMLN were harvested and cells analysed by flow cytometry. Representative plots and summary data showing the distribution of DC populations does not change in the **(a)** colon or **(b)** cMLN after seven days of antibiotic treatment compared with controls. Data are shown as the percentage of DC populations among live cells. Error bars represent S.D.; statistical analysis was carried out using a Mann-Whitney test.

We next compared expression of TIM4 on total colonic DC and CD64$^+$ MHCII$^+$ macrophages between antibiotic-treated and control mice, and found that depletion of the microbiota did not affect the expression of TIM4 on either cell population (Figure 5. 12a). There was also no DC population-specific change in TIM4 expression in the LP (Figure 5. 12b).

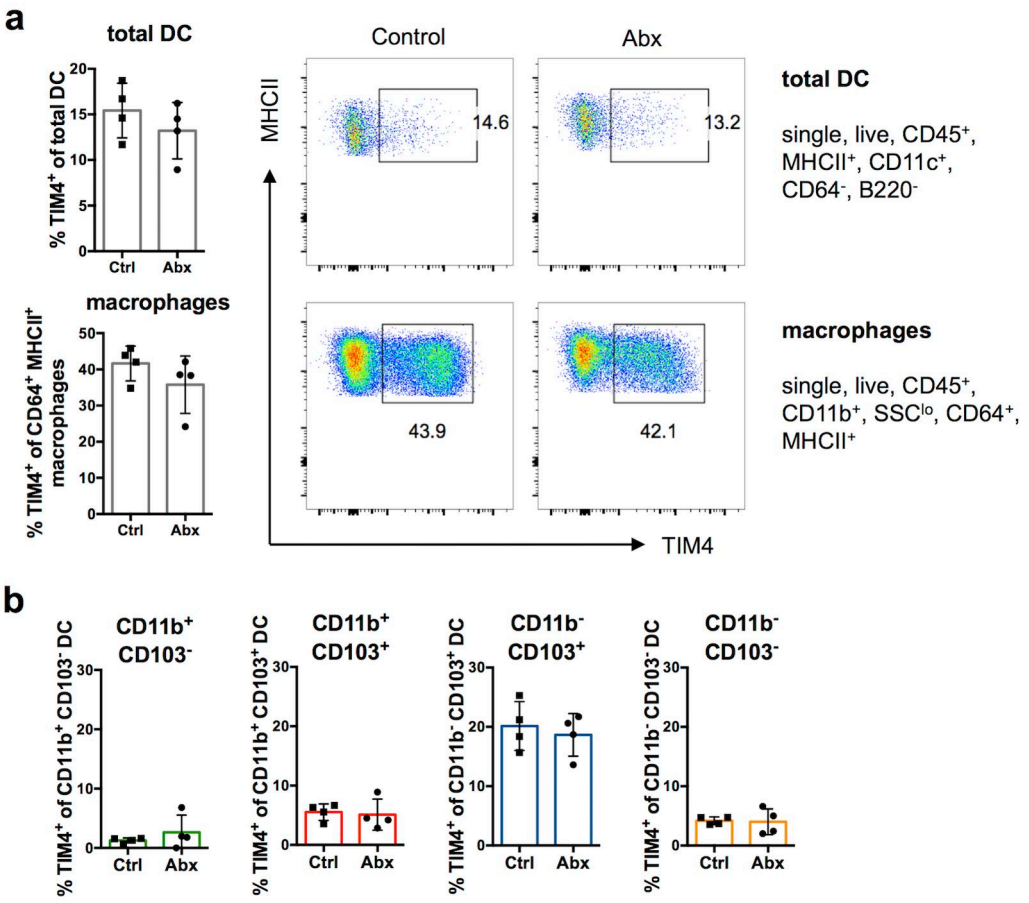

Figure 5. 12: TIM4 expression does not change on colonic DC or macrophages after antibiotic treatment

C57BL/6 mice were given drinking water supplemented with five antibiotics and saccharin (Abx), or saccharin alone (Ctrl), for seven days. After this, colons were harvested and LP cells analysed by flow cytometry. **(a)** Representative plots and summary data showing percentage of TIM4$^+$ cells among total LP DC and CD64$^+$ MHCII$^+$ macrophages after seven days of antibiotic treatment compared with controls. **(b)** Summary data showing percentage of TIM4+ cells among colonic LP DC subsets after seven days of antibiotic treatment compared with controls. Error bars represent S.D.; statistical analysis was carried out using a Mann-Whitney test.

As expected, we found a similar result in the cMLN, where TIM4 expression on both resident and migratory DC was unaffected by antibiotic treatment (Figure 5. 13a). We also analysed DC from the ILN to account for any gut-specific effects, and surprisingly found a trend towards a higher percentage of TIM4$^+$ cells among resident DC in control mice compared with antibiotic-treated mice, although this did not reach significance (Figure 5. 13b).

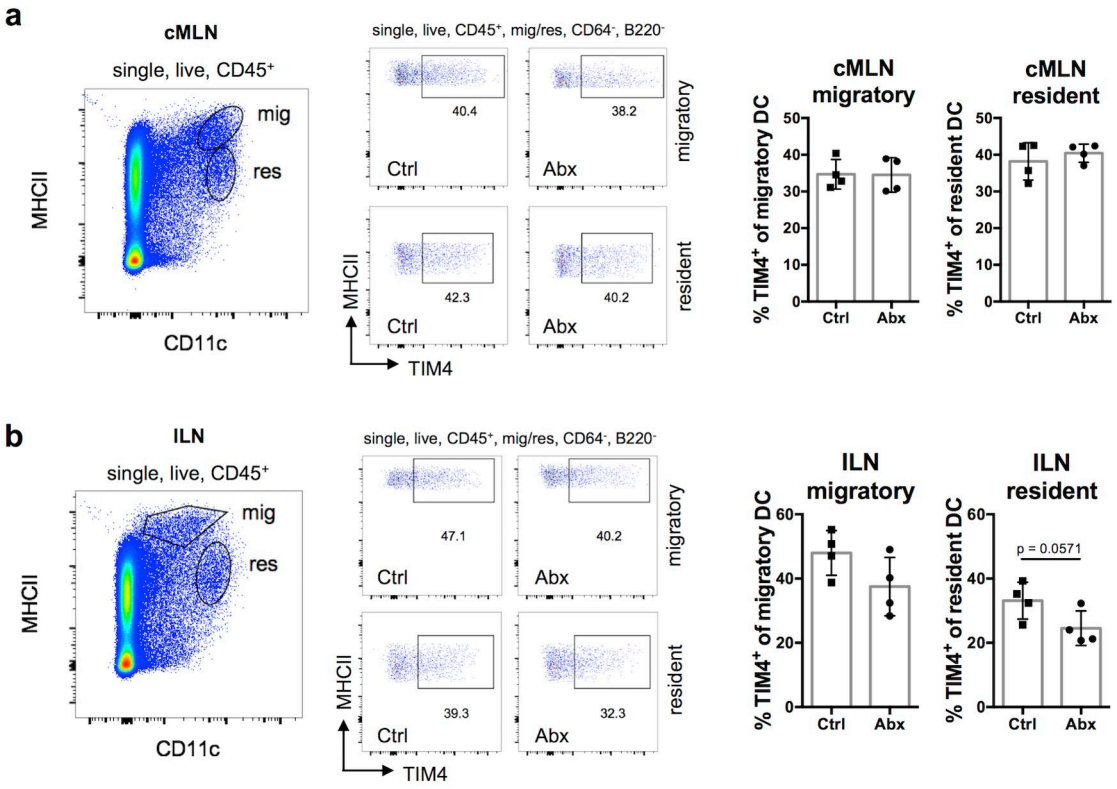

Figure 5. 13: Expression of TIM4 on LN resident and migratory populations of DC does not change after antibiotic treatment

C57BL/6 mice were given drinking water supplemented with five antibiotics and saccharin (Abx), or saccharin alone (Ctrl), for seven days. After this, cMLN and ILN were harvested and cells analysed by flow cytometry. Representative plots showing TIM4 staining on migratory and resident DC populations in the **(a)** cMLN and **(b)** ILN after seven days of antibiotic treatment compared with controls. Summary data are shown as the percentage of TIM4$^+$ cells among total migratory and resident DC populations in the **(c)** cMLN and **(d)** ILN. Error bars represent S.D.; statistical analysis was carried out using a Mann-Whitney test.

Finally, TIM4 expression on the four cMLN migratory DC populations was not dependent on an intact microbiota (Figure 5. 14).

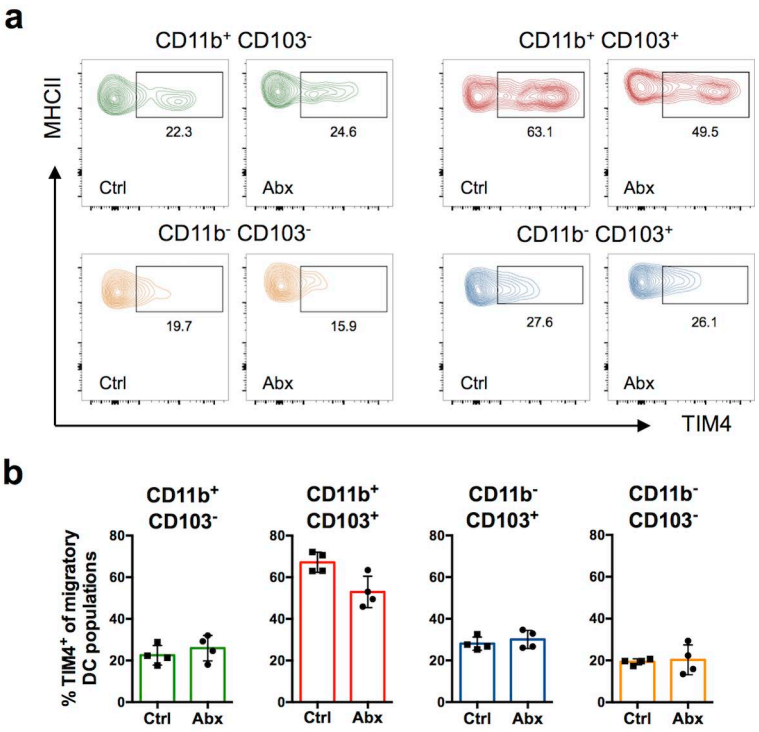

Figure 5. 14: Expression of TIM4 on migratory cMLN DC populations does not significantly change after antibiotic treatment

C57BL/6 mice were given drinking water supplemented with five antibiotics and saccharin (Abx), or saccharin alone (Ctrl), for seven days. After this, cMLN were harvested and cells analysed by flow cytometry. **(a)** Representative plots showing TIM4 expression on migratory cMLN DC subsets, gated on single, live, $CD45^+$, $MHCII^{hi}$ (migratory), $CD11c^+$, $B220^-$, $CD64^-$ cells. **(b)** Summary data are shown as the percentage of $TIM4^+$ cells among migratory DC populations after seven days of treatment with antibiotics compared with controls. Error bars represent S.D.; statistical analysis was carried out using a Mann-Whitney test.

5.2.4 Population-specific expression of TIM4 increases on colonic DC during infection with *C. rodentium*

Because depletion of the microbiota by antibiotics did not decrease the expression of TIM4 on DC in the colon or cMLN, we investigated if bacterial infection would lead to an increased frequency of $TIM4^+$ DC in these tissues. To achieve this, we infected mice with *C. rodentium*, an A/E bacterial pathogen which colonises the colon and rectum of infected mice. We found that induction of a Th17 response was detectable at seven days p. i. in the colon (Figure 5. 15a). Due to the involvement of the distal colon and rectum in *C. rodentium* infection, we included the caudal LN in our analysis and pooled these with the caecal and colon draining MLN (collectively referred to as cMLN). A similar trend towards increased $CD44^+$ IL-$17A^+$ $CD4^+$ T cells was also detected in the cMLN of infected

mice at seven days p. i. compared with PBS-treated controls (Figure 5. 15b). In all the following experiments, we therefore harvested tissues at this time point for analysis.

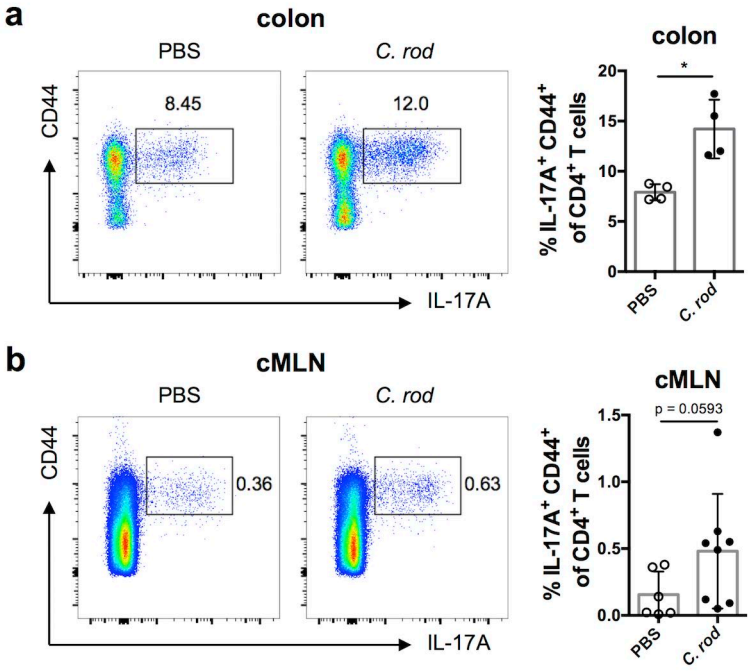

Figure 5. 15: Infection with *C. rodentium* induces a Th17 response seven days post-infection

Mice were given PBS or infected with 2×10^9 CFU *C. rodentium* by oral gavage. Seven days p. i., colons and cMLN (caecal, colonic and caudal) were harvested, cells stimulated with phorbol 12-myristate 13-acetate (PMA) and ionomycin and analysed by flow cytometry. **(a)** Representative plots showing $CD44^+$ $IL\text{-}17A^+$ cells in the colonic LP gated on single, live, $CD45^+$, $CD3^+$, $CD4^+$ T cells. Summary data are shown as the percentage of $CD44^+$ $IL\text{-}17A^+$ cells among $CD4^+$ T cells. **(b)** Representative plots showing $CD44^+$ $IL\text{-}17A^+$ cells in the cMLN gated on single, live, $CD45^+$, $CD3^+$, $CD4^+$ T cells. Summary data are shown as the percentage of $CD44^+$ $IL\text{-}17A^+$ cells among $CD4^+$ T cells. Error bars represent S.D.; statistical analysis carried out using Mann-Whitney test. * $p < 0.05$.

When we compared expression of TIM4 on total DC (Figure 5. 16a) and macrophages (Figure 5. 16b) in the colonic LP, we did not observe any significant changes, although there was a trend towards increased expression on DC.

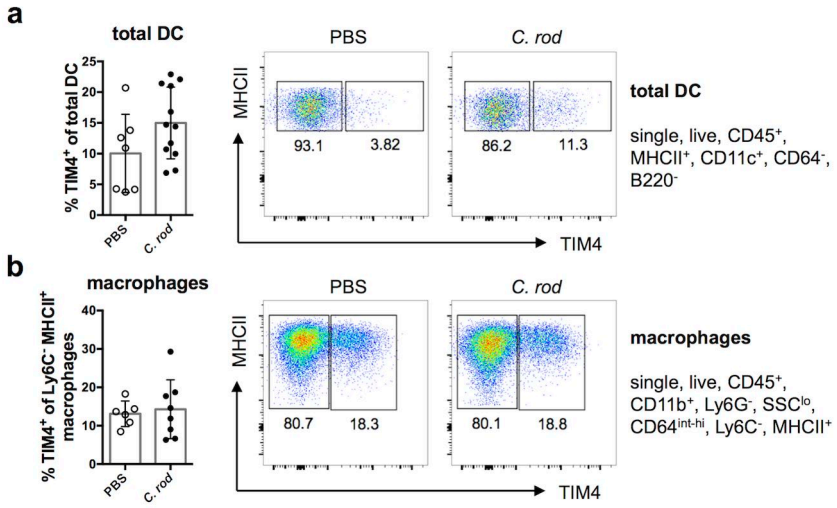

Figure 5. 16: Infection with *C. rodentium* does not significantly change expression on total colonic DC or macrophages

Mice were given PBS or infected with 2×10^9 CFU *C. rodentium* by oral gavage. Seven days p. i., colons were harvested and LP cells analysed by flow cytometry. Representative plots and summary data showing percentage of $TIM4^+$ cells among **(a)** total DC and **(b)** macrophages of infected (*C. rod*) and control (PBS) animals. DC were gated on single, live, $CD45^+$, $MHCII^+$, $CD11c^+$, $CD64^-$, $B220^-$ cells. Macrophages were gated on single, live, $CD45^+$, $CD11b^+$, $Ly6G^-$, SSC^{lo}, $CD64^{int\text{-}hi}$, $Ly6C^-$, $MHCII^+$ cells. Error bars represent S.D.; statistical analysis was carried out using a Mann-Whitney test.

In order to dissect this further, we first determined if colonic LP population frequencies were altered in infected mice. However, neither percentages nor the absolute number of DC populations changed in the colon seven days p. i. (Figure 5. 17).

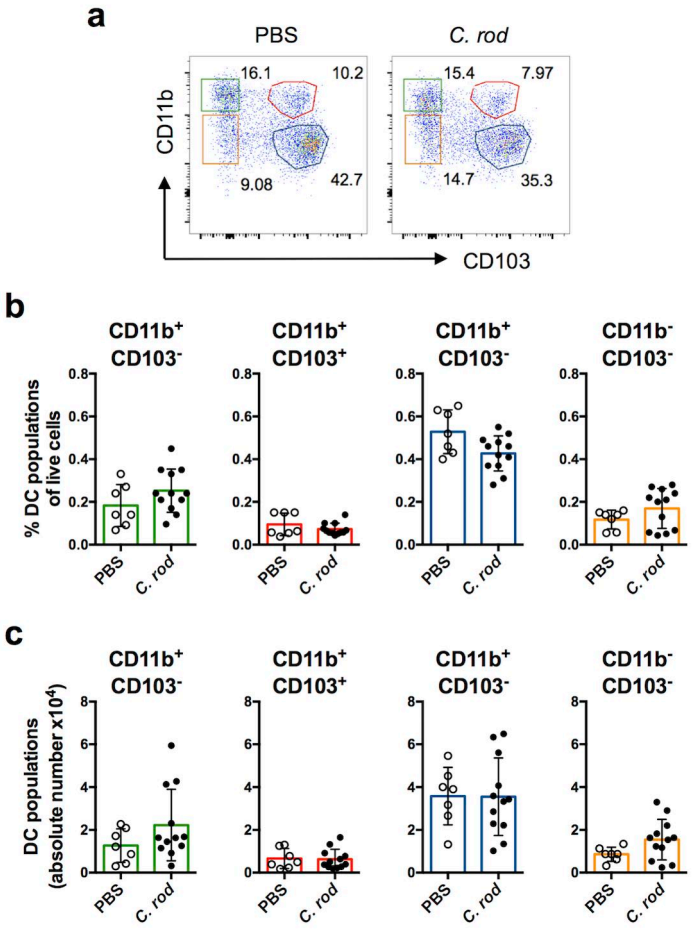

Figure 5. 17: Infection with *C. rodentium* does not significantly alter the distribution of colonic DC populations

Mice were given PBS or infected with 2×10^9 CFU *C. rodentium* by oral gavage. Seven days p. i., colons were harvested and LP cells analysed by flow cytometry. **(a)** Representative plots show DC populations gated on single, live, $CD45^+$, $MHCII^+$, $CD11c^+$, $CD64^-$, $B220^-$ cells. **(b)** Summary data are shown as the percentage of DC populations among live cells. Error bars represent S.D.; statistical analysis carried out using a Mann-Whitney test.

We did, on the other hand, detect a significant increase in the frequency of TIM4$^+$ CD11b$^+$ CD103$^-$ DC and CD11b$^-$ CD103$^-$ DC in infected mice (Figure 5. 18).

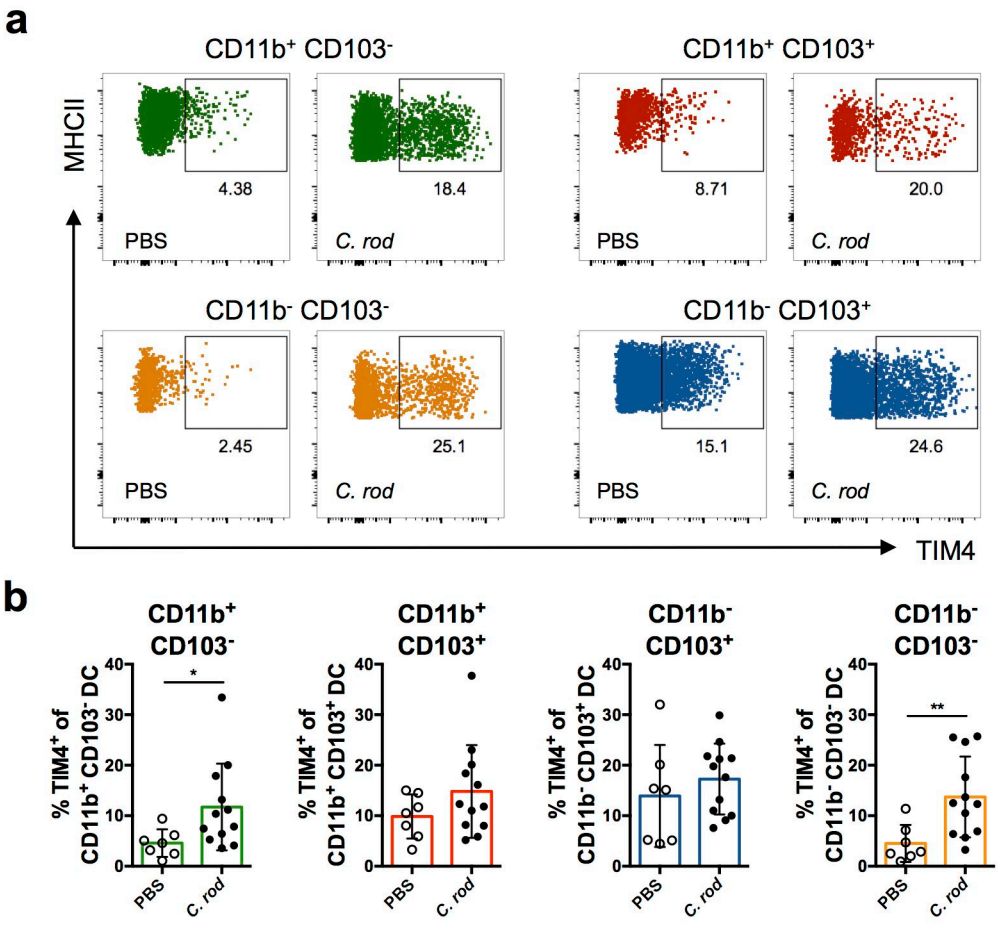

Figure 5. 18: TIM4 expression increases on colonic CD11b$^+$ CD103$^-$ and CD11b$^-$ CD103$^-$ DC during infection with *C. rodentium*

Mice were given PBS or infected with 2 × 10^9 CFU *C. rodentium* by oral gavage. Seven days p. i., colons were harvested and LP cells analysed by flow cytometry. **(a)** Representative plots showing TIM4 expression on colonic DC subsets from PBS-treated and infected (*C. rod*) mice. **(b)** Summary data shown as percentage of TIM4$^+$ cells among DC populations. Error bars represent S.D.; statistical analysis carried out using a Mann-Whitney test. * $p < 0.05$, ** $p < 0.01$

We had previously seen that colonic TIM4$^+$ CD11b$^-$ CD103$^+$ DC from naïve mice had greater expression of *Ccr7* and *Il1b* mRNA than their TIM4- counterparts (Figure 4. 20). Unfortunately, due to technical issues we were unable to accurately determine the transcript levels of *Ccr7* and *Il1b* in CD11b$^-$ CD103$^+$ DC from infected mice. However, in order to determine if the increase in TIM4 expression on CD11b$^+$ CD103$^-$ DC correlated with higher transcript levels for *Ccr7* and *Il1b*, we FACS-purified colonic CD11b$^+$ CD103$^-$ DC from PBS-treated and infected mice for qRT-PCR analysis (Figure 5. 19a). Surprisingly, we did not observe an upregulation of *Ccr7* expression after infection with *C. rodentium* (Figure 5. 19b). Furthermore, while there was a trend towards decreased expression of *Il1b* expression in CD11b$^+$ CD103$^-$ DC from infected animals, this was not statistically significant (Figure 5. 19b).

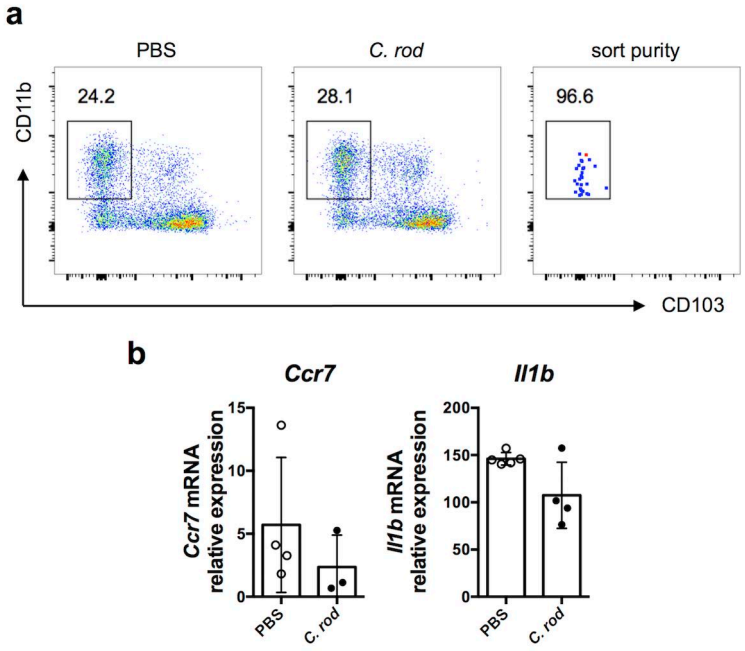

Figure 5. 19: Expression of *Ccr7* and *Il1b* mRNA in colonic CD11b$^+$ CD103$^-$ DC does not significantly change during infection with *C. rodentium*

Mice were given PBS or infected with 2 × 10^9 CFU *C. rodentium* by oral gavage. Seven days post-infection, colons were harvested and CD11b$^+$ CD103$^-$ DC FACS-sorted for qRT-PCR analysis. **(a)** Representative plots showing FACS sort gating and purity for CD11b$^+$ CD103$^-$ DC in PBS-treated and *C. rodentium* (*C. rod*) infected mice, gated on single, live, CD45$^+$, MHCII$^+$, CD11c$^+$, CD64$^-$, B220$^-$ cells. **(b)** Level of *Ccr7* and *Il1b* mRNA in colonic CD11b$^+$ CD103$^-$ DC from PBS-treated and *C. rod* infected mice as measured by qRT-PCR. Summary data are shown as *Ccr7* and *Il1b* mRNA expression relative to the housekeeping gene *Tbp*. Error bars represent S.D.; statistical analysis was carried out using a Mann-Whitney test.

TIM4 expression on lymph DC from cMLNx mice was unaffected by infection with *C. rodentium* (Figure 5. 20).

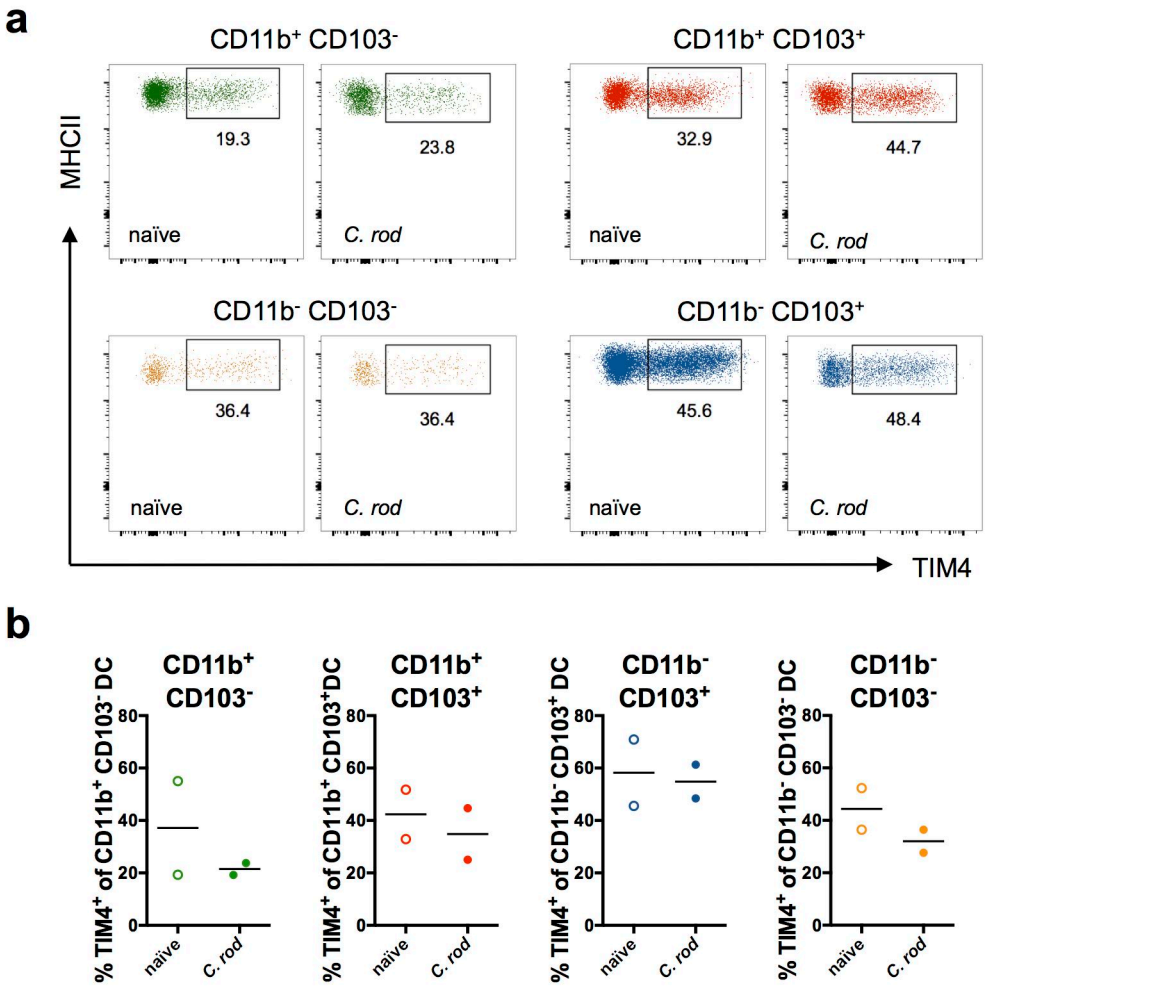

Figure 5. 20: TIM4 expression does not change on cMLNx lymph DC during infection with *C. rodentium*

Mice that had previously undergone colonic mesenteric lymphadenectomy (cMLNx) were infected with *C. rodentium* (*C. rod*). Six days p. i. thoracic duct cannulation was carried out with non-infected naïve cMLNx animals serving as controls. Lymph was collected over 16-24 h and cells analysed by flow cytometry. **(a)** Representative plots showing expression of TIM4 on cMLNx lymph DC populations gated on single, live, MHCII$^+$, CD11c$^+$, B220$^-$ cells. **(b)** Summary data are shown as the percentage of TIM4$^+$ cells among DC populations.

We next compared the frequency of the individual migratory DC populations in the cMLN between infected and uninfected mice. As in the colon, we found no significant changes in the frequency of migratory DC populations (Figure 5. 21).

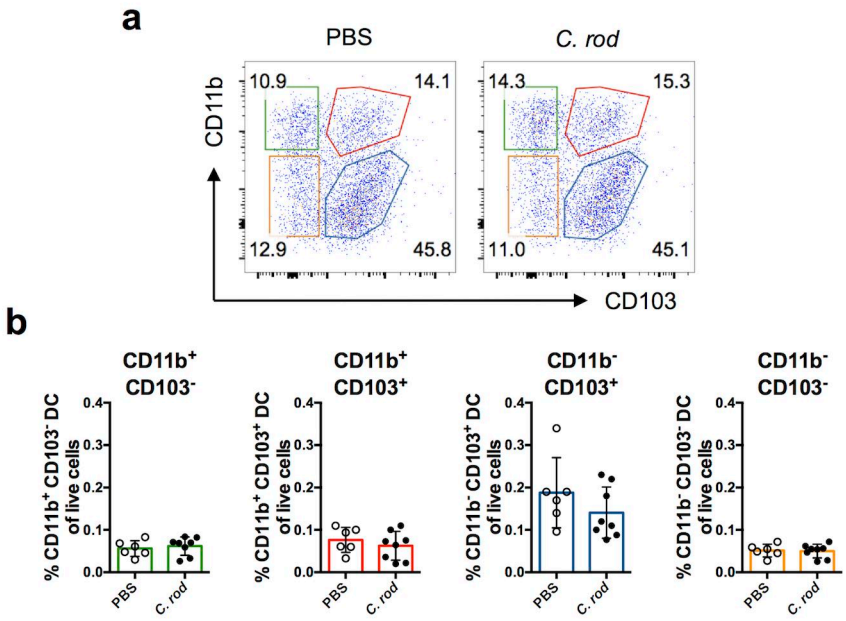

Figure 5. 21: The distribution of migratory DC populations in the cMLN does not change significantly during infection with *C. rodentium*

Mice were given PBS or infected with 2×10^9 CFU *C. rodentium* by oral gavage. Seven days p. i. cMLN were harvested and cells analysed by flow cytometry. **(a)** Representative plots showing DC populations gated on single, live, $CD45^+$, $MHCII^{hi}$, $CD11c^+$, $CD64^-$, $B220^-$ cells. **(b)** Summary data are shown as the percentage of DC populations among live cells. Error bars represent S.D.; statistical analysis carried out using a Mann-Whitney test.

However, contrary to the LP, TIM4 expression levels remained constant, with only a slight decrease on CD11b^{+} CD103^{+} DC that was not statistically significant (Figure 5. 22).

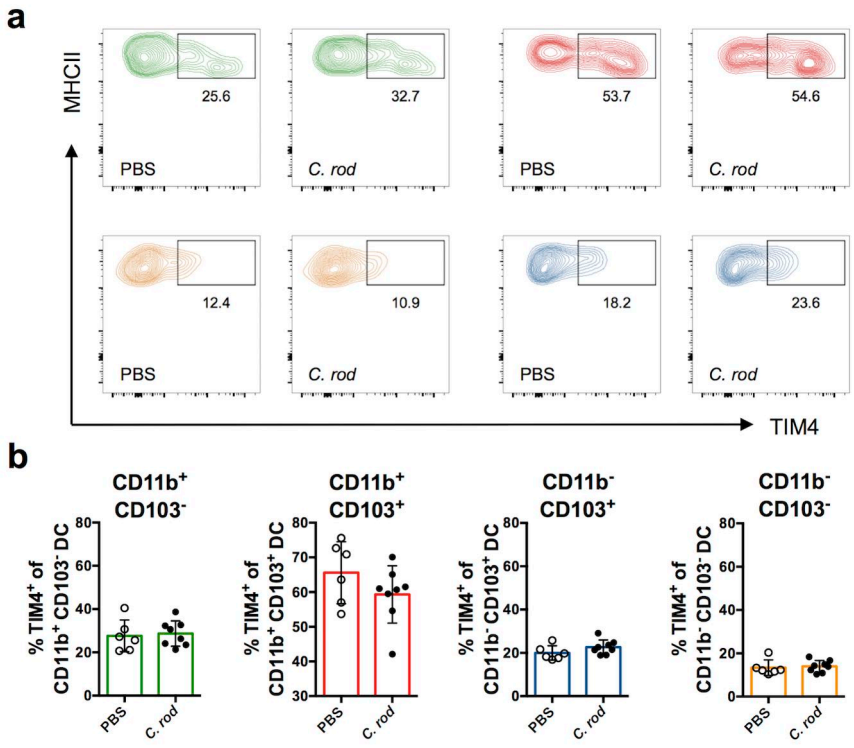

Figure 5. 22: TIM4 expression does not change on cMLN DC populations during infection with *C. rodentium*

Mice were given PBS or infected with 2 × 10^{9} CFU *C. rodentium* by oral gavage. Seven days p. i., cMLN (caecal, colonic and caudal LN) were harvested and cells analysed by flow cytometry. **(a)** Representative plots showing TIM4 expression on cMLN DC populations from PBS-treated and infected (*C. rod*) mice. **(b)** Summary data shown as percentage of TIM4^{+} cells among DC populations. Error bars represent S.D.; statistical analysis carried out using a Mann-Whitney test.

5.3 Discussion

Our previous work showed that TIM4 expression on DC was both population- and tissue-specific. We therefore set out to determine what factors might be involved in driving its expression. Firstly, we hypothesised that TIM4 was regulated by cytokines released in the local environment that acted on DC. IL-4 seemed a promising candidate, due to the importance of STAT6 signalling in driving TIM4 upregulation in a model of food allergy *in vivo* (Yang et al. 2016) and the reported role of TIM4 in inducing Th2 responses after treatment of human MNP with staphylococcal enterotoxin B (Liu et al. 2007). We therefore characterised the expression of TIM4 on DC from KN2 mice, which have had both copies of the *Il4* gene replaced by human CD2 (Mohrs et al. 2005), and compared them with KN2het mice, which are IL-4 sufficient. KN2 mice had normal DC population frequencies in the colonic LP and the cMLN, and TIM4 expression in these was not reduced compared with KN2het mice. In fact, there was a trend towards increased expression on total DC and macrophages in the LP of KN2 animals, although this did not reach statistical significance. More biological replicates would be required to determine if this difference is indeed consistently observed. IL-4 deficiency did not alter TIM4 expression on lung $CD103^+$ DC.

One explanation for these findings could be that the requirement for STAT6 in upregulating TIM4 expression observed previously (Yang et al. 2016) is dependent on IL-13 rather than IL-4 (Kaplan et al. 1996). A second reason for this independence of IL-4 could be the low basal levels of IL-4 in the gut and the lung. During parasite infections and allergic responses, large amounts of IL-4 are produced by a range of cells including $CD4^+$ T cells (Connor et al. 2014), mast cells (Wang et al. 1999), basophils (Motomura et al. 2014) and ILC2 (Pelly et al. 2016). However, less is known about the release of IL-4 at steady state. Recently, group 2 invariant natural killer T cells (NKT2) have been identified as producers of IL-4 in the MLN of naïve mice, leading to STAT6 phosphorylation on $CD4^+$ T cells (Lee, Wang, et al. 2015). This effect was especially pronounced in BALB/c mice, and significantly lower in C57BL/6 mice (Lee, Wang, et al. 2015), in concordance with the differential propensity of these strains to elicit Th2 responses (Locksley et al. 1987). There is evidence to suggest that the intestinal microbiota act to dampen baseline Th2 responses (Sudo et al. 1997, Wu et al. 2016). Together, these findings suggest that IL-4 availability in the intestine is tightly regulated in naïve mice. The fact that we saw no reduction of TIM4 on DC from IL-4-deficient animals suggests that TIM4 expression in the gut and the lung is IL-4 independent at steady state. Our results do not, however, negate the possibility that

TIM4 expression may be increased by IL-4 secretion during a Th2 challenge. Some work has been carried out in food allergy models in the small intestine using challenge with cholera toxin (Hilligan et al. 2016, Yang et al. 2016). However, as others (Hilligan et al. 2016) and we have found, basal levels of TIM4 on DC are low in the small intestine and it is difficult to assess the physiological relevance of these models in understanding tissue-specific regulation of TIM4 expression. Little is known about its regulation in more physiological models of Th2 induction in the colon and lung such as helminth infections or house dust mite challenge. These could be useful systems in which to test the hypothesis that TIM4 is indeed upregulated by IL-4 signalling and is important in the induction of Th2 responses in the tissues that actually contain TIM4 expressing DC.

Having found no role for homeostatic IL-4 in the induction of TIM4 expression, we next investigated if TGFβ signalling might be an important factor driving the cell and tissue-specific expression pattern we had observed. In the bone marrow, TGFβ supports the differentiation of conventional DC from CDP (Felker et al. 2010) and TGFβ signalling on DC is required for differentiation of $CD11b^{+}$ $CD103^{+}$ DC in the small intestine and to a lesser extent $CD11b^{-}$ $CD103^{+}$ DC in the colon and lung (Bain and Montgomery et al., *in press*). Furthermore, DC-specific deficiency in Smad7, a potent negative regulator of TGB-β signalling, increased the frequency of splenic $CD8\alpha^{+}$ $CD103^{+}$ DC *in vivo* (Lukas et al. 2017). $CD11b^{-}$ $CD103^{+}$ DC at mucosal sites and $CD8\alpha^{+}$ DC in the spleen are members of the same lineage of conventional DC (cDC1) (Guilliams et al. 2014), based on their shared transcriptional profile (Guilliams et al. 2016), and ability to cross-present antigen (Haan et al. 2000, Desch et al. 2011, Cerovic et al. 2014b). Expression of the cDC1-associated transcription factor IRF8 is upregulated by TGFβ (Ju et al. 2007), a further indication of its importance in regulating the development of cDC1. TGFβ is produced in a latent form that requires activation by the integrin αvβ8 (Travis et al. 2007), which is most highly expressed on intestinal $CD103^{+}$ DC (Worthington et al. 2011). Furthermore, IRF8 is required for the expression of αvβ8 on DC (Yoshida et al. 2014). Together, these observations suggest that TGFβ is an important factor influencing the function of cDC1, possibly via an autocrine mechanism (Belladonna et al. 2008, Kashiwagi et al. 2015). This is especially intriguing in the context of apoptotic cell uptake, as this induces TGFβ production by antigen-presenting cells (Torchinsky et al. 2009), which in turn could convey autocrine signals to the DC and lead to the sustained upregulation of ACR. TGFβ positively regulates

expression of Axl on Langerhans cells (Bauer et al. 2012) and a similar mechanism might be applicable to TIM4.

Based on these findings and the preferential expression of TIM4 on cDC1 in the colon and the lung, we hypothesised that TGFβ signalling may be important in its regulation. To test this, we used mice that lacked TGFβR1 on CD11c$^+$ cells (CD11c-Cre *Tgfbr1*$^{fl/fl}$ *Rag1*$^{-/-}$), therefore abrogating the effects of TGFβ signalling on DC and macrophages. These mice had a decrease in colonic CD11b$^-$ CD103$^+$ DC, thus confirming previous reports (Bain and Montgomery et al., *in press*), however, we did not detect a change in lung CD103$^+$ DC frequencies. When we analysed TIM4 expression on DC subsets in the colonic LP, we found that the frequency of TIM4$^+$ cells did not, as anticipated, decrease on CD11b$^-$ CD103$^+$ with lack of TGFβ signalling. On the other hand, CD11b$^+$ CD103$^+$ DC from Cre$^+$ mice did exhibit a significant decrease in TIM4$^+$ cells compared with Cre$^-$ littermate controls. This was unexpected, and given the low baseline expression of TIM4 on this subset of DC in the LP, difficult to interpret. It would have been interesting to investigate if CD11b$^+$ CD103$^+$ DC in the MLN also had decreased expression of TIM4 in Cre$^+$ animals. Unfortunately, due to the need to keep mice on a *Rag1*$^{-/-}$ background, the resultant lack of properly formed LN made this impossible.

We did not find a significant change in the frequency of TIM4$^+$ cells among colonic macrophages. Schridde et al. (2017) have shown that TGFβ signalling is required for colonic macrophage differentiation and the accompanying upregulation of genes involved in tissue repair. Both they and we have found that TIM4 is expressed on fully differentiated macrophages (Schridde et al. 2017). However, *Timd4* gene expression was not significantly downregulated in colonic macrophages from CD11c-Cre *Tgfbr1*$^{fl/fl}$ *Rag1*$^{-/-}$ mice (Schridde et al. 2017), although a trend towards decreased expression was observed (A. Schridde, *personal communication*). This may explain why we also did not find a clear difference.

TIM4 expression on colonic CD11b$^-$ CD103$^+$ DC did not significantly change. In the lung, on the other hand, while we saw no change in subset frequency, we did find a significant increase in TIM4$^+$ cells among CD103$^+$ DC (from 80% TIM4$^+$ cells in Cre$^-$ to 90% in Cre$^+$ animals). These findings could be explained in two ways; firstly, instead of inducing TIM4 expression on cDC1, TGFβ signalling serves as a negative regulator. However, the changes observed are small and as CD103$^+$ DC in the lung already express high levels of TIM4, this explanation seems unlikely. An alternative explanation could be that the observed changes

are secondary to the loss of TGFβR1 on DC, rather than due to a cell intrinsic mechanism. For example, loss of TGFβ signalling in DC could affect their regulatory function within the tissue, which in turn could shift the microenvironment to a more pro-inflammatory state and increase the rate of epithelial cell apoptosis. There is some evidence that such a feedback mechanism might be in place in the colon, as CD11c-Cre *Tgfbr2*$^{fl/fl}$ mice develop spontaneous colitis characterised by dysbiosis and goblet cell depletion (Ihara et al. 2016). In contrast to the inflammation observed in our mice if not maintained on a *Rag1*$^{-/-}$ background, this is not likely to be due to a reduction of Treg cell frequencies induced by the deletion of TGFβR2 on T cells, as expression of the receptor and TGFβ induced Smad2 signalling in these was not altered (Ihara et al. 2016). Lack of TGFβ signalling was shown to elevate Notch ligand expression in colonic DC and Cre^{+} epithelial cells exhibited a concomitant rise in *Hes1* transcript levels *in vivo* (Ihara et al. 2016). IEC-specific constitutive activation of Notch signalling leads to lack of goblet cell differentiation and IEC apoptosis (Fre et al. 2005). These findings point to a possible crosstalk mechanism between intestinal DC and epithelial cells that is dependent on DC intrinsic TGFβ signalling. The enhanced apoptosis that may ensue as a result of abrogating this interaction could lead to an increase in ACR such as TIM4 that is secondary to deletion of the TGFβR. However, to test this hypothesis, further experiments would need to be designed. These, in turn, may reveal an alternative or additional mechanisms connecting TIM4 and TGFβ.

An additional secondary factor in these mice might be the targeted deletion of TGFβR1 on alveolar macrophages, which also express CD11c. Indeed, when TGFβR2 was specifically deleted on macrophages using a LysM-Cre system, mice exhibited increased granulocyte infiltration in the lung, as well as reduction in epidermal growth factor expression, an important regulator of epithelial cell homeostasis (Heitmann et al. 2012). These findings support the conclusion that increased TIM4 expression on CD103^{+} DC in the lung may in fact be secondary to pro-inflammatory changes and increased apoptosis in the tissue induced by DC-epithelial cell interactions or off-target TGFβR1 deletion. To test this hypothesis, the extent of apoptosis in the epithelium should have been assessed in the epithelium Cre^{+} mice and changes in TIM4 expression analysed in mice treated with a caspase-3 inhibitor. An unfortunate confounding factor that must be considered when interpreting our results is that the mice used in this experiment had concurrent pinworm infection. This colonic infection was accompanied by an increase in SiglecF^{+} eosinophils in the colonic LP (data not shown) and may have had a significant effect on LP DC subset

function. Furthermore, given previous indications of a role of TIM4 in Th2 responses (Liu et al. 2007, Yang et al. 2016), it is possible that this strong Th2 stimulus could have increased TIM4 expression on DC, thus masking a potential decrease in Cre^+ mice.

Using our systems we were unable to show that TIM4 expression is dependent on either IL-4 or TGFβ signalling in the colon and lung. Given the higher frequency of $TIM4^+$ cells in the colon when compared with the small intestine, our second main hypothesis was that TIM4 expression on DC is controlled by the microbiota. *In vitro* evidence of TIM4 upregulation by flagellin on bone marrow derived mast cells (Li et al. 2014) and by LPS activation of bone marrow derived macrophages (Ji et al. 2014) indicates that PAMPs may indeed be important regulators of TIM4 expression. We therefore treated WT C57BL/6 mice with a cocktail of antibiotics for seven days to deplete a broad spectrum of the microbiota and analysed DC subsets and their expression of TIM4 in different tissues. We found that the distribution of DC subsets in the colonic LP and cMLN were not altered in mice that had received antibiotics compared with controls. Previously, antibiotic treatment has been shown to increase the frequency of $CD103^+$ and $CD103^-$ DC subsets in the MLN (Diehl et al. 2013), although this apparent discrepancy with our findings may be due to the shorter treatment duration used in our study (one week as opposed to four weeks). Of note, antibiotic induced changes in DC frequencies were not observed in a more recent study, where antibiotic treatment had no effect on the number of $CD103^+$ DC in the MLN (Hägerbrand et al. 2015), or in our own unpublished work. GF mice have been reported to have fewer total $CD11c^+$ (Walton et al. 2006, Chung et al. 2012) and $CD11c^+$ $CD103^+$ cells in the MLN (Niess et al. 2008), as well as fewer $CD11c^+$ $CX3CR1^+$ $CD103^-$ cells in the colonic LP (Niess et al. 2008). Given that macrophages also express CD11c and CX3CR1, these cell populations are likely to be composed of a mixture of $CD11b^+$ $CD103^+$ DC and macrophages, therefore making it difficult to draw a valid conclusion from these findings. Much more definitive data was provided by analysis of DC subset proportions in mesenteric lymph from GF and SPF mice, which were unchanged (Hägerbrand et al. 2015). This is consistent with our findings that DC subset composition is stable even after depletion of the microbiota.

We did not detect any significant changes in the expression of TIM4 on either total DC or individual DC subsets, or macrophages in the colonic DC after antibiotic treatment. Furthermore, TIM4 expression was not significantly altered on resident and migratory populations of DC in the cMLN or the ILN, included as a peripheral LN control. There

was, however, a trend towards a greater percentage of TIM4$^+$ cells in resident ILN DC of control mice. Contrary to the antibiotic-treated mice, tail bite wounds were evident in these mice, suggesting that they had been fighting. The trend that we observed may therefore be due to skin involvement, rather than microbiota-specific changes, especially given that no difference was seen in the cMLN. This admits the intriguing possibility that inflammation increases the expression of TIM4 on LN DC, but further work would be required to confirm this observation.

Microbiota-derived metabolites such as SCFA have strong immunomodulatory functions. The production of SCFA is dependent of the metabolism of dietary fibre by anaerobic bacteria. Interestingly, mice fed a high fibre diet have an increased proportion and RALDH activity of MLN CD103$^+$ DC compared with mice maintained on a fibre-deficient diet (Tan et al. 2016). This effect was specific to the SCFA butyrate and acetate (Tan et al. 2016). It is unclear, however, by what mechanism these metabolites influence the distribution of DC subsets in the MLN. The same report also showed that the proportional increase in CD103$^+$ DC after high fibre feeding was in part dependent on MyD88 signalling, thereby implicating PAMPs as a second important microbiota-derived signal that influences DC subsets (Tan et al. 2016). However, it is as yet unknown how the microbiota influences expression of ACR on antigen-presenting cells. Gas6 was reduced in the oral mucosa of GF mice (Nassar et al. 2017), implicating microbiota derived signals in its induction. Yet the expression pattern of other ACR in GF mice compared with SPF control animals remains unclear. Moreover, the role of TLR signalling induced by PAMPs, or SCFA signalling in regulating the expression of TIM4 or other ACR has not yet been clarified.

There is evidence to suggest that maturation of small intestinal DC induced by cholera toxin increases the expression of TIM4 on CD11b$^+$ CD103$^+$ DC in the LP and MLN (Hilligan et al. 2016). Furthermore, TIM4^{hi} DC in the MLN had greater expression levels of co-stimulatory molecules compared with TIM4$^-$ DC (Hilligan et al. 2016). Together with our observation that TIM4 is upregulated in lymph, these findings suggest the possibility that DC maturation can lead to TIM4 expression. MyD88 signalling in DC is required for DC maturation (Sporri and Reis e Sousa 2005, Yarovinsky et al. 2006). In the intestine, steady state migration of CD11b$^+$ CD103$^+$ and CD11b$^-$ CD103$^+$ DC to the MLN is dependent on MyD88 signalling (Hägerbrand et al. 2015). Given, however, that DC migration is not changed in GF mice, it is likely that MyD88 activation in intestinal DC is not limited to PAMPs, but could also be constituted by DAMPs from dying cells

(Hägerbrand et al. 2015). Furthermore, apoptotic cell inclusions can also be found in MLN DC of GF rats (Huang et al. 2000), suggesting that expression of ACR is not exclusively dependent on the microbiota. Taken together, these findings could explain why we did not observe a decrease in TIM4 expression in antibiotic-treated mice.

We next investigated if bacteria-induced inflammation in the intestine had any effect on TIM4 regulation by infecting mice with *C. rodentium*, an A/E pathogen that induces a robust colonic Th17 response (Mangan et al. 2006). Previous reports have shown the peak of infection to take place around ten days p.i. (Symonds et al. 2009). However, we were able to detect the induction of Th17 cells already at seven days p.i. in both the colonic LP and the cMLN, which in these experiments included the caudal LN due to involvement of rectal pathology (Wiles et al. 2006). This suggests that the infection has established and the tissue environment become pro-inflammatory at this time point. Nonetheless, it is early enough to detect and explore how changes in DC might influence T cell priming before the peak of infection is reached. We therefore chose this time point in our subsequent investigations.

Depletion of DC leads to decreased survival of *C. rodentium* infected mice, which fail to induce T cell priming and differentiation into the Th17 lineage (Schreiber et al. 2013). Furthermore, MyD88 signalling in $CD11c^+$ cells is required for animal survival and clearance of *C. rodentium* (Longman et al. 2014), suggesting that recognition of PAMPs by DC is likely to contribute to the mounting of a protective immune response against the pathogen. In particular, pathogen clearance relies on Notch2-dependent $CD11b^+$ DC (Satpathy et al. 2013), which have further been implicated functionally as sources of IL-23 in the tissue, thus helping maintain the Th17 pool and inducing IL-22 production by ILC3 (Satpathy et al. 2013, Aychek et al. 2015). BATF3 deficiency, on the other hand, depletes $CD11b^-$ $CD103^+$ DC (cDC1) in the intestine (Edelson et al. 2010), and *Batf3*$^{-/-}$ mice do not succumb to infection with *C. rodentium*, in contrast to CD11c-Cre *Notch2*$^{fl/fl}$ mice (Satpathy et al. 2013), suggesting that these DC are not essential for clearance of the pathogen. Interestingly, IL-23 deficiency during infection with *C. rodentium* leads to enhanced production of IL-12 by $CD11b^-$ $CD103^+$ DC, and subsequent IFNγ-induced immunopathology (Aychek et al. 2015), suggesting that tight regulation of this populations's function is essential to prevent an inappropriately strong Th1 response. We found no evidence of a change in DC population frequency in the LP or cMLN of infected animals. However, further experiments would be required to determine if *C. rodentium*

infection impacts DC function in a population-specific manner, and if this is dependent on TIM4 expression.

C. rodentium induces IEC apoptosis, dependent on effector protein EspF (Torchinsky et al. 2009), and an increase in TIM4 expression on DC and macrophages in response to this higher apoptotic burden is therefore plausible. Next to DC, macrophages are important players that help orchestrate the protective immune response against *C. rodentium*. For example, production of IL-23 by CX3CR1^{+} cells, likely to be mainly mature macrophages, is an important driver of IL-22 production (Longman et al. 2014, Aychek et al. 2015). We therefore aimed to ascertain if expression of TIM4 on either DC or macrophages changes during infection, thereby helping further define a function for this molecule in shaping downstream immunity. We found that while the percentage of TIM4^{+} Ly6C^{-} MHCII^{+} mature macrophages did not change seven days p.i. with *C. rodentium*, there was a trend towards increased TIM4 expression on total DC in the colonic LP. Furthermore, when we assessed if TIM4 expression changed in a subset-specific manner on DC, we found that it was indeed increased only on CD11b^{+} CD103^{-} and CD11b^{-} CD103^{-} DC.

Uptake of apoptotic cells by phagocytes has been shown to induce a regulatory phenotype (Torchinsky et al. 2009, Cummings et al. 2016) and reduce the production of IL-23 (Stark et al. 2005). However, the intracellular presence of TLR ligands due to phagocytosis of infected apoptotic cells can instead induce the production of IL-6 (Torchinsky et al. 2009). It is conceivable that this can also activate the inflammasome via NLR to induce IL-1β production (Rathinam et al. 2012), which in turn can stimulate the differentiation of Th17 cells (Ghoreschi et al. 2010). Furthermore, NOD2 expression in human MNP is required for the production of IL-23 after stimulation with TLR ligands (van Beelen et al. 2007), highlighting the importance of intracellular PAMP sensing in production of this mediator. We reasoned that increased expression of TIM4 on CD11b^{+} CD103^{-} DC during *C. rodentium* infection would have a downstream effect on their expression profile of pro-inflammatory mediators. We therefore measured the transcript levels of *Il1b* in FACS-sorted colonic CD11b^{+} CD103^{-} DC from infected and PBS-treated animals, but were unable to detect a significant difference between the two groups. Given the importance of IL-23 production by CD11b^{+} DC during *C. rodentium* infection, a more comprehensive investigation should have also included transcript level assessment of *Il23p19*. Furthermore, analysis of *Il6* expression and that of its receptor *Il6ra* could also have been

informative, due to the importance of IL-6 trans-presentation by DC in Th17 induction (Heink et al. 2017).

The increased expression of TIM4 on colonic LP CD11b^{+} CD103^{-} DC did not translate to the colon draining lymph or cMLN of infected mice. We had previously shown that TIM4 expression on DC increases in lymph, and suggested that this could be indicative of a more mature migratory phenotype. The fact that *C. rodentium* infection did not further increase this proportion seems to provide evidence against this hypothesis, as previous work investigating the maturation of DC in response to infection with *S.* Typhimurium has shown that expression of co-stimulatory molecules on migratory MLN DC increases under these circumstances (Sundquist and Wick 2005). Interestingly, the essential role of DC in orchestrating protective immunity to *C. rodentium* seems to be restricted to DC in the LP, as *Ccr7*$^{-/-}$ mice don't exhibit decreased survival compared with WT animals (Satpathy et al. 2013). As well as being indicative of a tissue-specific response to enhanced apoptosis, upregulation of TIM4 on colonic rather than cMLN DC may therefore also be important for shaping DC production of pro-inflammatory mediators in the LP.

While having shown that TIM4 expression is increased in a population-specific manner in the colonic LP during *C. rodentium* infection, our experimental approach was not comprehensive enough to identify the upstream signals that induced this upregulation. In the first place, it would have been important to confirm that in our hands and at the time point chosen, infection with *C. rodentium* indeed does induce enhanced apoptosis in the colon, thereby providing a potential trigger for the upregulation of TIM4. *In vivo* inhibition of caspases during *C. rodentium* infection decreases IEC apoptosis (Torchinsky et al. 2009) and a similar approach could have helped provide evidence for a functional link between the two. Alternatively, TIM4 expression on DC could have been assessed during DSS colitis, which induces widespread apoptosis in the colonic epithelium (Edelblum et al. 2008, Araki et al. 2010), and could have been used as a comparison to infective colitis. Consequently, it would also have been useful to confirm if TIM4 upregulation was a MyD88-dependent mechanism initiated by the phagocytosis of dying infected cells. Use of bacterial mutants defective in specific TLR ligands such as flagellin could help to answer this question, although the lack of pathogenicity that often characterises these strains might limit their usefulness in elucidating this *in vivo*.

We were also unable to establish if TIM4 upregulation has any functional effect on CD11b^{+} CD103^{-} DC during infection. For example, it would have been of interest to FACS-sort

$TIM4^+$ and $TIM4^-$ $CD11b^+$ $CD103^-$ DC during infection and compare their ability to take up apoptotic bodies *in vitro*. The small number of $TIM4^+$ cells recovered and the difficulty in maintaining LP DC *ex vivo* does place some constraints on this approach. More comprehensive transcriptional profiling of $TIM4^+$ and $TIM4^-$ populations would be a further informative and important way of testing the hypothesis that $TIM4^+$ cells upregulate the expression of pro-inflammatory mediators after phagocytosing infected apoptotic cells. Based on the work carried out by Torchinsky et al. (2009), it is tempting to speculate that increased TIM4 expression on DC during *C. rodentium* infection is protective by enhancing their ability to help establish Th17 responses. However, more functional experiments are required to confirm if this truly is the case.

Chapter 6: TIM4 function in the intestine and MLN

6.1 Aims and hypotheses

TIM4 expression may correlate with a migratory signature on DC and is upregulated in a population-specific manner in the colonic LP during *C. rodentium* infection. These findings indicate three possible roles for this molecule in regulating DC function. First, it may directly be involved in DC migration to the LN, by interacting with integrins or other glycoproteins on the lymphatic endothelium. The presence of an RGD peptide motif in its Ig domain, and the great number of O-linked glycosylation sites found in the mucin domain of TIM4 support this as a likely hypothesis. We therefore used Kaede mice to determine if DC migration to the LN was indeed dependent on functional TIM4.

Second, expression of TIM4 is upregulated in lymph and remains high on DC in the MLN, indicating that it may also have a role in antigen presentation. TIM4 is the ligand for TIM1 (Meyers et al. 2005), which is induced on T cells upon activation (de Souza et al. 2005). Ligation of TIM1 in the presence of co-stimulatory signals induces polyclonal T cell proliferation independently of TCR engagement (Mariat et al. 2009). Based on these observations, it is possible that TIM4 expressed on DC in the MLN can help sustain and amplify T cell activation. An alternative role during antigen presentation could be given by its native function as a PSR. During TCR ligation, the membrane surrounding the immunological synapse undergoes rearrangement (Gagnon et al. 2012), leading to the limited exposure of PS (Fischer et al. 2006, Albacker et al. 2013) on the cell surface. Recognition of PS by TIM4^{+} DC during antigen presentation could therefore allow further tethering and stabilisation of the immunological synapse. To address this question, we assessed the ability of MLN DC populations to drive an antigen-specific T cell response *in vitro* whilst concomitantly blocking TIM4.

Finally, as well as a possible role in supporting these functions in naïve mice, TIM4 may also shape DC function during bacterial-induced intestinal inflammation, as we found colonic DC upregulate TIM4 expression during *C. rodentium* infection. This could be due to the increased level of IEC apoptosis, or the increased abundance of PAMPs in the colonic LP of infected mice. However, it is unknown if TIM4-mediated uptake of apoptotic cells in this setting is required for instructing T cell differentiation during antigen presentation. Infection with both *C. rodentium* (Torchinsky et al. 2009) and

S. Typhimurium (Liu et al. 2010, Srikanth et al. 2010) causes the upregulation of apoptotic pathways in the colonic epithelium but contrary to *C. rodentium*, *S.* Typhimurium elicits a mixed Th1 and Th17 response (Lee et al. 2012). Given the importance of apoptotic cell uptake in the induction of Th17 responses to *C. rodentium* (Torchinsky et al. 2009), we asked if TIM4 upregulation on DC during infection was a driving factor for this. We therefore compared the importance of TIM4 in skewing T cell responses in these two different bacterial infections to help further elucidate its function.

6.2 Results

6.2.1 TIM4 function in DC migration to the cMLN

To test the hypothesis that TIM4 played a role in directly enhancing the efficiency of DC migration to the cMLN, we injected Kaede mice with αTIM4 antibody or Rat IgG2a isotype control 24 h before photoconverting the proximal colon using violet light (Figure 6. 1). After 48 h we harvested the cMLN and analysed the proportion of Kaede-red^{+} DC that had migrated from the colon (Figure 6. 1).

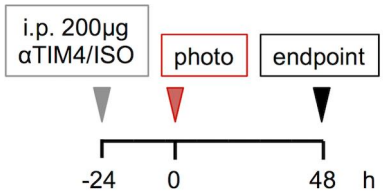

Figure 6. 1: Experimental setup to investigate the function of TIM4 in steady state DC migration to the cMLN

Schematic showing experimental setup, where Kaede mice were given 200 µg αTIM4 antibody or Rat IgG2a (ISO) by intraperitoneal (i.p.) injection 24 h before laparotomy and photoconversion (photo) of the proximal colon using violet light. Tissues were harvested 48 h post-photoconversion and cells analysed by flow cytometry.

The rate of colonic photoconversion in mice receiving αTIM4 or isotype control was comparable (Figure 6. 2a). Furthermore, TIM4 staining on colonic and cMLN DC was drastically reduced in mice that had received the blocking antibody compared with the isotype control (Figure 6. 2b, c).

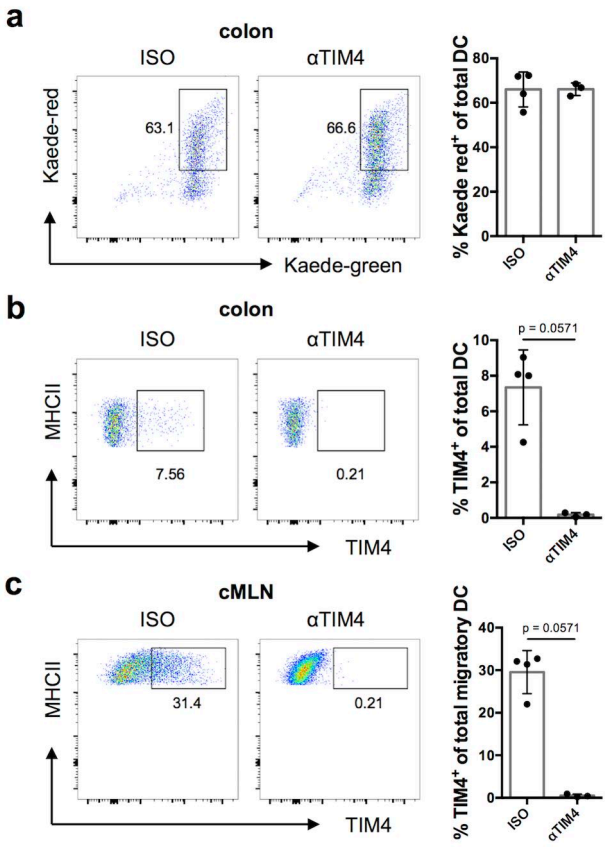

Figure 6. 2: The photoconversion rate between groups is comparable and TIM4 staining is reduced on colonic and cMLN DC

Kaede mice were given 200 µg αTIM4 antibody or Rat IgG2a (ISO) by intraperitoneal (i.p.) injection 24 h before laparotomy and photoconversion of the proximal colon using violet light. Colons and cMLN were harvested 48 h post-photoconversion and cells analysed by flow cytometry. **(a)** Representative plots showing total Kaede-red$^+$ DC in the colonic LP from αTIM4- and ISO-treated mice gated on single, live, CD45$^+$, MHCII$^+$, CD11c$^+$, CD64$^-$, B220$^-$ cells. Summary data are shown as percentage of Kaede-red$^+$ cells among total DC. **(b)** Representative plots showing total TIM4$^+$ colonic DC gated on single, live, CD45$^+$, MHCII$^+$, CD11c$^+$, CD64$^-$, B220$^-$ cells. Summary data are shown as percentage of TIM4$^+$ cells among total DC. **(c)** Representative plots showing total TIM4$^+$ migratory DC in the cMLN gated on single, live, CD45$^+$, MHCII^{hi}, CD11c$^+$, CD64$^-$, B220$^-$ cells. Summary data are shown as the percentage of TIM4$^+$ cells among total DC. Error bars represent the S.D.; statistical analysis carried out using a Mann-Whitney test.

To confirm that this decrease was not caused by the selective depletion of TIM4$^+$ DC in the colonic LP or cMLN, we compared the percentage and number of DC for each population in these tissues and found no significant change with αTIM4 treatment (Figure 6. 3 and Figure 6. 4). We concluded, therefore, that the reduction in TIM4 staining we had observed was either due to its internalisation or masking by the circulating injected antibody. We reasoned that its function would likely to be compromised in either case. Indeed, previously published work indicates that this approach successfully abolishes TIM4 function *in vivo* (Yeung et al. 2013, Ji et al. 2014).

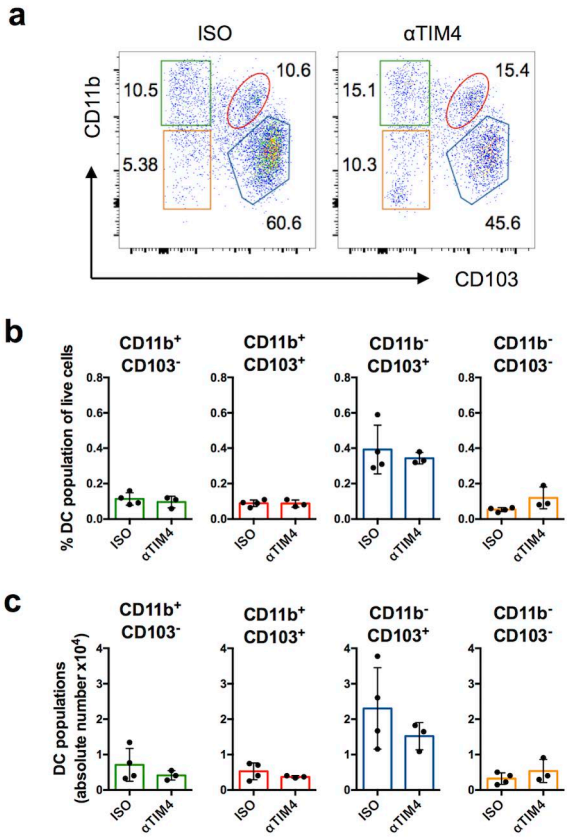

Figure 6. 3: Colonic DC population distribution does not change significantly after TIM4 blocking

Kaede mice were given 200 µg αTIM4 antibody or Rat IgG2a (ISO) by intraperitoneal (i.p.) injection 24 h before laparotomy and photoconversion of the proximal colon using violet light. Colons were harvested 48 h post-photoconversion and cells analysed by flow cytometry. **(a)** Representative plots showing DC populations in the colonic LP from αTIM4- and ISO-treated mice gated on single, live, CD45$^+$, MHCII$^+$, CD11c$^+$, CD64$^-$, B220$^-$ cells. Summary data are shown as **(b)** percentage of DC populations among live cells and **(c)** absolute cell number. Error bars represent S.D.; statistical analysis was carried out using a Mann-Whitney test.

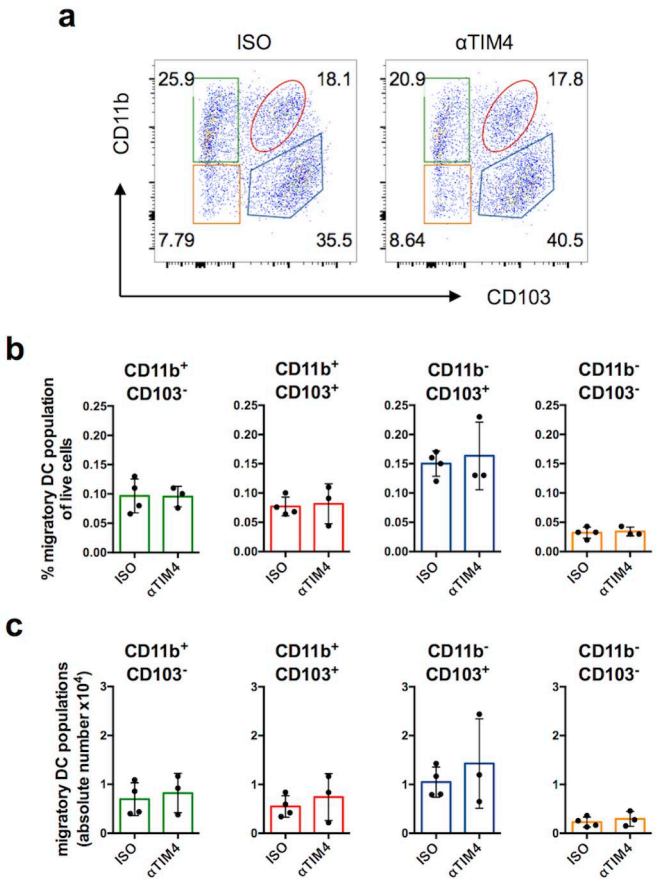

Figure 6. 4: Migratory DC population distribution in the cMLN does not change significantly after TIM4 blocking

Kaede mice were given 200 µg αTIM4 antibody or Rat IgG2a (ISO) by intraperitoneal (i.p.) injection 24 h before laparotomy and photoconversion of the proximal colon using violet light. Colon draining MLN (cMLN) were harvested 48 h post-photoconversion and cells analysed by flow cytometry. **(a)** Representative plots showing migratory DC populations in the cMLN from αTIM4- and ISO-treated mice gated on single, live, $CD45^+$, $MHCII^{hi}$, $CD11c^+$, $CD64^-$, $B220^-$ cells. Summary data are shown as **(b)** percentage of DC populations among live cells and **(c)** absolute cell number. Error bars represent S.D.; statistical analysis was carried out using a Mann-Whitney test.

When we compared the migratory DC compartment in the cMLN of mice given αTIM4 with those that had received the isotype control, we found no difference in the percentage or number of Kaede-red$^+$ DC between the two groups (Figure 6. 5). Moreover, this was true for all migratory DC subsets (Figure 6. 6).

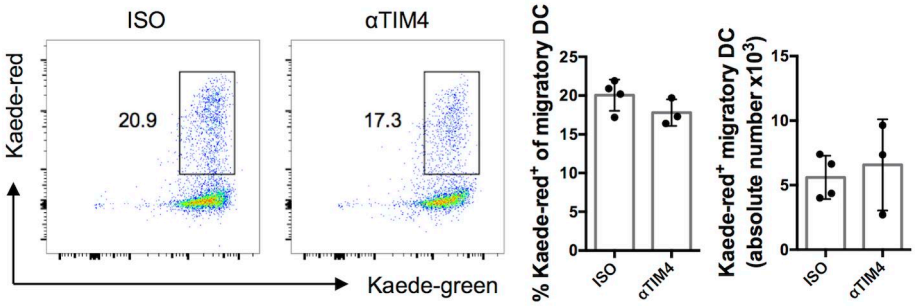

Figure 6. 5: Blocking TIM4 *in vivo* does not significantly decrease Kaede-red$^+$ migratory DC proportions or numbers in the cMLN

Kaede mice were given 200 µg αTIM4 antibody or Rat IgG2a (ISO) by intraperitoneal (i.p.) injection 24 h before laparotomy and photoconversion of the proximal colon using violet light. Colon draining MLN (cMLN) were harvested 48 h post-photoconversion and cells analysed by flow cytometry. Representative plots show Kaede-red$^+$ migratory DC in the cMLN from αTIM4- and ISO-treated mice gated on single, live, CD45$^+$, MHCII^{hi}, CD11c$^+$, CD64$^-$, B220$^-$ cells. Summary data are shown as the absolute cell number and percentage of Kaede-red$^+$ cells among migratory DC. Error bars represent S.D; statistical analysis carried out using a Mann-Whitney test.

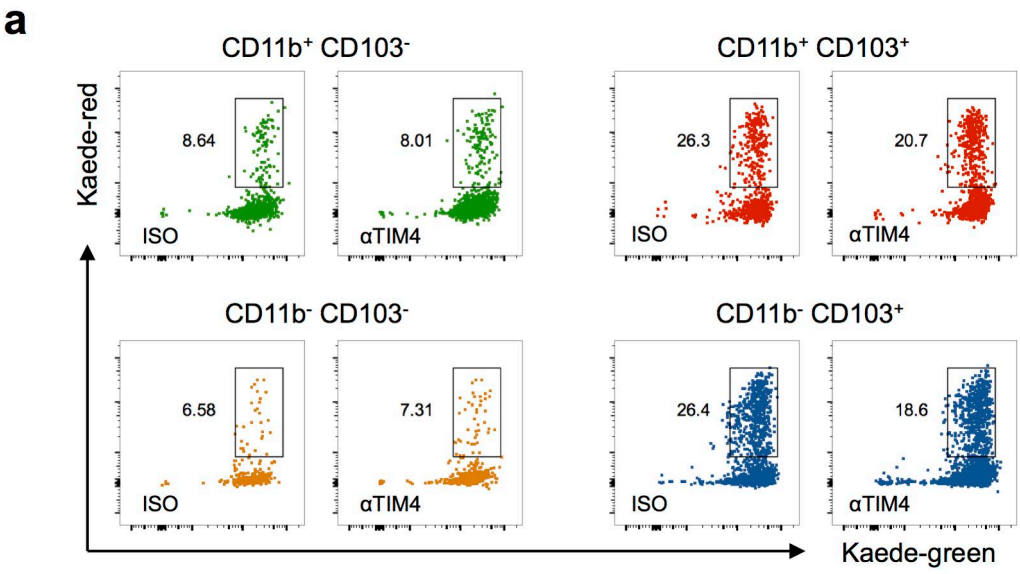

Figure 6.6 continued on next page

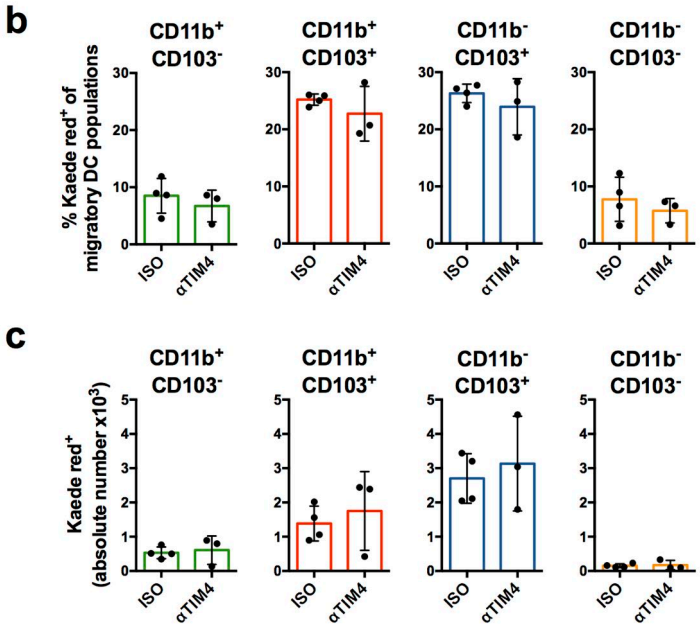

Figure 6. 6: Blocking TIM4 does not alter the percentage or number of Kaede-red$^+$ cells among cMLN migratory DC populations

Kaede mice were given 200 µg αTIM4 antibody or Rat IgG2a (ISO) by intraperitoneal (i.p.) injection 24 h before laparotomy and photoconversion of the proximal colon using violet light. Colon draining MLN (cMLN) were harvested 48 h post-photoconversion and cells analysed by flow cytometry. **(a)** Representative plots show Kaede-red$^+$ cells among each migratory DC subset in the cMLN from αTIM4- and ISO-treated mice gated on single, live, CD45$^+$, MHCII^{hi}, CD11c$^+$, CD64$^-$, B220$^-$ cells. Summary data show as **(b)** the percentage of Kaede-red$^+$ cells among each DC subset and **(c)** their absolute cell number. Error bars represent S.D.; statistical analysis carried out using a Mann-Whitney test.

6.2.2 TIM4 function in antigen presentation on MLN DC

Having seen little evidence for a role of TIM4 in directly facilitating DC migration to the MLN *in vivo*, we used an *in vitro* system to determine if TIM4 was required for efficient antigen-specific T cell proliferation. Total MLN migratory DC subsets were FACS-sorted (Figure 6. 7) and pulsed with OVA protein before co-culturing for three days with CFSE-labelled OT-II MLN cells in the presence of αTIM4 antibody or Rat IgG2a isotype control.

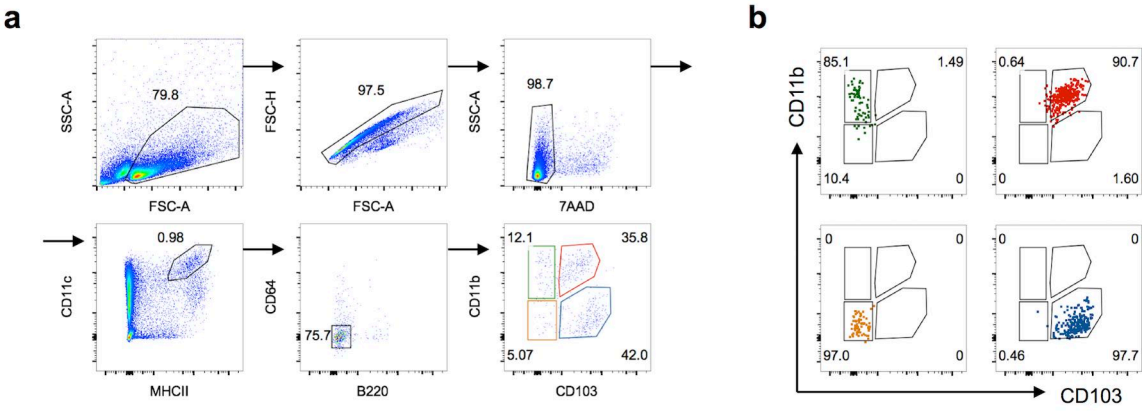

Figure 6. 7: FACS sort gating and purity for MLN DC migratory populations

Whole MLN from naïve C57BL/6 mice were harvested and migratory DC populations FACS sorted for co-culture with OT-II and OT-I MLN cells. **(a)** Representative plots showing gating strategy for MLN migratory DC populations, gated on single, live, $MHCII^{hi}$, $CD11c^{+}$, $CD64^{-}$, $B220^{-}$ cells. **(b)** Representative plots showing sort purity of DC populations.

All DC subsets were able to induce antigen-specific proliferation of CD4⁺ T cells, with CD11b⁺ CD103⁻ DC eliciting the strongest response (Figure 6. 8). However, blocking TIM4 *in vitro* had no effect on the ability of DC subsets to induce CD4⁺ T cell proliferation (Figure 6. 8).

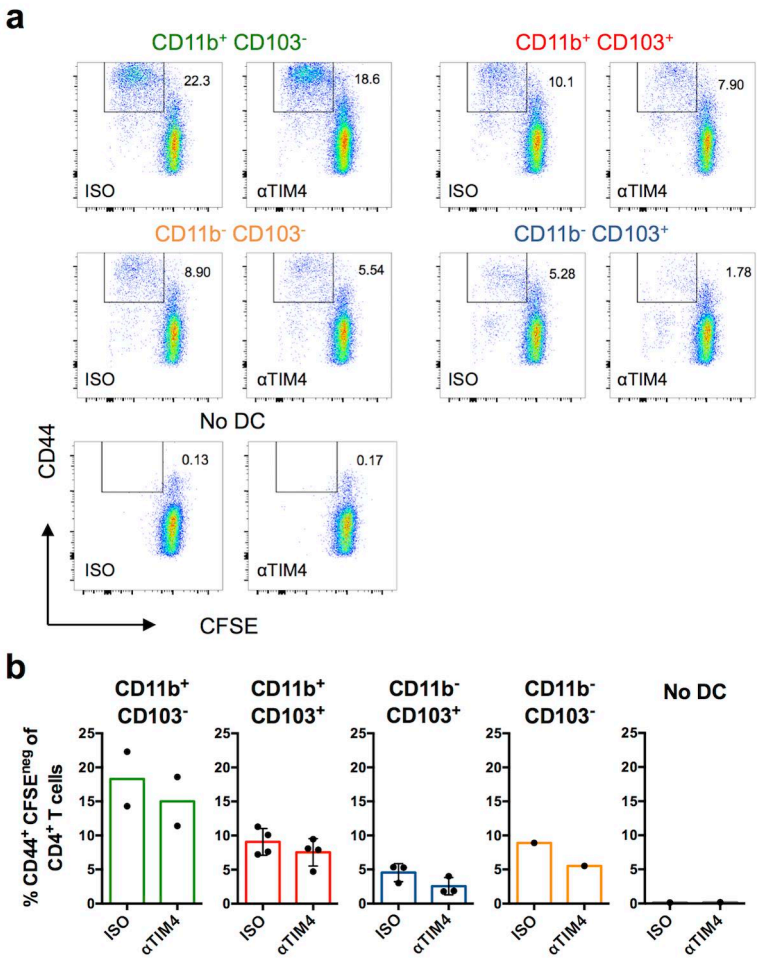

Figure 6. 8: Blocking TIM4 does not alter antigen-specific proliferation of CD4⁺ T cells *in vitro*

Whole MLN from naïve C57BL/6 mice were harvested and migratory DC subsets FACS sorted for co-culture with OT-II MLN cells. For each subset, 7,500 DC were incubated with 2 mg/ml OVA for two hours and subsequently co-cultured with 200,000 CFSE-labelled OT-II MLN cells in the presence of 5 µg/ml αTIM4 or Rat IgG2a isotype control (ISO) for three days. OT-II MLN cells were then analysed by flow cytometry. **(a)** Representative plots showing proliferated CD44⁺ CFSE^{neg} cells gated on single, live, CD3⁺ CD4⁺ T cells. A control without added DC was included to discount any non-specific proliferation ("No DC"). **(b)** Summary data shown as the percentage of CD44⁺ CFSE^{neg} cells among CD4⁺ T cells. Error bars represent S.D.; statistical analysis was carried out using a Mann-Whitney test.

On the other hand, a small but significant decrease in the proportion of proliferated T cells expression CCR9 was observed after blocking TIM4 in cultures with CD11b$^+$ CD103$^+$ DC (Figure 6. 9).

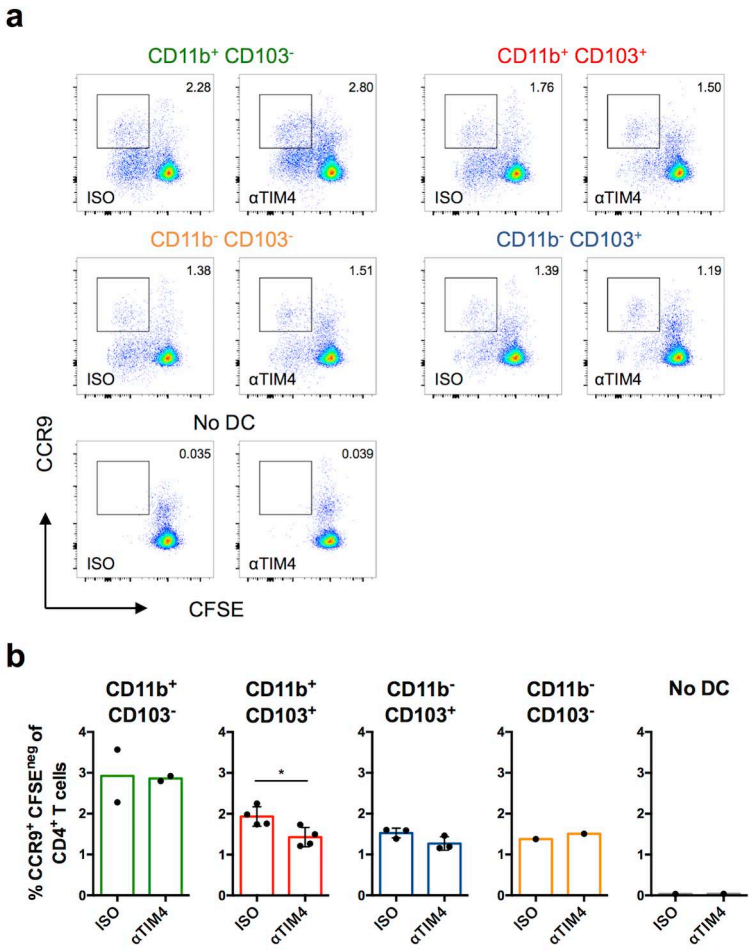

Figure 6. 9: Blocking TIM4 reduces CCR9 induction on CD4$^+$ T cells by CD11b$^+$ CD103$^+$ DC *in vitro*

Whole MLN from naïve C57BL/6 mice were harvested and migratory DC subsets FACS sorted for co-culture with OT-II MLN cells. For each subset, 7,500 DC were incubated with 2 mg/ml OVA for two hours and subsequently co-cultured with 200,000 CFSE-labelled OT-II MLN cells in the presence of 5 µg/ml αTIM4 or Rat IgG2a isotype control (ISO) for three days. OT-II MLN cells were then analysed by flow cytometry. **(a)** Representative plots showing CCR9$^+$ CFSE^{neg} cells gated on single, live, CD3$^+$, CD4$^+$ T cells. A control without added DC was included to discount any non-specific proliferation ("No DC"). **(b)** Summary data shown as the percentage of CCR9+ CFSE^{neg} cells among CD4+ T cells. Error bars represent S.D.; statistical analysis was carried out using a Mann-Whitney test. * $p < 0.05$.

Conversely, expression of the integrin β7 was not reduced when OT-II cells were co-cultured with DC in the presence of αTIM4 (Figure 6. 10).

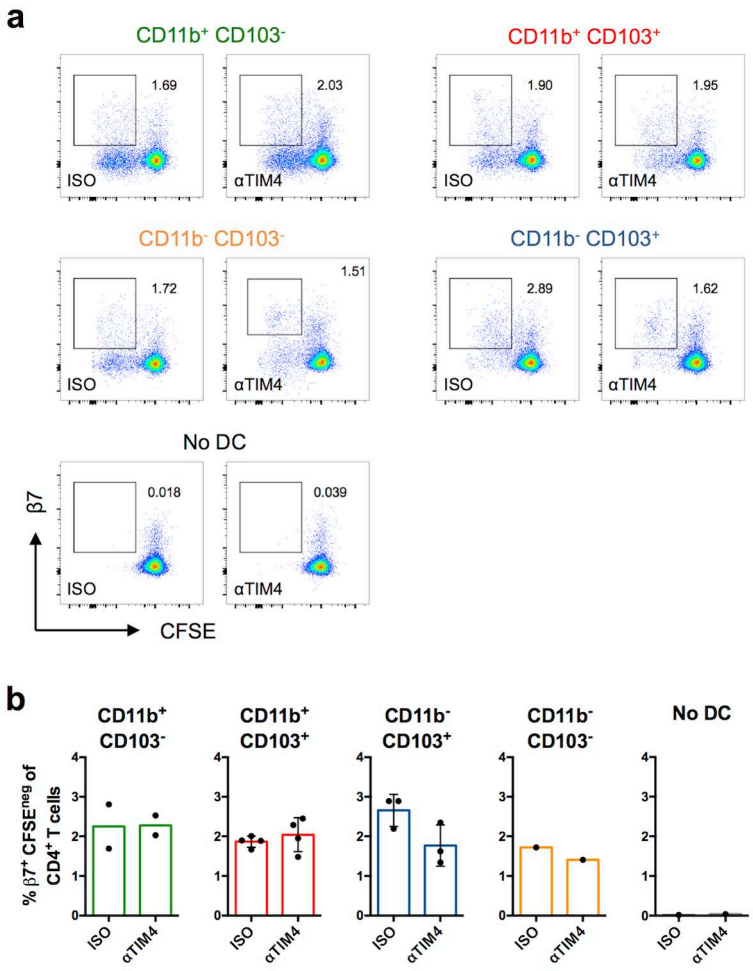

Figure 6. 10: Blocking TIM4 *in vitro* does not significantly change integrin β7 expression on CD4⁺ T cells after antigen-specific proliferation

Whole MLN from naïve C57BL/6 mice were harvested and migratory DC subsets FACS sorted for co-culture with OT-II MLN cells. For each subset, 7,500 DC were incubated with 2 mg/ml OVA for two hours and subsequently co-cultured with 200,000 CFSE-labelled OT-II MLN cells in the presence of 5 μg/ml αTIM4 or Rat IgG2a isotype control (ISO) for three days. OT-II MLN cells were then analysed by flow cytometry. **(a)** Representative plots showing $\beta7^+$ $CFSE^{neg}$ cells gated on single, live, $CD3^+$, $CD4^+$ T cells. A control without added DC was included to discount any non-specific proliferation ("No DC"). **(b)** Summary data shown as the percentage of $\beta7^+$ $CFSE^{neg}$ cells among $CD4^+$ T cells. Error bars represent S.D.; statistical analysis was carried out using a Mann-Whitney test.

Given the ability of CD11b$^-$ CD103$^+$ DC to cross-present self-derived antigen, we tested if TIM4 had any functional role in this process *in vitro*. We co-cultured OVA-pulsed MLN migratory CD11b$^-$ CD103$^+$ DC with OT-I MLN cells in the presence of αTIM4 antibody or Rat IgG2a isotype control for three days. As seen before with OT-II cells, proliferation of OT-I CD8$^+$ T cells was not impacted by blocking TIM4 *in vitro* (Figure 6. 11).

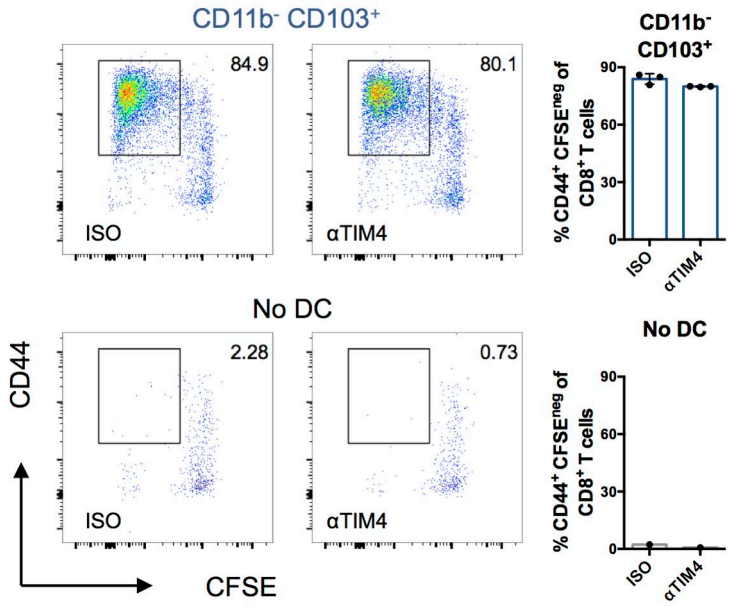

Figure 6. 11: Blocking TIM4 does not alter antigen-specific proliferation of CD8$^+$ T cells *in vitro*

Whole MLN from naïve C57BL/6 mice were harvested and migratory CD11b$^-$ CD103$^+$ DC FACS sorted for co-culture with OT-I MLN cells. To achieve this, 7,500 CD11b$^-$ CD103$^+$ DC were incubated with 2 mg/ml OVA for two hours and subsequently co-cultured with 200,000 CFSE-labelled OT-I MLN cells in the presence of 5 μg/ml αTIM4 or Rat IgG2a isotype control (ISO) for three days. OT-I MLN cells were then analysed by flow cytometry. Representative plots show CD44$^+$ CFSE^{neg} cells gated on single, live, CD3$^+$, CD8$^+$ T cells. A control without added DC was included to discount any non-specific proliferation ("No DC"). Summary data are shown as the percentage of CD44$^+$ CFSE^{neg} cells among CD8$^+$ T cells. Error bars represent S.D.; statistical analysis carried out using a Mann-Whitney test.

Furthermore, expression of CCR9 and integrin β7 (Figure 6. 12) were also unchanged on proliferated CD8⁺ T cells

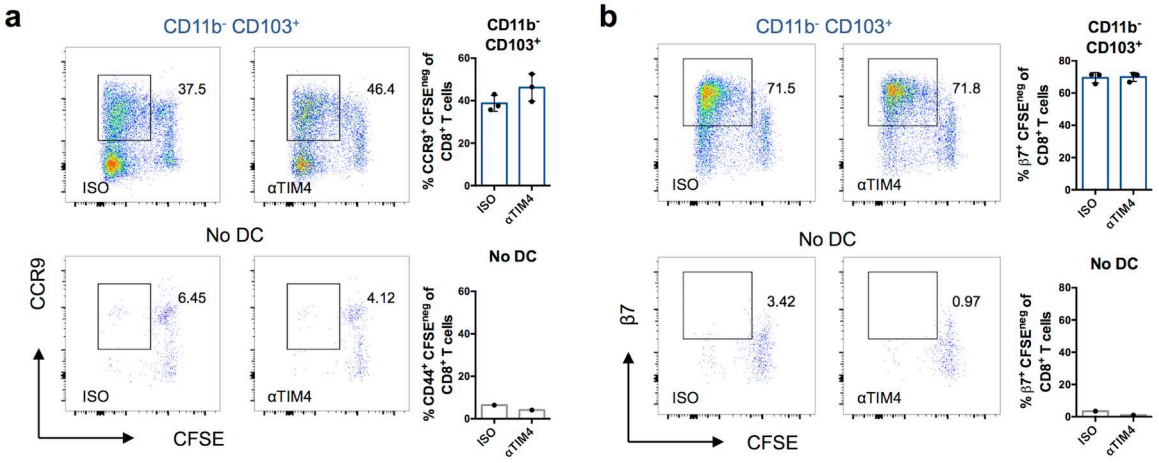

Figure 6. 12: Blocking TIM4 does not alter induction of intestinal homing markers on CD8⁺ T cells *in vitro*

Whole MLN from naïve C57BL/6 mice were harvested and migratory CD11b⁻ CD103⁺ DC FACS sorted for co-culture with OT-I MLN cells. To achieve this, 7,500 CD11b⁻ CD103⁺ DC were incubated with 2 mg/ml OVA for two hours and subsequently co-cultured with 200,000 CFSE-labelled OT-I MLN cells in the presence of 5 μg/ml αTIM4 or Rat IgG2a isotype control (ISO) for three days. OT-I MLN cells were then analysed by flow cytometry. A control without added DC was included to discount any non-specific proliferation ("No DC"). **(a)** Representative plots show CCR9⁺ CFSE^{neg} cells gated on single, live, CD3⁺, CD8⁺ T cells. Summary data are shown as the percentage of CCR9⁺ CFSE^{neg} cells among CD8⁺ T cells. **(b)** Representative plots show β7⁺ CFSE^{neg} cells gated on single, live, CD3⁺, CD8⁺ T cells. Summary data are shown as the percentage of β7⁺ CFSE^{neg} cells among CD8⁺ T cells. Error bars represent S.D.; statistical analysis carried out using a Mann-Whitney test.

We next assessed whether antigen-specific activation of CD4$^+$ and CD8$^+$ T cells by MLN DC *in vitro* could induce TIM1 expression, as had previously been reported in other systems (de Souza et al. 2005). Interestingly, we did not detect any TIM1 induction on proliferated OT-II CD4$^+$ T cells, while a small proportion of OT-I CD8$^+$ T cells did upregulate TIM1 after proliferation, independently of blocking TIM4 (Figure 6. 13).

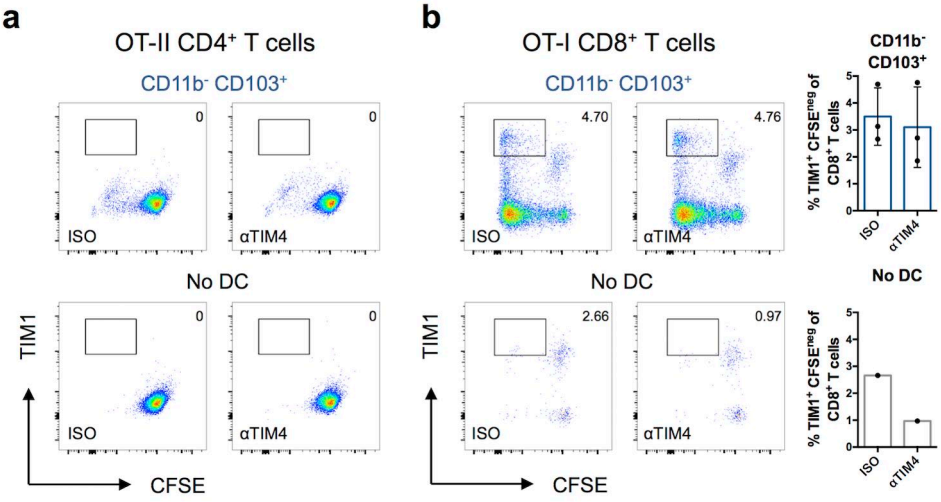

Figure 6. 13: TIM1 is induced on CD8$^+$ but not CD4$^+$ T cells *in vitro* independently of TIM4 blocking

Whole MLN from naïve C57BL/6 mice were harvested and migratory CD11b$^-$ CD103$^+$ DC FACS sorted for co-culture with OT-II or OT-I MLN cells. To achieve this, 7,500 CD11b$^-$ CD103$^+$ DC were incubated with 2 mg/ml OVA for two hours and subsequently co-cultured with 200,000 CFSE-labelled OT-II or OT-I MLN cells in the presence of 5 µg/ml αTIM4 or Rat IgG2a isotype control (ISO) for three days. OT-II and OT-I MLN cells were then analysed by flow cytometry. A control without added DC was included to discount any non-specific proliferation ("No DC"). **(a)** Representative plots showing TIM1$^+$ CFSE^{neg} cells gated on single, live, CD3$^+$, CD4$^+$ OT-II T cells. **(b)** Representative plots showing TIM1$^+$ CFSE^{neg} cells gated on single, live, CD3$^+$, CD8$^+$ OT-I T cells. Summary data are shown as the percentage of TIM1$^+$ CFSE^{neg} cells among CD8$^+$ T cells. Error bars represent S.D.; statistical analysis was carried out using a Mann-Whitney test.

6.2.3 TIM4 function in *C. rodentium* infection

During *C. rodentium* infection we the percentage of TIM4$^+$ cells increased for CD11b$^+$ CD103$^-$ and CD11b$^-$ CD103$^-$ DC in the colonic LP (Figure 5. 18). Given the importance of apoptotic cell uptake in initiation of Th17 responses (Torchinsky et al. 2009), we tested if TIM4 had a functional role in facilitating this *in vivo*. We infected mice with bioluminescent *C. rodentium* for seven days, during which time we treated them twice with αTIM4 antibody or Rat IgG2a isotype control by intraperitoneal (i.p.) injection (Figure 6. 14).

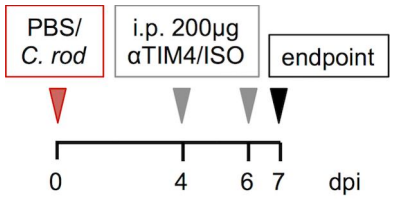

Figure 6. 14: Experimental setup for investigating the role of TIM4 during infection with *C. rodentium*

Schematic showing experimental setup, where mice were given PBS of infected with 2×10^9 CFU bioluminescent *C. rodentium* (*C. rod*) by oral gavage. Four and six days p. i. (dpi), infected mice were treated with intraperitoneal (i.p.) injections of 200 µg αTIM4 antibody or Rat IgG2a isotype control (ISO). Seven days p. i., tissues were harvested and cells analysed by flow cytometry.

We did not observe any differences in bacterial burden at the rectum after seven days in the two infected groups (Figure 6. 15).

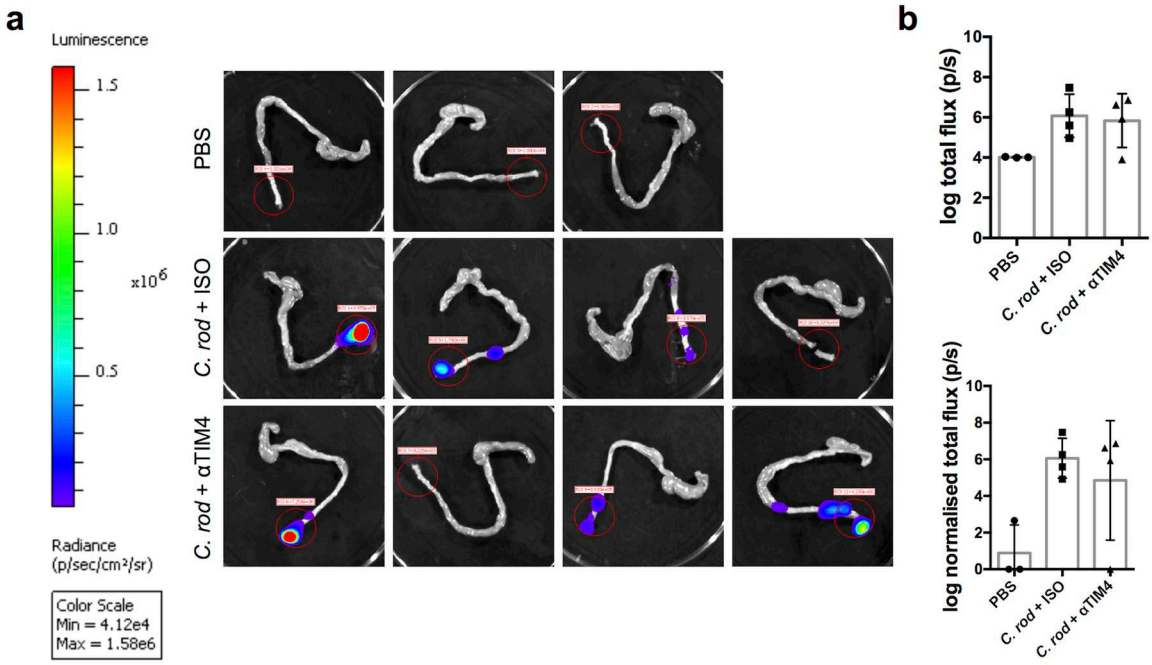

Figure 6. 15: Blocking TIM4 during *C. rodentium* infection does not have an impact on bacterial burden

Mice were given PBS of infected with 2×10^9 CFU bioluminescent *C. rodentium* (*C. rod*) by oral gavage. Four and six days p. i. (dpi), infected mice were treated with intraperitoneal (i.p.) injections of 200 µg αTIM4 antibody or Rat IgG2a isotype control (ISO). Seven days p. i. colons and caeca were harvested. **(a)** Bacterial luminescence in the organs was measured and images acquired using an IVIS Spectrum Imaging System. For each specimen the rectum was identified as a region of interest (ROI) for quantification of luminescence. **(b)** Total flux (photons/s) was measured for individual ROI and subsequently normalised by subtracting the mean total flux of uninfected PBS controls to eliminate background luminescence.

As described previously, there was a trend towards increased TIM4 expression on total colonic LP DC after infection with *C. rodentium* in the group given the isotype control, but treatment with αTIM4 significantly reduced TIM4 staining (Figure 6. 16a). This reduction was also seen on colonic Ly6C$^-$ MHCII$^+$ macrophages (Figure 6. 16b), and on migratory DC in the cMLN (Figure 6. 16c).

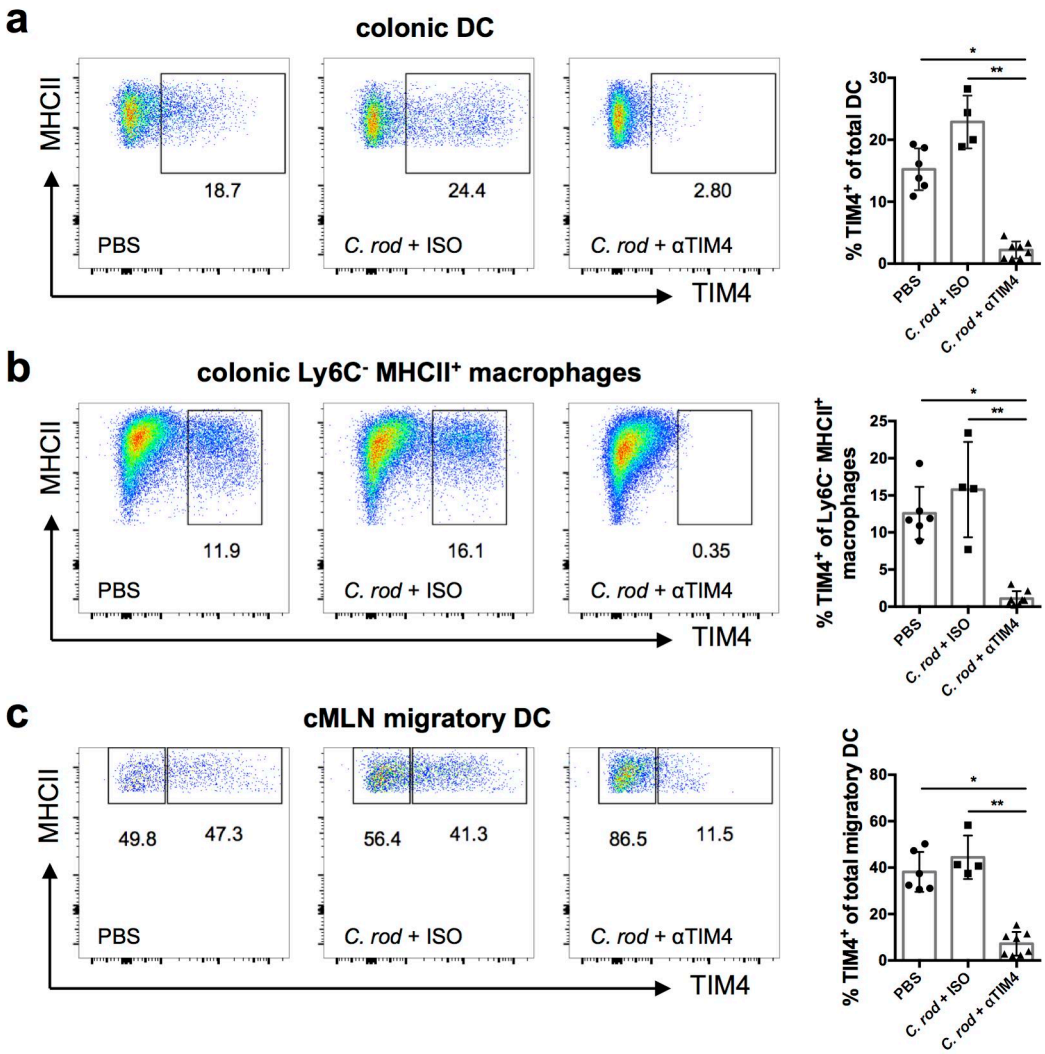

Figure 6. 16: Percentage of TIM4$^+$ DC and macrophages during infection with *C. rodentium* and concurrent blocking of TIM4

Mice were given PBS or infected with 2 × 10^9 CFU bioluminescent *C. rodentium* (*C. rod*) by oral gavage. Four and six days p. i., infected mice were treated with intraperitoneal (i.p.) injections of 200 µg αTIM4 antibody or Rat IgG2a isotype control (ISO). Seven days p. i., colons and cMLN were harvested and cells analysed by flow cytometry. **(a)** Representative plots showing TIM4$^+$ colonic LP DC gated on single, live, CD45$^+$, MHCII$^+$, CD11c$^+$, CD64$^-$, B220$^-$ cells. Summary data are shown as TIM4$^+$ cells among total LP DC. **(b)** Representative plots showing TIM4$^+$ colonic macrophages gated on single, live, CD45$^+$, CD11b$^+$, (Ly6G$^-$), SSC^{lo}, CD64$^{int\text{-}hi}$, Ly6C$^-$, MHCII$^+$ cells. Summary data are shown as TIM4$^+$ cells among Ly6C$^-$ MHCII$^+$ macrophages. **(c)** Representative plots showing TIM4$^+$ cMLN migratory total DC gated on single, live, CD45$^+$, MHCII^{hi}, CD11c$^+$, CD64$^-$, B220$^-$ cells. Summary data are shown as percentage of TIM4$^+$ cells among total migratory DC. Error bars represent S.D.; statistical analysis carried out using a Kruskal-Wallis test with a Dunn's post-test for multiple comparisons. * $p < 0.05$, ** $p < 0.01$.

Analysis of colonic LP DC subsets revealed, as previously observed, that *C. rodentium* infection reduced the percentage of CD11b$^-$ CD103+ DC (Figure 6. 17a, b), but not their absolute cell number (Figure 6. 17c). Furthermore, this was not impacted by blocking TIM4 (Figure 6. 17).

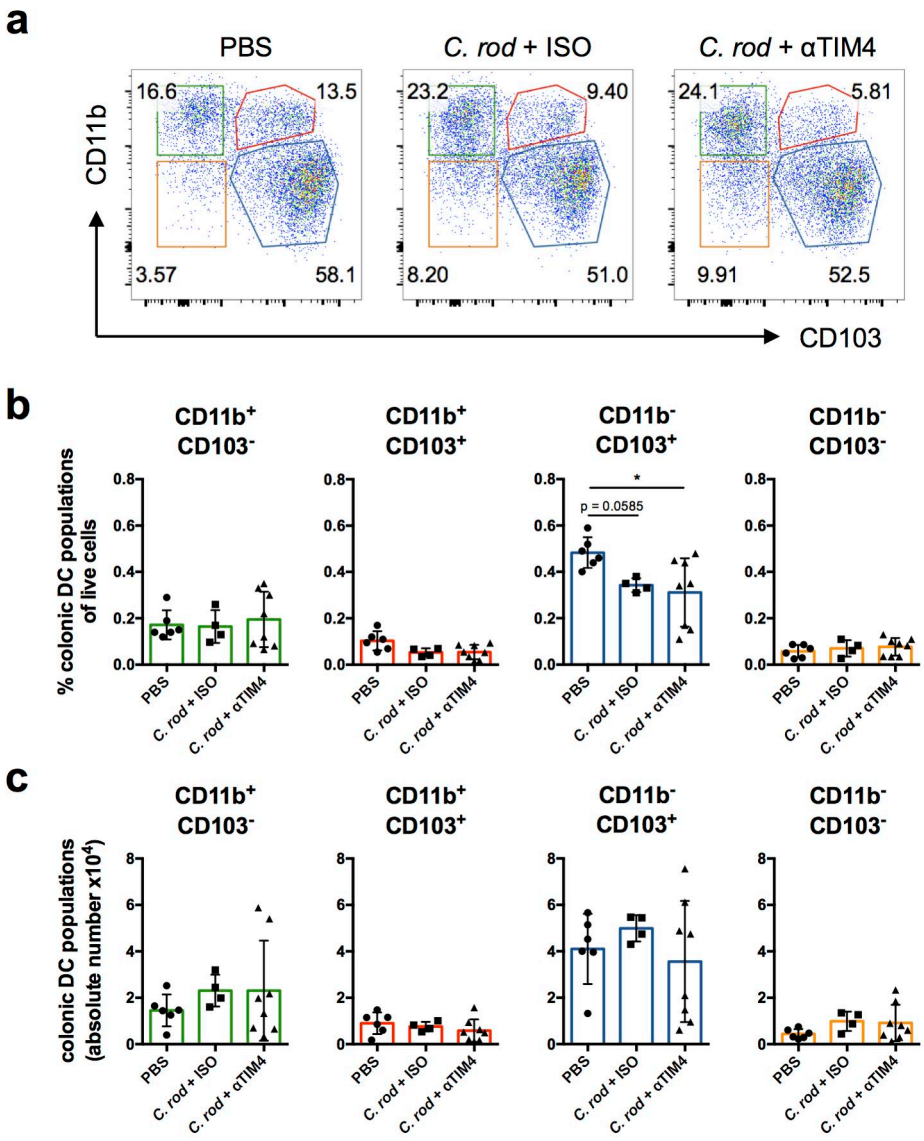

Figure 6. 17: The distribution of colonic DC populations is not impacted by TIM4 blocking during *C. rodentium* infection

Mice were given PBS or infected with 2 × 10^9 CFU bioluminescent *C. rodentium* (*C. rod*) by oral gavage. Four and six days p. i., infected mice were treated with intraperitoneal (i.p.) injections of 200 µg αTIM4 antibody or Rat IgG2a isotype control (ISO). Seven days p. i., colons were harvested and LP cells analysed by flow cytometry. **(a)** Representative plots showing colonic DC subsets from uninfected (PBS) and infected mice treated with αTIM4 antibody or ISO, gated on single, live, CD45$^+$, MHCII$^+$, CD11c$^+$, CD64$^-$, B220$^-$ cells. Summary data shown as **(b)** the percentage of DC populations among live cells and **(c)** their absolute cell number. Error bars represent S.D.; statistical analysis carried out using a Kruskal-Wallis test with a Dunn's post-test for multiple comparisons. * $p < 0.05$.

Nonetheless, the effect of TIM4 blockade may have been to reduce capacity to phagocytose apoptotic material on CD11b$^-$ CD103$^+$ DC, impacting downstream functions, such as maturation and cytokine production. We therefore FACS-sorted CD11b$^-$ CD103$^+$ DC for gene transcription analysis from the colons of PBS-treated mice and from *C. rodentium* infected mice, that had or hadn't received αTIM4 antibody (Figure 6. 18a). In order to assess if TIM4 blocking reduces the maturation of DC, we assessed the expression of *Ccr7* mRNA in CD11b$^-$ CD103$^+$ DC isolated from the three groups. However, we saw no significant changes in transcript levels of *Ccr7* (Figure 6. 18b). Given the importance of both IL-1β and TGFβ in the induction of Th17 responses (Mangan et al. 2006, Veldhoen et al. 2006, Ghoreschi et al. 2010), we used the same approach to assess the expression of *Il1b* and the TGFβ activating integrin beta8 (*Itgb8*) in CD11b$^-$ CD103$^+$ DC. However, we found no difference in expression levels in CD11b$^-$ CD103$^+$ DC from the three experimental groups (Figure 6. 18b).

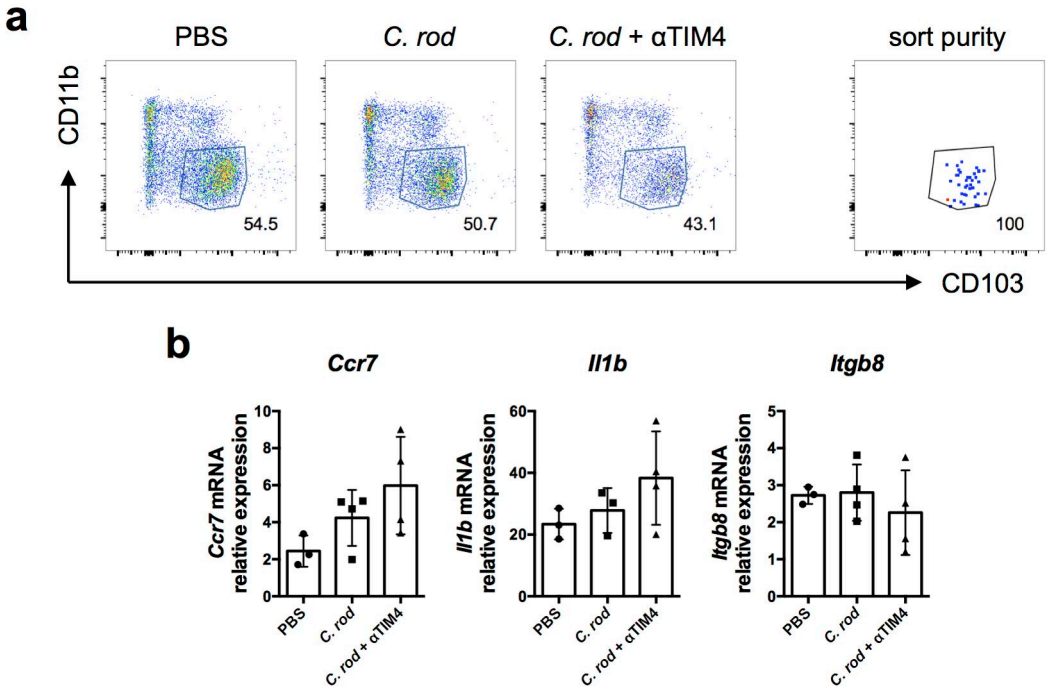

Figure 6. 18: Gene expression in colonic CD11b$^-$ CD103$^+$ DC during *C. rodentium* infection does not change with TIM4 blocking

Mice were given PBS or infected with 2 × 10^9 CFU bioluminescent *C. rodentium* (*C. rod*) by oral gavage. Four and six days p. i., a group of infected mice was treated with intraperitoneal (i.p.) injections of 200 µg αTIM4 antibody. Seven days p. i., colons were harvested and CD11b$^-$ CD103$^+$ FACS sorted for gene expression analysis by qRT-PCR. **(a)** Representative plots showing sort gating and purity of CD11b$^-$ CD103$^+$ DC. These were gated as single, live, CD45$^+$, MHCII$^+$, CD11c$^+$, CD64$^-$, B220$^-$ cells. **(b)** Expression levels of *Ccr7*, *Il1b*, and *Itgb8* mRNA normalised to housekeeping gene *Tbp*. Error bars represent S.D.; statistical analysis was carried out using a Kruskal-Wallis test with a Dunn's post-test for multiple comparisons.

In order to determine if blocking TIM4 during *C. rodentium* infection had any impact on the severity of the elicited inflammatory response, we analysed the frequency and number of CD11b$^+$ Ly6G$^+$ neutrophils in the colonic LP. However, this was unaffected in mice that had received αTIM4 compared with those administered the isotype control (Figure 6. 19).

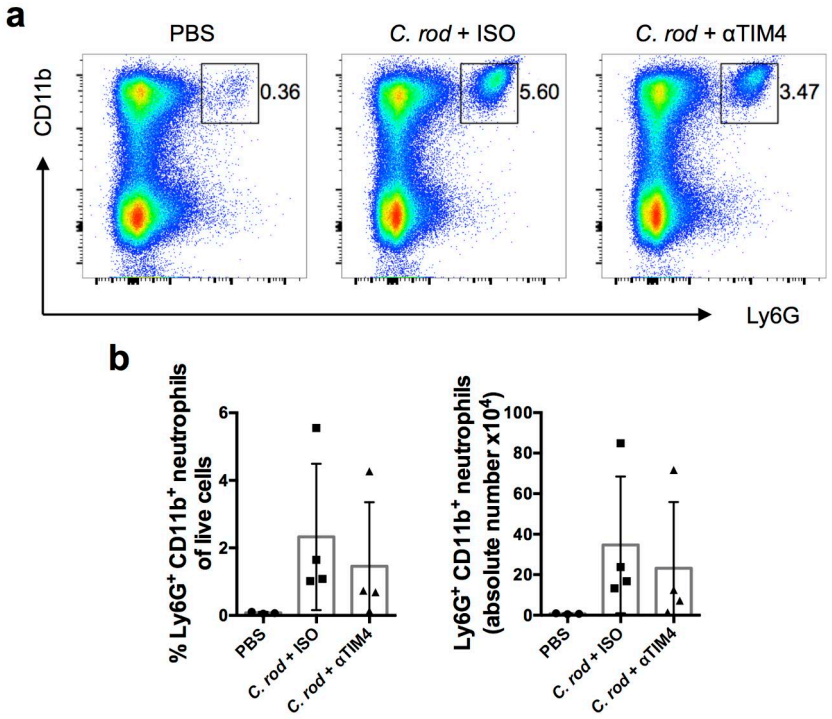

Figure 6. 19: Blocking TIM4 does not significantly alter neutrophil frequencies during *C. rodentium* infection

Mice were given PBS or infected with 2 × 10^9 CFU bioluminescent *C. rodentium* (*C. rod*) by oral gavage. Four and six days p. i., infected mice were treated with intraperitoneal (i.p.) injections of 200 µg αTIM4 antibody or Rat IgG2a isotype control (ISO). Seven days p. i., colons were harvested and LP cells analysed by flow cytometry. **(a)** Representative plots show colonic CD11b$^+$ Ly6G$^+$ neutrophils from PBS-treated and infected mice given αTIM4 or ISO, gated on single, live, CD45$^+$ cells. **(b)** Summary data are shown as percentage of CD11b$^+$ Ly6G$^+$ neutrophils among total live cells, and their absolute cell number. Error bars represent S.D.; statistical analysis was carried out using a Kruskal-Wallis test with a Dunn's post-test for multiple comparisons.

The influx of Ly6C$^+$ MHCII$^-$ and Ly6C$^+$ MHCII$^+$ monocytes into the colon is another indication of on-going tissue inflammation. Indeed, infected animals treated with the isotype control had significantly more monocytes infiltrating the colonic LP compared with PBS-treated controls (Figure 6. 20). This was not true, however, after blocking TIM4 (Figure 6. 20). Mature colonic macrophages also express TIM4, and exhibited loss of TIM4 staining upon administration of αTIM4 (Figure 6. 20b). While infection with *C. rodentium* significantly increased the number of Ly6C$^-$ MHCII$^+$ macrophages, this was not the case for αTIM4-treated infected mice, as seen in the monocyte compartment (Figure 6. 20).

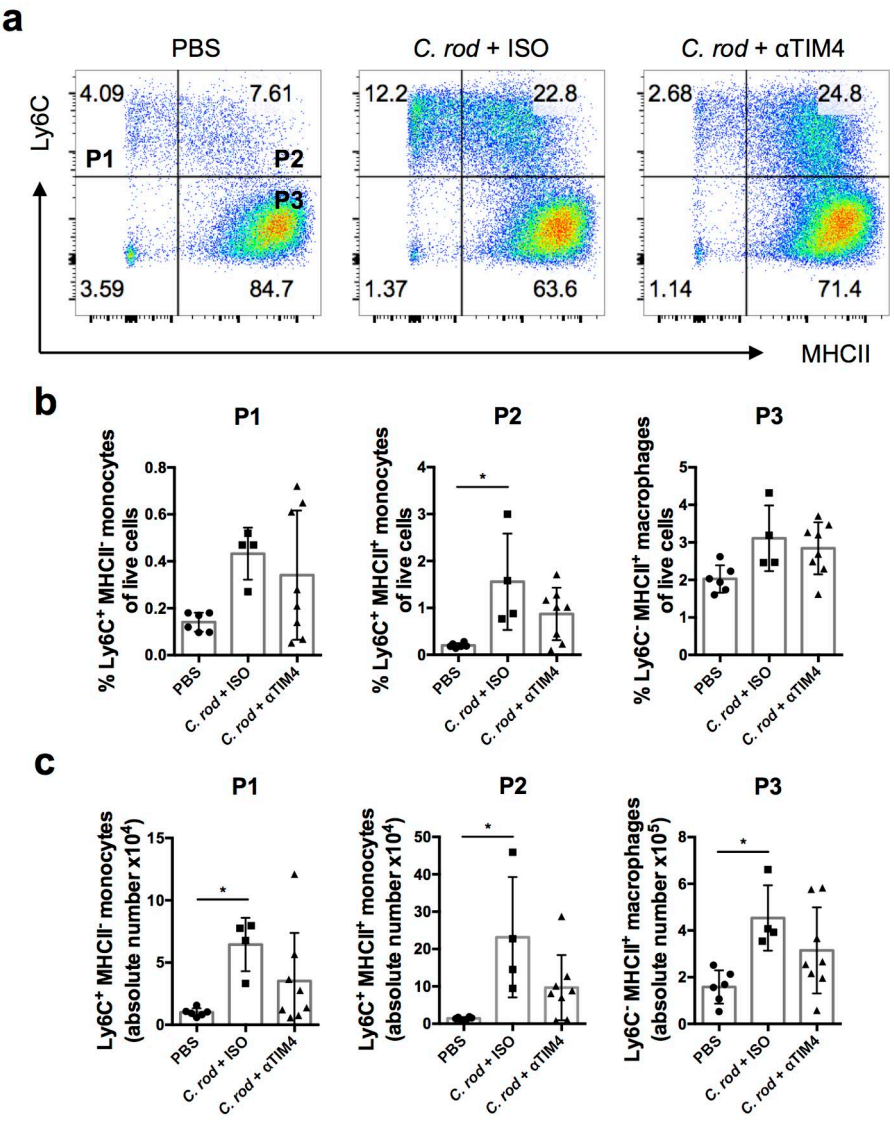

Figure 6. 20: Blocking TIM4 does not significantly alter colonic monocyte and macrophage frequencies during *C. rodentium* infection

Mice were given PBS or infected with 2×10^9 CFU bioluminescent *C. rodentium* (*C. rod*) by oral gavage. Four and six days p. i., infected mice were treated with intraperitoneal (i.p.) injections of 200 µg αTIM4 antibody or Rat IgG2a isotype control (ISO). Seven days p. i., colons were harvested and LP cells analysed by flow cytometry. **(a)** Representative plots showing Ly6C$^+$ MHCII$^-$ (P1) and Ly6C$^+$ MHCII$^+$ (P2) monocyte populations, and Ly6C$^-$ MHCII$^+$ (P3) macrophages from PBS-treated and infected mice given αTIM4 or ISO, gated on single, live, CD45$^+$, CD11b$^+$, (Ly6G$^-$), SSC^{lo}, CD64$^{int\text{-}hi}$ cells. Summary data are shown as **(b)** the percentage of P1, P2 and P3 populations among total live cells, and **(c)** their absolute cell number. Error bars represent S.D.; statistical analysis was carried out using a Kruskal-Wallis test with a Dunn's post-test for multiple comparisons. * $p < 0.05$.

We next ascertained if the percentage and number of migratory DC present in the cMLN was impacted by blocking TIM4 during *C. rodentium* infection. While infected mice that had received blocking antibody exhibited significantly reduced frequencies of all migratory DC populations except CD11b$^+$ CD103$^-$ DC in the cMLN compared with PBS-treated mice, there was no statistical difference between αTIM4- and isotype control-treated animals

(Figure 6. 21a, b). Furthermore, the reduction in proportion did not translate to changes in absolute cell number (Figure 6. 21c).

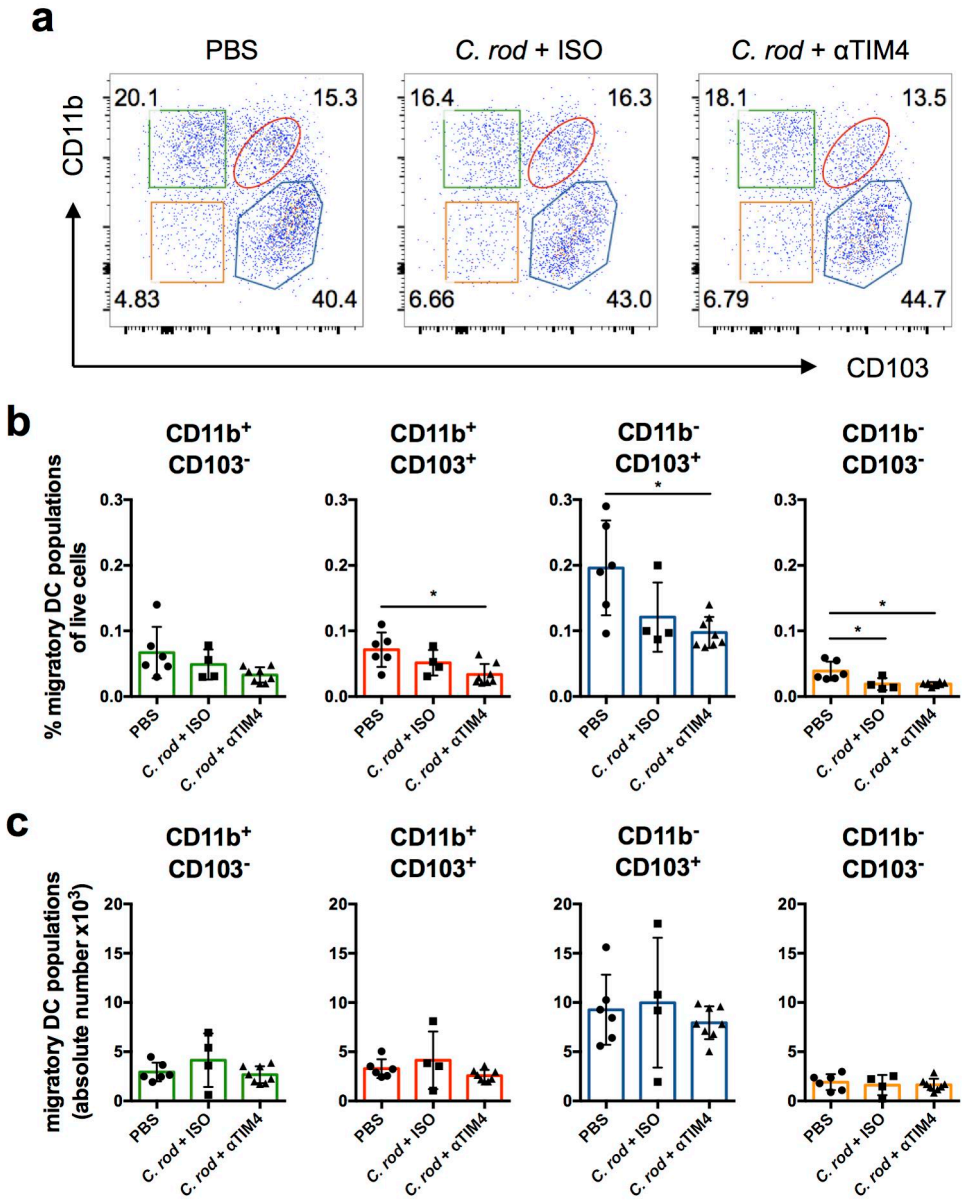

Figure 6. 21: Blocking TIM4 does not significantly alter cMLN migratory DC population frequencies

Mice were given PBS or infected with 2×10^9 CFU bioluminescent *C. rodentium* (*C. rod*) by oral gavage. Four and six days p. i., infected mice were treated with intraperitoneal (i.p.) injections of 200 µg αTIM4 antibody or Rat IgG2a isotype control (ISO). Seven days p. i., cMLN were harvested and cells analysed by flow cytometry. **(a)** Representative plots showing cMLN DC populations from PBS-treated and infected mice given αTIM4 or ISO, gated on single, live, $CD45^+$, $MHCII^{hi}$, $CD11c^+$, $CD64^-$ $B220^-$ cells. Summary data are shown as **(b)** the percentage of DC populations among total live cells and **(c)** their absolute cell number. Error bars represent S.D.; statistical analysis was carried out using a Kruskal-Wallis test with a Dunn's post-test for multiple comparisons. * $p < 0.05$.

Finally, we investigated the importance of TIM4 in the induction of T cell responses during infection with *C. rodentium*. Blocking TIM4 did not change the percentage or number of activated IL-17A$^+$ or IFNγ$^+$ CD4$^+$ T cells in the cMLN (Figure 6. 22a, b). Interestingly, the proportion of FoxP3$^+$ CD4$^+$ Treg cells in the cMLN dropped significantly during infection, but not if TIM4 was blocked (Figure 6. 22c). This was only true for the percentage, but not for the absolute number of Treg cells (Figure 6. 22c).

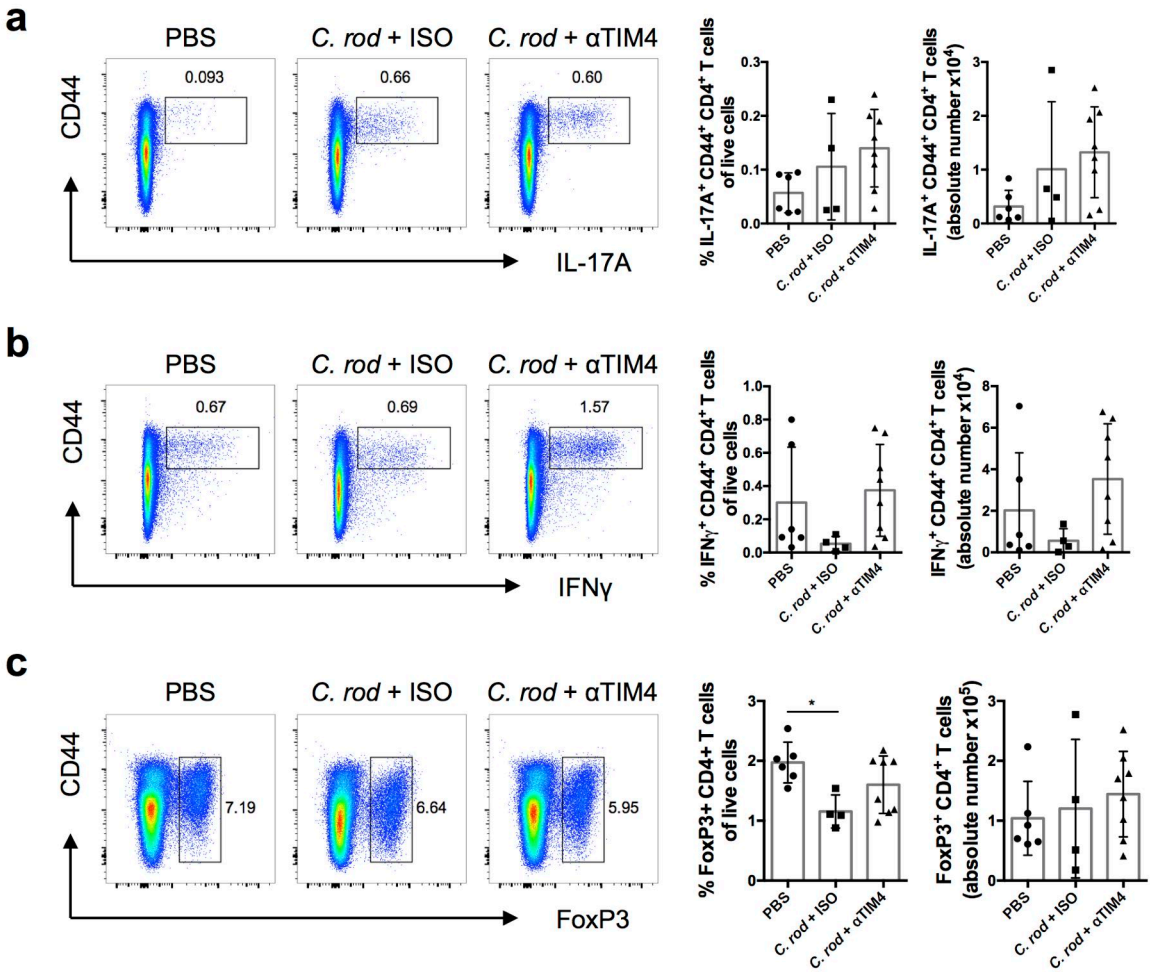

Figure 6. 22: CD4$^+$ T cell responses in the cMLN do not change significantly with TIM4 blocking during *C. rodentium* infection

Mice were given PBS or infected with 2 × 10^9 CFU bioluminescent *C. rodentium* (*C. rod*) by oral gavage. Four and six days p. i., infected mice were treated with intraperitoneal (i.p.) injections of 200 µg αTIM4 antibody or Rat IgG2a isotype control (ISO). Seven days p. i., cMLN were harvested, cells stimulated with PMA and Ionomycin, and analysed by flow cytometry. Evaluation of **(a)** IL-17A$^+$ CD44$^+$ CD4$^+$ T cells, **(b)** IFNγ$^+$ CD44$^+$ CD4$^+$ T cells and **(c)** FoxP3$^+$ CD4$^+$ Treg cells in the cMLN of PBS-treated and infected mice given αTIM4 or ISO. Representative plots show cytokine or transcription factor stained cells gated on single, live, CD45$^+$, CD3$^+$, CD4$^+$ T cells. Summary data are shown as the percentage of Th17, Th1 and Treg cells among total live cells, as well as their absolute cell number. Error bars represent S.D.; statistical analysis was carried out using a Kruskal-Wallis test with a Dunn's post-test for multiple comparisons. * $p < 0.05$.

As seen with CD4$^+$ T cells, the induction of IFNγ$^+$ CD8$^+$ T cells in the cMLN was also independent of TIM4 (Figure 6. 23).

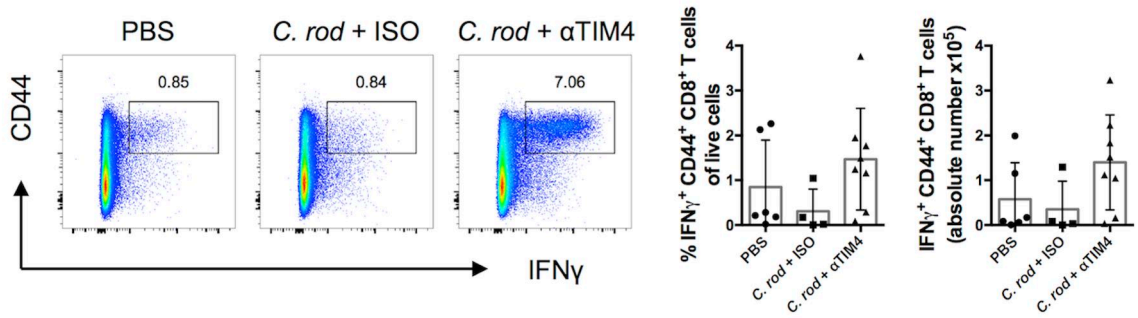

Figure 6. 23: Blocking TIM4 during *C. rodentium* infection does not significantly alter CD8$^+$ T cell responses in the cMLN

Mice were given PBS or infected with 2 × 10^9 CFU bioluminescent *C. rodentium* (*C. rod*) by oral gavage. Four and six days p. i., infected mice were treated with intraperitoneal (i.p.) injections of 200 µg αTIM4 antibody or Rat IgG2a isotype control (ISO). Seven days p. i., cMLN were harvested, cells stimulated with PMA and Ionomycin, and analysed by flow cytometry. Representative plots show IFNγ$^+$ CD44$^+$ CD8$^+$ T cells from the cMLN of PBS-treated and infected mice given αTIM4 or ISO, gated on single, live, CD45$^+$, CD3$^+$, CD8$^+$ T cells. Summary data are shown as the percentage of IFNγ$^+$ CD44$^+$ CD8$^+$ T cells among total live cells, and as their absolute cell number. Error bars represent S.D.; statistical analysis was carried out using a Kruskal-Wallis test with a Dunn's post-test for multiple comparisons.

Production of both IL-17A and IFNγ by stimulated colonic CD4⁺ T cells was low and TIM4 blocking had no effect on the levels produced during infection (Figure 6. 24a, b). The percentage of CD8⁺ IFNγ⁺ T cells in the colonic LP was negligible across groups (data not shown). Moreover, in contrast to the cMLN, where *C. rodentium* infection was found to increase the proportion of FoxP3⁺ CD4⁺ Treg cells, this was not true in the colon and blocking TIM4 had no impact on the percentage or number of Treg cells in the LP (Figure 6. 24c).

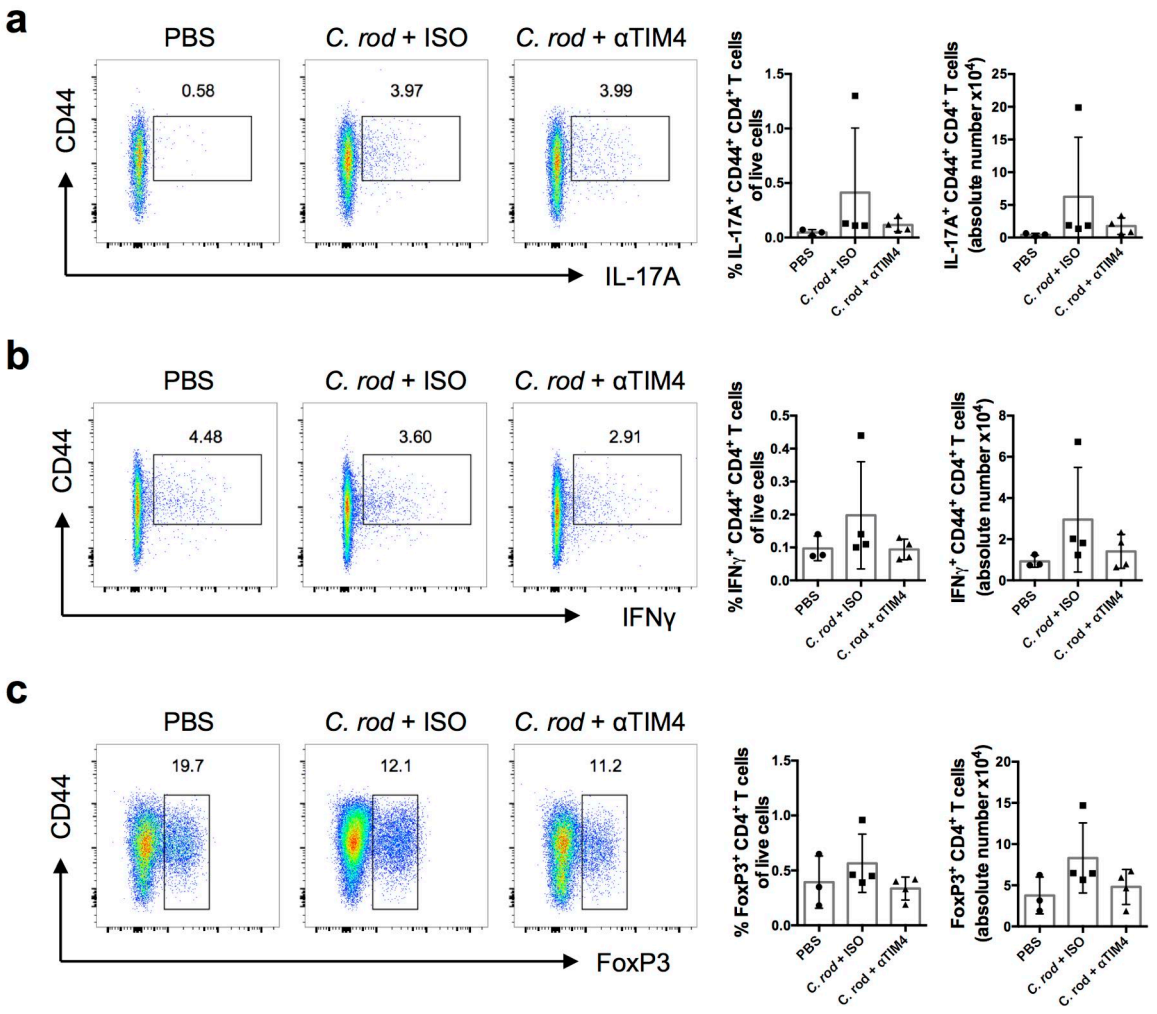

Figure 6. 24: Colonic CD4⁺ T cell responses are not significantly changed during infection with *C. rodentium* and concurrent blocking of TIM4

Mice were given PBS or infected with 2 × 10^9 CFU bioluminescent *C. rodentium* (*C. rod*) by oral gavage. Four and six days p. i, infected mice were treated with intraperitoneal (i.p.) injections of 200 µg αTIM4 antibody or Rat IgG2a isotype control (ISO). Seven days p. i., colons were harvested, LP cells stimulated with PMA and Ionomycin, and analysed by flow cytometry. Evaluation of **(a)** IL-17A⁺ CD44⁺ CD4⁺ T cells, **(b)** IFNγ⁺ CD44⁺ CD4⁺ T cells and **(c)** FoxP3⁺ CD4⁺ Treg cells in the colonic LP of PBS-treated and infected mice given αTIM4 or ISO. Representative plots show cytokine or transcription factor stained cells gated on single, live, CD45⁺, CD3⁺, CD4⁺ T cells. Summary data are shown as the percentage of Th17, Th1 and Treg cells among total live cells, as well as their absolute cell number. Error bars represent S.D.; statistical analysis was carried out using a Kruskal-Wallis test with a Dunn's post-test for multiple comparisons. * $p < 0.05$.

6.2.4 TIM4 function in *S.* Typhimurium infection

We were unable to find any evidence that blocking TIM4 had any significant impact on innate or adaptive responses to *C. rodentium*. We next aimed to determine if this was also the case with *S.* Typhimurium infection, which induces a mixed Th1/Th17 response (Lee et al. 2012). To this end we used a well-established model (Barthel et al. 2003), involving pre-treatment with oral streptomycin 24 h before infection with *S.* Typhimurium. Concurrently, animals were given i.p. injections of either αTIM4 blocking antibody or Rat IgG2a isotype control (Figure 6. 25). The next day, animals were either given PBS or orally infected with *S.* Typhimurium (Figure 6. 25).

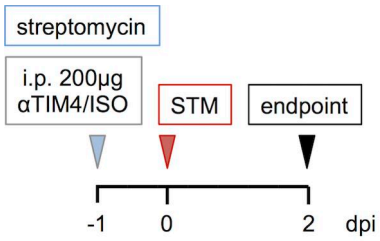

Figure 6. 25: Experimental setup for investigating the function of TIM4 in *S.* Typhimurium infection

Schematic describing experimental setup, where C57BL/6 mice were treated with 20 mg streptomycin by oral gavage and given 200 µg αTIM4 antibody or Rat IgG2a (ISO) by intraperitoneal (i.p.) injection 24 h before infection with 6×10^7 CFU *S.* Typhimurium (STM) per mouse, or treatment with PBS, by oral gavage. Two days p. i. (dpi) tissues were harvested and cells analysed by flow cytometry.

Weight loss over the course of infection was comparable between αTIM4 and isotype control-treated mice (Figure 6. 26a). Two days p. i. we measured colon lengths and found no differences between mice that had received αTIM4 compared with control mice in PBS-treated or infected groups (Figure 6. 26b).

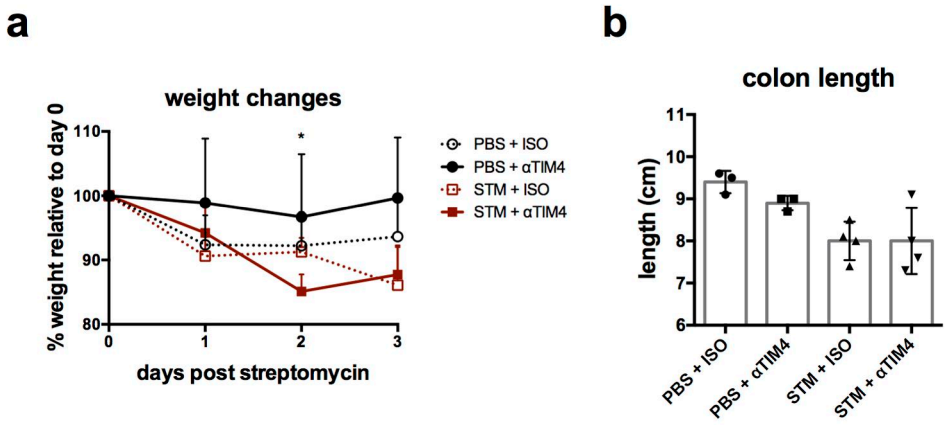

Figure 6. 26: Blocking TIM4 does not significantly impact weight loss or colon shortening during *S.* Typhimurium infection

C57BL/6 mice were treated with 20 mg streptomycin by oral gavage and given 200 µg αTIM4 antibody or Rat IgG2a (ISO) by intraperitoneal (i.p.) injection 24 h before infection with 6×10^7 CFU *S.* Typhimurium (STM) per mouse, or treatment with PBS, by oral gavage. **(a)** Weights were monitored throughout. Data are shown as the percentage weight relative to that before streptomycin treatment. **(b)** At two days p. i., colon lengths were determined. Error bars represent S.D.; statistical analysis was carried out using a Kruskal-Wallis test with a Dunn's post-test for multiple comparisons. * $p < 0.05$ between PBS + αTIM4 and STM + αTIM4.

As in previous experiments, blocking TIM4 systemically reduced the percentage of TIM4$^+$ DC in the colon and cMLN, as well as TIM4$^+$ colonic macrophages (Figure 6. 27).

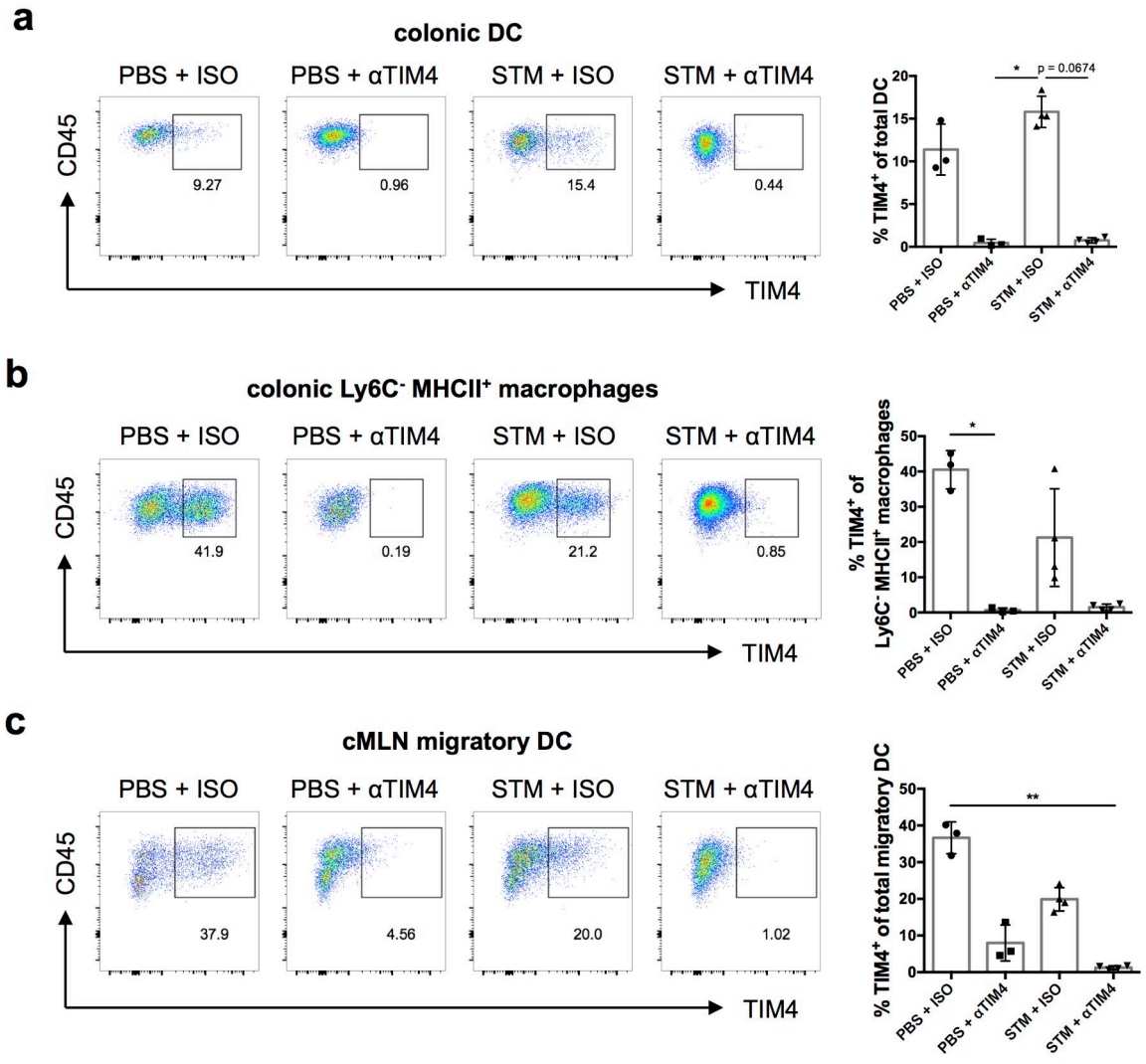

Figure 6. 27: Percentage of TIM4$^+$ DC and macrophages during *S.* Typhimurium infection and TIM4 blockade

C57BL/6 mice were treated with 20 mg streptomycin by oral gavage and given 200 µg αTIM4 antibody or Rat IgG2a (ISO) by intraperitoneal (i.p.) injection 24 h before infection with 6×10^7 CFU *S.* Typhimurium (STM) per mouse, or treatment with PBS, by oral gavage. Two days p. i. colons and cMLN were harvested and cells analysed by flow cytometry. **(a)** Representative plots show the expression of TIM4 on total colonic DC gated on single, live, CD45$^+$, MHCII$^+$, CD11c$^+$, CD64$^-$, B220 cells. Summary data are shown as the percentage of TIM4$^+$ cells among total LP DC. **(b)** Representative plots show the expression of TIM4 on Ly6C$^-$ MHCII$^+$ colonic macrophages gated on single, live, CD45$^+$, CD11b$^+$, SSC^{lo}, CD64$^{int\text{-}hi}$, Ly6C$^-$, MHCII$^+$ cells. Summary data are shown as the percentage of TIM4$^+$ cells among total colonic macrophages. **(c)** Representative plots show the expression of TIM4 on total cMLN DC, gated on single, live, CD45$^+$, MHCII$^+$, CD11c$^+$, CD64$^-$, B220$^-$ cells. Summary data are shown as the percentage of TIM4$^+$ cells among total cMLN DC. Error bars represent S.D.; statistical analysis was carried out using a Kruskal-Wallis test with a Dunn's post-test for multiple comparisons. * $p < 0.05$, ** $p < 0.01$.

Comparing the expression of TIM4 on DC from isotype-treated mice that had either received PBS or were infected with *S.* Typhimurium, we found a trend towards increased expression of TIM4 on CD11b$^+$ CD103$^+$ and CD11b$^-$ CD103$^-$ DC in the colonic LP of infected animals, though this was not statistically significant (Figure 6. 28).

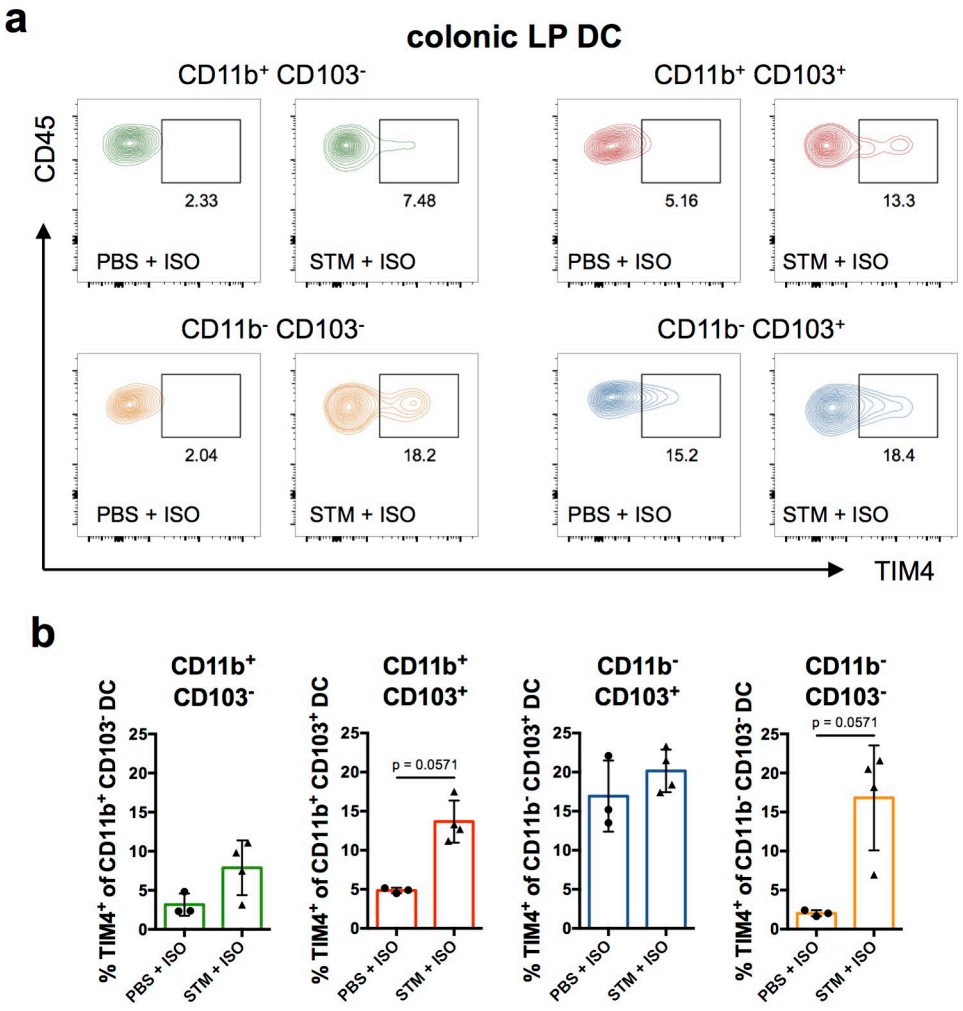

Figure 6. 28: The percentage of TIM4$^+$ cells among colonic DC populations does not change significantly with *S.* Typhimurium infection

C57BL/6 mice were treated with 20 mg streptomycin by oral gavage and given 200 µg αTIM4 antibody or Rat IgG2a (ISO) by intraperitoneal (i.p.) injection 24 h before infection with 6 × 10^7 CFU *S.* Typhimurium (STM) per mouse, or treatment with PBS, by oral gavage. Two days p. i. colons were harvested and LP cells analysed by flow cytometry. **(a)** Representative plots showing TIM4$^+$ cells among DC populations from PBS-treated and *S.* Typhimurium infected mice, both of which had received ISO antibody. DC are gated on single, live, CD45$^+$, MHCII$^+$, CD11c$^+$, CD64$^-$, B220$^-$ cells. **(b)** Summary data are shown as the percentage of TIM4$^+$ cells among DC populations. Error bars represent S.D.; statistical analysis was carried out using a Mann-Whitney test.

Interestingly, we found the opposite to be true in the cMLN, with a trend towards downregulation in TIM4 on CD11b$^+$ CD103$^-$ and CD11b$^+$ CD103$^+$ DC (Figure 6. 29).

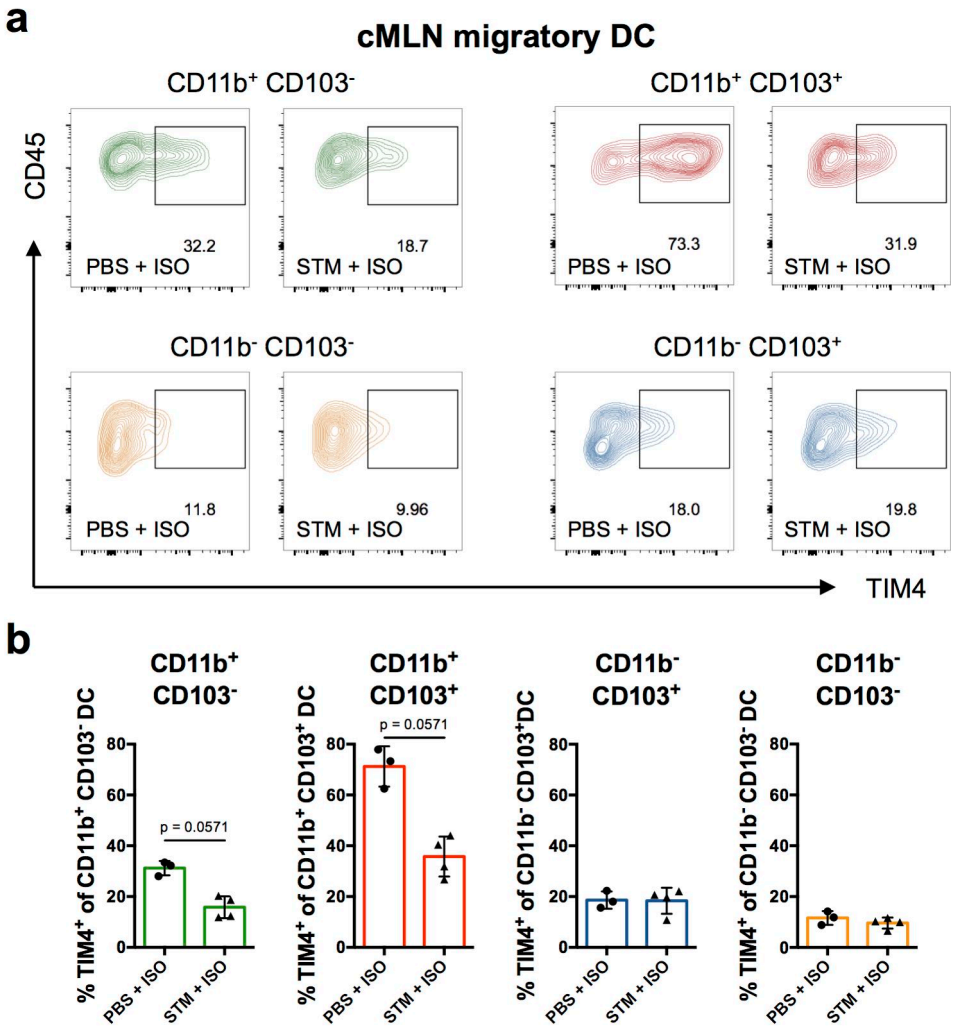

Figure 6. 29: The percentage of TIM4$^+$ cells among cMLN migratory DC populations does not change significantly with *S.* Typhimurium infection

C57BL/6 mice were treated with 20 mg streptomycin by oral gavage and given 200 µg αTIM4 antibody or Rat IgG2a (ISO) by intraperitoneal (i.p.) injection 24 h before infection with 6 × 10^7 CFU *S.* Typhimurium (STM) per mouse, or treatment with PBS, by oral gavage. Two days p. i. cMLN were harvested and cells analysed by flow cytometry. **(a)** Representative plots showing TIM4$^+$ cells among DC subsets from PBS-treated and *S.* Typhimurium infected mice, both of which had received ISO antibody. DC are gated on single, live, CD45$^+$, MHCII$^+$, CD11c$^+$, CD64$^-$, B220$^-$ cells. **(b)** Summary data are shown as the percentage of TIM4$^+$ cells among DC subsets. Error bars represent S.D.; statistical analysis was carried out using a Mann-Whitney test.

When we analysed the distribution of colonic DC subsets, we found that neither *S.* Typhimurium infection, nor blocking TIM4 had any significant effect on the percentage or number of DC within each subset (Figure 6. 30).

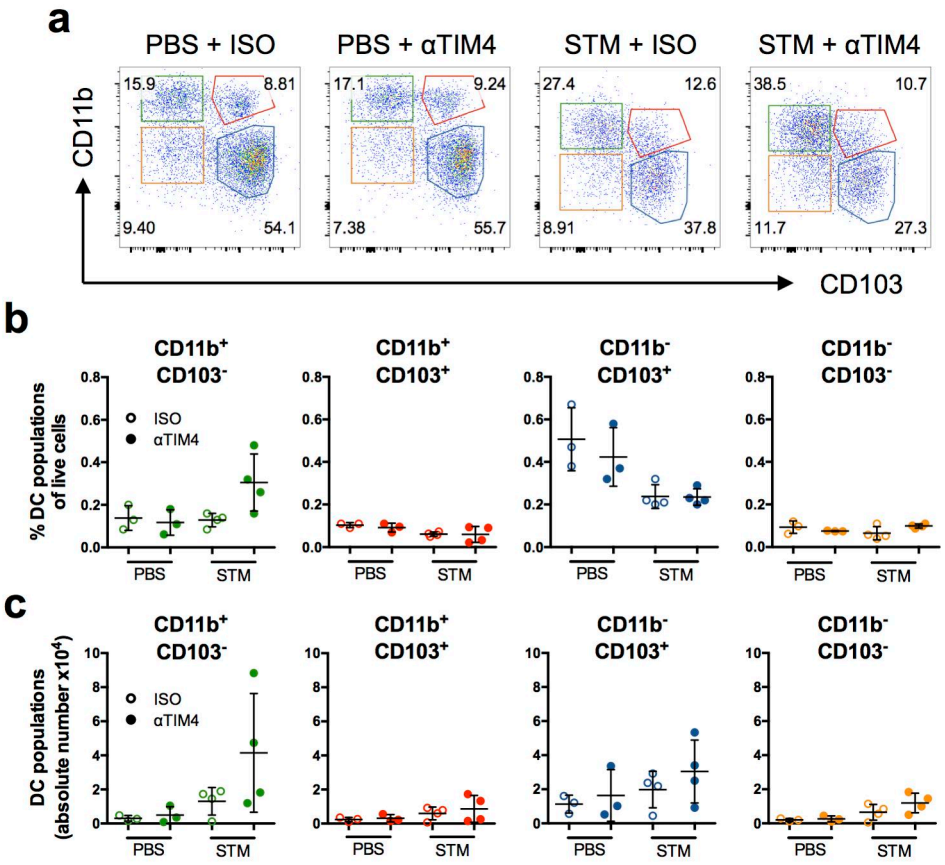

Figure 6. 30: Blocking TIM4 does not significantly impact colonic DC population distribution during *S.* Typhimurium infection

C57BL/6 mice were treated with 20 mg streptomycin by oral gavage and given 200 µg αTIM4 antibody or Rat IgG2a (ISO) by intraperitoneal (i.p.) injection 24 h before infection with 6×10^7 CFU *S.* Typhimurium (STM) per mouse, or treatment with PBS, by oral gavage. Two days p. i. colons were harvested and LP cells analysed by flow cytometry. **(a)** Representative plots show colonic LP DC populations, gated on single, live, $CD45^+$, $MHCII^+$, $CD11c^+$, $CD64^-$, $B220^-$ cells. Summary data are shown as **(b)** the percentage of DC subsets among total live cells and **(c)** their absolute cell number. Error bars represent S.D.; statistical analysis was carried out using a Kruskal-Wallis test with a Dunn's post-test for multiple comparisons.

S. Typhimurium-infected and αTIM4-treated mice did, however, have a significantly higher proportion of infiltrating Ly6C$^+$ MHCII$^-$ and Ly6C$^+$ MHCII$^-$ monocytes in the colonic LP compared with PBS controls (Figure 6. 31). This was accompanied by a similar trend in Ly6C$^+$ MHCII$^+$ monocyte numbers (Figure 6. 31c). Isotype control-treated infected animals also had a trend towards increased monocytes, although this was not statistically significant (Figure 6. 31).

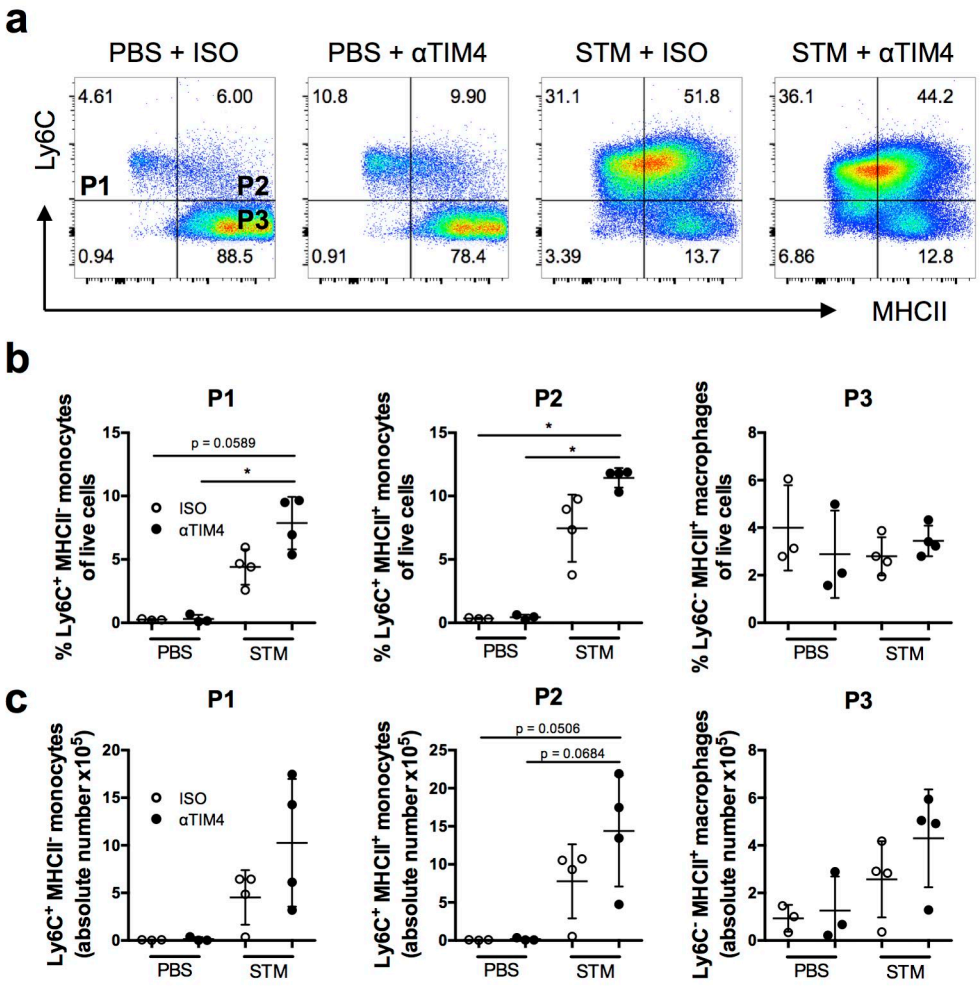

Figure 6. 31: Colonic monocyte and macrophage populations are not significantly altered with TIM4 blocking during *S.* Typhimurium infection

C57BL/6 mice were treated with 20 mg streptomycin by oral gavage and given 200 µg αTIM4 antibody or Rat IgG2a (ISO) by intraperitoneal (i.p.) injection 24 h before infection with 6×10^7 CFU *S.* Typhimurium (STM) per mouse, or treatment with PBS, by oral gavage. Two days p. i. colons were harvested and LP cells analysed by flow cytometry. **(a)** Representative plots show Ly6C$^+$ MHCII$^-$ (P1) monocyte, Ly6C$^+$ MHCII$^+$ (P2) monocyte and Ly6C$^-$ MHCII$^+$ (P3) macrophage populations, gated on single, live, CD45$^+$, CD11b$^+$, SSC^{lo}, CD64$^{int\text{-}hi}$ cells. Summary data are shown as **(b)** the percentage of P1 and P2 monocyte populations and P3 macrophages among total live cells, and **(c)** as their absolute cell number. Error bars represent S.D.; statistical analysis was carried out using a Kruskal-Wallis test with a Dunn's post-test for multiple comparisons.
* $p < 0.05$.

To further determine if TIM4 blocking interfered with antigen presentation in the cMLN, we first assessed if the distribution of DC populations was altered upon infection and TIM4 blockade. Unfortunately, we were unable to differentiate migratory and resident populations of DC in these samples based on the level of MHCII staining (data not shown), but instead gated on total MHCII$^+$ CD11c$^+$ cells, which will therefore represent a mixture of migratory and resident DC. Infection with *S.* Typhimurium did not alter DC population distribution in the cMLN, and neither did blocking TIM4 systemically (Figure 6. 32).

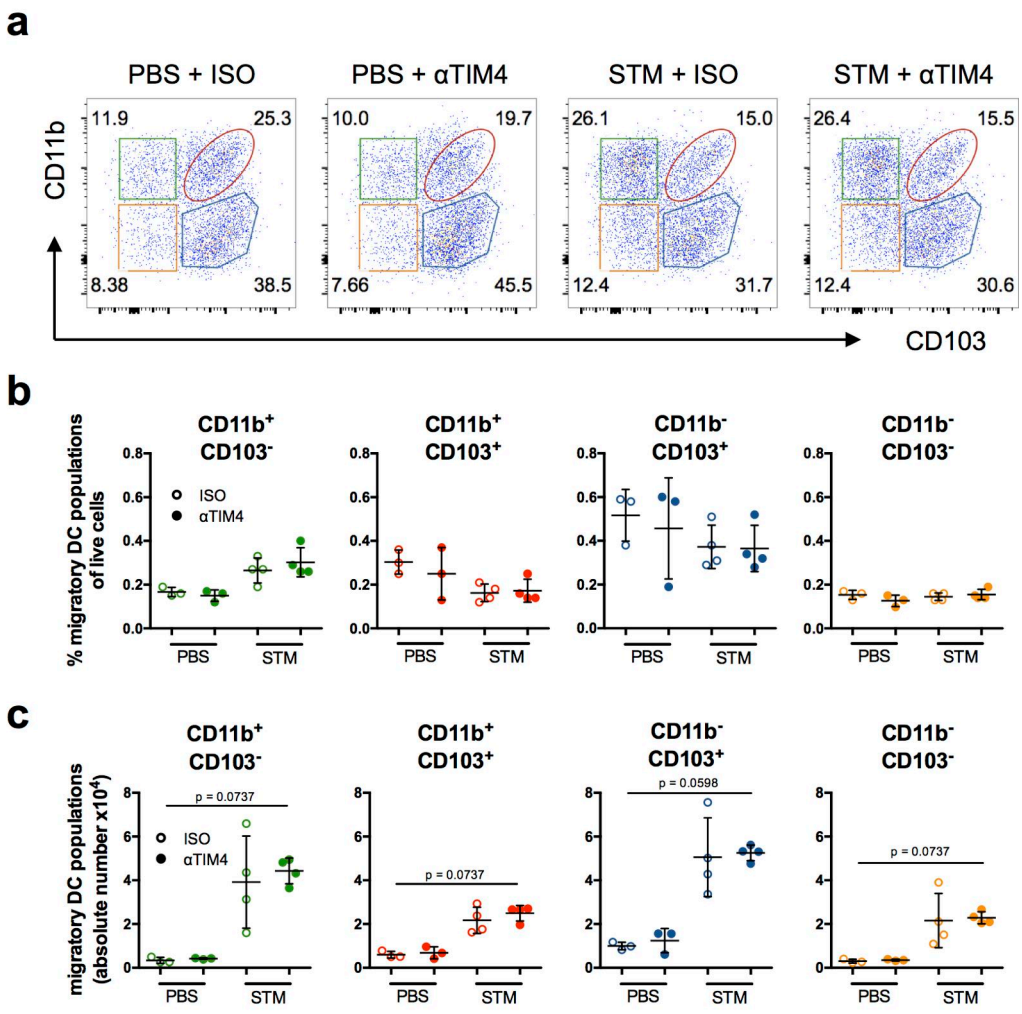

Figure 6. 32: Blocking TIM4 does not significantly alter cMLN DC population frequencies during *S.* Typhimurium infection

C57BL/6 mice were treated with 20 mg streptomycin by oral gavage and given 200 µg αTIM4 antibody or Rat IgG2a (ISO) by intraperitoneal (i.p.) injection 24 h before infection with 6×10^7 CFU *S.* Typhimurium (STM) per mouse, or treatment with PBS, by oral gavage. Two days p. i. cMLN were harvested and cells analysed by flow cytometry. **(a)** Representative plots showing cMLN DC populations gated on single, live, CD45$^+$, MHCII$^+$, CD11c$^+$, CD64$^-$, B220$^-$ cells. Summary data are shown as **(b)** the percentage of DC populations among total live cells and **(c)** their absolute cell number. Error bars represent S.D.; statistical analysis was carried out using a Kruskal-Wallis test with a Dunn's post-test for multiple comparisons.

While we observed a trend towards an increased proportion of IFNγ$^+$ CD44$^+$ CD4$^+$ T cells in the cMLN and colons of infected mice, this was not statistically significant and was not affected by blocking TIM4 (Figure 6. 33).

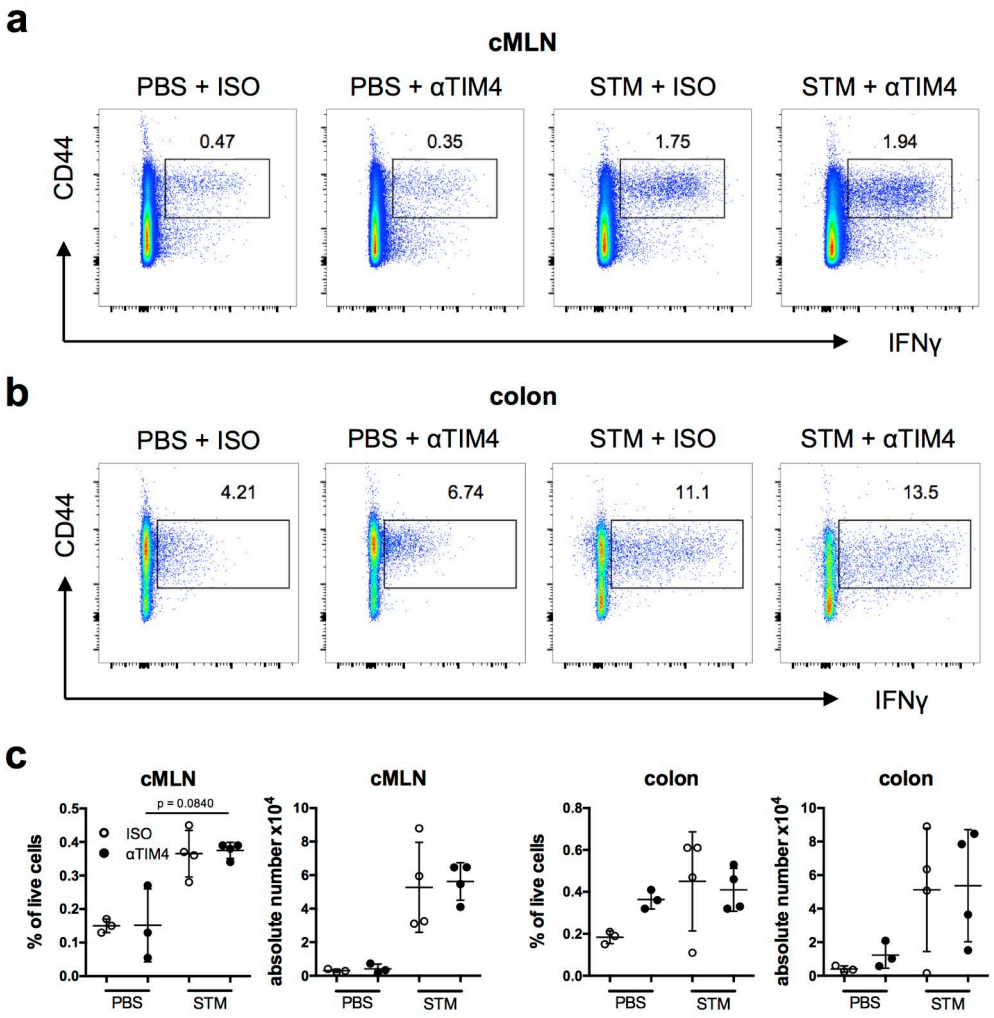

Figure 6. 33: Blocking TIM4 has no effect on the cMLN or colonic Th1 response during *S.* Typhimurium infection

C57BL/6 mice were treated with 20 mg streptomycin by oral gavage and given 200 µg αTIM4 antibody or Rat IgG2a (ISO) by intraperitoneal (i.p.) injection 24 h before infection with 6×10^7 CFU *S.* Typhimurium (STM) per mouse, or treatment with PBS, by oral gavage. Two days p. i. cMLN and colons were harvested, cells stimulated with PMA and Ionomycin, and analysed by flow cytometry. Representative plots showing IFNγ$^+$ CD44$^+$ CD4$^+$ T cells in **(a)** the cMLN and **(b)** the colonic LP. Cells were gated on single, live, CD45$^+$, CD3$^+$, CD4$^+$ T cells. **(c)** Summary data are shown as the percentage of IFNγ+ CD44$^+$ CD4$^+$ T cells among total live cells in the colon and cMLN, and as their absolute cell number. Error bars represent S.D.; statistical analysis was carried out using a Kruskal-Wallis test with a Dunn's post-test for multiple comparisons.

Infection with *S.* Typhimurium did not induce a strong colonic Th17 response either in the cMLN or the LP (Figure 6. 34), and there was no difference between mice that had received αTIM4 compared with those administered isotype control (Figure 6. 34).

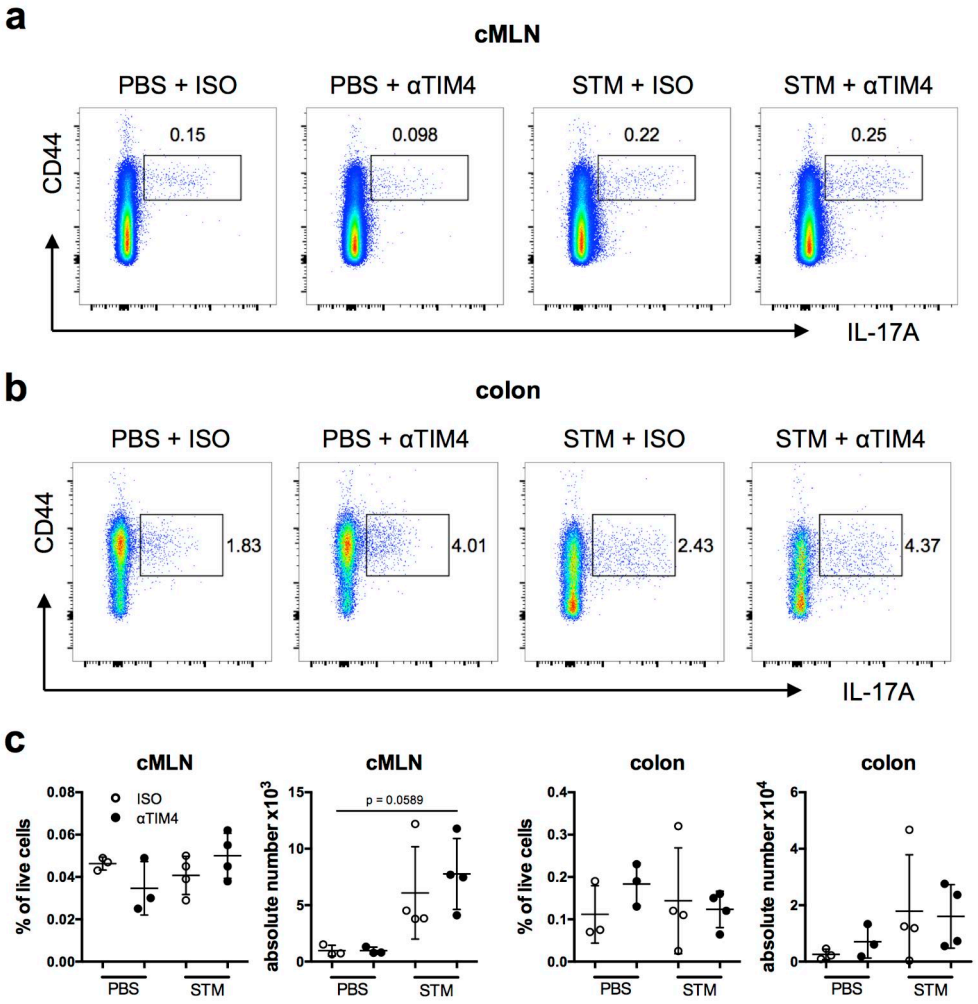

Figure 6. 34: Th17 responses in the cMLN and colon are not affected by blocking TIM4 during *S.* Typhimurium infection

C57BL/6 mice were treated with 20 mg streptomycin by oral gavage and given 200 µg αTIM4 antibody or Rat IgG2a (ISO) by intraperitoneal (i.p.) injection 24 h before infection with 6×10^7 CFU *S.* Typhimurium (STM) per mouse, or treatment with PBS, by oral gavage. Two days p. i. cMLN and colons were harvested, cells stimulated with PMA and Ionomycin, and analysed by flow cytometry. Representative plots showing IL-17A$^+$ CD44$^+$ CD4$^+$ T cells in **(a)** the cMLN and **(b)** the colonic LP. Cells were gated on single, live, CD45$^+$, CD3$^+$, CD4$^+$ T cells. **(c)** Summary data are shown as the percentage of IL-17A$^+$ CD44$^+$ CD4$^+$ T cells among total live cells in the colon and cMLN, and as their absolute cell number. Error bars represent S.D.; statistical analysis was carried out using a Kruskal-Wallis test with a Dunn's post-test for multiple comparisons.

We had found that mice infected with *C. rodentium* had a reduced proportion of Treg cells in the cMLN (Figure 6. 22c). However, this was not the case in *S.* Typhimurium infected mice (Figure 6. 35a, c). In the colon of mice that had received αTIM4, on the other hand, infection with *S.* Typhimurium did significantly decrease the proportion, but not number, of Treg cells when compared with PBS-treated mice. However, overall TIM4 blocking had no impact on Treg cell frequencies or number in the cMLN or colon during *S.* Typhimurium infection (Figure 6. 35).

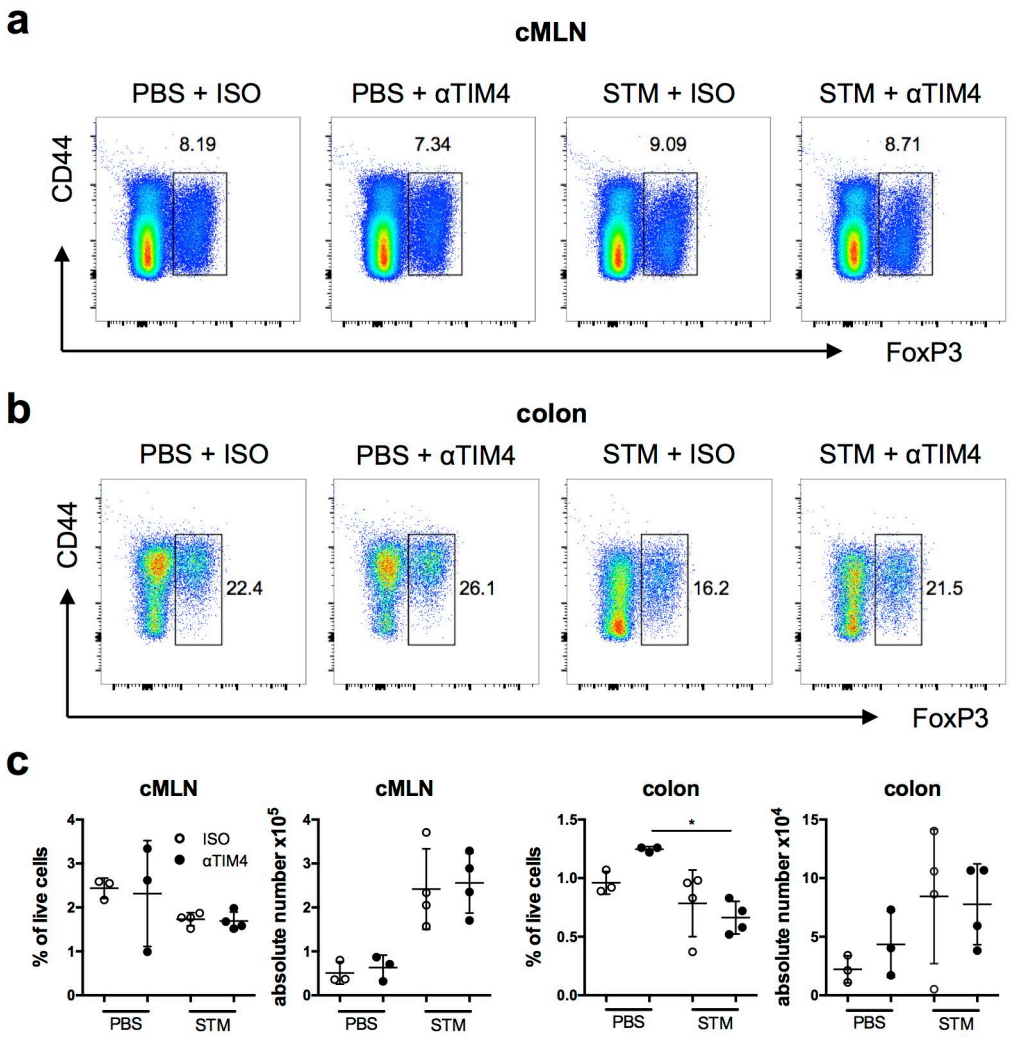

Figure 6. 35: Blocking TIM4 has no effect on Treg cell frequencies in the cMLN or colon during *S.* Typhimurium infection

C57BL/6 mice were treated with 20 mg streptomycin by oral gavage and given 200 µg αTIM4 antibody or Rat IgG2a (ISO) by intraperitoneal (i.p.) injection 24 h before infection with 6×10^7 CFU *S.* Typhimurium (STM) per mouse, or treatment with PBS, by oral gavage. Two days p. i. cMLN and colons were harvested, cells stimulated with PMA and Ionomycin, and analysed by flow cytometry. Representative plots showing FoxP3$^+$ CD4$^+$ T cells in **(a)** the cMLN and **(b)** the colonic LP. Cells were gated on single, live, CD45$^+$, CD3$^+$, CD4$^+$ T cells. **(c)** Summary data are shown as the percentage of FoxP3$^+$ CD4$^+$ T cells among total live cells in the colon and cMLN, and as their absolute cell number. Error bars represent S.D.; statistical analysis was carried out using a Kruskal-Wallis test with a Dunn's post-test for multiple comparisons. * $p < 0.05$.

Finally, IFNγ$^+$ CD8$^+$ T cells were generally increased in frequency and number, though not always significantly, during *S.* Typhimurium infection in both the cMLN and colon (Figure 6. 36). As seen with CD4$^+$ T cells, this was not affected by blocking TIM4 (Figure 6. 36).

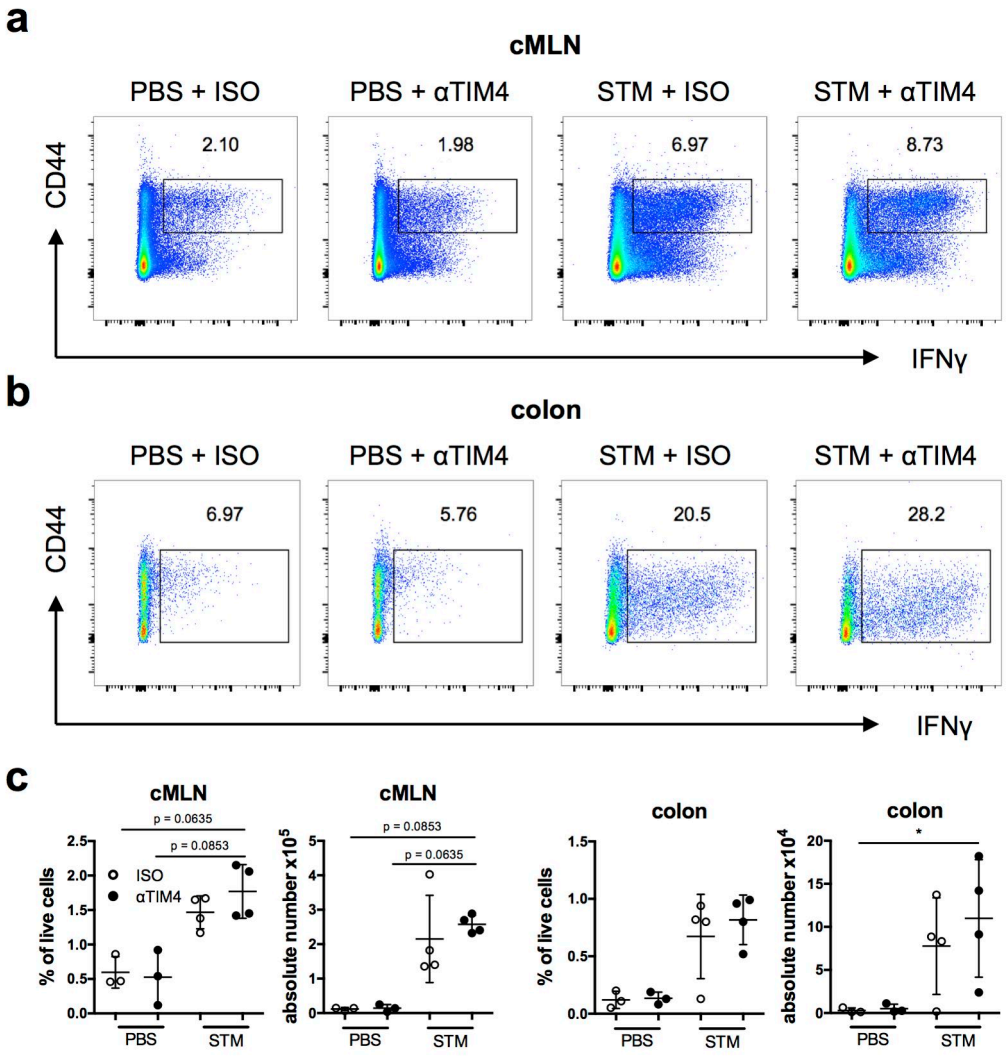

Figure 6. 36: CD8$^+$ T cell responses in the cMLN and colon remain unchanged by TIM4 blocking during *S.* Typhimurium infection

C57BL/6 mice were treated with 20 mg streptomycin by oral gavage and given 200 µg αTIM4 antibody or Rat IgG2a (ISO) by intraperitoneal (i.p.) injection 24 h before infection with 6 × 10^7 CFU *S.* Typhimurium (STM) per mouse, or treatment with PBS, by oral gavage. Two days p. i. cMLN and colons were harvested, cells stimulated with PMA and Ionomycin, and analysed by flow cytometry. **(a)** Representative plots showing IFNγ$^+$ CD44$^+$ CD8$^+$ T cells in the cMLN, gated on single, live, CD45$^+$, CD3$^+$, CD8$^+$ T cells. **(b)** Representative plots showing IFNγ$^+$ CD8$^+$ T cells in the colonic LP gated on single, live, CD45$^+$, CD3$^+$, CD8$^+$ T cells. **(c)** Summary data are shown as the percentage of IFNγ$^+$ (CD44$^+$) CD8$^+$ T cells among total live cells in the colon and cMLN, and as their absolute cell number. Error bars represent S.D.; statistical analysis was carried out using a Kruskal-Wallis test with a Dunn's post-test for multiple comparisons. * $p < 0.05$.

6.3 Discussion

Instead of being ubiquitously expressed on DC, we found that TIM4 expression was tightly controlled. It was upregulated upon migration and remained high in the cMLN on CD11b$^+$ DC. Furthermore, bacterial-induced inflammation increased its expression on DC in the colonic LP. However, it remains unclear whether or not the function of TIM4 in these different settings is limited to that of a PSR, or if its expression on DC is important in shaping adaptive immunity. We therefore tested three hypotheses to begin to address these questions; firstly, we postulated that if TIM4 expression on DC were required for efficient migration to the MLN, blocking TIM4 *in vivo* would reduce the number of migratory DC in the MLN. Secondly, having found that a sizeable proportion of DC expressed TIM4 in the MLN, we hypothesised that it played a role in antigen presentation. Lastly, as TIM4 is upregulated on DC during bacterial induced colonic inflammation, we determined if it was required for the induction of protective T cell responses in the cMLN and colon during infection.

Previously, we had found that after photoconverting the proximal colon of Kaede mice, TIM4$^+$ migratory DC in the cMLN showed a trend towards a higher percentage of Kaede-red$^+$ cells compared with TIM4$^-$ DC. Using a similar approach, we quantified Kaede-red$^+$ DC in the cMLN 48 h post photoconversion after having blocked TIM4 *in vivo* using an αTIM4 antibody. However, we found that this did not significantly change the migration efficiency of DC. It is possible, but unlikely, that this was caused by incomplete blocking of the molecule, as we showed antibody staining of TIM4 on cMLN DC was substantially decreased on DC. Moreover, previous investigations have successfully used this approach to abrogate TIM4 function *in vivo* (Yeung et al. 2013, Ji et al. 2014). The antibodies used for our investigations *in vivo* and for detection by flow cytometry were different clones, but both were originally raised against the entire extracellular domain of TIM4 (Nakayama et al. 2009, Yeung et al. 2013). There is a possibility, therefore, that they bind to the same epitope. While we attempted to determine if lack of TIM4 staining was due to epitope shielding by surface-bound antibody, we were unable to succeed technically, and further experiments would be required to confirm if this is indeed the case, or if TIM4 is internalised upon antibody binding. We saw no overall changes in colonic LP DC population distribution, suggesting that *in vivo* administration does not selectively induce antibody-dependent depletion of TIM4$^+$ cells. This was also confirmed by analysing

$CD103^+$ DC in the lungs of αTIM4-treated animals, which have a much higher expression level than their colonic counterparts (data not shown).

From our results, we cannot conclude that TIM4 has any role in directly mediating DC migration to the MLN. This is perhaps not surprising, given previous work that has demonstrated that mice lacking all major integrin homodimers do not exhibit any migratory defects (Lämmermann et al. 2008). Instead, DC migration to LN is chemokine driven and dependent on the expression of CCR7 (Förster et al. 1999). This ability to move independently of the cellular and tissue environment is underpinned by actin rearrangements that cause cellular protrusions independently of cell adhesion (Lämmermann et al. 2008). Furthermore, TIM4 expression on lymph DC is not ubiquitous, with between 20-40% expression depending on the tissue it is draining, which also speaks against a fundamental role in orchestrating migration.

We next investigated if blocking TIM4 on MLN DC had any effect on antigen-specific T cell proliferation. However, OVA-specific $CD4^+$ T cell proliferation was not impacted by blocking TIM4 *in vitro*. Further experiments confirming no dose-dependent effect would have been necessary to fully optimise this approach. The concentration of antibody was chosen based on previous work using different antibody clones that reported efficient inhibition of phagocytosis by blocking TIM4 *in vitro* (Kobayashi et al. 2007). However, subsequent publications detail use at six-fold (Nakayama et al. 2009) and even 20-fold (Yeung et al. 2013) concentrations for co-culture assays of $CD11c^+$ cells with T cells. It is possible, therefore, that a higher concentration of antibody in our hands would have yielded different results.

We were able to show, however, that blocking TIM4 *in vitro* slightly, but significantly, reduced the induction of CCR9 on proliferated $CD4^+$ T cells by $CD11b^+$ $CD103^+$ MLN DC. Previously, we had been unable to ascertain if $TIM4^+$ total $CD11b^+$ MLN DC had any enhanced ability to induce CCR9 expression on $CD4^+$ T cells *in vitro*, possibly due to the extended culture time of five days rather than three. This would be an important approach required to confirm our results. It would also be of interest to determine if this phenomenon is dose-dependent. CCR9 directs cell homing to the small intestine via interactions with its cognate chemokine ligand CCL25 (Svensson et al. 2002), which within the gastrointestinal tract is only expressed in the small intestinal epithelium (Kunkel et al. 2000). The contribution of sMLN DC within the total MLN cells used in our experiment will be greater than that of cMLN DC, and it is therefore likely that our results mirror a

small intestinal rather than a colonic phenotype. This is consistent with the importance of CCR9 in small intestinal homing. However, to confirm this, it would be necessary to specifically sort sMLN and cMLN DC separately. Unfortunately, while not impossible, the small number of cMLN DC makes this a technically difficult task.

Induction of CCR9 expression on T cells is dependent on RA production by $CD103^+$ DC (Iwata et al. 2004, Jaensson et al. 2008). Previously we had found that $TIM4^+$ $CD11b^+$ $CD103^+$ DC in the sMLN had a trend towards a higher percentage of $Aldefluor^+$ cells, indicating greater RALDH activity in this population compared with $TIM4^-$ cells. This had not, however, been the case for cMLN DC. Moreover, *Aldh1a2* transcript levels were similar in $TIM4^+$ and $TIM4^-$ total $CD11b^+$ DC from the sMLN, indicating that while their baseline capacity to make RA is unchanged, the actual production levels differ. Interestingly, $CD103^+$ DC that have taken up apoptotic cell antigen *in vivo* have elevated levels of *Aldh1a2* mRNA (Cummings et al. 2016), which indicates a possible link between the uptake of apoptotic cells and the production of RA by DC. The level of apoptosis taking place in our *in vitro* culture system is likely to be quite high, and blocking TIM4 on $CD11b^+$ $CD103^+$ DC could have decreased the rate of uptake by these cells. Further experiments would be required to confirm this, however. One important point to make when assessing the role of TIM4 on MLN DC is that, due to the higher proportion of sMLN DC in our culture system, the overall percentage of $TIM4^+$ cells will be fairly low, given its lower expression on sMLN DC (20%) compared with their counterparts in the cMLN (40%). This could be one reason why the effect on CCR9 induction induced by blocking TIM4 was not very pronounced.

RA signalling also imprints the expression of α4β7 on T cells (Iwata et al. 2004), the integrin that recognises MAdCAM-1 on vascular endothelial cells in the small intestine (Hamann et al. 1994). We did not, however, find that blocking TIM4 *in vitro* significantly reduced the expression of the β7 subunit on proliferating T cells. One caveat to interpreting these results is the absence of the α4 staining in our analysis. The β7 subunit can also dimerise with integrin αE, which together constitute the CD103 molecule. As a well-functioning antibody to the entire heterodimer is not yet commercially available to the best of our knowledge, it would have been important to include staining for CD103 to be confident in our identification of α4β7. Nonetheless, our findings suggest that TIM4 function on DC does not play a role in its induction on T cells.

We could not find a role for TIM4 on any other MLN DC subset in the experimental readouts we investigated in this system, but the small number of repeats, especially for CD11b$^+$ CD103$^-$ and CD11b$^-$ CD103$^-$ DC make sound conclusions impossible. To assess whether TIM4 is required functionally for cross-presentation and induction of homing markers on CD8$^+$ T cells, we co-cultured OVA-pulsed CD11b$^-$ CD103$^+$ DC with OT-I MLN cells in the presence of αTIM4 blocking antibody. However, blocking TIM4 had no effect on the proliferation or induction of CCR9 or β7 on antigen-specific CD8$^+$ T cells. Together with our observations from evaluating homing markers on CD4$^+$ T cells, these data indicate that TIM4 on MLN CD11b$^-$ CD103$^+$ DC is not involved in this process. This also correlates with the lower expression level of TIM4 on CD11b$^-$ CD103$^+$ DC compared with CD11b$^+$ CD103$^+$ DC in the MLN.

We had hypothesised that TIM4 on DC might interact with T cells during antigen presentation via ligand binding to TIM1. However, we could only detect TIM1 staining on CD8$^+$ T cells and not CD4$^+$ T cells. One reason for this could be the lack of pro-inflammatory stimuli in our system. Previous identification of TIM1 on activated CD4$^+$ T cells has either been limited to a very small percentage (de Souza et al. 2005), or induced after incubation with concanavalin A (Meyers et al. 2005), a strong polyclonal activation stimulus. Furthermore, Mizui et al. (2008) showed that activation of CD4$^+$ T cells *in vitro* using αCD3/28 treatment led to an increase in TIM1 transcript but not protein levels, which is more in line with our findings of non-detectable TIM1 staining on antigen-specific CD4$^+$ T cells. Moreover, in our hands expression on CD8$^+$ T cells was limited to a small population of cells that had completed all rounds of replication detected through loss of CFSE staining, as well as a population of unproliferated cells. Together with the fact that blocking TIM4 in OT-I co-cultures did not reduce proliferation, these results do not provide any evidence that interactions between TIM1 and TIM4 occur or are vital for T cell proliferation under steady state conditions *in vitro*. This may, however, change in a pro-inflammatory setting afforded, for example, by bacterial infection. Future investigations should take this into account.

Our final hypothesis was that TIM4 played a role in determining DC functions during bacterial-induced inflammation in the colon. We therefore compared the inflammation caused during infection with two different enteric pathogens, *C. rodentium* and *S.* Typhimurium, and its dependency on TIM4 *in vivo* by administering systemic αTIM4 blocking antibody. We did not see a significant difference in bacterial colonisation during

C. rodentium infection, suggesting that the host's ability to take up apoptotic cell material through TIM4 is not a limiting factor in bacterial colonisation and replication. Furthermore, animal weight loss was comparable between groups during *S.* Typhimurium infection, as was colon shortening. These findings indicate that blocking TIM4 has no effect on the course or overall severity of infection. It would, however, have been useful to assess the pathology exhibited in the different groups by histological examination of colonic tissue, thus affording a more detailed comparison of outcome.

S. Typhimurium-infected mice displayed a trend towards more $TIM4^+$ cells among $CD11b^+$ $CD103^+$ and $CD11b^-$ $CD103^-$ colonic DC. We had previously seen a similar effect on $CD11b^+$ $CD103^-$ DC during *C. rodentium* infection. Interestingly, however, *S.* Typhimurium-infected mice also exhibited a trend towards decreased TIM4 expression on cMLN $CD11b^+$ $CD103^+$ DC, which had not previously been found during infection with *C. rodentium*. These differences may stem from the heightened severity of inflammation caused by *S.* Typhimurium. There is evidence to suggest that metabolites enriched in the MLN during *S.* Typhimurium infection can lead to lymphocyte apoptosis (Hulme et al. 2017). Furthermore, mice lacking the ACR CD300a exhibited greater bacterial dissemination after infection with *S.* Typhimurium (Nakahashi-Oda et al. 2015), indicating that the uptake of apoptotic cells is important for limiting systemic spread of bacteria. Based on these observations, it appears counterintuitive that expression of an ACR would decrease in the cMLN during infection. However, this reduction could also be caused by selective killing of $TIM4^+$ DC by *S.* Typhimurium after uptake of infected apoptotic cells, given the ability of this pathogen to induce caspase-1-dependent cell death in $CD11c^+$ cells (van der Velden et al. 2003) and macrophages (Hersh et al. 1999). Determining the number of viable *S.* Typhimurium in $TIM4^+$ and $TIM4^-$ MLN DC during infection could begin to give some indication of whether or not this is a valid hypothesis. On the other hand, we did not detect a significant decrease in the number of cMLN $CD11b^+$ $CD103^+$ DC during infection, which would be expected if this hypothesis were indeed true. Furthermore, blocking TIM4 in *S.* Typhimurium-infected animals did not have any effect on percentages or cell number of any DC population in the colonic LP or cMLN. Similarly, infection with *C. rodentium* also did not alter the distribution of DC populations in these tissues.

Transcript levels of *Ccr7*, *Il1b* and *Itgb8* in $CD11b^-$ $CD103^+$ colonic DC did not change after blocking TIM4 in *C. rodentium* infected animals, indicating that TIM4-mediated uptake of apoptotic cells during infection has little impact on $CD11b^-$ $CD103^+$ DC activation. Further

investigation would be required with a broader approach in gene expression profiling and with an appropriate control constituted by *C. rodentium*-infected mice treated with isotype control antibody to investigate this fully, however. On the other hand, it could be indicative of a less prominent role of these DC in mediating TIM4-mediated uptake of apoptotic cells during infection. This is especially plausible given that TIM4 expression does not increase on this subset during infection, when it does on colonic CD11b$^+$ CD103$^-$ DC. It would have therefore been interesting to investigate if blocking TIM4 alters gene expression in these cells, and although attempted during our investigation, this was not successful technically.

Both *C. rodentium* and *S.* Typhimurium induced an elevated influx of Ly6C$^+$ monocytes into the colonic LP. However, in *C. rodentium* infected mice that had received αTIM4 antibody, this increase was not statistically significant, indicating a slightly less pronounced response. Interestingly, this trend was reversed during *S.* Typhimurium infection, with αTIM4-treated mice showing a significant increase in Ly6C$^+$ MHCII$^+$ monocytes compared with uninfected controls, while the increase in isotype-treated infected animals did not reach statistical significance. These results require confirmation by further repeats, but may indicate that blocking TIM4 impacts inflammation severity differently during *C. rodentium* and *S.* Typhimurium infection.

Even though we were unable to provide any evidence for the regulation of steady state T cell proliferation by TIM4-TIM1 interactions *in vitro*, TIM4-mediated interactions with T cells may still be important *in vivo* during inflammation. Given that TIM4 has been implicated in the negative regulation of T cell activation (Mizui et al. 2008, Cao et al. 2011), the decreased percentage of TIM4$^+$ CD11b$^+$ CD103$^+$ DC in the cMLN of *S.* Typhimurium infected mice could be required for allowing adequate activation for mounting a protective immune response. We did not find, however, that blocking TIM4 *in vivo* during infection with either *S.* Typhimurium or *C. rodentium* had any effect on T cell differentiation. While we could show that *S.* Typhimurium induced a more robust IFNγ response in both CD4$^+$ and CD8$^+$ T cells than *C. rodentium*, this was independent of TIM4 function. However, to fully discount an inhibitory role for TIM4 in this context, further investigations would be necessary involving constitutive expression of TIM4 on DC. Previous work has shown that the induction of apoptosis during *C. rodentium* infection is required for the development of a Th17 response *in vivo* (Torchinsky et al. 2009), pointing to a possible role for TIM4 in facilitating this. Conversely, plate-bound TIM4-Fc can reduce IL-17 production from naïve T cells cultured under Th17-differentiating conditions *in vitro* (Cao et al. 2011). We could

not, in fact, find any evidence that Th17 induction during *C. rodentium* infection was either dependent on or negatively regulated by TIM4. The lack of any difference between αTIM4- and isotype-treated animals in the level of neutrophil influx into the colon during *C. rodentium* infection further suggests that TIM4 does not play a vital role in IL-17-mediated pathology. Previously, blocking TIM4 *in vivo* has been shown to increase Treg cell expansion in a skin allograft model (Yeung et al. 2013). We showed that Treg cell frequencies decreased significantly in the cMLN during *C. rodentium* infection in mice that had received isotype control, but not αTIM4 antibody. A similar proportional decrease was seen during *S.* Typhimurium infection compared with PBS controls, but in the colonic LP rather than the cMLN. In both cases this was not mirrored by absolute cell numbers, suggesting instead increased expansion of another cell type, such as possibly B cells, during infection. Nevertheless, as seen for both Th1 and Th17 responses, blocking TIM4 did not significantly change the Treg response during infection.

A problem faced in these investigations was the high variability encountered between individual mice. This could be due to differences in colonisation or development of infection, and could be overcome with more experimental repeats. Furthermore, the cell death pathways initiated during bacterial infection are likely to not only be represented by apoptosis, but also be comprised of responses such as necrosis and pyroptosis. Little is as yet known about the role of TIM4 in mediating uptake of cells that have undergone cell death via apoptosis distinct mechanisms. This could be a further factor increasing the variability observed in this *in vivo* approach. However, the at times low level detection of intracellular cytokines produced by T cells and the resulting variability between samples could also stem from technical issues. The use of PMA and Ionomyin to activate T cells and stimulate cytokine production, while routinely used, is also not a highly physiologically relevant indication of the differentiation state of T cells upon restimulation. In order to address this, a better approach would be to mimic restimulation by incubating T cells with αCD3 and αCD28 antibodies. Alternatively, transcription factor staining can be used to discriminate between T cell subsets. Finally, the use of bacteria expressing a model antigen would have allowed identification of antigen-specific T cells and a more accurate indication of whether or not blocking TIM4 has an effect on T cell priming during infection.

In conclusion, we were unable to clearly identify a functional role for TIM4 in mediating DC migration, antigen presentation, or control of innate and adaptive responses during

bacterial infection in the intestine. Our results do, on the other hand, point to the possibility that TIM4$^+$ DC might be important in the induction of CCR9 on T cells. Further work will be needed to determine if this is the case *in vivo* and, supposing this is limited to the sMLN, what the function of the more abundant TIM4$^+$ DC is in the cMLN, where RA production plays a less prominent part in orchestrating mucosal immunity.

Chapter 7: Final discussion and conclusions

7.1 Final discussion

We have investigated some of the cellular and molecular mechanisms that underpin bacterial infection and the induction of inflammation in the intestinal mucosa. Specifically, we characterised the intestinal immune response to infection with CD-associated AIEC strain NRG857c. We have also used infection with *C. rodentium* and *S.* Typhimurium to better understand the role of apoptotic cell antigen uptake in regulating T cell responses during inflammation. Whilst *C. rodentium* and *S.* Typhimurium are specialised enteric pathogens that employ a range of virulence factors facilitating robust colonisation and invasion, NRG857c is a commensal thought to have the capacity to act as a pathobiont under certain circumstances.

Previous work had demonstrated a significant level of chronic inflammation induced by NRG857c infection of WT mice after perturbation of the microbiota using a single treatment with oral streptomycin (Small et al. 2013). In order to further elucidate the cellular mechanisms of inflammation in this model, we performed a comprehensive characterisation of the intestinal immune response to infection with NRG857c *in vivo*. We showed that NRG857c was indeed able to colonise the lumen of mice and be shed in the faeces for up to nine weeks after infection. However, this was not accompanied by any signs of weight loss or tissue pathology in mice. Moreover, infection did not alter the frequency or number of infiltrating innate or adaptive immune cell populations in the LP. We also found no evidence for increased number or activation of T cells in the MLN. These observations indicate that NRG857c infection in our hands is not sufficient to drive chronic tissue inflammation. When we additionally caused perturbations in intestinal homeostasis by feeding mice a diet deficient in fibre, we did not observe any induction of intestinal inflammation by NRG857c. Furthermore, treatment with low-level DSS also did not enhance this strain's ability to invade and cause immune activation. Therefore, despite our extensive attempts to detect signs of inflammation both at steady state and after disruption of intestinal homeostasis by insult or lack of SCFA, we conclude that NRG857c does not cause chronic intestinal inflammation. This critical observation thereby denies the fulfilment of the Henle-Koch postulates (Carter 1985) by this strain of *E. coli*. While our work supports the hypothesis that AIEC, whilst correlative, is not causative in CD, the

limitations of comparing murine models with the human disease setting cannot be overlooked. Our model fails to account for differences in microbiota composition between mice and humans, as well as the role of prior insults and the contribution of host susceptibility factors. Moreover, great heterogeneity exists within both clinical presentation and disease-associated genetic risk in CD. Murine models only allow limited investigation of the pathogenic mechanisms involved, and there is therefore a need for more detailed study of the interaction between these factors and the microbiota in well-defined patient cohorts.

Given the elevated rate of apoptosis that occurs in the inflamed mucosa of IBD patients, we next carried out an in-depth characterisation of the expression of ACR, specifically TIM4, on DC and macrophage populations. We found that TIM4 is expressed on a subset of mature macrophages in the small intestine and colon (Figure 7. 1). Moreover, about 10% of cDC1 in the colon (Figure 7. 1) and 90% of cDC1 in the lung expressed TIM4, highlighting a potentially important role of this molecule in mediating the uptake of apoptotic cell antigen for cross-presentation by cDC1 at mucosal sites. All DC populations were shown to upregulate TIM4 upon migration in mesenteric lymph (Figure 7. 1), and cDC2 further increased expression once in the cMLN. $CD11b^+$ $CD103^+$ DC had the highest frequency of $TIM4^+$ cells in both sMLN and cMLN compared with the other migratory DC populations (Figure 7. 1). Across the LP, lymph and MLN, more colonic DC expressed TIM4 than small intestinal DC, indicating that TIM4 is not only controlled in a population specific manner, but is also tissue-dependent. We were not, however, able to show any role for IL-4 or TGFβR signalling on DC, or the microbiota in controlling TIM4 expression *in vivo*. Instead, *C. rodentium* infection did increase the percentage of $TIM4^+$ cells among colonic LP $CD11b^+$ $CD103^-$ and $CD11b^-$ $CD103^-$ DC.

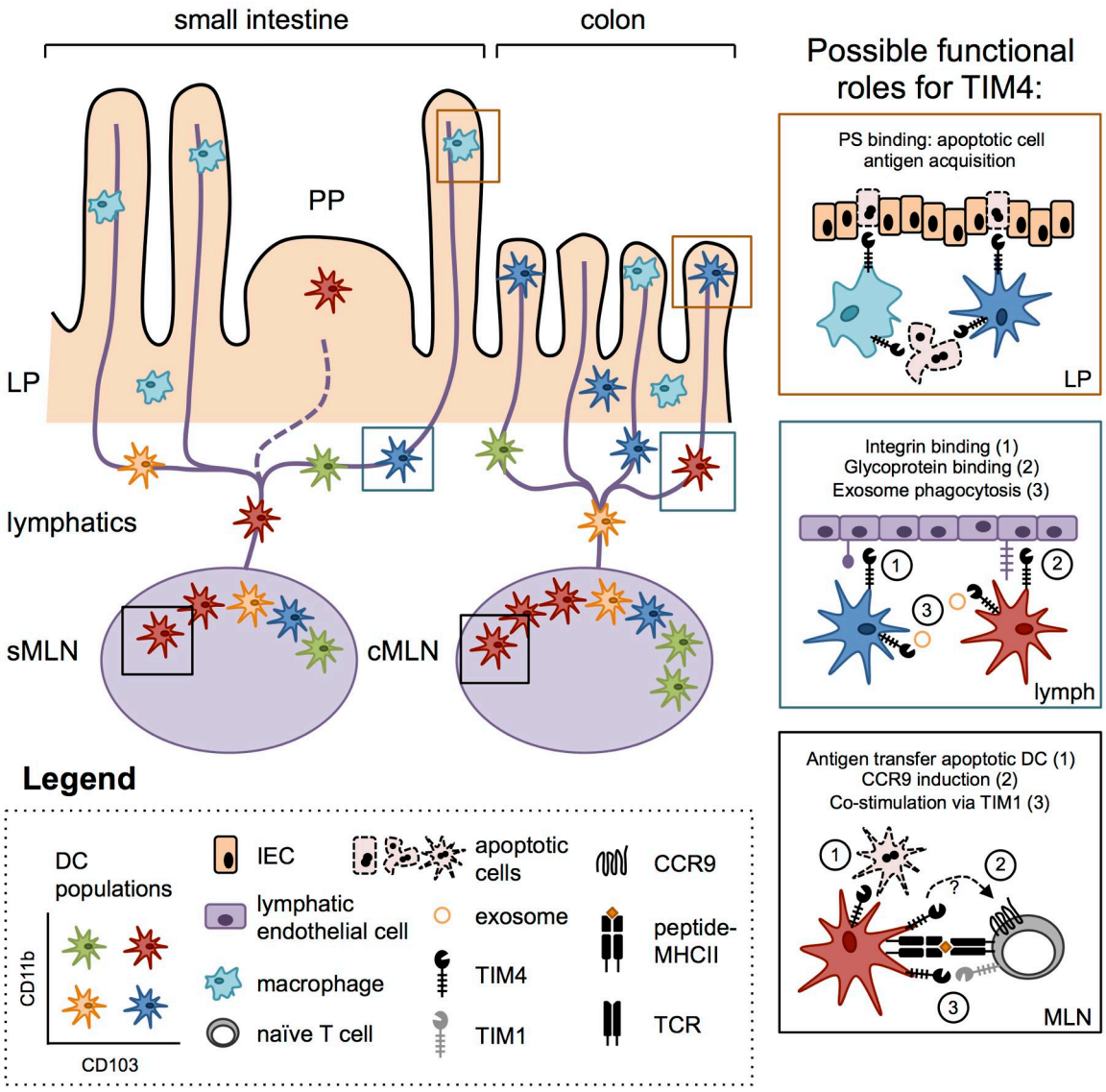

Figure 7. 1: Expression pattern of TIM4 on MNP in the intestine and potential tissue-dependent functions

Schematic representation of the small intestinal and colonic LP, lymphatics and MLN, showing cell populations that express TIM4 in the various tissues. In the LP of both small intestine and colon, TIM4 is expressed by macrophages, but only colonic CD11b$^-$ CD103$^+$ express TIM4. All migratory DC populations upregulate TIM4 in lymph, and the frequency of TIM4$^+$ cDC2, especially CD11b$^+$ CD103$^+$ further increases in the MLN. Inset boxes give an overview of potential functions mediated by TIM4 on DC in the various tissues.

Taken together, these data indicate that TIM4 may have context-dependent roles on DC (Figure 7. 1). In the LP, TIM4 is likely to function as a *bona fide* PSR and facilitate the uptake of apoptotic cells both in the epithelium and the LP by macrophages and cDC1 (Figure 7. 1). We found that TIM4$^+$ cDC1 had higher expression levels of *Ccr7* and *Il1b* mRNA, indicating that they may be more mature and ready to migrate to the MLN. However, more work will be required to fully understand the downstream effects of apoptotic cell uptake via TIM4 in these cells. For example, it remains unclear if these could be mediated by TIM4 itself, of which as yet no intrinsic signalling capability has been

reported, or if TIM4-mediated phagocytosis and subsequent activation of autophagy-associated pathways may play a role in DC maturation. Our observation that the frequency of TIM4^{+} DC increases during infection with *C. rodentium* in a population-specific manner indicates that it may have further important functions during bacterial-induced intestinal inflammation. In this context, the elevated expression of TIM4 may be due to the increased levels of TLR ligands and activation of downstream MyD88 signalling. It could also be controlled by a cell-intrinsic mechanism, where phagocytic uptake of apoptotic cells during infection leads to upregulation of the PSR on the cell membrane. However, more in depth *in vitro* and *in vivo* approaches will be required to elucidate what mechanisms control TIM4 expression in this setting. Blocking TIM4 *in vivo* had no effect on the generation of protective Th17 responses in *C. rodentium* infected mice, indicating that despite the increase in expression, TIM4 is likely to play a redundant role together with other ACR in sampling apoptotic cell antigen in the LP and supporting Th17 cell differentiation. Furthermore, the innate protective responses in these mice characterised by the influx of monocytes or neutrophils to the LP were also not significantly changed after blocking TIM4.

Together with the observations that TIM4^{+} LP cDC1 have higher *Ccr7* mRNA levels than their TIM4^{-} counterparts, and that an increased frequency of DC express TIM4 in mesenteric lymph compared with the LP, we hypothesised that TIM4 is important during DC migration to the MLN. This could be supported by integrin binding on lymphatic endothelial cells via the RGD motif in its IgV domain, or by interactions between the highly glycosylated mucin domain and other glycoproteins on the endothelium (Figure 7. 1). However, blocking TIM4 *in vivo* did not significantly decrease the migration efficiency of DC, indicating that while these interactions may indeed play a part in supporting DC entry into, migration through, or exit out of the lymphatics, TIM4 is not essential for these functions. Again, the lack of an effect after TIM4 blockade may reflect the large amount of redundancy for cell adhesion molecules in DC migration, which to date has been shown only to be dependent on CCR7 (Lämmermann et al. 2008). A second possible role for TIM4 on migrating DC in lymph is its ability to bind PS on exosomes (Miyanishi et al. 2007, Nakai et al. 2016). These can traffic via the lymphatics (Srinivasan et al. 2016) and have indeed been found to be present in substantial quantities in mesenteric lymph (Milling, *personal communication*). While the ability of DC to take up antigen after the initiation of migration to the MLN has not yet been demonstrated, TIM4-mediated

exosome uptake represents an intriguing possibility that warrants further investigation (Figure 7. 1).

We found that both migratory and resident DC populations express TIM4 in the MLN. In this context it may serve several purposes. First, TIM4 could allow for antigen transfer from apoptotic DC to either resident or newly arrived migratory DC (Figure 7. 1). However, we were unable to test this hypothesis *in vitro* or *in vivo* and further work will be required to ascertain if this indeed takes place and if so, what downstream effects on T cell differentiation this might have. On the other hand, we did find that $TIM4^+$ $CD11b^+$ $CD103^+$ sMLN DC had higher RALDH activity than their $TIM4^-$ counterparts and that blocking TIM4 on $CD11b^+$ $CD103^+$ MLN DC *in vitro* led to a small, but significant, reduction in the induction of CCR9 expression on antigen-specific $CD4^+$ T cells. Given that this is a small intestinal homing marker (Stenstad et al. 2006, Jaensson et al. 2008), but the frequency of $TIM4^+$ DC is higher in the cMLN compared with the sMLN, the relevance of these findings, especially with respect to cMLN DC, is unclear. More in-depth investigation in relation to these observations will be required to fully ascertain if TIM4-mediated uptake of apoptotic cell antigen in the MLN indeed stimulates the production of RA by DC, and what other downstream effects this might have in the cMLN, where this metabolite plays a less important role.

A substantial, but somewhat contradictory, body of literature exists in support of interactions between TIM4 and TIM1 on T cells being important positive or negative regulators of T cell activation and differentiation. We were unable to show that TIM1 was upregulated upon antigen-specific activation of $CD4^+$ T cells, although we could detect it on a small population of proliferated $CD8^+$ T cells *in vitro*. $TIM4^+$ DC did not show any altered ability to prime and skew antigen-specific $CD4^+$ T cell responses *in vitro* compared with $TIM4^-$ DC. Moreover, blocking TIM4 on MLN DC also had no effect on the proliferation of $CD4^+$ or $CD8^+$ T cells *in vitro*. We therefore do not have any evidence to support the hypothesis that TIM4 binding of TIM1 acts as a co-stimulatory or inhibitory signal at steady state. Nevertheless, this could become evident in settings of inflammation. Indeed, mice infected with *S.* Typhimurium had a reduced frequency of $CD11b^+$ $CD103^+$ DC that expressed TIM4 in the cMLN compared with uninfected controls. We were unable to show, however, that blocking TIM4 had a significant effect on altering T cell differentiation in mice infected with *S.* Typhimurium or *C. rodentium*.

A number of open questions therefore remain regarding the function of TIM4 on MLN DC during steady state and inflammation. Even though our functional investigations did not yield any significant findings, the observation that TIM4 is enriched on CD11b^{+} CD103^{+} DC in the migratory population indicates that it may have a role in regulating the function of these DC. Further work comparing its expression of other ACR on this population, as well as transcriptomic profiling of CD11b^{+} CD103^{+} MLN DC from *Timd4*$^{-/-}$ and WT mice would help to further shed light on this issue.

7.2 Final conclusion

Herein we have provided evidence that the expression pattern of the ACR TIM4 on murine DC is both tissue- and subset-specific. While enriched on cDC1 in the mucosa of lung and colon, it is upregulated on all DC populations in mesenteric lymph and remains high on cDC2 in the cMLN. We were unable to investigate its role on DC in a chronic intestinal inflammatory setting due to the failure to demonstrate that CD-associated AIEC strain NRG857c induced intestinal disease in mice. We instead showed that TIM4 expression increases on LP DC during *C. rodentium* infection, but showed that it does not play an essential role in DC migration or the induction of protective T cell immunity to enteric bacterial pathogens. Having therefore begun to characterise this molecule's expression and function in the murine intestine, further work will be required to understand its role on human MNP in the healthy gut and during IBD, where recognition of apoptosis and the clearance of bacteria are likely to be vital for disease remission.

References

Adolph, T. E., Tomczak, M. F., Niederreiter, L., Ko, H.-J., Bock, J., Martinez-Naves, E., Glickman, J. N., Tschurtschenthaler, M., Hartwig, J., Hosomi, S., Flak, M. B., Cusick, J. L., Kohno, K., Iwawaki, T., Billmann-Born, S., Raine, T., Bharti, R., Lucius, R., Kweon, M.-N., Marciniak, S. J., Choi, A., Hagen, S. J., Schreiber, S., Rosenstiel, P., Kaser, A., and Blumberg, R. S., 2013. Paneth cells as a site of origin for intestinal inflammation. *Nature*, 503 (7475), 272–276.

Albacker, L. A., Karisola, P., Chang, Y.-J., Umetsu, S. E., Zhou, M., Akbari, O., Kobayashi, N., Baumgarth, N., Freeman, G. J., Umetsu, D. T., and Dekruyff, R. H., 2010. TIM-4, a Receptor for Phosphatidylserine, Controls Adaptive Immunity by Regulating the Removal of Antigen-Specific T Cells. *The Journal of Immunology*, 185 (11), 6839–6849.

Albacker, L. A., Yu, S., Bedoret, D., Lee, W.-L., Umetsu, S. E., Monahan, S., Freeman, G. J., Umetsu, D. T., and DeKruyff, R. H., 2013. TIM-4, expressed by medullary macrophages, regulates respiratory tolerance by mediating phagocytosis of antigen-specific T cells. *Mucosal Immunology*, 6 (3), 580–590.

Ando, R., Hama, H., Yamamoto-Hino, M., Mizuno, H., and Miyawaki, A., 2002. An optical marker based on the UV-induced green-to-red photoconversion of a fluorescent protein. *Proc Natl Acad Sci U S A*, 99 (20), 12651–12656.

Angiari, S. and Constantin, G., 2014. Regulation of T cell trafficking by the T cell immunoglobulin and mucin domain 1 glycoprotein. *Trends in Molecular Medicine*, 20 (12), 675–684.

Araki, Y., Mukaisyo, K.-I., Sugihara, H., Fujiyama, Y., and Hattori, T., 2010. Increased apoptosis and decreased proliferation of colonic epithelium in dextran sulfate sodium-induced colitis in mice. *Oncology Reports*, 24 (4), 869–874.

Ardawi, M. S. and Newsholme, E. A., 1985. Fuel utilization in colonocytes of the rat. *Biochemical Journal*, 231 (3), 713–719.

Arias, C. A. and Murray, B. E., 2012. The rise of the Enterococcus: beyond vancomycin resistance. *Nature Reviews Microbiology*, 10 (4), 266–278.

Arrode, G., Boccaccio, C., Lule, J., Allart, S., Moinard, N., Abastado, J. P., Alam, A., and Davrinche, C., 2000. Incoming human cytomegalovirus pp65 (UL83) contained in apoptotic infected fibroblasts is cross-presented to CD8(+) T cells by dendritic cells. *Journal of Virology*, 74 (21), 10018–10024.

Atarashi, K., Tanoue, T., Ando, M., Kamada, N., Nagano, Y., Narushima, S., Suda, W., Imaoka, A., Setoyama, H., Nagamori, T., Ishikawa, E., Shima, T., Hara, T., Kado, S., Jinnohara, T., Ohno, H., Kondo, T., Toyooka, K., Watanabe, E., Yokoyama, S.-I., Tokoro, S., Mori, H., Noguchi, Y., Morita, H., Ivanov, I. I., Sugiyama, T., Nuñez, G., Camp, J. G., Hattori, M., Umesaki, Y., and Honda, K., 2015. Th17 cell induction by adhesion of microbes to intestinal epithelial cells. *Cell*, 1–15.

Atarashi, K., Tanoue, T., Oshima, K., Suda, W., Nagano, Y., Nishikawa, H., Fukuda, S., Saito, T., Narushima, S., Hase, K., Kim, S., Fritz, J. V., Wilmes, P., Ueha, S., Matsushima, K., Ohno, H., Olle, B., Sakaguchi, S., Taniguchi, T., Morita, H., Hattori, M., and Honda, K., 2013. Treg induction by a rationally selected mixture of *Clostridia* strains from the human microbiota. *Nature*, 500 (7461), 232–236.

Atarashi, K., Tanoue, T., Shima, T., Imaoka, A., Kuwahara, T., Momose, Y., Cheng, G., Yamasaki, S., Saito, T., Ohba, Y., Taniguchi, T., Takeda, K., Hori, S., Ivanov, I. I., Umesaki, Y., Itoh, K., and Honda, K., 2011. Induction of colonic regulatory T cells by indigenous *Clostridium* species. *Science*, 331 (6015), 337–341.

Aychek, T., Mildner, A., Yona, S., Kim, K.-W., Lampl, N., Reich-Zeliger, S., Boon, L., Yogev, N., Waisman, A., Cua, D. J., and Jung, S., 2015. IL-23-mediated mononuclear phagocyte crosstalk protects mice from *Citrobacter rodentium*-induced colon immunopathology. *Nature Communications*, 6, 6525.

Ayres, J. S., Trinidad, N. J., and Vance, R. E., 2012. Lethal inflammasome activation by a multidrug-resistant pathobiont upon antibiotic disruption of the microbiota. *Nature Medicine*, 18 (5), 799–806.

Azukizawa, H., Dohler, A., Kanazawa, N., Nayak, A., Lipp, M., Malissen, B., Autenrieth, I., Katayama, I., Riemann, M., Weih, F., Berberich-Siebelt, F., and Lutz, M. B., 2011. Steady state migratory RelB+ langerin+ dermal dendritic cells mediate peripheral induction of antigen-specific CD4+ CD25+ Foxp3+ regulatory T cells. *European Journal of Immunology*, 41 (5), 1420–1434.

Backert, I., Koralov, S. B., Wirtz, S., Kitowski, V., Billmeier, U., Martini, E., Hofmann, K., Hildner, K., Wittkopf, N., Brecht, K., Waldner, M., Rajewsky, K., Neurath, M. F., Becker, C., and Neufert, C., 2014. STAT3 Activation in Th17 and Th22 cells controls IL-22-mediated epithelial host defense during infectious colitis. *The Journal of Immunology*, 193 (7), 3779–3791.

Bain, C. C., Bravo-Blas, A., Scott, C. L., Gomez Perdiguero, E., Geissmann, F., Henri, S., Malissen, B., Osborne, L. C., Artis, D., and Mowat, A. M., 2014. Constant replenishment from circulating monocytes maintains the macrophage pool in the intestine of adult mice. *Nature Immunology*, 15 (10), 929–937.

Bain, C. C., Scott, C. L., Uronen-Hansson, H., Gudjonsson, S., Jansson, O., Grip, O., Guilliams, M., Malissen, B., Agace, W. W., and Mowat, A. M. I., 2013. Resident and pro-inflammatory macrophages in the colon represent alternative context-dependent fates of the same Ly6C(hi) monocyte precursors. *Mucosal Immunology*, 6 (3), 498–510.

Bank, S., Skytt Andersen, P., Burisch, J., Pedersen, N., Roug, S., Galsgaard, J., Ydegaard Turino, S., Broder Brodersen, J., Rashid, S., Kaiser Rasmussen, B., Avlund, S., Bastholm Olesen, T., Jürgen Hoffmann, H., Kragh Thomsen, M., Østergaard Thomsen, V., Frydenberg, M., Andersen Nexø, B., Sode, J., Vogel, U., and Andersen, V., 2014. Polymorphisms in the inflammatory pathway genes TLR2, TLR4, TLR9, LY96, NFKBIA, NFKB1, TNFA ,TNFRSF1A, IL6R, IL10, IL23R, PTPN22, and PPARG are associated with susceptibility of inflammatory bowel disease in a Danish cohort. *PLoS ONE*, 9 (6), e98815.

Bao, S., Beagley, K. W., France, M. P., Shen, J., and Husband, A. J., 2000. Interferon-gamma plays a critical role in intestinal immunity against *Salmonella* Typhimurium infection. *Immunology*, 99 (3), 464–472.

Barnett Foster, D., Abul-Milh, M., Huesca, M., and Lingwood, C. A., 2000. Enterohemorrhagic *Escherichia coli* induces apoptosis which augments bacterial binding and phosphatidylethanolamine exposure on the plasma membrane outer leaflet. *Infection and Immunity*, 68 (6), 3108–3115.

Barnich, N. and Darfeuille-Michaud, A., 2007. Role of bacteria in the etiopathogenesis of inflammatory bowel disease. *World Journal of Gastroenterology*, 13 (42), 5571–5576.

Barrett, J. C., Hansoul, S., Nicolae, D. L., Cho, J. H., Duerr, R. H., Rioux, J. D., Brant, S. R., Silverberg, M. S., Taylor, K. D., Barmada, M. M., Bitton, A., Dassopoulos, T., Datta, L. W., Green, T., Griffiths, A. M., Kistner, E. O., Murtha, M. T., Regueiro, M. D., Rotter, J. I., Schumm, et al., 2008. Genome-wide association defines more than 30 distinct susceptibility loci for Crohn's disease. *Nature Genetics*, 40 (8), 955–962.

Barthel, M., Hapfelmeier, S., Quintanilla-Martínez, L., Kremer, M., Rohde, M., Hogardt, M., Pfeffer, K., Rüssmann, H., and Hardt, W.-D., 2003. Pretreatment of mice with streptomycin provides a *Salmonella enterica* serovar Typhimurium colitis model that allows analysis of both pathogen and host. *Infection and Immunity*, 71 (5), 2839–2858.

Bauer, T., Zagorska, A., Jurkin, J., Yasmin, N., Koffel, R., Richter, S., Gesslbauer, B., Lemke, G., and Strobl, H., 2012. Identification of Axl as a downstream effector of TGFbeta1 during Langerhans cell differentiation and epidermal homeostasis. *Journal of Experimental Medicine*, 209 (11), 2033–2047.

Becker, M., Güttler, S., Bachem, A., Hartung, E., Mora, A., Jäkel, A., Hutloff, A., Henn, V., Mages, H. W., Gurka, S., and Kroczek, R. A., 2014. Ontogenic, phenotypic, and functional characterization of XCR1+ dendritic cells leads to a consistent classification of intestinal dendritic cells based on the expression of XCR1 and SIRPalpha. *Frontiers in Immunology*, 5, 2107.

Beg, A. A. and Baltimore, D., 1996. An essential role for NF-kappaB in preventing TNF-alpha-induced cell death. *Science*, 274 (5288), 782–784.

Behnsen, J., Jellbauer, S., Wong, C. P., Edwards, R. A., George, M. D., Ouyang, W., and Raffatellu, M., 2014. The cytokine IL-22 promotes pathogen colonization by suppressing related commensal bacteria. *Immunity*, 40 (2), 262–273.

Belladonna, M. L., Volpi, C., Bianchi, R., Vacca, C., Orabona, C., Pallotta, M. T., Boon, L., Gizzi, S., Fioretti, M. C., Grohmann, U., and Puccetti, P., 2008. Cutting edge: Autocrine TGFbeta sustains default tolerogenesis by IDO-competent dendritic cells. *Journal of Immunology*, 181 (8), 5194–5198.

Bergsbaken, T. and Bevan, M. J., 2015. Proinflammatory microenvironments within the intestine regulate the differentiation of tissue-resident CD8(+) T cells responding to infection. *Nature Immunology*, 16 (4), 406–414.

Berlin, C., Berg, E. L., Briskin, M. J., Andrew, D. P., Kilshaw, P. J., Holzmann, B., Weissman, I. L., Hamann, A., and Butcher, E. C., 1993. Alpha 4 beta 7 integrin mediates lymphocyte binding to the mucosal vascular addressin MAdCAM-1. *Cell*, 74 (1), 185–195.

Bettelli, E., Carrier, Y., Gao, W., Korn, T., Strom, T. B., Oukka, M., Weiner, H. L., and Kuchroo, V. K., 2006. Reciprocal developmental pathways for the generation of pathogenic effector TH17 and regulatory T cells. *Nature*, 441 (7090), 235–238.

Binne, L. L., Scott, M. L., and Rennert, P. D., 2007. Human TIM-1 associates with the TCR complex and up-regulates T cell activation signals. *Journal of Immunology*, 178 (7), 4342–4350.

Black, R. E., Cousens, S., Johnson, H. L., Lawn, J. E., Rudan, I., Bassani, D. G., Jha, P., Campbell, H., Walker, C. F., Cibulskis, R., Eisele, T., Liu, L., and Mathers, C., 2010. Global, regional, and national causes of child mortality in 2008: a systematic analysis. *The Lancet*, 375 (9730), 1969–1987.

Bogunovic, M., Ginhoux, F., Helft, J., Shang, L., Hashimoto, D., Greter, M., Liu, K., Jakubzick, C., Ingersoll, M. A., Leboeuf, M., Stanley, E. R., Nussenzweig, M., Lira, S. A., Randolph, G. J., and Merad, M., 2009. Origin of the lamina propria dendritic cell network. *Immunity*, 31 (3), 513–525.

Bollrath, J. and Powrie, F. M., 2013. Controlling the frontier: Regulatory T cells and intestinal homeostasis. *Seminars in Immunology*, 25 (5), 352–357.

Borisenko, G. G., Matsura, T., Liu, S.-X., Tyurin, V. A., Jianfei, J., Serinkan, F. B., and Kagan, V. E., 2003. Macrophage recognition of externalized phosphatidylserine and phagocytosis of apoptotic Jurkat cells--existence of a threshold. *Archives of Biochemistry and Biophysics*, 413 (1), 41–52.

Borkowski, T. A., Letterio, J. J., Farr, A. G., and Udey, M. C., 1996. A role for endogenous transforming growth factor beta 1 in Langerhans cell biology: the skin of transforming growth factor beta 1 null mice is devoid of epidermal Langerhans cells. *Journal of Experimental Medicine*, 184 (6), 2417–2422.

Bouskra, D., Brezillon, C., Berard, M., Werts, C., Varona, R., Boneca, I. G., and Eberl, G., 2008. Lymphoid tissue genesis induced by commensals through NOD1 regulates intestinal homeostasis. *Nature*, 456 (7221), 507–U34.

Breese, E. J., Michie, C. A., Nicholls, S. W., Murch, S. H., Williams, C. B., Domizio, P., Walker-Smith, J. A., and MacDonald, T. T., 1994. Tumor necrosis factor alpha-producing cells in the intestinal mucosa of children with inflammatory bowel disease. *Gastroenterology*, 106 (6), 1455–1466.

Breton, G., Lee, J., Zhou, Y. J., Schreiber, J. J., Keler, T., Puhr, S., Anandasabapathy, N., Schlesinger, S., Caskey, M., Liu, K., and Nussenzweig, M. C., 2015. Circulating precursors of human CD1c+ and CD141+ dendritic cells. *Journal of Experimental Medicine*, 212 (3), 401–413.

Brown, A. J., Goldsworthy, S. M., Barnes, A. A., Eilert, M. M., Tcheang, L., Daniels, D., Muir, A. I., Wigglesworth, M. J., Kinghorn, I., Fraser, N. J., Pike, N. B., Strum, J. C., Steplewski, K. M., Murdock, P. R., Holder, J. C., Marshall, F. H., Szekeres, P. G., Wilson, S., Ignar, D. M., Foord, S. M., Wise, A., and Dowell, S. J., 2003. The Orphan G protein-coupled receptors GPR41 and GPR43 are activated by propionate and other short chain carboxylic acids. *Journal of Biological Chemistry*, 278 (13), 11312–11319.

Brzostek, J., Gascoigne, N. R. J., and Rybakin, V., 2016. Cell type-specific regulation of immunological synapse dynamics by B7 ligand recognition. *Frontiers in Immunology*, 7, 24.

Bullen, T. F., Forrest, S., Campbell, F., Dodson, A. R., Hershman, M. J., Pritchard, D. M., Turner, J. R., Montrose, M. H., and Watson, A. J. M., 2006. Characterization of epithelial cell shedding from human small intestine. *Laboratory Investigation*, 86 (10), 1052–1063.

Cai, P. C., Hu, L. H., Cui, T. P., Li, Y. R., Chen, F. H., and Wu, Q. W., 2009. Association of TIM4 promoter polymorphism -1419G>A with childhood asthma in a Chinese Han population. *Tissue Antigens*, 74 (1), 11–16.

Calfon, M., Zeng, H., Urano, F., Till, J. H., Hubbard, S. R., Harding, H. P., Clark, S. G., and Ron, D., 2002. IRE1 couples endoplasmic reticulum load to secretory capacity by processing the XBP-1 mRNA. *Nature*, 415 (6867), 92–96.

Camerini, V., Panwala, C., and Kronenberg, M., 1993. Regional specialization of the mucosal immune system. Intraepithelial lymphocytes of the large intestine have a different phenotype and function than those of the small intestine. *Journal of Immunology*, 151 (4), 1765–1776.

Cao, L., Chang, H., Shi, X., Peng, C., and He, Y., 2016. Keratin mediates the recognition of apoptotic and necrotic cells through dendritic cell receptor DEC205/CD205. *Proceedings of the National Academy of Sciences*, 113(47), 13438–13443.

Cao, L., Shi, X., Chang, H., Zhang, Q., and He, Y., 2015. pH-Dependent recognition of apoptotic and necrotic cells by the human dendritic cell receptor DEC205. *Proceedings of the National Academy of Sciences*, 112 (23), 7237–7242.

Cao, W., Ryan, M., Buckley, D., O'Connor, R., and Clarkson, M. R., 2011. Tim-4 inhibition of T-cell activation and T helper type 17 differentiation requires both the immunoglobulin V and mucin domains and occurs via the mitogen-activated protein kinase pathway. *Immunology*, 133 (2), 179–189.

Carneiro, L. A. M., Travassos, L. H., Soares, F., Tattoli, I., Magalhães, J. G., Bozza, M. T., Plotkowski, M. C., Sansonetti, P. J., Molkentin, J. D., Philpott, D. J., and Girardin, S. E., 2009. *Shigella* induces mitochondrial dysfunction and cell death in nonmyleoid cells. *Cell Host and Microbe*, 5 (2), 123–136.

Carter, K. C., 1985. Koch's postulates in relation to the work of Jacob Henle and Edwin Klebs. *Medical History*, 29 (4), 353–374.

Carter, P. B. and Collins, F. M., 1974. The route of enteric infection in normal mice. *Journal of Experimental Medicine*, 139 (5), 1189–1203.

Carvalho, F. A., Barnich, N., Sauvanet, P., Darcha, C., Gelot, A., and Darfeuille-Michaud, A., 2008. Crohn's disease-associated *Escherichia coli* LF82 aggravates colitis in injured mouse colon via signaling by flagellin. *Inflammatory Bowel Diseases*, 14 (8), 1051–1060.

Carvalho, F. A., Barnich, N., Sivignon, A., Darcha, C., Chan, C. H., Stanners, C. P., and Darfeuille-Michaud, A., 2009. Crohn's disease adherent-invasive *Escherichia coli* colonize and induce strong gut inflammation in transgenic mice expressing human CEACAM. *Journal of Experimental Medicine*, 206 (10), 2179–2189.

Caulin, C., Salvesen, G. S., and Oshima, R. G., 1997. Caspase cleavage of keratin 18 and reorganization of intermediate filaments during epithelial cell apoptosis. *The Journal of Cell Biology*, 138 (6), 1379–1394.

Cepek, K. L., Shaw, S. K., Parker, C. M., Russell, G. J., Morrow, J. S., Rimm, D. L., and Brenner, M. B., 1994. Adhesion between epithelial cells and T lymphocytes mediated by E-cadherin and the alpha E beta 7 integrin. *Nature*, 372 (6502), 190–193.

Cerovic, V., Bain, C. C., Mowat, A. M., and Milling, S. W., 2014a. Intestinal macrophages and dendritic cells: what's the difference? *Trends in Immunology*, 35 (6), 270–277.

Cerovic, V., Houston, S. A., Scott, C. L., Aumeunier, A., Yrlid, U., Mowat, A. M., and Milling, S. W. F., 2013. Intestinal CD103(-) dendritic cells migrate in lymph and prime effector T cells. *Mucosal Immunology*, 6 (1), 104–113.

Cerovic, V., Houston, S. A., Westlund, J., Utriainen, L., Davison, E. S., Scott, C. L., Bain, C. C., Joeris, T., Agace, W. W., Kroczek, R. A., Mowat, A. M., Yrlid, U., and Milling, S. W., 2014b. Lymph-borne CD8alpha dendritic cells are uniquely able to cross-prime CD8 T cells with antigen acquired from intestinal epithelial cells. *Mucosal Immunology*, 8(1), 38-48.

Cerovic, V., Jenkins, C. D., Barnes, A. G. C., Milling, S. W. F., MacPherson, G. G., and Klavinskis, L. S., 2009. Hyporesponsiveness of intestinal dendritic cells to TLR stimulation is limited to TLR4. *Journal of Immunology*, 182 (4), 2405–2415.

Chan, C. H. and Stanners, C. P., 2004. Novel mouse model for carcinoembryonic antigen-based therapy. *Molecular Therapy*, 9 (6), 775–785.

Chang, P. V., Hao, L., Offermanns, S., and Medzhitov, R., 2014. The microbial metabolite butyrate regulates intestinal macrophage function via histone deacetylase inhibition. *Proceedings of the National Academy of Sciences*, 111 (6), 2247–2252.

Chatterjee, B., Smed-Sorensen, A., Cohn, L., Chalouni, C., Vandlen, R., Lee, B.-C., Widger, J., Keler, T., Delamarre, L., and Mellman, I., 2012. Internalization and endosomal degradation of receptor-bound antigens regulate the efficiency of cross presentation by human dendritic cells. *Blood*, 120 (10), 2011–2020.

Chen, M., Wang, Y.-H., Wang, Y., Huang, L., Sandoval, H., Liu, Y.-J., and Wang, J., 2006. Dendritic cell apoptosis in the maintenance of immune tolerance. *Science*, 311 (5764), 1160–1164.

Chen, W., Jin, W., Hardegen, N., Lei, K.-J., Li, L., Marinos, N., McGrady, G., and Wahl, S. M., 2003. Conversion of peripheral CD4+ CD25- naive T cells to CD4+ CD25+ regulatory T cells by TGFbeta induction of transcription factor Foxp3. *J Exp Med*, 198 (12), 1875–1886.

Cherrington, C. A., Hinton, M., Pearson, G. R., and Chopra, I., 1991. Short-chain organic acids at pH 5.0 kill *Escherichia coli* and *Salmonella* spp. without causing membrane perturbation. *The Journal of Applied Bacteriology*, 70 (2), 161–165.

Chieppa, M., Rescigno, M., Huang, A. Y. C., and Germain, R. N., 2006. Dynamic imaging of dendritic cell extension into the small bowel lumen in response to epithelial cell TLR engagement. *Journal of Experimental Medicine*, 203 (13), 2841–2852.

Chu, D. K., Jimenez-Saiz, R., Verschoor, C. P., Walker, T. D., Goncharova, S., Llop-Guevara, A., Shen, P., Gordon, M. E., Barra, N. G., Bassett, J. D., Kong, J., Fattouh, R., McCoy, K. D., Bowdish, D. M., Erjefalt, J. S., Pabst, O., Humbles, A. A., Kolbeck, R., Waserman, S., and Jordana, M., 2014. Indigenous enteric eosinophils control DCs to initiate a primary Th2 immune response *in vivo*. *Journal of Experimental Medicine*, 211 (8), 1657–1672.

Chu, V. T., Beller, A., Rausch, S., Strandmark, J., Zanker, M., Arbach, O., Kruglov, A., and Berek, C., 2014. Eosinophils promote generation and maintenance of immunoglobulin-A-expressing plasma cells and contribute to gut immune homeostasis. *Immunity*, 40 (4), 582–593.

Chung, E. Y., Liu, J., Homma, Y., Zhang, Y., Brendolan, A., Saggese, M., Han, J., Silverstein, R., Selleri, L., and Ma, X., 2007. Interleukin-10 expression in macrophages during phagocytosis of apoptotic cells is mediated by homeodomain proteins Pbx1 and Prep-1. *Immunity*, 27 (6), 952–964.

Chung, H., Pamp, S. J., Hill, J. A., Surana, N. K., Edelman, S. M., Troy, E. B., Reading, N. C., Villablanca, E. J., Wang, S., Mora, J. R., Umesaki, Y., Mathis, D., Benoist, C., Relman, D. A., and Kasper, D. L., 2012. Gut immune maturation depends on colonization with a host-specific microbiota. *Cell*, 149 (7), 1578–1593.

Chung, Y., Chang, J.-H., Kweon, M.-N., Rennert, P. D., and Kang, C.-Y., 2005. CD8alpha-11b+ dendritic cells but not CD8alpha+ dendritic cells mediate cross-tolerance toward intestinal antigens. *Blood*, 106 (1), 201–206.

Cieza, R. J., Hu, J., Ross, B. N., Sbrana, E., and Torres, A. G., 2015. The IbeA invasin of adherent-invasive *Escherichia coli* mediates interaction with intestinal epithelia and macrophages. *Infection and Immunity*, 83 (5), 1904–1918.

Clark, M. A., Jepson, M. A., Simmons, N. L., and Hirst, B. H., 1994. Preferential interaction of *Salmonella* Typhimurium with mouse Peyer's patch M cells. *Research in Microbiology*, 145 (7), 543–552.

Clarke, R. M., 1970. A new method of measuring the rate of shedding of epithelial cells from the intestinal villus of the rat. *Gut*, 11 (12), 1015–1019.

Cleynen, I., Boucher, G., Jostins, L., Schumm, P., Zeissig, S., Ahmad, T., Andersen, V., Andrews, J. M., Annese, V., Brand, S., Brant, S. R., Cho, J. H., Daly, M. J., Dubinsky, M., Duerr, R. H., Ferguson, L. R., Franke, A., Gearry, R. B., Goyette, P., Hakonarson, H., et al., 2015. Inherited determinants of Crohn's disease and ulcerative colitis phenotypes: a genetic association study. *The Lancet*, 387(10014), 1–12.

Cliffe, L. J., Humphreys, N. E., Lane, T. E., Potten, C. S., Booth, C., and Grencis, R. K., 2005. Accelerated intestinal epithelial cell turnover: a new mechanism of parasite expulsion. *Science*, 308 (5727), 1463–1465.

Connor, L. M., Tang, S.-C., Camberis, M., Le Gros, G., and Ronchese, F., 2014. Helminth-conditioned dendritic cells prime CD4+ T cells to IL-4 production *in vivo*. *Journal of Immunology*, 193 (6), 2709–2717.

Coombes, J. L., Siddiqui, K. R. R., Arancibia-Carcamo, C. V., Hall, J., Sun, C.-M., Belkaid, Y., and Powrie, F., 2007. A functionally specialized population of mucosal CD103(+) DCs induces Foxp3(+) regulatory T cells via a TGFbeta- and retinoic acid-dependent mechanism. *Journal of Experimental Medicine*, 204 (8), 1757–1764.

Cooney, R., Baker, J., Brain, O., Danis, B., Pichulik, T., Allan, P., Ferguson, D. J. P., Campbell, B. J., Jewell, D., and Simmons, A., 2010. NOD2 stimulation induces autophagy in dendritic cells influencing bacterial handling and antigen presentation. *Nature Medicine*, 16 (1), 90–97.

Corazza, N., Muller, S., Brunner, T., Kagi, D., and Mueller, C., 2000. Differential contribution of Fas- and perforin-mediated mechanisms to the cell-mediated cytotoxic activity of naive and *in vivo*-primed intestinal intraepithelial lymphocytes. *Journal of Immunology*, 164 (1), 398–403.

Corbin, B. D., Seeley, E. H., Raab, A., Feldmann, J., Miller, M. R., Torres, V. J., Anderson, K. L., Dattilo, B. M., Dunman, P. M., Gerads, R., Caprioli, R. M., Nacken, W., Chazin, W. J., and Skaar, E. P., 2008. Metal chelation and inhibition of bacterial growth in tissue abscesses. *Science*, 319 (5865), 962–965.

Creamer, B., Shorter, R. G., and Bamforth, J., 1961a. The turnover and shedding of epithelial cells. I. The turnover in the gastro-intestinal tract. *Gut*, 2, 110–118.

Creamer, B., Shorter, R. G., and Bamforth, J., 1961b. The turnover and shedding of epithelial cells: Part II The shedding in the small intestine. *Gut*, 2 (2), 117–118.

Cullender, T. C., Chassaing, B., Janzon, A., Kumar, K., Muller, C. E., Werner, J. J., Angenent, L. T., Bell, M. E., Hay, A. G., Peterson, D. A., Walter, J., Vijay-Kumar, M., Gewirtz, A. T., and Ley, R. E., 2013. Innate and adaptive immunity interact to quench microbiome flagellar motility in the gut. *Cell Host and Microbe*, 14 (5), 571–581.

Cummings, J. H., Hill, M. J., Bone, E. S., Branch, W. J., and Jenkins, D. J., 1979. The effect of meat protein and dietary fiber on colonic function and metabolism. II. Bacterial metabolites in feces and urine. *The American Journal of Clinical Nutrition*, 32 (10), 2094–2101.

Cummings, R. J., Barbet, G., Bongers, G., Hartmann, B. M., Gettler, K., Muniz, L., Furtado, G. C., Cho, J., Lira, S. A., and Blander, J. M., 2016. Different tissue phagocytes sample apoptotic cells to direct distinct homeostasis programs. *Nature*, 539 (7630), 565–569.

Czuczman, M. A., Fattouh, R., van Rijn, J. M., Canadien, V., Osborne, S., Muise, A. M., Kuchroo, V. K., Higgins, D. E., and Brumell, J. H., 2014. *Listeria monocytogenes* exploits efferocytosis to promote cell-to-cell spread. *Nature*, 509 (7499), 230–234.

Dai, X. and Zhu, B. T., 2010. Indoleamine 2,3-dioxygenase tissue distribution and cellular localization in mice: implications for its biological functions. *Journal of Histochemistry and Cytochemistry*, 58 (1), 17–28.

Darfeuille-Michaud, A., Boudeau, J., Bulois, P., Neut, C., Glasser, A. L., Barnich, N., Bringer, M. A., Swidsinski, A., Beaugerie, L., and Colombel, J. F., 2004. High prevalence of adherent-invasive *Escherichia coli* associated with ileal mucosa in Crohn's disease. *Gastroenterology*, 127 (2), 412–421.

Darfeuille-Michaud, A., Neut, C., Barnich, N., Lederman, E., Di Martino, P., Desreumaux, P., Gambiez, L., Joly, B., Cortot, A., and Colombel, J. F., 1998. Presence of adherent *Escherichia coli* strains in ileal mucosa of patients with Crohn's disease. *Gastroenterology*, 115 (6), 1405–1413.

de Souza, A. J., Oriss, T. B., O'malley, K. J., Ray, A., and Kane, L. P., 2005. T cell Ig and mucin 1 (TIM-1) is expressed on *in vivo*-activated T cells and provides a costimulatory signal for T cell activation. *Proceedings of the National Academy of Sciences*, 102 (47), 17113–17118.

Deng, W., Vallance, B. A., Li, Y., Puente, J. L., and Finlay, B. B., 2003. Citrobacter rodentium translocated intimin receptor (Tir) is an essential virulence factor needed for actin condensation, intestinal colonization and colonic hyperplasia in mice. *Molecular Microbiology*, 48 (1), 95–115.

Denning, T. L., Norris, B. A., Medina-Contreras, O., Manicassamy, S., Geem, D., Madan, R., Karp, C. L., and Pulendran, B., 2011. Functional specializations of intestinal dendritic cell and macrophage subsets that control Th17 and regulatory T cell responses are dependent on the T cell/APC ratio, source of mouse strain, and regional localization. *Journal of Immunology*, 187 (2), 733–747.

Denning, T. L., Wang, Y.-C., Patel, S. R., Williams, I. R., and Pulendran, B., 2007. Lamina propria macrophages and dendritic cells differentially induce regulatory and interleukin 17-producing T cell responses. *Nature Immunology*, 8 (10), 1086–1094.

Deriu, E., Liu, J. Z., Pezeshki, M., Edwards, R. A., Ochoa, R. J., Contreras, H., Libby, S. J., Fang, F. C., and Raffatellu, M., 2013. Probiotic bacteria reduce *Salmonella* Typhimurium intestinal colonization by competing for iron. *Cell Host and Microbe*, 14 (1), 26–37.

Desch, A. N., Henson, P. M., and Jakubzick, C. V., 2013. Pulmonary dendritic cell development and antigen acquisition. *Immunological Research*, 55 (1-3), 178–186.

Desch, A. N., Randolph, G. J., Murphy, K., Gautier, E. L., Kedl, R. M., Lahoud, M. H., Caminschi, I., Shortman, K., Henson, P. M., and Jakubzick, C. V., 2011. CD103+ pulmonary dendritic cells preferentially acquire and present apoptotic cell-associated antigen. *Journal of Experimental Medicine*, 208 (9), 1789–1797.

Di Sabatino, A., Ciccocioppo, R., Luinetti, O., Ricevuti, L., Morera, R., Cifone, M. G., Solcia, E., and Corazza, G. R., 2003. Increased enterocyte apoptosis in inflamed areas of Crohn's disease. *Diseases of the Colon and Rectum*, 46 (11), 1498–1507.

Diao, J., Winter, E., Cantin, C., Chen, W., Xu, L., Kelvin, D., Phillips, J., and Cattral, M. S., 2006. *In situ* replication of immediate dendritic cell (DC) precursors contributes to conventional DC homeostasis in lymphoid tissue. *Journal of Immunology*, 176 (12), 7196–7206.

Dicksved, J., Halfvarson, J., Rosenquist, M., Järnerot, G., Tysk, C., Apajalahti, J., Engstrand, L., and Jansson, J. K., 2008. Molecular analysis of the gut microbiota of identical twins with Crohn's disease. *The ISME Journal*, 2 (7), 716–727.

Diehl, G. E., Longman, R. S., Zhang, J.-X., Breart, B., Galan, C., Cuesta, A., Schwab, S. R., and Littman, D. R., 2013. Microbiota restricts trafficking of bacteria to mesenteric lymph nodes by CX3CR1hi cells. *Nature*, 494 (7435), 116–120.

Dieleman, L. A., Ridwan, B. U., Tennyson, G. S., Beagley, K. W., Bucy, R. P., and Elson, C. O., 1994. Dextran sulfate sodium-induced colitis occurs in severe combined immunodeficient mice. *Gastroenterology*, 107 (6), 1643–1652.

Ding, Q., Yeung, M., Camirand, G., Zeng, Q., Akiba, H., Yagita, H., Chalasani, G., Sayegh, M. H., Najafian, N., and Rothstein, D. M., 2011. Regulatory B cells are identified by expression of TIM-1 and can be induced through TIM-1 ligation to promote tolerance in mice. *The Journal of Clinical Investigation*, 121 (9), 3645–3656.

Domka, J., Lee, J., and Wood, T. K., 2006. YliH (BssR) and YceP (BssS) regulate *Escherichia coli* K-12 biofilm formation by influencing cell signaling. *Applied and Environmental Microbiology*, 72 (4), 2449–2459.

Donohoe, D. R., Garge, N., Zhang, X., Sun, W., O'Connell, T. M., Bunger, M. K., and Bultman, S. J., 2011. The microbiome and butyrate regulate energy metabolism and autophagy in the mammalian colon. *Cell Metabolism*, 13 (5), 517–526.

Dorner, B. G., Dorner, M. B., Zhou, X., Opitz, C., Mora, A., Güttler, S., Hutloff, A., Mages, H. W., Ranke, K., Schaefer, M., Jack, R. S., Henn, V., and Kroczek, R. A., 2009. Selective expression of the chemokine receptor XCR1 on cross-presenting dendritic cells determines cooperation with CD8+ T cells. *Immunity*, 31 (5), 823–833.

Duncan, S. H., Barcenilla, A., Stewart, C. S., Pryde, S. E., and Flint, H. J., 2002. Acetate utilization and butyryl coenzyme A (CoA):acetate-CoA transferase in butyrate-producing bacteria from the human large intestine. *Applied and Environmental Microbiology*, 68 (10), 5186–5190.

Eaves-Pyles, T., Allen, C. A., Taormina, J., Swidsinski, A., Tutt, C. B., Eric Jezek, G., Islas-Islas, M., and Torres, A. G., 2008. *Escherichia coli* isolated from a Crohn's disease patient adheres, invades, and induces inflammatory responses in polarized intestinal epithelial cells. *International Journal of Medical Microbiology*, 298 (5–6), 397–409.

Eberl, G. and Littman, D. R., 2004. Thymic origin of intestinal alphabeta T cells revealed by fate mapping of RORgammat+ cells. *Science*, 305 (5681), 248–251.

Eckburg, P. B., Bik, E. M., Bernstein, C. N., Purdom, E., Dethlefsen, L., Sargent, M., Gill, S. R., Nelson, K. E., and Relman, D. A., 2005. Diversity of the human intestinal microbial flora. *Science*, 308 (5728), 1635–1638.

Edelblum, K. L., Singh, G., Odenwald, M. A., Lingaraju, A., Bissati, El, K., McLeod, R., Sperling, A. I., and Turner, J. R., 2015. Gamma-delta intraepithelial lymphocyte migration limits transepithelial pathogen invasion and systemic disease in mice. *Gastroenterology*, 148 (7), 1417–1426.

Edelblum, K. L., Washington, M. K., Koyama, T., Robine, S., Baccarini, M., and Polk, D. B., 2008. Raf protects against colitis by promoting mouse colon epithelial cell survival through NF-kappaB. *Gastroenterology*, 135 (2), 539–551.

Edelson, B. T., Kc, W., Juang, R., Kohyama, M., Benoit, L. A., Klekotka, P. A., Moon, C., Albring, J. C., Ise, W., Michael, D. G., Bhattacharya, D., Stappenbeck, T. S., Holtzman, M. J., Sung, S.-S. J., Murphy, T. L., Hildner, K., and Murphy, K. M., 2010. Peripheral CD103+ dendritic cells form a unified subset developmentally related to CD8α+ conventional dendritic cells. *The Journal of Experimental Medicine*, 207 (4), 823–836.

Eisenhauer, P. B., Harwig, S. S., and Lehrer, R. I., 1992. Cryptdins: antimicrobial defensins of the murine small intestine. *Infection and Immunity*, 60 (9), 3556–3565.

Eisenhoffer, G. T., Loftus, P. D., Yoshigi, M., Otsuna, H., Chien, C.-B., Morcos, P. A., and Rosenblatt, J., 2012. Crowding induces live cell extrusion to maintain homeostatic cell numbers in epithelia. *Nature* 484 (7395), 546-549.

Fadok, V. A., Bratton, D. L., Konowal, A., Freed, P. W., Westcott, J. Y., and Henson, P. M., 1998. Macrophages that have ingested apoptotic cells in vitro inhibit proinflammatory cytokine production through autocrine/paracrine mechanisms involving TGFbeta, PGE2, and PAF. *The Journal of Clinical Investigation*, 101 (4), 890–898.

Fadok, V. A., Voelker, D. R., Campbell, P. A., Cohen, J. J., Bratton, D. L., and Henson, P. M., 1992. Exposure of phosphatidylserine on the surface of apoptotic lymphocytes triggers specific recognition and removal by macrophages. *Journal of Immunology*, 148 (7), 2207–2216.

Fagarasan, S., Muramatsu, M., Suzuki, K., Nagaoka, H., Hiai, H., and Honjo, T., 2002. Critical roles of activation-induced cytidine deaminase in the homeostasis of gut flora. *Science*, 298 (5597), 1424–1427.

Faith, J. J., McNulty, N. P., Rey, F. E., and Gordon, J. I., 2011. Predicting a human gut microbiota's response to diet in gnotobiotic mice. *Science*, 333 (6038), 101–104.

Farache, J., Koren, I., Milo, I., Gurevich, I., Kim, K.-W., Zigmond, E., Furtado, G. C., Lira, S. A., and Shakhar, G., 2013. Luminal bacteria recruit CD103+ dendritic cells into the intestinal epithelium to sample bacterial antigens for presentation. *Immunity*, 38 (3), 581–595.

Farstad, I. N., Halstensen, T. S., Kvale, D., Fausa, O., and Brandtzaeg, P., 1997. Topographic distribution of homing receptors on B and T cells in human gut-associated lymphoid tissue: relation of L-selectin and integrin alpha 4 beta 7 to naive and memory phenotypes. *The American Journal of Pathology*, 150 (1), 187–199.

Felker, P., Sere, K., Lin, Q., Becker, C., Hristov, M., Hieronymus, T., and Zenke, M., 2010. TGFbeta1 accelerates dendritic cell differentiation from common dendritic cell progenitors and directs subset specification toward conventional dendritic cells. *Journal of Immunology*, 185 (9), 5326–5335.

Ferguson, T. A., Herndon, J., Elzey, B., Griffith, T. S., Schoenberger, S., and Green, D. R., 2002. Uptake of apoptotic antigen-coupled cells by lymphoid dendritic cells and cross-priming of CD8(+) T cells produce active immune unresponsiveness. *Journal of Immunology*, 168 (11), 5589–5595.

Fischer, K., Voelkl, S., Berger, J., Andreesen, R., Pomorski, T., and Mackensen, A., 2006. Antigen recognition induces phosphatidylserine exposure on the cell surface of human CD8+ T cells. *Blood*, 108 (13), 4094–4101.

Flannagan, R. S., Canton, J., Furuya, W., Glogauer, M., and Grinstein, S., 2014. The phosphatidylserine receptor TIM4 utilizes integrins as coreceptors to effect phagocytosis. *Molecular Biology of the Cell*, 25 (9), 1511–1522.

Fletcher, S. M., McLaws, M.-L., and Ellis, J. T., 2013. Prevalence of gastrointestinal pathogens in developed and developing countries: systematic review and meta-analysis. *Journal of Public Health Research*, 2 (1), 42–53.

Fogg, D. K., Sibon, C., Miled, C., Jung, S., Aucouturier, P., Littman, D. R., Cumano, A., and Geissmann, F., 2006. A clonogenic bone marrow progenitor specific for macrophages and dendritic cells. *Science*, 311 (5757), 83–87.

Fontenot, J. D., Gavin, M. A., and Rudensky, A. Y., 2003. Foxp3 programs the development and function of CD4+CD25+ regulatory T cells. *Nature Immunology*, 4 (4), 330–336.

Förster, R., Schubel, A., Breitfeld, D., Kremmer, E., Renner-Müller, I., Wolf, E., and Lipp, M., 1999. CCR7 coordinates the primary immune response by establishing functional microenvironments in secondary lymphoid organs. *Cell*, 99 (1), 23–33.

Frank, D. N., Robertson, C. E., Hamm, C. M., Kpadeh, Z., Zhang, T., Chen, H., Zhu, W., Sartor, R. B., Boedeker, E. C., Harpaz, N., Pace, N. R., and Li, E., 2011. Disease phenotype and genotype are associated with shifts in intestinal-associated microbiota in inflammatory bowel diseases. *Inflammatory Bowel Diseases*, 17 (1), 179–184.

Frank, D. N., St Amand, A. L., Feldman, R. A., Boedeker, E. C., Harpaz, N., and Pace, N. R., 2007. Molecular-phylogenetic characterization of microbial community imbalances in human inflammatory bowel diseases. *Proceedings of the National Academy of Sciences*, 104 (34), 13780–13785.

Frankel, G. and Phillips, A. D., 2008. Attaching effacing *Escherichia coli* and paradigms of Tir-triggered actin polymerization: getting off the pedestal. *Cellular Microbiology*, 10 (3), 549–556.

Fre, S., Huyghe, M., Mourikis, P., Robine, S., Louvard, D., and Artavanis-Tsakonas, S., 2005. Notch signals control the fate of immature progenitor cells in the intestine. *Nature*, 435 (7044), 964–968.

Freeman, G. J., Casasnovas, J. M., Umetsu, D. T., and Dekruyff, R. H., 2010. TIM genes: a family of cell surface phosphatidylserine receptors that regulate innate and adaptive immunity. *Immunological Reviews*, 235 (1), 172–189.

Fukata, M., 2005. Toll-like receptor-4 is required for intestinal response to epithelial injury and limiting bacterial translocation in a murine model of acute colitis. *AJP: Gastrointestinal and Liver Physiology*, 288 (5), G1055–G1065.

Fukata, M. and Arditi, M., 2013. The role of pattern recognition receptors in intestinal inflammation. *Mucosal Immunology*, 6 (3), 451–463.

Fukuda, S., Toh, H., Hase, K., Oshima, K., Nakanishi, Y., Yoshimura, K., Tobe, T., Clarke, J. M., Topping, D. L., Suzuki, T., Taylor, T. D., Itoh, K., Kikuchi, J., Morita, H., Hattori, M., and Ohno, H., 2011. *Bifidobacteria* can protect from enteropathogenic infection through production of acetate. *Nature*, 469 (7331), 543–547.

Furusawa, Y., Obata, Y., Fukuda, S., Endo, T. A., Nakato, G., Takahashi, D., Nakanishi, Y., Uetake, C., Kato, K., Kato, T., Takahashi, M., Fukuda, N. N., Murakami, S., Miyauchi, E., Hino, S., Atarashi, K., Onawa, S., Fujimura, Y., Lockett, T., Clarke, J. M., Topping, D. L., Tomita, M., Hori, S., Ohara, O., Morita, T., Koseki, H., Kikuchi, J., Honda, K., Hase, K., and Ohno, H., 2013. Commensal microbe-derived butyrate induces the differentiation of colonic regulatory T cells. *Nature*, 504 (7480), 446–450.

Futterer, A., Mink, K., Luz, A., Kosco-Vilbois, M. H., and Pfeffer, K., 1998. The lymphotoxin beta receptor controls organogenesis and affinity maturation in peripheral lymphoid tissues. *Immunity*, 9 (1), 59–70.

Gagliani, N., Palm, N. W., de Zoete, M. R., and Flavell, R. A., 2014. Inflammasomes and intestinal homeostasis: regulating and connecting infection, inflammation and the microbiota. *International Immunology*, 26 (9), 495–499.

Gagnon, E., Schubert, D. A., Gordo, S., Chu, H. H., and Wucherpfennig, K. W., 2012. Local changes in lipid environment of TCR microclusters regulate membrane binding by the CD3ε cytoplasmic domain. *The Journal of Experimental Medicine*, 209 (13), 2423–2439.

Gantois, I., Ducatelle, R., Pasmans, F., Haesebrouck, F., Hautefort, I., Thompson, A., Hinton, J. C., and Van Immerseel, F., 2006. Butyrate specifically down-regulates *Salmonella* pathogenicity island 1 gene expression. *Applied and Environmental Microbiology*, 72 (1), 946–949.

Gatto, D., Wood, K., Caminschi, I., Murphy-Durland, D., Schofield, P., Christ, D., Karupiah, G., and Brink, R., 2013. The chemotactic receptor EBI2 regulates the homeostasis, localization and immunological function of splenic dendritic cells. *Nature Immunology*, 14 (5), 446–453.

Gerbe, F., Sidot, E., Smyth, D. J., Ohmoto, M., Matsumoto, I., Dardalhon, V., Cesses, P., Garnier, L., Pouzolles, M., Brulin, B., Bruschi, M., Harcus, Y., Zimmermann, V. S., Taylor, N., Maizels, R. M., and Jay, P., 2016. Intestinal epithelial tuft cells initiate type 2 mucosal immunity to helminth parasites. *Nature*, 529 (7585), 226–230.

Gewirtz, A. T., Siber, A. M., Madara, J. L., and McCormick, B. A., 1999. Orchestration of neutrophil movement by intestinal epithelial cells in response to *Salmonella* Typhimurium can be uncoupled from bacterial internalization. *Infection and Immunity*, 67 (2), 608–617.

Ghoreschi, K., Laurence, A., Yang, X.-P., Tato, C. M., McGeachy, M. J., Konkel, J. E., Ramos, H. L., Wei, L., Davidson, T. S., Bouladoux, N., Grainger, J. R., Chen, Q., Kanno, Y., Watford, W. T., Sun, H.-W., Eberl, G., Shevach, E. M., Belkaid, Y., Cua, D. J., Chen, W., and O'Shea, J. J., 2010. Generation of pathogenic T(H)17 cells in the absence of TGFbeta signalling. *Nature*, 467 (7318), 967–971.

Ginhoux, F., Liu, K., Helft, J., Bogunovic, M., Greter, M., Hashimoto, D., Price, J., Yin, N., Bromberg, J., Lira, S. A., Stanley, E. R., Nussenzweig, M., and Merad, M., 2009. The origin and development of nonlymphoid tissue CD103+ DCs. *The Journal of Experimental Medicine*, 206 (13), 3115–3130.

Girard, J.-P., Moussion, C., and Förster, R., 2012. HEVs, lymphatics and homeostatic immune cell trafficking in lymph nodes. *Nature Reviews Immunology*, 12 (11), 762–773.

Glasser, A.-L., Boudeau, J., Barnich, N., Perruchot, M.-H., Colombel, J.-F., and Darfeuille-Michaud, A., 2001. Adherent invasive *Escherichia coli* strains from patients with Crohn's disease survive and replicate within macrophages without inducing host cell death. *Infection and Immunity*, 69 (9), 5529–5537.

Glocker, E.-O., Kotlarz, D., Boztug, K., Gertz, E. M., Schaffer, A. A., Noyan, F., Perro, M., Diestelhorst, J., Allroth, A., Murugan, D., Hatscher, N., Pfeifer, D., Sykora, K.-W., Sauer, M., Kreipe, H., Lacher, M., Nustede, R., Woellner, C., Baumann, U., Salzer, U., et al., 2009. Inflammatory bowel disease and mutations affecting the interleukin-10 receptor. *New England Journal of Medicine*, 361 (21), 2033–2045.

Goetz, D. H., Holmes, M. A., Borregaard, N., Bluhm, M. E., Raymond, K. N., and Strong, R. K., 2002. The neutrophil lipocalin NGAL is a bacteriostatic agent that interferes with siderophore-mediated iron acquisition. *Molecular Cell*, 10 (5), 1033–1043.

Gomez Perdiguero, E., Klapproth, K., Schulz, C., Busch, K., Azzoni, E., Crozet, L., Garner, H., Trouillet, C., de Bruijn, M. F., Geissmann, F., and Rodewald, H.-R., 2015. Tissue-resident macrophages originate from yolk-sac-derived erythro-myeloid progenitors. *Nature*, 518 (7540), 547–551.

Gophna, U., Sommerfeld, K., Gophna, S., Doolittle, W. F., and Veldhuyzen van Zanten, S. J. O., 2006. Differences between tissue-associated intestinal microfloras of patients with Crohn's disease and ulcerative colitis. *Journal of Clinical Microbiology*, 44 (11), 4136–4141.

Green, D. R., Ferguson, T., Zitvogel, L., and Kroemer, G., 2009. Immunogenic and tolerogenic cell death. *Nature Reviews Immunology*, 9 (5), 353–363.

Griffin, A. J. and McSorley, S. J., 2011. Development of protective immunity to *Salmonella*, a mucosal pathogen with a systemic agenda. *Mucosal Immunology*, 4 (4), 371–382.

Griffin, G. K., Newton, G., Tarrio, M. L., Bu, D.-X., Maganto-Garcia, E., Azcutia, V., Alcaide, P., Grabie, N., Luscinskas, F. W., Croce, K. J., and Lichtman, A. H., 2012. IL-17 and TNFα Sustain Neutrophil Recruitment During Inflammation Through Synergistic Effects on Endothelial Activation. *The Journal of Immunology*, 188 (12), 6287–6299.

Griseri, T., Arnold, I. C., Pearson, C., Krausgruber, T., Schiering, C., Franchini, F., Schulthess, J., McKenzie, B. S., Crocker, P. R., and Powrie, F., 2015. Granulocyte macrophage colony-stimulating factor-activated eosinophils promote interleukin-23 driven chronic colitis. *Immunity*, 43 (1), 187–199.

Gu, S., Chen, D., Zhang, J.-N., Lv, X., Wang, K., Duan, L.-P., Nie, Y., and Wu, X.-L., 2013. Bacterial community mapping of the mouse gastrointestinal tract. *PLoS ONE*, 8 (10), e74957.

Gu, Y., Forostyan, T., Sabbadini, R., and Rosenblatt, J., 2011. Epithelial cell extrusion requires the sphingosine-1-phosphate receptor 2 pathway. *The Journal of Cell Biology*, 193 (4), 667–676.

Guilliams, M., Dutertre, C.-A., Scott, C. L., McGovern, N., Sichien, D., Chakarov, S., Van Gassen, S., Chen, J., Poidinger, M., De Prijck, S., Tavernier, S. J., Low, I., Irac, S. E., Mattar, C. N., Sumatoh, H. R., Low, G. H. L., Chung, T. J. K., Chan, D. K. H., Tan, K. K., Hon, T. L. K., et al., 2016. Unsupervised high-dimensional analysis aligns dendritic cells across tissues and species. *Immunity*, 45 (3), 669–684.

Guilliams, M., Ginhoux, F., Jakubzick, C., Naik, S. H., Onai, N., Schraml, B. U., Segura, E., Tussiwand, R., and Yona, S., 2014. Dendritic cells, monocytes and macrophages: a unified nomenclature based on ontogeny. *Nature Reviews Immunology*, 14 (8), 571–578.

Gunn, M. D., Tangemann, K., Tam, C., Cyster, J. G., Rosen, S. D., and Williams, L. T., 1998. A chemokine expressed in lymphoid high endothelial venules promotes the adhesion and chemotaxis of naive T lymphocytes. *Proceedings of the National Academy of Sciences*, 95 (1), 258–263.

Guttman, J. A., Li, Y., Wickham, M. E., Deng, W., Vogl, A. W., and Finlay, B. B., 2006. Attaching and effacing pathogen-induced tight junction disruption *in vivo*. *Cellular Microbiology*, 8 (4), 634–645.

Guttman, J. A., Samji, F. N., Li, Y., Vogl, A. W., and Finlay, B. B., 2006. Evidence that tight junctions are disrupted due to intimate bacterial contact and not inflammation during attaching and effacing pathogen infection *in vivo*. *Infection and Immunity*, 74 (11), 6075–6084.

Haan, den, J. M., Lehar, S. M., and Bevan, M. J., 2000. CD8(+) but not CD8(-) dendritic cells cross-prime cytotoxic T cells *in vivo*. *Journal of Experimental Medicine*, 192 (12), 1685–1696.

Hadis, U., Wahl, B., Schulz, O., Hardtke-Wolenski, M., Schippers, A., Wagner, N., Mueller, W., Sparwasser, T., Foerster, R., and Pabst, O., 2011. Intestinal tolerance requires gut homing and expansion of FoxP3(+) regulatory T cells in the lamina propria. *Immunity*, 34 (2), 237–246.

Hägerbrand, K., Westlund, J., Yrlid, U., Agace, W., and Johansson-Lindbom, B., 2015. MyD88 signaling regulates steady-state migration of intestinal CD103+ dendritic cells independently of TNF-α and the gut microbiota. *The Journal of Immunology*, 195 (6), 2888–2899.

Hagiwara, C., Tanaka, M., and Kudo, H., 2002. Increase in colorectal epithelial apoptotic cells in patients with ulcerative colitis ultimately requiring surgery. *Journal of Gastroenterology and Hepatology*, 17 (7), 758–764.

Hall, P. A., Coates, P. J., Ansari, B., and Hopwood, D., 1994. Regulation of cell number in the mammalian gastrointestinal tract: the importance of apoptosis. *Journal of Cell Science*, 107 (Pt 12), 3569–3577.

Halle, S., Bumann, D., Herbrand, H., Willer, Y., Dahne, S., Förster, R., and Pabst, O., 2007. Solitary intestinal lymphoid tissue provides a productive port of entry for *Salmonella enterica* serovar Typhimurium. *Infection and Immunity*, 75 (4), 1577–1585.

Hamann, A., Andrew, D. P., Jablonski-Westrich, D., Holzmann, B., and Butcher, E. C., 1994. Role of alpha 4-integrins in lymphocyte homing to mucosal tissues *in vivo*. *Journal of Immunology*, 152 (7), 3282–3293.

Hammerschmidt, S. I., Ahrendt, M., Bode, U., Wahl, B., Kremmer, E., Förster, R., and Pabst, O., 2008. Stromal mesenteric lymph node cells are essential for the generation of gut-homing T cells *in vivo*. *The Journal of Experimental Medicine*, 205 (11), 2483–2490.

Han, H., Iwanaga, T., Uchiyama, Y., and Fujita, T., 1993. Aggregation of macrophages in the tips of intestinal villi in guinea pigs: their possible role in the phagocytosis of effete epithelial cells. *Cell and Tissue Reseach*, 271 (3), 407–416.

Harrington, S. M., Sheikh, J., Henderson, I. R., Ruiz-Perez, F., Cohen, P. S., and Nataro, J. P., 2009. The Pic protease of enteroaggregative *Escherichia coli* promotes intestinal colonization and growth in the presence of mucin. *Infection and Immunity*, 77 (6), 2465–2473.

Hartland, E. L., Batchelor, M., Delahay, R. M., Hale, C., Matthews, S., Dougan, G., Knutton, S., Connerton, I., and Frankel, G., 1999. Binding of intimin from enteropathogenic *Escherichia coli* to Tir and to host cells. *Molecular Microbiology*, 32 (1), 151–158.

Hase, K., Kawano, K., Nochi, T., Pontes, G. S., Fukuda, S., Ebisawa, M., Kadokura, K., Tobe, T., Fujimura, Y., Kawano, S., Yabashi, A., Waguri, S., Nakato, G., Kimura, S., Murakami, T., Iimura, M., Hamura, K., Fukuoka, S., Lowe, A. W., Itoh, K., Kiyono, H., and Ohno, H., 2009. Uptake through glycoprotein 2 of FimH(+) bacteria by M cells initiates mucosal immune response. *Nature*, 462 (7270), 226–230.

Hashimoto, D., Chow, A., Noizat, C., Teo, P., Beasley, M. B., Leboeuf, M., Becker, C. D., See, P., Price, J., Lucas, D., Greter, M., Mortha, A., Boyer, S. W., Forsberg, E. C., Tanaka, M., Van Rooijen, N., Garcia-Sastre, A., Stanley, E. R., Ginhoux, F., Frenette, P. S., and Merad, M., 2013. Tissue-resident macrophages self-maintain locally throughout adult life with minimal contribution from circulating monocytes. *Immunity*, 38 (4), 792–804.

He, G., Shankar, R. A., Chzhan, M., Samouilov, A., Kuppusamy, P., and Zweier, J. L., 1999. Noninvasive measurement of anatomic structure and intraluminal oxygenation in the gastrointestinal tract of living mice with spatial and spectral EPR imaging. *Proceedings of the National Academy of Sciences*, 96 (8), 4586–4591.

Heink, S., Yogev, N., Garbers, C., Herwerth, M., Aly, L., Gasperi, C., Husterer, V., Croxford, A. L., Moller-Hackbarth, K., Bartsch, H. S., Sotlar, K., Krebs, S., Regen, T., Blum, H., Hemmer, B., Misgeld, T., Wunderlich, T. F., Hidalgo, J., Oukka, M., Rose-John, S., Schmidt-Supprian, M., Waisman, A., and Korn, T., 2017. Trans-presentation of IL-6 by dendritic cells is required for the priming of pathogenic TH17 cells. *Nature Immunology*, 18 (1), 74–85.

Heitmann, L., Rani, R., Dawson, L., Perkins, C., Yang, Y., Downey, J., Hölscher, C., and Herbert, D. R., 2012. TGFbeta-responsive myeloid cells suppress type 2 immunity and emphysematous pathology after hookworm infection. *The American Journal of Pathology*, 181 (3), 897–906.

Helft, J., Böttcher, J., Chakravarty, P., Zelenay, S., Huotari, J., Schraml, B. U., Goubau, D., and Reis e Sousa, C., 2015. GM-CSF mouse bone marrow cultures comprise a heterogeneous population of CD11c+ MHCII+ macrophages and dendritic cells. *Immunity*, 42 (6), 1197–1211.

Hemrajani, C., Berger, C. N., Robinson, K. S., Marches, O., Mousnier, A., and Frankel, G., 2010. NleH effectors interact with Bax inhibitor-1 to block apoptosis during enteropathogenic *Escherichia coli* infection. *Proceedings of the National Academy of Sciences*, 107 (7), 3129–3134.

Hersh, D., Monack, D. M., Smith, M. R., Ghori, N., Falkow, S., and Zychlinsky, A., 1999. The *Salmonella* invasin SipB induces macrophage apoptosis by binding to caspase-1. *Proceedings of the National Academy of Sciences*, 96 (5), 2396–2401.

Higgins, L. M., Frankel, G., Douce, G., Dougan, G., and MacDonald, T. T., 1999. *Citrobacter rodentium* infection in mice elicits a mucosal Th1 cytokine response and lesions similar to those in murine inflammatory bowel disease. *Infection and Immunity*, 67 (6), 3031–3039.

Hildner, K., Edelson, B. T., Purtha, W. E., Diamond, M., Matsushita, H., Kohyama, M., Calderon, B., Schraml, B. U., Unanue, E. R., Diamond, M. S., Schreiber, R. D., Murphy, T. L., and Murphy, K. M., 2008. Batf3 deficiency reveals a critical role for CD8alpha+ dendritic cells in cytotoxic T cell immunity. *Science*, 322 (5904), 1097–1100.

Hilligan, K. L., Connor, L. M., Schmidt, A. J., and Ronchese, F., 2016. Activation-induced TIM-4 expression identifies differential responsiveness of intestinal CD103+ CD11b+ dendritic cells to a mucosal adjuvant. *PLoS ONE*, 11 (7), e0158775.

Hlavaty, T., Pierik, M., Henckaerts, L., Ferrante, M., Joossens, S., van Schuerbeek, N., Noman, M., Rutgeerts, P., and Vermeire, S., 2005. Polymorphisms in apoptosis genes predict response to infliximab therapy in luminal and fistulizing Crohn's disease. *Alimentary Pharmacology and Therapeutics*, 22 (7), 613–626.

Hobbie, S., Chen, L. M., Davis, R. J., and Galan, J. E., 1997. Involvement of mitogen-activated protein kinase pathways in the nuclear responses and cytokine production induced by *Salmonella* Typhimurium in cultured intestinal epithelial cells. *Journal of Immunology*, 159 (11), 5550–5559.

Hong, P.-Y., Croix, J. A., Greenberg, E., Gaskins, H. R., and Mackie, R. I., 2011. Pyrosequencing-based analysis of the mucosal microbiota in healthy individuals reveals ubiquitous bacterial groups and micro-heterogeneity. *PLoS ONE*, 6 (9), e25042.

Hormann, N., Brandao, I., Jackel, S., Ens, N., Lillich, M., Walter, U., and Reinhardt, C., 2014. Gut microbial colonization orchestrates TLR2 expression, signaling and epithelial proliferation in the small intestinal mucosa. *PLoS ONE*, 9 (11), e113080.

Houston, S. A., Cerovic, V., Thomson, C., Brewer, J., Mowat, A. M., and Milling, S., 2016. The lymph nodes draining the small intestine and colon are anatomically separate and immunologically distinct. *Mucosal Immunology*, 9 (2), 468–478.

Hoyler, T., Klose, C. S. N., Souabni, A., Turqueti-Neves, A., Pfeifer, D., Rawlins, E. L., Voehringer, D., Busslinger, M., and Diefenbach, A., 2012. The transcription factor GATA-3 controls cell fate and maintenance of type 2 innate lymphoid cells. *Immunity*, 37 (4), 634–648.

Huang, F. P., Platt, N., Wykes, M., Major, J. R., Powell, T. J., Jenkins, C. D., and MacPherson, G. G., 2000. A discrete subpopulation of dendritic cells transports apoptotic intestinal epithelial cells to T cell areas of mesenteric lymph nodes. *Journal of Experimental Medicine*, 191 (3), 435–444.

Huang, J. Y., Lee, S. M., and Mazmanian, S. K., 2011. The human commensal *Bacteroides fragilis* binds intestinal mucin. *Anaerobe*, 17 (4), 137–141.

Hulme, H. E., Meikle, L. M., Wessel, H., Strittmatter, N., Swales, J., Thomson, C., Nilsson, A., Nibbs, R. J. B., Milling, S., Andren, P. E., Mackay, C. L., Dexter, A., Bunch, J., Goodwin, R. J. A., Burchmore, R., and Wall, D. M., 2017. Mass spectrometry imaging identifies palmitoylcarnitine as an immunological mediator during *Salmonella* Typhimurium infection. *Scientific Reports*, 7 (1), 2786.

Huppa, J. B. and Davis, M. M., 2003. T-cell-antigen recognition and the immunological synapse. *Nature Reviews Immunology*, 3 (12), 973–983.

Ichimura, T., Bonventre, J. V., Bailly, V., Wei, H., Hession, C. A., Cate, R. L., and Sanicola, M., 1998. Kidney injury molecule-1 (KIM-1), a putative epithelial cell adhesion molecule containing a novel immunoglobulin domain, is up-regulated in renal cells after injury. *Journal of Biological Chemistry*, 273 (7), 4135–4142.

Ihara, S., Hirata, Y., Serizawa, T., Suzuki, N., Sakitani, K., Kinoshita, H., Hayakawa, Y., Nakagawa, H., Ijichi, H., Tateishi, K., and Koike, K., 2016. TGFbeta signaling in dendritic cells governs colonic homeostasis by controlling epithelial differentiation and the luminal microbiota. *Journal of Immunology*, 196 (11), 4603–4613.

Inohara, N., Ogura, Y., Chen, F. F., Muto, A., and Nuñez, G., 2001. Human Nod1 confers responsiveness to bacterial lipopolysaccharides. *Journal of Biological Chemistry*, 276 (4), 2551–2554.

Ivanov, I. I., Atarashi, K., Manel, N., Brodie, E. L., Shima, T., Karaoz, U., Wei, D., Goldfarb, K. C., Santee, C. A., Lynch, S. V., Tanoue, T., Imaoka, A., Itoh, K., Takeda, K., Umesaki, Y., Honda, K., and Littman, D. R., 2009. Induction of intestinal Th17 cells by segmented filamentous bacteria. *Cell*, 139 (3), 485–498.

Iwamoto, M., Koji, T., Makiyama, K., Kobayashi, N., and Nakane, P. K., 1996. Apoptosis of crypt epithelial cells in ulcerative colitis. *The Journal of Pathology*, 180 (2), 152–159.

Iwanaga, T., Han, H., Adachi, K., and Fujita, T., 1993. A novel mechanism for disposing of effete epithelial cells in the small intestine of guinea pigs. *Gastroenterology*, 105 (4), 1089–1097.

Iwata, M., Hirakiyama, A., Eshima, Y., Kagechika, H., Kato, C., and Song, S. Y., 2004. Retinoic acid imprints gut-homing specificity on T cells. *Immunity*, 21 (4), 527–538.

Iyoda, T., Shimoyama, S., Liu, K., Omatsu, Y., Akiyama, Y., Maeda, Y., Takahara, K., Steinman, R. M., and Inaba, K., 2002. The CD8+ dendritic cell subset selectively endocytoses dying cells in culture and *in vivo*. *Journal of Experimental Medicine*, 195 (10), 1289–1302.

Jaensson, E., Uronen-Hansson, H., Pabst, O., Eksteen, B., Tian, J., Coombes, J. L., Berg, P.-L., Davidsson, T., Powrie, F., Johansson-Lindbom, B., and Agace, W. W., 2008. Small intestinal CD103(+) dendritic cells display unique functional properties that are conserved between mice and humans. *Journal of Experimental Medicine*, 205 (9), 2139–2149.

Jang, M. H., Sougawa, N., Tanaka, T., Hirata, T., Hiroi, T., Tohya, K., Guo, Z., Umemoto, E., Ebisuno, Y., Yang, B.-G., Seoh, J.-Y., Lipp, M., Kiyono, H., and Miyasaka, M., 2006. CCR7 is critically important for migration of dendritic cells in intestinal lamina propria to mesenteric lymph nodes. *Journal of Immunology*, 176 (2), 803–810.

Jarvis, K. G., Giron, J. A., Jerse, A. E., McDaniel, T. K., Donnenberg, M. S., and Kaper, J. B., 1995. Enteropathogenic *Escherichia coli* contains a putative type III secretion system necessary for the export of proteins involved in attaching and effacing lesion formation. *Proc Natl Acad Sci U S A*, 92 (17), 7996–8000.

Jepson, M. A., Clark, M. A., Simmons, N. L., and Hirst, B. H., 1993. Actin accumulation at sites of attachment of indigenous apathogenic segmented filamentous bacteria to mouse ileal epithelial cells. *Infection and Immunity*, 61 (9), 4001–4004.

Ji, H., Liu, Y., Zhang, Y., Shen, X.-D., Gao, F., Busuttil, R. W., Kuchroo, V. K., and Kupiec-Weglinski, J. W., 2014. T-cell immunoglobulin and mucin domain 4 (TIM-4) signaling in innate immune-mediated liver ischemia-reperfusion injury. *Hepatology*, 60 (6), 2052–2064.

Jin, U.-H., Lee, S.-O., Sridharan, G., Lee, K., Davidson, L. A., Jayaraman, A., Chapkin, R. S., Alaniz, R., and Safe, S., 2014. Microbiome-derived tryptophan metabolites and their aryl hydrocarbon receptor-dependent agonist and antagonist activities. *Molecular Pharmacology*, 85 (5), 777–788.

Johansson, M. E. V., Phillipson, M., Petersson, J., Velcich, A., Holm, L., and Hansson, G. C., 2008. The inner of the two Muc2 mucin-dependent mucus layers in colon is devoid of bacteria. *Proceedings of the National Academy of Sciences*, 105 (39), 15064–15069.

Jones, B. D., Ghori, N., and Falkow, S., 1994. *Salmonella* Typhimurium initiates murine infection by penetrating and destroying the specialized epithelial M cells of the Peyer's patches. *Journal of Experimental Medicine*, 180 (1), 15–23.

Jostins, L., Ripke, S., Weersma, R. K., Duerr, R. H., McGovern, D. P., Hui, K. Y., Lee, J. C., Schumm, L. P., Sharma, Y., Anderson, C. A., Essers, J., Mitrovic, M., Ning, K., Cleynen, I., Theatre, E., Spain, S. L., Raychaudhuri, S., Goyette, P., Wei, Z., Abraham, C., et al., 2012. Host-microbe interactions have shaped the genetic architecture of inflammatory bowel disease. *Nature*, 491 (7422), 119–124.

Ju, X.-S., Ruau, D., Jantti, P., Sere, K., Becker, C., Wiercinska, E., Bartz, C., Erdmann, B., Dooley, S., and Zenke, M., 2007. Transforming growth factor beta1 up-regulates interferon regulatory factor 8 during dendritic cell development. *European Journal of Immunology*, 37 (5), 1174–1183.

Kaech, S. M. and Wherry, E. J., 2007. Heterogeneity and cell-fate decisions in effector and memory CD8+ T cell differentiation during viral infection. *Immunity*, 27 (3), 393–405.

Kamada, N., Hisamatsu, T., Honda, H., Kobayashi, T., Chinen, H., Kitazume, M. T., Takayama, T., Okamoto, S., Koganei, K., Sugita, A., Kanai, T., and Hibi, T., 2009. Human CD14+ macrophages in intestinal lamina propria exhibit potent antigen-presenting ability. *Journal of Immunology*, 183 (3), 1724–1731.

Kamada, N., Kim, Y.-G., Sham, H. P., Vallance, B. A., Puente, J. L., Martens, E. C., and Nuñez, G., 2012. Regulated virulence controls the ability of a pathogen to compete with the gut microbiota. *Science*, 336 (6086), 1325–1329.

Kaplan, M. H., Schindler, U., Smiley, S. T., and Grusby, M. J., 1996. Stat6 is required for mediating responses to IL-4 and for development of Th2 cells. *Immunity*, 4 (3), 313–319.

Kaser, A., Lee, A.-H., Franke, A., Glickman, J. N., Zeissig, S., Tilg, H., Nieuwenhuis, E. E. S., Higgins, D. E., Schreiber, S., Glimcher, L. H., and Blumberg, R. S., 2008. XBP1 inks ER stress to intestinal inflammation and confers genetic risk for human inflammatory bowel disease. *Cell*, 134 (5), 743–756.

Kashiwagi, I., Morita, R., Schichita, T., Komai, K., Saeki, K., Matsumoto, M., Takeda, K., Nomura, M., Hayashi, A., Kanai, T., and Yoshimura, A., 2015. Smad2 and Smad3 inversely regulate TGFbeta autoinduction in *Clostridium butyricum*-activated dendritic cells. *Immunity*, 43 (1), 65–79.

Kato, H., Sato, S., Yoneyama, M., Yamamoto, M., Uematsu, S., Matsui, K., Tsujimura, T., Takeda, K., Fujita, T., Takeuchi, O., and Akira, S., 2005. Cell type-specific involvement of RIG-I in antiviral response. *Immunity*, 23 (1), 19–28.

Kel, J. M., Girard-Madoux, M. J. H., Reizis, B., and Clausen, B. E., 2010. TGFbeta is required to maintain the pool of immature Langerhans cells in the epidermis. *Journal of Immunology*, 185 (6), 3248–3255.

Khademi, M., Illes, Z., Gielen, A. W., Marta, M., Takazawa, N., Baecher-Allan, C., Brundin, L., Hannerz, J., Martin, C., Harris, R. A., Hafler, D. A., Kuchroo, V. K., Olsson, T., Piehl, F., and Wallstrom, E., 2004. T Cell Ig- and mucin-domain-containing molecule-3 (TIM-3) and TIM-1 molecules are differentially expressed on human Th1 and Th2 cells and in cerebrospinal fluid-derived mononuclear cells in multiple sclerosis. *Journal of Immunology*, 172 (11), 7169–7176.

Kim, B.-H., Shenoy, A. R., Kumar, P., Bradfield, C. J., and MacMicking, J. D., 2012. IFN-inducible GTPases in host cell defense. *Cell Host and Microbe*, 12 (4), 432–444.

Kim, J. M., Eckmann, L., Savidge, T. C., Lowe, D. C., Witthöft, T., and Kagnoff, M. F., 1998. Apoptosis of human intestinal epithelial cells after bacterial invasion. *The Journal of Clinical Investigation*, 102 (10), 1815–1823.

Kim, M., Ashida, H., Ogawa, M., Yoshikawa, Y., Mimuro, H., and Sasakawa, C., 2010. Bacterial interactions with the host epithelium. *Cell Host and Microbe*, 8 (1), 20–35.

Kim, S. V., Xiang, W. V., Kwak, C., Yang, Y., Lin, X. W., Ota, M., Sarpel, U., Rifkin, D. B., Xu, R., and Littman, D. R., 2013. GPR15-mediated homing controls immune homeostasis in the large intestine mucosa. *Science*, 340 (6139), 1456–1459.

Kimura, S., Yamakami-Kimura, M., Obata, Y., Hase, K., Kitamura, H., Ohno, H., and Iwanaga, T., 2014. Visualization of the entire differentiation process of murine M cells: suppression of their maturation in cecal patches. *Mucosal Immunology*, 8 (3), 650-660.

Kinchen, J. M. and Ravichandran, K. S., 2008. Phagosome maturation: going through the acid test. *Nature Reviews Molecular Cell Biology*, 9 (10), 781–795.

Kinoshita, M., Suzuki, Y., and Saito, Y., 2002. Butyrate reduces colonic paracellular permeability by enhancing PPARgamma activation. *Biochemical and Biophysical Research Communications*, 293 (2), 827–831.

Kiss, E. A., Vonarbourg, C., Kopfmann, S., Hobeika, E., Finke, D., Esser, C., and Diefenbach, A., 2011. Natural aryl hydrocarbon receptor ligands control organogenesis of intestinal lymphoid follicles. *Science*, 334 (6062), 1561–1565.

Klebanoff, C. A., Spencer, S. P., Torabi-Parizi, P., Grainger, J. R., Roychoudhuri, R., Ji, Y., Sukumar, M., Muranski, P., Scott, C. D., Hall, J. A., Ferreyra, G. A., Leonardi, A. J., Borman, Z. A., Wang, J., Palmer, D. C., Wilhelm, C., Cai, R., Sun, J., Napoli, J. L., Danner, R. L., Gattinoni, L., Belkaid, Y., and Restifo, N. P., 2013. Retinoic acid controls the homeostasis of pre-cDC-derived splenic and intestinal dendritic cells. *Journal of Experimental Medicine*, 210 (10), 1961–1976.

Kleinclauss, F., Perruche, S., Masson, E., de Carvalho Bittencourt, M., Biichle, S., Remy-Martin, J.-P., Ferrand, C., Martin, M., Bittard, H., Chalopin, J.-M., Seilles, E., Tiberghien, P., and Saas, P., 2006. Intravenous apoptotic spleen cell infusion induces a TGFbeta-dependent regulatory T-cell expansion. *Cell Death and Differentiation*, 13 (1), 41–52.

Knodler, L. A., Finlay, B. B., and Steele-Mortimer, O., 2005. The *Salmonella* effector protein SopB protects epithelial cells from apoptosis by sustained activation of Akt. *Journal of Biological Chemistry*, 280 (10), 9058–9064.

Knodler, L. A., Vallance, B. A., Celli, J., Winfree, S., Hansen, B., Montero, M., and Steele-Mortimer, O., 2010. Dissemination of invasive Salmonella via bacterial-induced extrusion of mucosal epithelia. *Proceedings of the National Academy of Sciences*, 107 (41), 17733–17738.

Knoop, K. A., McDonald, K. G., Kulkarni, D. H., and Newberry, R. D., 2015. Antibiotics promote inflammation through the translocation of native commensal colonic bacteria. *Gut* 65 (7), 1100-1109

Kobayashi, N., Karisola, P., Pena-Cruz, V., Dorfman, D. M., Jinushi, M., Umetsu, S. E., Butte, M. J., Nagumo, H., Chernova, I., Zhu, B., Sharpe, A. H., Ito, S., Dranoff, G., Kaplan, G. G., Casasnovas, J. M., Umetsu, D. T., Dekruyff, R. H., and Freeman, G. J., 2007. TIM-1 and TIM-4 glycoproteins bind phosphatidylserine and mediate uptake of apoptotic cells. *Immunity*, 27 (6), 927–940.

Kontoyiannis, D., Pasparakis, M., Pizarro, T. T., Cominelli, F., and Kollias, G., 1999. Impaired on/off regulation of TNF biosynthesis in mice lacking TNF AU-rich elements: implications for joint and gut-associated immunopathologies. *Immunity*, 10 (3), 387–398.

Kraal, G., Breel, M., Janse, M., and Bruin, G., 1986. Langerhans' cells, veiled cells, and interdigitating cells in the mouse recognized by a monoclonal antibody. *The Journal of Experimental Medicine*, 163 (4), 981–997.

Kuchroo, V. K., Umetsu, D. T., Dekruyff, R. H., and Freeman, G. J., 2003. The TIM gene family: emerging roles in immunity and disease. *Nature Reviews Immunology*, 3 (6), 454–462.

Kullberg, M. C., Jankovic, D., Feng, C. G., Hue, S., Gorelick, P. L., McKenzie, B. S., Cua, D. J., Powrie, F., Cheever, A. W., Maloy, K. J., and Sher, A., 2006. IL-23 plays a key role in *Helicobacter hepaticus*–induced T cell–dependent colitis. *The Journal of Experimental Medicine*, 203 (11), 2485–2494.

Kullberg, M. C., Ward, J. M., Gorelick, P. L., Caspar, P., Hieny, S., Cheever, A., Jankovic, D., and Sher, A., 1998. *Helicobacter hepaticus* triggers colitis in specific-pathogen-free interleukin-10 (IL-10)-deficient mice through an IL-12- and gamma interferon-dependent mechanism. *Infection and Immunity*, 66 (11), 5157–5166.

Kum, W. W. S., Lo, B. C., Yu, H. B., and Finlay, B. B., 2011. Protective role of Akt2 in *Salmonella enterica* serovar Typhimurium-induced gastroenterocolitis. *Infection and Immunity*, 79 (7), 2554–2566.

Kunisawa, J., Gohda, M., Hashimoto, E., Ishikawa, I., Higuchi, M., Suzuki, Y., Goto, Y., Panea, C., Ivanov, I. I., Sumiya, R., Aayam, L., Wake, T., Tajiri, S., Kurashima, Y., Shikata, S., Akira, S., Takeda, K., and Kiyono, H., 2013. Microbe-dependent CD11b+ IgA+ plasma cells mediate robust early-phase intestinal IgA responses in mice. *Nature Communications*, 4, 1772.

Kunkel, E. J., Campbell, J. J., Haraldsen, G., Pan, J., Boisvert, J., Roberts, A. I., Ebert, E. C., Vierra, M. A., Goodman, S. B., Genovese, M. C., Wardlaw, A. J., Greenberg, H. B., Parker, C. M., Butcher, E. C., Andrew, D. P., and Agace, W. W., 2000. Lymphocyte CC chemokine receptor 9 and epithelial thymus-expressed chemokine (TECK) expression distinguish the small intestinal immune compartment: Epithelial expression of tissue-specific chemokines as an organizing principle in regional immunity. *Journal of Experimental Medicine*, 192 (5), 761–768.

Kunkel, E. J., Kim, C. H., Lazarus, N. H., Vierra, M. A., Soler, D., Bowman, E. P., and Butcher, E. C., 2003. CCR10 expression is a common feature of circulating and mucosal epithelial tissue IgA Ab-secreting cells. *The Journal of Clinical Investigation*, 111 (7), 1001–1010.

Kushwah, R., Oliver, J. R., Zhang, J., Siminovitch, K. A., and Hu, J., 2009. Apoptotic dendritic cells induce tolerance in mice through suppression of dendritic cell maturation and induction of antigen-specific regulatory T cells. *The Journal of Immunology*, 183 (11), 7104–7118.

Kwon, J. H., 2002. Colonic epithelial cells are a major site of macrophage inflammatory protein 3alpha (MIP-3alpha) production in normal colon and inflammatory bowel disease. *Gut*, 51 (6), 818–826.

la Fuente, De, M., Franchi, L., Araya, D., Díaz-Jiménez, D., Olivares, M., Álvarez-Lobos, M., Golenbock, D., González, M.-J., López-Kostner, F., Quera, R., Nuñez, G., Vidal, R., and Hermoso, M. A., 2014. *Escherichia coli* isolates from inflammatory bowel diseases patients survive in macrophages and activate NLRP3 inflammasome. *International Journal of Medical Microbiology*, 304 (3–4), 384–392.

Lahdeniemi, I. A. K., Misiorek, J. O., Antila, C. J. M., Landor, S. K.-J., Stenvall, C.-G. A., Fortelius, L. E., Bergstrom, L. K., Sahlgren, C., and Toivola, D. M., 2017. Keratins regulate colonic epithelial cell differentiation through the Notch1 signalling pathway. *Cell Death and Differentiation*, 24 (6), 984–996.

Lamas, B., Richard, M. L., Leducq, V., Pham, H.-P., Michel, M.-L., Da Costa, G., Bridonneau, C., Jegou, S., Hoffmann, T. W., Natividad, J. M., Brot, L., Taleb, S., Couturier-Maillard, A., Nion-Larmurier, I., Merabtene, F., Seksik, P., Bourrier, A., Cosnes, J., Ryffel, B., Beaugerie, L., Launay, J.-M., Langella, P., Xavier, R. J., and Sokol, H., 2016. CARD9 impacts colitis by altering gut microbiota metabolism of tryptophan into aryl hydrocarbon receptor ligands. *Nature Medicine*, 22 (6), 598-605.

Lämmermann, T., Bader, B. L., Monkley, S. J., Worbs, T., Wedlich-Soldner, R., Hirsch, K., Keller, M., Förster, R., Critchley, D. R., Fassler, R., and Sixt, M., 2008. Rapid leukocyte migration by integrin-independent flowing and squeezing. *Nature*, 453 (7191), 51–55.

Lassen, K. G., Kuballa, P., Conway, K. L., Patel, K. K., Becker, C. E., Peloquin, J. M., Villablanca, E. J., Norman, J. M., Liu, T.-C., Heath, R. J., Becker, M. L., Fagbami, L., Horn, H., Mercer, J., Yilmaz, O. H., Jaffe, J. D., Shamji, A. F., Bhan, A. K., Carr, S. A., Daly, M. J., Virgin, H. W., Schreiber, S. L., Stappenbeck, T. S., and Xavier, R. J., 2014. Atg16L1 T300A variant decreases selective autophagy resulting in altered cytokine signaling and decreased antibacterial defense. *Proceedings of the National Academy of Sciences*, 111 (21), 7741–7746.

Latour, S., Tanaka, H., Demeure, C., Mateo, V., Rubio, M., Brown, E. J., Maliszewski, C., Lindberg, F. P., Oldenborg, A., Ullrich, A., Delespesse, G., and Sarfati, M., 2001. Bidirectional negative regulation of human T and dendritic cells by CD47 and its cognate receptor signal-regulator protein-alpha: down-regulation of IL-12 responsiveness and inhibition of dendritic cell activation. *Journal of Immunology*, 167 (5), 2547–2554.

Lavin, Y., Winter, D., Blecher-Gonen, R., David, E., Keren-Shaul, H., Merad, M., Jung, S., and Amit, I., 2014. Tissue-resident macrophage enhancer landscapes are shaped by the local microenvironment. *Cell*, 159 (6), 1312–1326.

Le Bourhis, L., Magalhaes, J. G., Selvanantham, T., Travassos, L. H., Geddes, K., Fritz, J. H., Viala, J., Tedin, K., Girardin, S. E., and Philpott, D. J., 2009. Role of Nod1 in mucosal dendritic cells during *Salmonella* pathogenicity island 1-independent *Salmonella enterica* serovar Typhimurium infection. *Infection and Immunity*, 77 (10), 4480–4486.

Leach, M. W., Bean, A. G., Mauze, S., Coffman, R. L., and Powrie, F., 1996. Inflammatory bowel disease in C.B-17 Scid mice reconstituted with the CD45RBhigh subset of CD4+ T cells. *The American Journal of Pathology*, 148 (5), 1503–1515.

Lee, J., Breton, G., Oliveira, T. Y. K., Zhou, Y. J., Aljoufi, A., Puhr, S., Cameron, M. J., Sékaly, R.-P., Nussenzweig, M. C., and Liu, K., 2015. Restricted dendritic cell and monocyte progenitors in human cord blood and bone marrow. *The Journal of Experimental Medicine*, 212 (3), 385–399.

Lee, S.-J., McLachlan, J. B., Kurtz, J. R., Fan, D., Winter, S. E., Bäumler, A. J., Jenkins, M. K., and McSorley, S. J., 2012. Temporal expression of bacterial proteins instructs host CD4 T cell expansion and Th17 development. *PLoS Pathogens*, 8 (1), e1002499.

Lee, Y. J., Wang, H., Starrett, G. J., Phuong, V., Jameson, S. C., and Hogquist, K. A., 2015. Tissue-specific distribution of iNKT cells impacts their cytokine response. *Immunity*, 43 (3), 566–578.

Lelouard, H., Fallet, M., de Bovis, B., Meresse, S., and Gorvel, J.-P., 2012. Peyer's patch dendritic cells sample antigens by extending dendrites through M cell-specific transcellular pores. *Gastroenterology*, 142 (3), 592–601.e3.

Lemke, G., 2013. Biology of the TAM Receptors. *Cold Spring Harbor Perspectives in Biology*, 5:a009076.

Lepage, P., Seksik, P., Sutren, M., la Cochetiere, de, M.-F., Jian, R., Marteau, P., and Dore, J., 2005. Biodiversity of the mucosa-associated microbiota is stable along the distal digestive tract in healthy individuals and patients with IBD. *Inflammatory Bowel Diseases*, 11 (5), 473–480.

Leventis, P. A. and Grinstein, S., 2010. The distribution and function of phosphatidylserine in cellular membranes. *Annual Review of Biophysics*, 39, 407–427.

Levine, B. and Kroemer, G., 2008. Autophagy in the pathogenesis of disease. *Cell*, 132 (1), 27–42.

Lewis, K. L., Caton, M. L., Bogunovic, M., Greter, M., Grajkowska, L. T., Ng, D., Klinakis, A., Charo, I. F., Jung, S., Gommerman, J. L., Ivanov, I. I., Liu, K., Merad, M., and Reizis, B., 2011. Notch2 receptor signaling controls functional differentiation of dendritic cells in the spleen and intestine. *Immunity*, 35 (5), 780–791.

Lécuyer, E., Rakotobe, S., Lengliné-Garnier, H., Lebreton, C., Picard, M., Juste, C., Fritzen, R., Eberl, G., McCoy, K. D., Macpherson, A. J., Reynaud, C.-A., Cerf-Bensussan, N., and Gaboriau-Routhiau, V., 2014. Segmented filamentous bacterium uses secondary and tertiary lymphoid tissues to induce gut IgA and specific T helper 17 cell responses. *Immunity*, 40 (4), 608–620.

Li, H., Limenitakis, J. P., Fuhrer, T., Geuking, M. B., Lawson, M. A., Wyss, M., Brugiroux, S., Keller, I., Macpherson, J. A., Rupp, S., Stolp, B., Stein, J. V., Stecher, B., Sauer, U., McCoy, K. D., and Macpherson, A. J., 2015. The outer mucus layer hosts a distinct intestinal microbial niche. *Nature Communications*, 6, 8292.

Li, L., Mo, L., Hao, H., Yang, W., Zhou, Q., Xue, F., Shi, Z., Liu, Z., Yang, P.-C., and Feng, B., 2014. Flagellin modulates TIM4 expression in mast cells. *Cell Biology International*, 38 (11), 1330–1336.

Li, L.-J., Zeng, L., Li, X.-X., Mo, L.-H., Geng, X.-R., Zheng, P.-Y., Liu, Z.-G., Feng, B.-S., and Yang, P.-C., 2016. Induction of colitis in mice with food allergen-specific immune response. *Scientific Reports*, 6, 32765.

Li, Y., Innocentin, S., Withers, D. R., Roberts, N. A., Gallagher, A. R., Grigorieva, E. F., Wilhelm, C., and Veldhoen, M., 2011. Exogenous stimuli maintain intraepithelial lymphocytes via aryl hydrocarbon receptor activation. *Cell*, 147 (3), 629–640.

Liang, S., Alard, P., Zhao, Y., Parnell, S., Clark, S. L., and Kosiewicz, M. M., 2005. Conversion of CD4+ CD25- cells into CD4+ CD25+ regulatory T cells in vivo requires B7 costimulation, but not the thymus. *Journal of Experimental Medicine*, 201 (1), 127–137.

Lim, A. I., Verrier, T., Vosshenrich, C. A., and Di Santo, J. P., 2017. Developmental options and functional plasticity of innate lymphoid cells. *Current Opinion in Immunology*, 44, 61–68.

Liu, H. and Rohowsky-Kochan, C., 2008. Regulation of IL-17 in human CCR6+ effector memory T cells. *J Immunol*, 180 (12), 7948–7957.

Liu, J. Z., Jellbauer, S., Poe, A. J., Ton, V., Pesciaroli, M., Kehl-Fie, T. E., Restrepo, N. A., Hosking, M. P., Edwards, R. A., Battistoni, A., Pasquali, P., Lane, T. E., Chazin, W. J., Vogl, T., Roth, J., Skaar, E. P., and Raffatellu, M., 2012. Zinc sequestration by the neutrophil protein calprotectin enhances *Salmonella* growth in the inflamed gut. *Cell Host and Microbe*, 11 (3), 227–239.

Liu, K., Iyoda, T., Saternus, M., Kimura, Y., Inaba, K., and Steinman, R. M., 2002. Immune tolerance after delivery of dying cells to dendritic cells in situ. *Journal of Experimental Medicine*, 196 (8), 1091–1097.

Liu, K., Victora, G. D., Schwickert, T. A., Guermonprez, P., Meredith, M. M., Yao, K., Chu, F. F., Randolph, G. J., Rudensky, A. Y., and Nussenzweig, M., 2009. *In vivo* analysis of dendritic cell development and homeostasis. *Science*, 324, 392–397.

Liu, T., He, S.-H., Zheng, P.-Y., Zhang, T.-Y., Wang, B.-Q., and Yang, P.-C., 2007. Staphylococcal enterotoxin B increases TIM4 expression in human dendritic cells that drives naïve CD4 T cells to differentiate into Th2 cells. *Molecular Immunology*, 44 (14), 3580–3587.

Liu, X., Lu, R., Xia, Y., and Sun, J., 2010. Global analysis of the eukaryotic pathways and networks regulated by *Salmonella* Typhimurium in mouse intestinal infection *in vivo*. *BMC Genomics*, 11:722.

Locksley, R. M., Heinzel, F. P., Sadick, M. D., Holaday, B. J., and Gardner, K. D. J., 1987. Murine cutaneous leishmaniasis: susceptibility correlates with differential expansion of helper T-cell subsets. *Annales de l'Institut Pasteur. Immunology*, 138 (5), 744–749.

Longman, R. S., Diehl, G. E., Victorio, D. A., Huh, J. R., Galan, C., Miraldi, E. R., Swaminath, A., Bonneau, R., Scherl, E. J., and Littman, D. R., 2014. CX(3)CR1(+) mononuclear phagocytes support colitis-associated innate lymphoid cell production of IL-22. *Journal of Experimental Medicine*, 211 (8), 1571–1583.

Louis, P., Hold, G. L., and Flint, H. J., 2014. The gut microbiota, bacterial metabolites and colorectal cancer. *Nature Reviews Microbiology*, 12 (10), 661–672.

Lucas, M., Stuart, L. M., Savill, J., and Lacy-Hulbert, A., 2003. Apoptotic cells and innate immune stimuli combine to regulate macrophage cytokine secretion. *Journal of Immunology*, 171 (5), 2610–2615.

Lukas, D., Yogev, N., Kel, J. M., Regen, T., Mufazalov, I. A., Tang, Y., Wanke, F., Reizis, B., Muller, W., Kurschus, F. C., Prinz, M., Kleiter, I., Clausen, B. E., and Waisman, A., 2017. TGFβ inhibitor Smad7 regulates dendritic cell-induced autoimmunity. *Proceedings of the National Academy of Sciences*, 114 (8), E1480–E1489.

Luther, S. A., Tang, H. L., Hyman, P. L., Farr, A. G., and Cyster, J. G., 2000. Coexpression of the chemokines ELC and SLC by T zone stromal cells and deletion of the ELC gene in the plt/plt mouse. *Proceedings of the National Academy of Sciences*, 97 (23), 12694–12699.

Mabbott, N. A., Donaldson, D. S., Ohno, H., Williams, I. R., and Mahajan, A., 2013. Microfold (M) cells: important immunosurveillance posts in the intestinal epithelium. *Mucosal Immunology*, 6 (4), 666–677.

Macatonia, S. E., Hosken, N. A., Litton, M., Vieira, P., Hsieh, C. S., Culpepper, J. A., Wysocka, M., Trinchieri, G., Murphy, K. M., and O'Garra, A., 1995. Dendritic cells produce IL-12 and direct the development of Th1 cells from naive CD4+ T cells. *Journal of Immunology*, 154 (10), 5071–5079.

Macfarlane, G. T. and Gibson, G. R., 1991. Formation of glycoprotein degrading enzymes by *Bacteroides fragilis*. *FEMS Microbiology Letters*, 77 (2-3), 289–293.

Macia, L., Tan, J., Vieira, A. T., Leach, K., Stanley, D., Luong, S., Maruya, M., Ian McKenzie, C., Hijikata, A., Wong, C., Binge, L., Thorburn, A. N., Chevalier, N., Ang, C., Marino, E., Robert, R., Offermanns, S., Teixeira, M. M., Moore, R. J., Flavell, R. A., Fagarasan, S., and Mackay, C. R., 2015. Metabolite-sensing receptors GPR43 and GPR109A facilitate dietary fibre-induced gut homeostasis through regulation of the inflammasome. *Nature Communications*, 6, 6734.

MacMicking, J. D., 2012. Interferon-inducible effector mechanisms in cell-autonomous immunity. *Nature Reviews Immunology*, 12 (5), 367–382.

Macpherson, A. J. and Uhr, T., 2004. Induction of Protective IgA by Intestinal Dendritic Cells Carrying Commensal Bacteria. *Science*, 303 (5664), 1662–1665.

Maeda, A., Schwarz, A., Kernebeck, K., Gross, N., Aragane, Y., Peritt, D., and Schwarz, T., 2005. Intravenous infusion of syngeneic apoptotic cells by photopheresis induces antigen-specific regulatory T cells. *Journal of Immunology*, 174 (10), 5968–5976.

Mangan, P. R., Harrington, L. E., O'Quinn, D. B., Helms, W. S., Bullard, D. C., Elson, C. O., Hatton, R. D., Wahl, S. M., Schoeb, T. R., and Weaver, C. T., 2006. Transforming growth factor-beta induces development of the T(H)17 lineage. *Nature*, 441 (7090), 231–234.

Manichanh, C., Rigottier-Gois, L., Bonnaud, E., Gloux, K., Pelletier, E., Frangeul, L., Nalin, R., Jarrin, C., Chardon, P., Marteau, P., Roca, J., and Dore, J., 2006. Reduced diversity of faecal microbiota in Crohn's disease revealed by a metagenomic approach. *Gut*, 55 (2), 205–211.

Maraskovsky, E., 1996. Dramatic increase in the numbers of functionally mature dendritic cells in Flt3 ligand-treated mice: multiple dendritic cell subpopulations identified. *The Journal of Experimental Medicine*, 184 (5), 1953–1962.

Marches, O., Covarelli, V., Dahan, S., Cougoule, C., Bhatta, P., Frankel, G., and Caron, E., 2008. EspJ of enteropathogenic and enterohaemorrhagic *Escherichia coli* inhibits opsono-phagocytosis. *Cellular Microbiology*, 10 (5), 1104–1115.

Mariat, C., Degauque, N., Balasubramanian, S., Kenny, J., Dekruyff, R. H., Umetsu, D. T., Kuchroo, V., Zheng, X. X., and Strom, T. B., 2009. Tim-1 signaling substitutes for conventional signal 1 and requires costimulation to induce T cell proliferation. *The Journal of Immunology*, 182 (3), 1379–1385.

Marini, M., Bamias, G., Rivera-Nieves, J., Moskaluk, C. A., Hoang, S. B., Ross, W. G., Pizarro, T. T., and Cominelli, F., 2003. TNF-α neutralization ameliorates the severity of murine Crohn's-like ileitis by abrogation of intestinal epithelial cell apoptosis. *Proceedings of the National Academy of Sciences*, 100 (14), 8366–8371.

Markle, J. G. M., Frank, D. N., Mortin-Toth, S., Robertson, C. E., Feazel, L. M., Rolle-Kampczyk, U., Bergen, von, M., McCoy, K. D., Macpherson, A. J., and Danska, J. S., 2013. Sex differences in the gut microbiome drive hormone-dependent regulation of autoimmunity. *Science*, 339 (6123), 1084–1088.

Marsh, D. G., Neely, J. D., Breazeale, D. R., Ghosh, B., Freidhoff, L. R., Ehrlich-Kautzky, E., Schou, C., Krishnaswamy, G., and Beaty, T. H., 1994. Linkage analysis of IL4 and other chromosome 5q31.1 markers and total serum immunoglobulin E concentrations. *Science*, 264 (5162), 1152–1156.

Marsland, B. J., Battig, P., Bauer, M., Ruedl, C., Lassing, U., Beerli, R. R., Dietmeier, K., Ivanova, L., Pfister, T., Vogt, L., Nakano, H., Nembrini, C., Saudan, P., Kopf, M., and Bachmann, M. F., 2005. CCL19 and CCL21 induce a potent proinflammatory differentiation program in licensed dendritic cells. *Immunity*, 22 (4), 493–505.

Martin, B., Hirota, K., Cua, D. J., Stockinger, B., and Veldhoen, M., 2009. Interleukin-17-producing γδ T cells selectively expand in response to pathogen products and environmental signals. *Immunity*, 31 (2), 321–330.

Martin, H. M., Campbell, B. J., Hart, C. A., Mpofu, C., Nayar, M., Singh, R., Englyst, H., Williams, H. F., and Rhodes, J. M., 2004. Enhanced *Escherichia coli* adherence and invasion in Crohn's disease and colon cancer. *Gastroenterology*, 127 (1), 80–93.

Martinez, F. O., Helming, L., and Gordon, S., 2009. Alternative activation of macrophages: an immunologic functional perspective. *Annual Review of Immunology*, 27, 451-483.

Martinez, J., Almendinger, J., Oberst, A., Ness, R., Dillon, C. P., Fitzgerald, P., Hengartner, M. O., and Green, D. R., 2011. Microtubule-associated protein 1 light chain 3 alpha (LC3)-associated phagocytosis is required for the efficient clearance of dead cells. *Proceedings of the National Academy of Sciences*, 108 (42), 17396–17401.

Masahata, K., Umemoto, E., Kayama, H., Kotani, M., Nakamura, S., Kurakawa, T., Kikuta, J., Gotoh, K., Motooka, D., Sato, S., Higuchi, T., Baba, Y., Kurosaki, T., Kinoshita, M., Shimada, Y., Kimura, T., Okumura, R., Takeda, A., Tajima, M., Yoshie, O., Fukuzawa, M., Kiyono, H., Fagarasan, S., Iida, T., Ishii, M., and Takeda, K., 2014. Generation of colonic IgA-secreting cells in the caecal patch. *Nature Communications*, 5, 3704.

Mashayekhi, M., Sandau, M. M., Dunay, I. R., Frickel, E. M., Khan, A., Goldszmid, R. S., Sher, A., Ploegh, H. L., Murphy, T. L., Sibley, L. D., and Murphy, K. M., 2011. CD8alpha(+) dendritic cells are the critical source of interleukin-12 that controls acute infection by *Toxoplasma gondii* tachyzoites. *Immunity*, 35 (2), 249–259.

Maslowski, K. M., Vieira, A. T., Ng, A., Kranich, J., Sierro, F., Yu, D., Schilter, H. C., Rolph, M. S., Mackay, F., Artis, D., Xavier, R. J., Teixeira, M. M., and Mackay, C. R., 2009. Regulation of inflammatory responses by gut microbiota and chemoattractant receptor GPR43. *Nature*, 461 (7268), 1282–1286.

Masopust, D., Vezys, V., Wherry, E. J., Barber, D. L., and Ahmed, R., 2006. Cutting edge: gut microenvironment promotes differentiation of a unique memory CD8 T cell population. *Journal of Immunology*, 176 (4), 2079–2083.

Matsuyama, S., Llopis, J., Deveraux, Q. L., Tsien, R. Y., and Reed, J. C., 2000. Changes in intramitochondrial and cytosolic pH: early events that modulate caspase activation during apoptosis. *Nature cell biology*, 2 (6), 318–325.

Mayer, J. U., Demiri, M., Agace, W. W., MacDonald, A. S., Svensson-Frej, M., and Milling, S. W., 2017. Different populations of CD11b+ dendritic cells drive Th2 responses in the small intestine and colon. *Nature Communications*, 8, 15820.

McCormick, B. A., Parkos, C. A., Colgan, S. P., Carnes, D. K., and Madara, J. L., 1998. Apical secretion of a pathogen-elicited epithelial chemoattractant activity in response to surface colonization of intestinal epithelia by *Salmonella* Typhimurium. *Journal of Immunology*, 160 (1), 455–466.

McDaniel, T. K., Jarvis, K. G., Donnenberg, M. S., and Kaper, J. B., 1995. A genetic locus of enterocyte effacement conserved among diverse enterobacterial pathogens. *Proceedings of the National Academy of Sciences*, 92 (5), 1664–1668.

McDole, J. R., Wheeler, L. W., McDonald, K. G., Wang, B., Konjufca, V., Knoop, K. A., Newberry, R. D., and Miller, M. J., 2012. Goblet cells deliver luminal antigen to CD103+ dendritic cells in the small intestine. *Nature*, 483 (7389), 345–349.

McGeachy, M. J., Chen, Y., Tato, C. M., Laurence, A., Joyce-Shaikh, B., Blumenschein, W. M., McClanahan, T. K., O'Shea, J. J., and Cua, D. J., 2009. The interleukin 23 receptor is essential for the terminal differentiation of interleukin 17-producing effector T helper cells *in vivo*. *Nature Immunology*, 10 (3), 314–324.

McIntire, J. J., Umetsu, S. E., Akbari, O., Potter, M., Kuchroo, V. K., Barsh, G. S., Freeman, G. J., Umetsu, D. T., and DeKruyff, R. H., 2001. Identification of Tapr (an airway hyperreactivity regulatory locus) and the linked Tim gene family. *Nature Immunology*, 2 (12), 1109–1116.

McKenna, H. J., Stocking, K. L., Miller, R. E., Brasel, K., De Smedt, T., Maraskovsky, E., Maliszewski, C. R., Lynch, D. H., Smith, J., Pulendran, B., Roux, E. R., Teepe, M., Lyman, S. D., and Peschon, J. J., 2000. Mice lacking Flt3 ligand have deficient hematopoiesis affecting hematopoietic progenitor cells, dendritic cells, and natural killer cells. *Blood*, 95 (11), 3489–3497.

McPhee, J. B., Small, C. L., Reid-Yu, S. A., Brannon, J. R., Le Moual, H., and Coombes, B. K., 2014. Host defense peptide resistance contributes to colonization and maximal intestinal pathology by Crohn's disease-associated adherent-invasive *Escherichia coli*. *Infection and Immunity*, 82 (8), 3383–3393.

McSorley, S. J., Asch, S., Costalonga, M., Reinhardt, R. L., and Jenkins, M. K., 2002. Tracking *Salmonella*-specific CD4 T cells *in vivo* reveals a local mucosal response to a disseminated infection. *Immunity*, 16 (3), 365–377.

Meador, J. P., Caldwell, M. E., Cohen, P. S., and Conway, T., 2014. *Escherichia coli* pathotypes occupy distinct niches in the mouse intestine. *Infection and Immunity*, 82 (5), 1931–1938.

Meconi, S., Vercellone, A., Levillain, F., Payré, B., Saati, Al, T., Capilla, F., Desreumaux, P., Darfeuille-Michaud, A., and Altare, F., 2007. Adherent-invasive *Escherichia coli* isolated from Crohn's disease patients induce granulomas *in vitro*. *Cellular Microbiology*, 9 (5), 1252–1261.

Meyers, J. H., Chakravarti, S., Schlesinger, D., Illes, Z., Waldner, H., Umetsu, S. E., Kenny, J., Zheng, X. X., Umetsu, D. T., Dekruyff, R. H., Strom, T. B., and Kuchroo, V. K., 2005. TIM-4 is the ligand for TIM-1, and the TIM-1-TIM-4 interaction regulates T cell proliferation. *Nature Immunology*, 6 (5), 455–464.

Miao, E. A., Leaf, I. A., Treuting, P. M., Mao, D. P., Dors, M., Sarkar, A., Warren, S. E., Wewers, M. D., and Aderem, A., 2010a. Caspase-1-induced pyroptosis is an innate immune effector mechanism against intracellular bacteria. *Nature Immunology*, 11 (12), 1136–1142.

Miao, E. A., Mao, D. P., Yudkovsky, N., Bonneau, R., Lorang, C. G., Warren, S. E., Leaf, I. A., and Aderem, A., 2010b. Innate immune detection of the type III secretion apparatus through the NLRC4 inflammasome. *Proceedings of the National Academy of Sciences*, 107 (7), 3076–3080.

Miranda, R. L., Conway, T., Leatham, M. P., Chang, D.-E., Norris, W. E., Allen, J. H., Stevenson, S. J., Laux, D. C., and Cohen, P. S., 2004. Glycolytic and gluconeogenic growth of *Escherichia coli* O157:H7 (EDL933) and *E. coli* K-12 (MG1655) in the mouse intestine. *Infection and Immunity*, 72 (3), 1666–1676.

Mishra, A., Hogan, S. P., Lee, J. J., Foster, P. S., and Rothenberg, M. E., 1999. Fundamental signals that regulate eosinophil homing to the gastrointestinal tract. *The Journal of Clinical Investigation*, 103 (12), 1719–1727.

Miyanishi, M., Tada, K., Koike, M., Uchiyama, Y., Kitamura, T., and Nagata, S., 2007. Identification of Tim4 as a phosphatidylserine receptor. *Nature*, 450 (7168), 435–439.

Mizui, M., Shikina, T., Arase, H., Suzuki, K., Yasui, T., Rennert, P. D., Kumanogoh, A., and Kikutani, H., 2008. Bimodal regulation of T cell-mediated immune responses by TIM-4. *International Immunology*, 20 (5), 695–708.

Moayyedi, P., Surette, M. G., Kim, P. T., Libertucci, J., Wolfe, M., Onischi, C., Armstrong, D., Marshall, J. K., Kassam, Z., Reinisch, W., and Lee, C. H., 2015. Fecal microbiota transplantation induces remission in patients with active ulcerative colitis in a randomized controlled trial. *Gastroenterology*, 149 (1), 102–109.e6.

Mohrs, K., Wakil, A. E., Killeen, N., Locksley, R. M., and Mohrs, M., 2005. A two-step process for cytokine production revealed by IL-4 dual-reporter mice. *Immunity*, 23 (4), 419–429.

Molodecky, N. A., Soon, I. S., Rabi, D. M., Ghali, W. A., Ferris, M., Chernoff, G., Benchimol, E. I., Panaccione, R., Ghosh, S., Barkema, H. W., and Kaplan, G. G., 2012. Increasing incidence and prevalence of the inflammatory bowel diseases with time, based on systematic review. *Gastroenterology*, 142 (1), 46–54.

Moltke, von, J., Ji, M., Liang, H.-E., and Locksley, R. M., 2016. Tuft-cell-derived IL-25 regulates an intestinal ILC2-epithelial response circuit. *Nature*, 529 (7585), 221–225.

Monteleone, G., Parrello, T., Monteleone, I., Tammaro, S., Luzza, F., and Pallone, F., 1999. Interferon-gamma (IFN-gamma) and prostaglandin E2 (PGE2) regulate differently IL-12 production in human intestinal lamina propria mononuclear cells (LPMC). *Clinical and Experimental Immunology*, 117 (3), 469–475.

Monteleone, I., Platt, A. M., Jaensson, E., Agace, W. W., and Mowat, A. M., 2008. IL-10-dependent partial refractoriness to Toll-like receptor stimulation modulates gut mucosal dendritic cell function. *European Journal of Immunology*, 38 (6), 1533–1547.

Morgan, X. C., Tickle, T. L., Sokol, H., Gevers, D., Devaney, K. L., Ward, D. V., Reyes, J. A., Shah, S. A., LeLeiko, N., Snapper, S. B., Bousvaros, A., Korzenik, J., Sands, B. E., Xavier, R. J., and Huttenhower, C., 2012. Dysfunction of the intestinal microbiome in inflammatory bowel disease and treatment. *Genome Biology*, 13 (9), R79.

Moro, K., Yamada, T., Tanabe, M., Takeuchi, T., Ikawa, T., Kawamoto, H., Furusawa, J.-I., Ohtani, M., Fujii, H., and Koyasu, S., 2010. Innate production of T(H)2 cytokines by adipose tissue-associated c-Kit(+) Sca-1(+) lymphoid cells. *Nature*, 463 (7280), 540–544.

Moss, S. F., Calam, J., Agarwal, B., Wang, S., and Holt, P. R., 1996. Induction of gastric epithelial apoptosis by *Helicobacter pylori*. *Gut*, 38 (4), 498–501.

Motomura, Y., Morita, H., Moro, K., Nakae, S., Artis, D., Endo, T. A., Kuroki, Y., Ohara, O., Koyasu, S., and Kubo, M., 2014. Basophil-derived interleukin-4 controls the function of natural helper cells, a member of ILC2s, in lung inflammation. *Immunity*, 40 (5), 758–771.

Mowat, A. M. and Agace, W. W., 2014. Regional specialization within the intestinal immune system. *Nature Reviews Immunology*, 14 (10), 667–685.

Mrsny, R. J., Gewirtz, A. T., Siccardi, D., Savidge, T., Hurley, B. P., Madara, J. L., and McCormick, B. A., 2004. Identification of hepoxilin A3 in inflammatory events: a required role in neutrophil migration across intestinal epithelia. *Proceedings of the National Academy of Sciences,* 101 (19), 7421–7426.

Mundy, R., MacDonald, T. T., Dougan, G., Frankel, G., and Wiles, S., 2005. *Citrobacter rodentium* of mice and man. *Cellular Microbiology*, 7 (12), 1697–1706.

Murai, M., Turovskaya, O., Kim, G., Madan, R., Karp, C. L., Cheroutre, H., and Kronenberg, M., 2009. Interleukin 10 acts on regulatory T cells to maintain expression of the transcription factor Foxp3 and suppressive function in mice with colitis. *Nature Immunology*, 10 (11), 1178–1184.

Muralidharan, S. and Mandrekar, P., 2013. Cellular stress response and innate immune signaling: integrating pathways in host defense and inflammation. *Journal of Leukocyte Biology*, 94 (6), 1167–1184.

Murch, S. H., Braegger, C. P., Walker-Smith, J. A., and MacDonald, T. T., 1993. Location of tumour necrosis factor alpha by immunohistochemistry in chronic inflammatory bowel disease. *Gut*, 34 (12), 1705–1709.

Møller, A. K., Leatham, M. P., Conway, T., Nuijten, P. J. M., de Haan, L. A. M., Krogfelt, K. A., and Cohen, P. S., 2003. An *Escherichia coli* MG1655 lipopolysaccharide deep-rough core mutant grows and survives in mouse cecal mucus but fails to colonize the mouse large intestine. *Infection and Immunity*, 71 (4), 2142–2152.

Nagai, T., Abe, A., and Sasakawa, C., 2005. Targeting of enteropathogenic *Escherichia coli* EspF to host mitochondria is essential for bacterial pathogenesis: critical role of the 16th leucine residue in EspF. *Journal of Biological Chemistry*, 280 (4), 2998–3011.

Nagashima, R., Maeda, K., Imai, Y., and Takahashi, T., 1996. Lamina propria macrophages in the human gastrointestinal mucosa: their distribution, immunohistological phenotype, and function. *Journal of Histochemistry and Cytochemistry*, 44 (7), 721–731.

Naik, S. H., Metcalf, D., van Nieuwenhuijze, A., Wicks, I., Wu, L., O'Keeffe, M., and Shortman, K., 2006. Intrasplenic steady-state dendritic cell precursors that are distinct from monocytes. *Nature Immunology*, 7 (6), 663–671.

Naik, S. H., Sathe, P., Park, H.-Y., Metcalf, D., Proietto, A. I., Dakic, A., Carotta, S., O'Keeffe, M., Bahlo, M., Papenfuss, A., Kwak, J.-Y., Wu, L., and Shortman, K., 2007. Development of plasmacytoid and conventional dendritic cell subtypes from single precursor cells derived *in vitro* and *in vivo*. *Nature Immunology*, 8 (11), 1217–1226.

Nair, M. G., Gallagher, I. J., Taylor, M. D., Loke, P., Coulson, P. S., Wilson, R. A., Maizels, R. M., and Allen, J. E., 2005. Chitinase and Fizz family members are a generalized feature of nematode infection with selective upregulation of Ym1 and Fizz1 by antigen-presenting cells. *Infection and Immunity*, 73 (1), 385–394.

Nakahashi-Oda, C., Udayanga, K. G. S., Nakamura, Y., Nakazawa, Y., Totsuka, N., Miki, H., Iino, S., Tahara-Hanaoka, S., Honda, S.-I., Shibuya, K., and Shibuya, A., 2015. Apoptotic epithelial cells control the abundance of Treg cells at barrier surfaces. *Nature Immunology*, 17 (4), 441–450.

Nakai, W., Yoshida, T., Diez, D., Miyatake, Y., Nishibu, T., Imawaka, N., Naruse, K., Sadamura, Y., and Hanayama, R., 2016. A novel affinity-based method for the isolation of highly purified extracellular vesicles, *Scientific Reports*, 6, 33935.

Nakayama, M., Akiba, H., Takeda, K., Kojima, Y., Hashiguchi, M., Azuma, M., Yagita, H., and Okumura, K., 2009. Tim-3 mediates phagocytosis of apoptotic cells and cross-presentation. *Blood*, 113 (16), 3821–3830.

Nardone, G. and Compare, D., 2015. The human gastric microbiota: Is it time to rethink the pathogenesis of stomach diseases? *United European Gastroenterology Journal*, 3 (3), 255–260.

Nash, J. H., Villegas, A., Kropinski, A. M., Aguilar-Valenzuela, R., Konczy, P., Mascarenhas, M., Ziebell, K., Torres, A. G., Karmali, M. A., and Coombes, B. K., 2010. Genome sequence of adherent-invasive *Escherichia coli* and comparative genomic analysis with other *E. coli* pathotypes. *BMC Genomics*, 11, 667.

Nassar, M., Tabib, Y., Capucha, T., Mizraji, G., Nir, T., Pevsner-Fischer, M., Zilberman-Schapira, G., Heyman, O., Nussbaum, G., Bercovier, H., Wilensky, A., Elinav, E., Burstyn-Cohen, T., and Hovav, A.-H., 2017. GAS6 is a key homeostatic immunological regulator of host-commensal interactions in the oral mucosa. *Proceedings of the National Academy of Sciences*, 114 (3), E337–E346.

Nava, G. M., Friedrichsen, H. J., and Stappenbeck, T. S., 2011. Spatial organization of intestinal microbiota in the mouse ascending colon. *The ISME Journal*, 5 (4), 627–638.

Nava, P., Koch, S., Laukoetter, M. G., Lee, W. Y., Kolegraff, K., Capaldo, C. T., Beeman, N., Addis, C., Gerner-Smidt, K., Neumaier, I., Skerra, A., Li, L., Parkos, C. A., and Nusrat, A., 2010. Interferon-gamma regulates intestinal epithelial homeostasis through converging beta-catenin signaling pathways. *Immunity*, 32 (3), 392–402.

Neill, D. R., Wong, S. H., Bellosi, A., Flynn, R. J., Daly, M., Langford, T. K. A., Bucks, C., Kane, C. M., Fallon, P. G., Pannell, R., Jolin, H. E., and McKenzie, A. N. J., 2010. Nuocytes represent a new innate effector leukocyte that mediates type-2 immunity. *Nature*, 464 (7293), 1367–1370.

Neutra, M. R., Phillips, T. L., Mayer, E. L., and Fishkind, D. J., 1987. Transport of membrane-bound macromolecules by M cells in follicle-associated epithelium of rabbit Peyer's patch. *Cell and Tissue Reseach*, 247 (3), 537–546.

Newham, P., Craig, S. E., Seddon, G. N., Schofield, N. R., Rees, A., Edwards, R. M., Jones, E. Y., and Humphries, M. J., 1997. α4 integrin binding interfaces on VCAM-1 and MAdCAM-1: integrin binding footprints identify accessory binding sites that play a role in integrin specificity. *Journal of Biological Chemistry*, 272 (31), 19429–19440.

Nguyen, L. P., Pan, J., Dinh, T. T., Hadeiba, H., O'Hara Iii, E., Ebtikar, A., Hertweck, A., Gokmen, M. R., Lord, G. M., Jenner, R. G., Butcher, E. C., and Habtezion, A., 2014. Role and species-specific expression of colon T cell homing receptor GPR15 in colitis. *Nature Immunology*, 16 (2), 207-213.

Niess, J. H., Brand, S., Gu, X., Landsman, L., Jung, S., McCormick, B. A., Vyas, J. M., Boes, M., Ploegh, H. L., Fox, J. G., Littman, D. R., and Reinecker, H.-C., 2005. CX3CR1-mediated dendritic cell access to the intestinal lumen and bacterial clearance. *Science*, 307 (5707), 254–258.

Niess, J. H., Leithauser, F., Adler, G., and Reimann, J., 2008. Commensal gut flora drives the expansion of proinflammatory CD4 T cells in the colonic lamina propria under normal and inflammatory conditions. *Journal of Immunology*, 180 (1), 559–568.

Nishi, C., Toda, S., Segawa, K., and Nagata, S., 2014. Tim4- and MerTK-mediated engulfment of apoptotic cells by mouse resident peritoneal macrophages. *Molecular and Cellular Biology*, 34 (8), 1512–1520.

Notley, C. A., Brown, M. A., McGovern, J. L., Jordan, C. K., and Ehrenstein, M. R., 2015. Engulfment of activated apoptotic cells abolishes TGFbeta-mediated immunoregulation via the induction of IL-6. *Journal of Immunology*, 194 (4), 1621–1627.

Nougayrède, J.-P. and Donnenberg, M. S., 2004. Enteropathogenic *Escherichia coli* EspF is targeted to mitochondria and is required to initiate the mitochondrial death pathway. *Cellular Microbiology*, 6 (11), 1097–1111.

Ochman, H., Soncini, F. C., Solomon, F., and Groisman, E. A., 1996. Identification of a pathogenicity island required for *Salmonella* survival in host cells. *Proceedings of the National Academy of Sciences*, 93 (15), 7800–7804.

Ogura, Y., Bonen, D. K., Inohara, N., Nicolae, D. L., Chen, F. F., Ramos, R., Britton, H., Moran, T., Karaliuskas, R., Duerr, R. H., Achkar, J.-P., Brant, S. R., Bayless, T. M., Kirschner, B. S., Hanauer, S. B., Nuñez, G., and Cho, J. H., 2001. A frameshift mutation in *NOD2* associated with susceptibility to Crohn's disease. *Nature*, 411 (6837), 603–606.

Ohta, T., Sugiyama, M., Hemmi, H., Yamazaki, C., Okura, S., Sasaki, I., Fukuda, Y., Orimo, T., Ishii, K. J., Hoshino, K., Ginhoux, F., and Kaisho, T., 2016. Crucial roles of XCR1-expressing dendritic cells and the XCR1-XCL1 chemokine axis in intestinal immune homeostasis. *Scientific Reports*, 6, 23505.

Okazawa, H., Motegi, S.-I., Ohyama, N., Ohnishi, H., Tomizawa, T., Kaneko, Y., Oldenborg, P.-A., Ishikawa, O., and Matozaki, T., 2005. Negative regulation of phagocytosis in macrophages by the CD47-SHPS-1 system. *Journal of Immunology*, 174 (4), 2004–2011.

Olsen, T., Rismo, R., Cui, G., Goll, R., Christiansen, I., and Florholmen, J., 2011. TH1 and TH17 interactions in untreated inflamed mucosa of inflammatory bowel disease, and their potential to mediate the inflammation. *Cytokine*, 56 (3), 633–640.

Onai, N., Kurabayashi, K., Hosoi-Amaike, M., Toyama-Sorimachi, N., Matsushima, K., Inaba, K., and Ohteki, T., 2013. A clonogenic progenitor with prominent plasmacytoid dendritic cell developmental potential. *Immunity*, 38 (5), 943–957.

Onai, N., Obata-Onai, A., Schmid, M. A., Ohteki, T., Jarrossay, D., and Manz, M. G., 2007. Identification of clonogenic common Flt3+M-CSFR+ plasmacytoid and conventional dendritic cell progenitors in mouse bone marrow. *Nature Immunology*, 8 (11), 1207–1216.

Pabst, O., 2012. New concepts in the generation and functions of IgA. *Nature Reviews Immunology*, 12 (12), 821–832.

Pabst, O., Herbrand, H., Worbs, T., Friedrichsen, M., Yan, S., Hoffmann, M. W., Korner, H., Bernhardt, G., Pabst, R., and Förster, R., 2005. Cryptopatches and isolated lymphoid follicles: dynamic lymphoid tissues dispensable for the generation of intraepithelial lymphocytes. *European Journal of Immunology*, 35 (1), 98–107.

Pack, M., Trumpfheller, C., Thomas, D., Park, C. G., Granelli-Piperno, A., Münz, C., and Steinman, R. M., 2008. DEC-205/CD205+ dendritic cells are abundant in the white pulp of the human spleen, including the border region between the red and white pulp. *Immunology*, 123 (3), 438–446.

Paesold, G., Guiney, D. G., Eckmann, L., and Kagnoff, M. F., 2002. Genes in the *Salmonella* pathogenicity island 2 and the *Salmonella* virulence plasmid are essential for *Salmonella*-induced apoptosis in intestinal epithelial cells. *Cellular Microbiology*, 4 (11), 771–781.

Palm, N. W., de Zoete, M. R., Cullen, T. W., Barry, N. A., Stefanowski, J., Hao, L., Degnan, P. H., Hu, J., Peter, I., Zhang, W., Ruggiero, E., Cho, J. H., Goodman, A. L., and Flavell, R. A., 2014. Immunoglobulin A coating identifies colitogenic bacteria in inflammatory bowel disease. *Cell*, 158 (5), 1000–1010.

Pan, J. L., Kunkel, E. J., Gosslar, U., Lazarus, N., Langdon, P., Broadwell, K., Vierra, M. A., Genovese, M. C., Butcher, E. C., and Soler, D., 2000. Cutting edge: A novel chemokine ligand for CCR10 and CCR3 expressed by epithelial cells in mucosal tissues. *Journal of Immunology*, 165 (6), 2943–2949.

Park, D., Hochreiter-Hufford, A., and Ravichandran, K. S., 2009. The phosphatidylserine receptor TIM-4 does not mediate direct signaling. *Current Biology*, 19 (4), 346–351.

Pearson, J. S., Giogha, C., Ong, S. Y., Kennedy, C. L., Kelly, M., Robinson, K. S., Lung, T. W. F., Mansell, A., Riedmaier, P., Oates, C. V. L., Zaid, A., Mühlen, S., Crepin, V. F., Marches, O., Ang, C.-S., Williamson, N. A., O'Reilly, L. A., Bankovacki, A., Nachbur, U., Infusini, G., Webb, A. I., Silke, J., Strasser, A., Frankel, G., and Hartland, E. L., 2013. A type III effector antagonizes death receptor signalling during bacterial gut infection. *Nature*, 501 (7466), 247–251.

Pelly, V. S., Kannan, Y., Coomes, S. M., Entwistle, L. J., Ruckerl, D., Seddon, B., MacDonald, A. S., McKenzie, A., and Wilson, M. S., 2016. IL-4-producing ILC2s are required for the differentiation of TH2 cells following *Heligmosomoides polygyrus* infection. *Mucosal Immunology*, 9 (6), 1407–1417.

Pereira, F. C. and Berry, D., 2017. Microbial nutrient niches in the gut. *Environmental Microbiology*, 19 (4), 1366–1378.

Perruche, S., Zhang, P., Liu, Y., Saas, P., Bluestone, J. A., and Chen, W., 2008. CD3-specific antibody-induced immune tolerance involves transforming growth factor-beta from phagocytes digesting apoptotic T cells. *Nature Medicine*, 14 (5), 528–535.

Persson, E. K., Scott, C. L., Mowat, A. M., and Agace, W. W., 2013a. Dendritic cell subsets in the intestinal lamina propria: Ontogeny and function. *European Journal of Immunology*, 43 (12), 3098-3107.

Persson, E. K., Uronen-Hansson, H., Semmrich, M., Rivollier, A., Hägerbrand, K., Marsal, J., Gudjonsson, S., Hakansson, U., Reizis, B., Kotarsky, K., and Agace, W. W., 2013b. IRF4 transcription-factor-dependent CD103(+)CD11b(+) dendritic cells drive mucosal T helper 17 cell differentiation. *Immunity*, 38 (5), 958–969.

Petty, N. K., Bulgin, R., Crepin, V. F., Cerdeno-Tarraga, A. M., Schroeder, G. N., Quail, M. A., Lennard, N., Corton, C., Barron, A., Clark, L., Toribio, A. L., Parkhill, J., Dougan, G., Frankel, G., and Thomson, N. R., 2010. The *Citrobacter rodentium* genome sequence reveals convergent evolution with human pathogenic *Escherichia coli*. *Journal of Bacteriology*, 192 (2), 525–538.

Piguet, P. F., Vesin, C., Donati, Y., and Barazzone, C., 1999. TNF-induced enterocyte apoptosis and detachment in mice: induction of caspases and prevention by a caspase inhibitor, ZVAD-fmk. *Laboratory Investigation*, 79 (4), 495–500.

Pugh, C. W., MacPherson, G. G., and Steer, H. W., 1983. Characterization of nonlymphoid cells derived from rat peripheral lymph. *Journal of Experimental Medicine*, 157 (6), 1758–1779.

Qi, H., Cannons, J. L., Klauschen, F., Schwartzberg, P. L., and Germain, R. N., 2008. SAP-controlled T-B cell interactions underlie germinal centre formation. *Nature*, 455 (7214), 764–769.

Qiu, J., Heller, J. J., Guo, X., Chen, Z.-M. E., Fish, K., Fu, Y.-X., and Zhou, L., 2012. The aryl hydrocarbon receptor regulates gut immunity through modulation of innate lymphoid cells. *Immunity*, 36 (1), 92–104.

Raffatellu, M., George, M. D., Akiyama, Y., Hornsby, M. J., Nuccio, S.-P., Paixao, T. A., Butler, B. P., Chu, H., Santos, R. L., Berger, T., Mak, T. W., Tsolis, R. M., Bevins, C. L., Solnick, J. V., Dandekar, S., and Bäumler, A. J., 2009. Lipocalin-2 resistance confers an advantage to *Salmonella enterica* serotype Typhimurium for growth and survival in the inflamed intestine. *Cell Host and Microbe*, 5 (5), 476–486.

Raffatellu, M., Wilson, R. P., Chessa, D., Andrews-Polymenis, H., Tran, Q. T., Lawhon, S., Khare, S., Adams, L. G., and Bäumler, A. J., 2005. SipA, SopA, SopB, SopD, and SopE2 contribute to *Salmonella enterica* serotype Typhimurium invasion of epithelial cells. *Infection and Immunity*, 73 (1), 146–154.

Ramalingam, R., Larmonier, C. B., Thurston, R. D., Midura-Kiela, M. T., Zheng, S. G., Ghishan, F. K., and Kiela, P. R., 2012. Dendritic cell-specific disruption of TGFβ receptor II leads to altered regulatory T-cell phenotype and spontaneous multi-organ autoimmunity. *The Journal of Immunology*, 189 (8), 3878–3893.

Rathinam, V. A. K., Vanaja, S. K., and Fitzgerald, K. A., 2012. Regulation of inflammasome signaling. *Nature Immunology*, 13 (4), 333–342.

Read, S., Malmström, V., and Powrie, F., 2000. Cytotoxic T Lymphocyte–associated Antigen 4 plays an essential role in the function of CD25+ CD4+ regulatory cells that control intestinal inflammation. *The Journal of Experimental Medicine*, 192 (2), 295–302.

Reichardt, N., Duncan, S. H., Young, P., Belenguer, A., McWilliam Leitch, C., Scott, K. P., Flint, H. J., and Louis, P., 2014. Phylogenetic distribution of three pathways for propionate production within the human gut microbiota. *The ISME Journal*, 8 (6), 1323–1335.

Riedel, C. U., Casey, P. G., Mulcahy, H., O'Gara, F., Gahan, C. G. M., and Hill, C., 2007. Construction of p16Slux, a novel vector for improved bioluminescent labeling of gram-negative bacteria. *Applied and Environmental Microbiology*, 73 (21), 7092–7095.

Ringel, Y., Maharshak, N., Ringel-Kulka, T., Wolber, E. A., Sartor, R. B., and Carroll, I. M., 2015. High throughput sequencing reveals distinct microbial populations within the mucosal and luminal niches in healthy individuals. *Gut Microbes*, 6 (3), 173–181.

Rodriguez-Manzanet, R., Meyers, J. H., Balasubramanian, S., Slavik, J., Kassam, N., Dardalhon, V., Greenfield, E. A., Anderson, A. C., Sobel, R. A., Hafler, D. A., Strom, T. B., and Kuchroo, V. K., 2008. TIM-4 expressed on APCs induces T cell expansion and survival. *Journal of Immunology*, 180 (7), 4706–4713.

Rodriguez-Manzanet, R., Sanjuan, M. A., Wu, H. Y., Quintana, F. J., Xiao, S., Anderson, A. C., Weiner, H. L., Green, D. R., and Kuchroo, V. K., 2010. T and B cell hyperactivity and autoimmunity associated with niche-specific defects in apoptotic body clearance in TIM-4-deficient mice. *Proceedings of the National Academy of Sciences*, 107 (19), 8706–8711.

Roediger, W. E., 1980. Role of anaerobic bacteria in the metabolic welfare of the colonic mucosa in man. *Gut*, 21 (9), 793–798.

Rosas, M., Davies, L. C., Giles, P. J., Liao, C.-T., Kharfan, B., Stone, T. C., O'Donnell, V. B., Fraser, D. J., Jones, S. A., and Taylor, P. R., 2014. The transcription factor Gata6 links tissue macrophage phenotype and proliferative renewal. *Science*, 344 (6184), 645–648.

Rose, J. R., Williams, M. B., Rott, L. S., Butcher, E. C., and Greenberg, H. B., 1998. Expression of the mucosal homing receptor alpha4beta7 correlates with the ability of CD8+ memory T cells to clear rotavirus infection. *Journal of Virology*, 72 (1), 726–730.

Rosenblatt, J., Raff, M. C., and Cramer, L. P., 2001. An epithelial cell destined for apoptosis signals its neighbors to extrude it by an actin- and myosin-dependent mechanism. *Current Biology*, 11 (23), 1847–1857.

Rossen, N. G., Fuentes, S., van der Spek, M. J., Tijssen, J. G., Hartman, J. H. A., Duflou, A., Lowenberg, M., van den Brink, G. R., Mathus-Vliegen, E. M. H., de Vos, W. M., Zoetendal, E. G., D'Haens, G. R., and Ponsioen, C. Y., 2015. Findings from a randomized controlled trial of fecal transplantation for patients with ulcerative colitis. *Gastroenterology*, 149 (1), 110–118.e4.

Rossini, V., Zhurina, D., Radulovic, K., Manta, C., Walther, P., Riedel, C. U., and Niess, J. H., 2014. CX3CR1(+) cells facilitate the activation of CD4 T cells in the colonic lamina propria during antigen-driven colitis. *Mucosal Immunology*, 7 (3), 533–548.

Rothlin, C. V., Ghosh, S., Zuniga, E. I., Oldstone, M. B. A., and Lemke, G., 2007. TAM receptors are pleiotropic inhibitors of the innate immune response. *Cell*, 131 (6), 1124–1136.

Rovedatti, L., Kudo, T., Biancheri, P., Sarra, M., Knowles, C. H., Rampton, D. S., Corazza, G. R., Monteleone, G., Di Sabatino, A., and MacDonald, T. T., 2009. Differential regulation of interleukin 17 and interferon γ production in inflammatory bowel disease. *Gut*, 58 (12), 1629–1636.

Ryan, P., Kelly, R. G., Lee, G., Collins, J. K., O'Sullivan, G. C., O'Connell, J., and Shanahan, F., 2004. Bacterial DNA within granulomas of patients with Crohn's disease - detection by laser capture microdissection and PCR. *American Journal of Gastroenterology*, 99 (8), 1539–1543.

Saijo, S., Ikeda, S., Yamabe, K., Kakuta, S., Ishigame, H., Akitsu, A., Fujikado, N., Kusaka, T., Kubo, S., Chung, S.-H., Komatsu, R., Miura, N., Adachi, Y., Ohno, N., Shibuya, K., Yamamoto, N., Kawakami, K., Yamasaki, S., Saito, T., Akira, S., and Iwakura, Y., 2010. Dectin-2 recognition of α-mannans and induction of Th17 cell differentiation Is essential for host defense against *Candida albicans*. *Immunity*, 32 (5), 681–691.

Sallusto, F., Schaerli, P., Loetscher, P., Schaniel, C., Lenig, D., Mackay, C. R., Qin, S., and Lanzavecchia, A., 1998. Rapid and coordinated switch in chemokine receptor expression during dendritic cell maturation. *European Journal of Immunology*, 28 (9), 2760–2769.

Salzman, N. H., Hung, K., Haribhai, D., Chu, H., Karlsson-Sjoberg, J., Amir, E., Teggatz, P., Barman, M., Hayward, M., Eastwood, D., Stoel, M., Zhou, Y., Sodergren, E., Weinstock, G. M., Bevins, C. L., Williams, C. B., and Bos, N. A., 2010. Enteric defensins are essential regulators of intestinal microbial ecology. *Nature Immunology*, 11 (1), 76–83.

Sandborn, W. J., Feagan, B. G., Rutgeerts, P., Hanauer, S., Colombel, J.-F., Sands, B. E., Lukas, M., Fedorak, R. N., Lee, S., Bressler, B., Fox, I., Rosario, M., Sankoh, S., Xu, J., Stephens, K., Milch, C., and Parikh, A., 2013. Vedolizumab as induction and maintenance therapy for Crohn's disease. *New England Journal of Medicine*, 369 (8), 711–721.

Sanjuan, M. A., Dillon, C. P., Tait, S. W. G., Moshiach, S., Dorsey, F., Connell, S., Komatsu, M., Tanaka, K., Cleveland, J. L., Withoff, S., and Green, D. R., 2007. Toll-like receptor signalling in macrophages links the autophagy pathway to phagocytosis. *Nature*, 450 (7173), 1253–1257.

Santiago, C., Ballesteros, A., Martinez-Munoz, L., Mellado, M., Kaplan, G. G., Freeman, G. J., and Casasnovas, J. M., 2007. Structures of T cell immunoglobulin mucin protein 4 show a metal-Ion-dependent ligand binding site where phosphatidylserine binds. *Immunity*, 27 (6), 941–951.

Sarang, Z., Joos, G., Garabuczi, E., Ruhl, R., Gregory, C. D., and Szondy, Z., 2014. Macrophages engulfing apoptotic cells produce nonclassical retinoids to enhance their phagocytic capacity. *Journal of Immunology*, 192 (12), 5730–5738.

Sathe, P., Metcalf, D., Vremec, D., Naik, S. H., Langdon, W. Y., Huntington, N. D., Wu, L., and Shortman, K., 2014. Lymphoid tissue and plasmacytoid dendritic cells and macrophages do not share a common macrophage-dendritic cell-restricted progenitor. *Immunity*, 41 (1), 104–115.

Sato, A., 2007. Tuft cells. *Anatomical Science International*, 82 (4), 187–199.

Sato, T., van Es, J. H., Snippert, H. J., Stange, D. E., Vries, R. G., van den Born, M., Barker, N., Shroyer, N. F., van de Wetering, M., and Clevers, H., 2011. Paneth cells constitute the niche for Lgr5 stem cells in intestinal crypts. *Nature*, 469 (7330), 415–418.

Satpathy, A. T., Briseno, C. G., Lee, J. S., Ng, D., Manieri, N. A., Wumesh, K. C., Wu, X., Thomas, S. R., Lee, W.-L., Turkoz, M., McDonald, K. G., Meredith, M. M., Song, C., Guidos, C. J., Newberry, R. D., Ouyang, W., Murphy, T. L., Stappenbeck, T. S., Gommerman, J. L., Nussenzweig, M. C., Colonna, M., Kopan, R., and Murphy, K. M., 2013. Notch2-dependent classical dendritic cells orchestrate intestinal immunity to attaching-and-effacing bacterial pathogens. *Nature Immunology*, 14 (9), 937–948.

Scanlan, P. D., Shanahan, F., O'Mahony, C., and Marchesi, J. R., 2006. Culture-independent analyses of temporal variation of the dominant fecal microbiota and targeted bacterial subgroups in Crohn's disease. *Journal of Clinical Microbiology*, 44 (11), 3980–3988.

Schaubeck, M., Clavel, T., Calasan, J., Lagkouvardos, I., Haange, S. B., Jehmlich, N., Basic, M., Dupont, A., Hornef, M., Bergen, M. V., Bleich, A., and Haller, D., 2015. Dysbiotic gut microbiota causes transmissible Crohn's disease-like ileitis independent of failure in antimicrobial defence. *Gut*, (0), 1–13.

Schauber, J., Svanholm, C., Termén, S., Iffland, K., Menzel, T., Scheppach, W., Melcher, R., Agerberth, B., Lührs, H., and Gudmundsson, G. H., 2003. Expression of the cathelicidin LL-37 is modulated by short chain fatty acids in colonocytes: relevance of signalling pathways. *Gut*, 52 (5), 735–741.

Schauer, D. B. and Falkow, S., 1993. The eae gene of *Citrobacter freundii* biotype 4280 is necessary for colonization in transmissible murine colonic hyperplasia. *Infection and Immunity*, 61 (11), 4654–4661.

Schiavoni, G., Mattei, F., Sestili, P., Borghi, P., Venditti, M., Morse, H. C. 3., Belardelli, F., and Gabriele, L., 2002. ICSBP is essential for the development of mouse type I interferon-producing cells and for the generation and activation of CD8alpha(+) dendritic cells. *Journal of Experimental Medicine*, 196 (11), 1415–1425.

Schlitzer, A., McGovern, N., Teo, P., Zelante, T., Atarashi, K., Low, D., Ho, A. W. S., See, P., Shin, A., Wasan, P. S., Hoeffel, G., Malleret, B., Heiseke, A., Chew, S., Jardine, L., Purvis, H. A., Hilkens, C. M. U., Tam, J., Poidinger, M., Stanley, E. R., Krug, A. B., Renia, L., Sivasankar, B., Ng, L. G., Collin, M., Ricciardi-Castagnoli, P., Honda, K., Haniffa, M., and Ginhoux, F., 2013. IRF4 transcription factor-dependent CD11b+ dendritic cells in human and mouse control mucosal IL-17 cytokine responses. *Immunity*, 38 (5), 970–983.

Schlitzer, A., Sivakamasundari, V., Chen, J., Sumatoh, H. R. B., Schreuder, J., Lum, J., Malleret, B., Zhang, S., Larbi, A., Zolezzi, F., Renia, L., Poidinger, M., Naik, S., Newell, E. W., Robson, P., and Ginhoux, F., 2015. Identification of cDC1- and cDC2-committed DC progenitors reveals early lineage priming at the common DC progenitor stage in the bone marrow. *Nature Immunology*, 16 (7), 718–728.

Schmitt, C. K., Ikeda, J. S., Darnell, S. C., Watson, P. R., Bispham, J., Wallis, T. S., Weinstein, D. L., Metcalf, E. S., and O'Brien, A. D., 2001. Absence of all components of the flagellar export and synthesis machinery differentially alters virulence of *Salmonella enterica* serovar Typhimurium in models of typhoid fever, survival in macrophages, tissue culture invasiveness, and calf enterocolitis. *Infection and Immunity*, 69 (9), 5619–5625.

Schnupf, P., Gaboriau-Routhiau, V., Gros, M., Friedman, R., Moya-Nilges, M., Nigro, G., Cerf-Bensussan, N., and Sansonetti, P. J., 2015. Growth and host interaction of mouse segmented filamentous bacteria *in vitro*. *Nature*, (520), 99–103.

Schon, M. P., Arya, A., Murphy, E. A., Adams, C. M., Strauch, U. G., Agace, W. W., Marsal, J., Donohue, J. P., Her, H., Beier, D. R., Olson, S., Lefrancois, L., Brenner, M. B., Grusby, M. J., and Parker, C. M., 1999. Mucosal T lymphocyte numbers are selectively reduced in integrin alpha E (CD103)-deficient mice. *Journal of Immunology*, 162 (11), 6641–6649.

Schreiber, H. A., Loschko, J., Karssemeijer, R. A., Escolano, A., Meredith, M. M., Mucida, D., Guermonprez, P., and Nussenzweig, M. C., 2013. Intestinal monocytes and macrophages are required for T cell polarization in response to *Citrobacter rodentium*. *The Journal of Experimental Medicine*, 210 (10), 2025–2039.

Schridde, A., Bain, C. C., Mayer, J. U., Montgomery, J., Pollet, E., Denecke, B., Milling, S. W. F., Jenkins, S. J., Dalod, M., Henri, S., Malissen, B., Pabst, O., and Mcl Mowat, A., 2017. Tissue-specific differentiation of colonic macrophages requires TGFbeta receptor-mediated signaling. *Mucosal Immunology* (advance online publication), doi: 10.1038/mi.2016.142.

Scott, C. L., Bain, C. C., Wright, P. B., Sichien, D., Kotarsky, K., Persson, E. K., Luda, K., Guilliams, M., Lambrecht, B. N., Agace, W. W., Milling, S. W., and Mowat, A. M., 2014a. CCR2+ CD103- intestinal dendritic cells develop from DC-committed precursors and induce interleukin-17 production by T cells. *Mucosal Immunology*, 8 (2), 327–339.

Scott, C. L., Zangerle Murray, T. F. P., Beckham, K. S. H., Douce, G., and Mowat, A. M., 2014b. Signal regulatory protein alpha (SIRPα) regulates the homeostasis of CD103+ CD11b+ DCs in the intestinal lamina propria. *European Journal of Immunology*, 44 (12), 3658–3668.

See, P., Dutertre, C.-A., Chen, J., Gunther, P., McGovern, N., Irac, S. E., Gunawan, M., Beyer, M., Handler, K., Duan, K., Sumatoh, H. R. B., Ruffin, N., Jouve, M., Gea-Mallorqui, E., Hennekam, R. C. M., Lim, T., Yip, C. C., Wen, M., Malleret, B., Low, I., et al., 2017. Mapping the human DC lineage through the integration of high-dimensional techniques. *Science*, 356 (6342).

Sellon, R. K., Tonkonogy, S., Schultz, M., Dieleman, L. A., Grenther, W., Balish, E., Rennick, D. M., and Sartor, R. B., 1998. Resident enteric bacteria are necessary for development of spontaneous colitis and immune system activation in interleukin-10-deficient mice. *Infection and Immunity*, 66 (11), 5224–5231.

Seo, S.-U., Kuffa, P., Kitamoto, S., Nagao-Kitamoto, H., Rousseau, J., Kim, Y.-G., Nuñez, G., and Kamada, N., 2015. Intestinal macrophages arising from CCR2(+) monocytes control pathogen infection by activating innate lymphoid cells. *Nature Communications*, 6, 8010.

Sepehri, S., Khafipour, E., Bernstein, C. N., Coombes, B. K., Pilar, A. V., Karmali, M., Ziebell, K., and Krause, D. O., 2011. Characterization of *Escherichia coli* isolated from gut biopsies of newly diagnosed patients with inflammatory bowel disease. *Inflammatory Bowel Diseases*, 17 (7), 1451–1463.

Sepehri, S., Kotlowski, R., Bernstein, C. N., and Krause, D. O., 2007. Microbial diversity of inflamed and noninflamed gut biopsy tissues in inflammatory bowel disease. *Inflammatory Bowel Diseases*, 13 (6), 675–683.

Serafini, N., Vosshenrich, C. A. J., and Di Santo, J. P., 2015. Transcriptional regulation of innate lymphoid cell fate. *Nature Reviews Immunology*, 15 (7), 415–428.

Shakhov, A. N., Rybtsov, S., Tumanov, A. V., Shulenin, S., Dean, M., Kuprash, D. V., and Nedospasov, S. A., 2004. SMUCKLER/TIM4 is a distinct member of TIM family expressed by stromal cells of secondary lymphoid tissues and associated with lymphotoxin signaling. *European Journal of Immunology*, 34 (2), 494–503.

Sheridan, B. S., Pham, Q.-M., Lee, Y.-T., Cauley, L. S., Puddington, L., and Lefrancois, L., 2014. Oral infection drives a distinct population of intestinal resident memory CD8(+) T cells with enhanced protective function. *Immunity*, 40 (5), 747–757.

Shibahara, T., Sato, N., Waguri, S., Iwanaga, T., Nakahara, A., Fukutomi, H., and Uchiyama, Y., 1995. The fate of effete epithelial cells at the villus tips of the human small intestine. *Archives of Histology and Cytology*, 58 (2), 205–219.

Shin, R., Suzuki, M., and Morishita, Y., 2002. Influence of intestinal anaerobes and organic acids on the growth of enterohaemorrhagic *Escherichia coli* O157:H7. *Journal of Medical Microbiology*, 51 (3), 201–206.

Shkoda, A., Werner, T., Daniel, H., Gunckel, M., Rogler, G., and Haller, D., 2007. Differential protein expression profile in the intestinal epithelium from patients with inflammatory bowel disease. *Journal of Proteome Research*, 6 (3), 1114–1125.

Shouval, D. S., Biswas, A., Goettel, J. A., McCann, K., Conaway, E., Redhu, N. S., Mascanfroni, I. D., Adham, Al, Z., Lavoie, S., Ibourk, M., Nguyen, D. D., Samsom, J. N., Escher, J. C., Somech, R., Weiss, B., Beier, R., Conklin, L. S., Ebens, C. L., Santos, F. G. M. S., et al., 2014. Interleukin-10 receptor signaling in innate immune cells regulates mucosal immune tolerance and anti-inflammatory macrophage function. *Immunity*, 40 (5), 706–719.

Singer, M. and Sansonetti, P. J., 2004. IL-8 is a key chemokine regulating neutrophil recruitment in a new mouse model of *Shigella*-induced colitis. *The Journal of Immunology*, 173 (6), 4197–4206.

Sixt, M., Kanazawa, N., Selg, M., Samson, T., Roos, G., Reinhardt, D. P., Pabst, R., Lutz, M. B., and Sorokin, L., 2005. The conduit system transports soluble antigens from the afferent lymph to resident dendritic cells in the T cell area of the lymph node. *Immunity*, 22 (1), 19–29.

Small, C. L., Reid-Yu, S. A., McPhee, J. B., and Coombes, B. K., 2013. Persistent infection with Crohn's disease-associated adherent-invasive *Escherichia coli* leads to chronic inflammation and intestinal fibrosis. *Nature Communications*, 4, 1957.

Smith, K. M., Davidson, J. M., and Garside, P., 2002. T-cell activation occurs simultaneously in local and peripheral lymphoid tissue following oral administration of a range of doses of immunogenic or tolerogenic antigen although tolerized T cells display a defect in cell division. *Immunology*, 106 (2), 144–158.

Smith, P. M., Howitt, M. R., Panikov, N., Michaud, M., Gallini, C. A., Bohlooly-Y, M., Glickman, J. N., and Garrett, W. S., 2013. The microbial metabolites, short-chain fatty acids, regulate colonic Treg cell homeostasis. *Science*, 341 (6145), 569–573.

Smythies, L. E., Shen, R., Bimczok, D., Novak, L., Clements, R. H., Eckhoff, D. E., Bouchard, P., George, M. D., Hu, W. K., Dandekar, S., and Smith, P. D., 2010. Inflammation anergy in human intestinal macrophages is due to Smad-induced IkappaBalpha expression and NF-kappaB inactivation. *Journal of Biological Chemistry*, 285 (25), 19593–19604.

Snelgrove, R. J., Goulding, J., Didierlaurent, A. M., Lyonga, D., Vekaria, S., Edwards, L., Gwyer, E., Sedgwick, J. D., Barclay, A. N., and Hussell, T., 2008. A critical function for CD200 in lung immune homeostasis and the severity of influenza infection. *Nature Immunology*, 9 (9), 1074–1083.

Snijders, A., Kalinski, P., Hilkens, C. M., and Kapsenberg, M. L., 1998. High-level IL-12 production by human dendritic cells requires two signals. *International Immunology*, 10 (11), 1593–1598.

Sonnenberg, G. F., Fouser, L. A., and Artis, D., 2011. Border patrol: regulation of immunity, inflammation and tissue homeostasis at barrier surfaces by IL-22. *Nature Immunology*, 12 (5), 383–390.

Soroosh, P., Doherty, T. A., Duan, W., Mehta, A. K., Choi, H., Adams, Y. F., Mikulski, Z., Khorram, N., Rosenthal, P., Broide, D. H., and Croft, M., 2013. Lung-resident tissue macrophages generate Foxp3+ regulatory T cells and promote airway tolerance. *Journal of Experimental Medicine*, 210 (4), 775–788.

Sozzani, S., Allavena, P., D'Amico, G., Luini, W., Bianchi, G., Kataura, M., Imai, T., Yoshie, O., Bonecchi, R., and Mantovani, A., 1998. Differential regulation of chemokine receptors during dendritic cell maturation: a model for their trafficking properties. *Journal of Immunology*, 161 (3), 1083–1086.

Spehlmann, M. E., Dann, S. M., Hruz, P., Hanson, E., McCole, D. F., and Eckmann, L., 2009. CXCR2-dependent mucosal neutrophil influx protects against colitis-associated diarrhea caused by an attaching/effacing lesion-forming bacterial pathogen. *The Journal of Immunology*, 183 (5), 3332–3343.

Sporri, R. and Reis e Sousa, C., 2005. Inflammatory mediators are insufficient for full dendritic cell activation and promote expansion of CD4+ T cell populations lacking helper function. *Nature Immunology*, 6 (2), 163–170.

Srikanth, C. V., Wall, D. M., Maldonado-Contreras, A., Shi, H. N., Zhou, D., Demma, Z., Mumy, K. L., and McCormick, B. A., 2010. *Salmonella* pathogenesis and processing of secreted effectors by caspase-3. *Science*, 330 (6002), 390–393.

Srinivasan, S., Vannberg, F. O., and Dixon, J. B., 2016. Lymphatic transport of exosomes as a rapid route of information dissemination to the lymph node. *Scientific Reports*, 6, 24436.

Stark, M. A., Huo, Y., Burcin, T. L., Morris, M. A., Olson, T. S., and Ley, K., 2005. Phagocytosis of apoptotic neutrophils regulates granulopoiesis via IL-23 and IL-17. *Immunity*, 22 (3), 285–294.

Steinman, R. M. and Cohn, Z. A., 1973. Identification of a novel cell type in peripheral lymphoid organs of mice. I. Morphology, quantitation, tissue distribution. *Journal of Experimental Medicine*, 137 (5), 1142–1162.

Steinman, R. M., Turley, S., Mellman, I., and Inaba, K., 2000. The induction of tolerance by dendritic cells that have captured apoptotic cells. *Journal of Experimental Medicine*, 191 (3), 411–416.

Stenstad, H., Ericsson, A., Johansson-Lindbom, B., Svensson, M., Marsal, J., Mack, M., Picarella, D., Soler, D., Marquez, G., Briskin, M., and Agace, W. W., 2006. Gut-associated lymphoid tissue-primed CD4(+) T cells display CCR9-dependent and -independent homing to the small intesfine. *Blood*, 107 (9), 3447–3454.

Stenstad, H., Svensson, M., Cucak, H., Kotarsky, K., and Agace, W. W., 2007. Differential homing mechanisms regulate regionalized effector CD8alphabeta+ T cell accumulation within the small intestine. *Proceedings of the National Academy of Sciences,* 104 (24), 10122–10127.

Strater, J., Koretz, K., Gunthert, A. R., and Moller, P., 1995. *In situ* detection of enterocytic apoptosis in normal colonic mucosa and in familial adenomatous polyposis. *Gut*, 37 (6), 819–825.

Stritesky, G. L., Yeh, N., and Kaplan, M. H., 2008. IL-23 promotes maintenance but not commitment to the Th17 lineage. *Journal of Immunology*, 181 (9), 5948–5955.

Stuart, L. M., Lucas, M., Simpson, C., Lamb, J., Savill, J., and Lacy-Hulbert, A., 2002. Inhibitory effects of apoptotic cell ingestion upon endotoxin-driven myeloid dendritic cell maturation. *Journal of Immunology*, 168 (4), 1627–1635.

Sudo, N., Sawamura, S., Tanaka, K., Aiba, Y., Kubo, C., and Koga, Y., 1997. The requirement of intestinal bacterial flora for the development of an IgE production system fully susceptible to oral tolerance induction. *Journal of Immunology*, 159 (4), 1739–1745.

Sundquist, M. and Wick, M. J., 2005. TNF-alpha-dependent and -independent maturation of dendritic cells and recruited CD11c(int) CD11b+ cells during oral *Salmonella* infection. *Journal of Immunology*, 175 (5), 3287–3298.

Sunkara, L. T., Jiang, W., and Zhang, G., 2012. Modulation of antimicrobial host defense peptide gene expression by free fatty acids. *PLoS ONE*, 7 (11), e49558.

Svensson, M., Marsal, J., Ericsson, A., Carramolino, L., Broden, T., Márquez, G., and Agace, W. W., 2002. CCL25 mediates the localization of recently activated CD8alphabeta(+) lymphocytes to the small-intestinal mucosa. *The Journal of Clinical Investigation*, 110 (8), 1113–1121.

Symonds, E. L., Riedel, C. U., O'Mahony, D., Lapthorne, S., O'Mahony, L., and Shanahan, F., 2009. Involvement of T helper type 17 and regulatory T cell activity in *Citrobacter rodentium* invasion and inflammatory damage. *Clinical and Experimental Immunology*, 157 (1), 148–154.

Szabo, S. J., Kim, S. T., Costa, G. L., Zhang, X., Fathman, C. G., and Glimcher, L. H., 2000. A novel transcription factor, T-bet, directs Th1 lineage commitment. *Cell*, 100 (6), 655–669.

Takada, Y., Hisamatsu, T., Kamada, N., Kitazume, M. T., Honda, H., Oshima, Y., Saito, R., Takayama, T., Kobayashi, T., Chinen, H., Mikami, Y., Kanai, T., Okamoto, S., and Hibi, T., 2010. Monocyte chemoattractant protein-1 contributes to gut homeostasis and intestinal inflammation by composition of IL-10-producing regulatory macrophage subset. *Journal of Immunology*, 184 (5), 2671–2676.

Talham, G. L., Jiang, H. Q., Bos, N. A., and Cebra, J. J., 1999. Segmented filamentous bacteria are potent stimuli of a physiologically normal state of the murine gut mucosal immune system. *Infection and Immunity*, 67 (4), 1992–2000.

Tamoutounour, S., Henri, S., Lelouard, H., de Bovis, B., de Haar, C., van der Woude, C. J., Woltman, A. M., Reyal, Y., Bonnet, D., Sichien, D., Bain, C. C., Mowat, A. M., Reis e Sousa, C., Poulin, L. F., Malissen, B., and Guilliams, M., 2012. CD64 distinguishes macrophages from dendritic cells in the gut and reveals the Th1-inducing role of mesenteric lymph node macrophages during colitis. *European Journal of Immunology*, 42 (12), 3150–3166.

Tamura, T., Tailor, P., Yamaoka, K., Kong, H. J., Tsujimura, H., O'Shea, J. J., Singh, H., and Ozato, K., 2005. IFN regulatory factor-4 and -8 govern dendritic cell subset development and their functional diversity. *Journal of Immunology*, 174 (5), 2573–2581.

Tan, J., McKenzie, C., Vuillermin, P. J., Goverse, G., Vinuesa, C. G., Mebius, R. E., Macia, L., and Mackay, C. R., 2016. Dietary fiber and bacterial SCFA enhance oral tolerance and protect against food allergy through diverse cellular pathways. *Cell Reports*, 15 (12), 2809–2824.

Tannock, G. W., Lawley, B., Munro, K., Sims, I. M., Lee, J., Butts, C. A., and Roy, N., 2014. RNA-stable-isotope probing shows utilization of carbon from inulin by specific bacterial populations in the rat large bowel. *Applied and Environmental Microbiology*, 80 (7), 2240–2247.

Thornley, T. B., Fang, Z., Balasubramanian, S., Larocca, R. A., Gong, W., Gupta, S., Csizmadia, E., Degauque, N., Kim, B. S., Koulmanda, M., Kuchroo, V. K., and Strom, T. B., 2014. Fragile TIM-4-expressing tissue resident macrophages are migratory and immunoregulatory. *The Journal of Clinical Investigation*, 124 (8), 3443–3454.

Tietjen, G. T., Gong, Z., Chen, C.-H., Vargas, E., Crooks, J. E., Cao, K. D., Heffern, C. T. R., Henderson, J. M., Meron, M., Lin, B., Roux, B., Schlossman, M. L., Steck, T. L., Lee, K. Y. C., and Adams, E. J., 2014. Molecular mechanism for differential recognition of membrane phosphatidylserine by the immune regulatory receptor Tim4. *Proceedings of the National Academy of Sciences*, 111 (15), E1463–E1472.

Tilney, N. L., 1971. Patterns of lymphatic drainage in the adult laboratory rat. *Journal of Anatomy*, 109 (Pt 3), 369–383.

Toda, S., Hanayama, R., and Nagata, S., 2012. Two-step engulfment of apoptotic cells. *Molecular and Cellular Biology*, 32 (1), 118–125.

Tomura, M., Yoshida, N., Tanaka, J., Karasawa, S., Miwa, Y., Miyawaki, A., and Kanagawa, O., 2008. Monitoring cellular movement *in vivo* with photoconvertible fluorescence protein 'Kaede' transgenic mice. *Proceedings of the National Academy of Sciences*, 105 (31), 10871–10876.

Torchinsky, M. B., Garaude, J., Martin, A. P., and Blander, J. M., 2009. Innate immune recognition of infected apoptotic cells directs TH17 cell differentiation. *Nature*, 458 (7234), 78–82.

Travassos, L. H., Carneiro, L. A. M., Ramjeet, M., Hussey, S., Kim, Y.-G., Magalhães, J. G., Yuan, L., Soares, F., Chea, E., Le Bourhis, L., Boneca, I. G., Allaoui, A., Jones, N. L., Nuñez, G., Girardin, S. E., and Philpott, D. J., 2010. Nod1 and Nod2 direct autophagy by recruiting ATG16L1 to the plasma membrane at the site of bacterial entry. *Nature Immunology*, 11 (1), 55–62.

Travis, M. A., Reizis, B., Melton, A. C., Masteller, E., Tang, Q., Proctor, J. M., Wang, Y., Bernstein, X., Huang, X., Reichardt, L. F., Bluestone, J. A., and Sheppard, D., 2007. Loss of integrin alpha(v)beta8 on dendritic cells causes autoimmunity and colitis in mice. *Nature*, 449 (7160), 361–365.

Trompette, A., Gollwitzer, E. S., Yadava, K., Sichelstiel, A. K., Sprenger, N., Ngom-Bru, C., Blanchard, C., Junt, T., Nicod, L. P., Harris, N. L., and Marsland, B. J., 2014. Gut microbiota metabolism of dietary fiber influences allergic airway disease and hematopoiesis. *Nature Medicine*, 20 (2), 159–166.

Tschurtschenthaler, M., Adolph, T. E., Ashcroft, J. W., Niederreiter, L., Bharti, R., Saveljeva, S., Bhattacharyya, J., Flak, M. B., Shih, D. Q., Fuhler, G. M., Parkes, M., Kohno, K., Iwawaki, T., Janneke van der Woude, C., Harding, H. P., Smith, A. M., Peppelenbosch, M. P., Targan, S. R., Ron, D., Rosenstiel, P., Blumberg, R. S., and Kaser, A., 2017. Defective ATG16L1-mediated removal of IRE1α drives Crohn's disease–like ileitis. *The Journal of Experimental Medicine*, 214 (2), 401–422.

Tsolis, R. M., Adams, L. G., Ficht, T. A., and Baumler, A. J., 1999. Contribution of *Salmonella* Typhimurium virulence factors to diarrheal disease in calves. *Infection and Immunity*, 67 (9), 4879–4885.

Tsuji, M., Suzuki, K., Kitamura, H., Maruya, M., Kinoshita, K., Ivanov, I. I., Itoh, K., Littman, D. R., and Fagarasan, S., 2008. Requirement for lymphoid tissue-inducer cells in isolated follicle formation and T cell-independent immunoglobulin A generation in the gut. *Immunity*, 29 (2), 261–271.

Turnbaugh, P. J., Ley, R. E., Hamady, M., Fraser-Liggett, C. M., Knight, R., and Gordon, J. I., 2007. The human microbiome project. *Nature*, 449 (7164), 804–810.

Uematsu, S., Jang, M. H., Chevrier, N., Guo, Z., Kumagai, Y., Yamamoto, M., Kato, H., Sougawa, N., Matsui, H., Kuwata, H., Hemmi, H., Coban, C., Kawai, T., Ishii, K. J., Takeuchi, O., Miyasaka, M., Takeda, K., and Akira, S., 2006. Detection of pathogenic intestinal bacteria by Toll-like receptor 5 on intestinal CD11c+ lamina propria cells. *Nature Immunology*, 7 (8), 868–874.

Uhlen, M., Fagerberg, L., Hallstrom, B. M., Lindskog, C., Oksvold, P., Mardinoglu, A., Sivertsson, A., Kampf, C., Sjostedt, E., Asplund, A., Olsson, I., Edlund, K., Lundberg, E., Navani, S., Szigyarto, C. A.-K., Odeberg, J., Djureinovic, D., Takanen, J. O., Hober, S., Alm, T., et al., 2015. Proteomics. Tissue-based map of the human proteome. *Science*, 347 (6220), 1260419.

Umetsu, S. E., Lee, W.-L., McIntire, J. J., Downey, L., Sanjanwala, B., Akbari, O., Berry, G. J., Nagumo, H., Freeman, G. J., Umetsu, D. T., and Dekruyff, R. H., 2005. TIM-1 induces T cell activation and inhibits the development of peripheral tolerance. *Nature Immunology*, 6 (5), 447–454.

Van Antwerp, D. J., Martin, S. J., Kafri, T., Green, D. R., and Verma, I. M., 1996. Suppression of TNF-alpha-induced apoptosis by NF-kappaB. *Science*, 274 (5288), 787–789.

van Beelen, A. J., Zelinkova, Z., Taanman-Kueter, E. W., Muller, F. J., Hommes, D. W., Zaat, S. A., Kapsenberg, M. L., and de Jong, E. C., 2007. Stimulation of the intracellular bacterial sensor NOD2 programs dendritic cells to promote interleukin-17 production in human memory T cells. *Immunity*, 27 (4), 660–669.

Van den Abbeele, P., Van de Wiele, T., Verstraete, W., and Possemiers, S., 2011. The host selects mucosal and luminal associations of coevolved gut microorganisms: a novel concept. *FEMS Microbiology Reviews*, 35 (4), 681–704.

van der Velden, A. W. M., Velasquez, M., and Starnbach, M. N., 2003. *Salmonella* rapidly kill dendritic cells via a caspase-1-dependent mechanism. *Journal of Immunology*, 171 (12), 6742–6749.

van Schaik, F. D. M., Oldenburg, B., Hart, A. R., Siersema, P. D., Lindgren, S., Grip, O., Teucher, B., Kaaks, R., Bergmann, M. M., Boeing, H., Carbonnel, F., Jantchou, P., Boutron-Ruault, M.-C., Tjønneland, A., Olsen, A., Crowe, F. L., Peeters, P. H. M., van Oijen, M. G. H., and Bueno-de-Mesquita, H. B., 2013. Serological markers predict inflammatory bowel disease years before the diagnosis. *Gut*, 62 (5), 683–688.

Veenbergen, S., van Berkel, L. A., Pre, du, M. F., He, J., Karrich, J. J., Costes, L. M. M., Luk, F., Simons-Oosterhuis, Y., Raatgeep, H. C., Cerovic, V., Cupedo, T., Mowat, A. M., Kelsall, B. L., and Samsom, J. N., 2015. Colonic tolerance develops in the iliac lymph nodes and can be established independent of CD103+ dendritic cells. *Mucosal Immunology*, 9 (4), 894–906.

Veldhoen, M., Hirota, K., Westendorf, A. M., Buer, J., Dumoutier, L., Renauld, J.-C., and Stockinger, B., 2008. The aryl hydrocarbon receptor links TH17-cell-mediated autoimmunity to environmental toxins. *Nature*, 453 (7191), 106–109.

Veldhoen, M., Hocking, R. J., Atkins, C. J., Locksley, R. M., and Stockinger, B., 2006. TGF beta in the context of an inflammatory cytokine milieu supports *de novo* differentiation of IL-17-producing T cells. *Immunity*, 24 (2), 179–189.

Vezys, V., Olson, S., and Lefrancois, L., 2000. Expression of intestine-specific antigen reveals novel pathways of CD8 T cell tolerance induction. *Immunity*, 12 (5), 505–514.

Viladomiu, M., Kivolowitz, C., Abdulhamid, A., Dogan, B., Victorio, D., Castellanos, J. G., Woo, V., Teng, F., Tran, N. L., Sczesnak, A., Chai, C., Kim, M., Diehl, G. E., Ajami, N. J., Petrosino, J. F., Zhou, X. K., Schwartzman, S., Mandl, L. A., Abramowitz, M., Jacob, V., et al., 2017. IgA-coated *E. coli* enriched in Crohn's disease spondyloarthritis promote TH17-dependent inflammation. *Science Translational Medicine*, 9 (376), eaaf9655.

Vinolo, M. A. R., Ferguson, G. J., Kulkarni, S., Damoulakis, G., Anderson, K., Bohlooly-Y, M., Stephens, L., Hawkins, P. T., and Curi, R., 2011. SCFAs induce mouse neutrophil chemotaxis through the GPR43 receptor. *PLoS ONE*, 6 (6), e21205.

Vinolo, M. A. R., Rodrigues, H. G., Hatanaka, E., Sato, F. T., Sampaio, S. C., and Curi, R., 2011. Suppressive effect of short-chain fatty acids on production of proinflammatory mediators by neutrophils. *The Journal of Nutritional Biochemistry*, 22 (9), 849–855.

Voedisch, S., Koenecke, C., David, S., Herbrand, H., Förster, R., Rhen, M., and Pabst, O., 2009. Mesenteric lymph nodes confine dendritic cell-mediated dissemination of *Salmonella enterica* serovar Typhimurium and limit systemic disease in mice. *Infection and Immunity*, 77 (8), 3170–3180.

Walker, A. W., Ince, J., Duncan, S. H., Webster, L. M., Holtrop, G., Ze, X., Brown, D., Stares, M. D., Scott, P., Bergerat, A., Louis, P., McIntosh, F., Johnstone, A. M., Lobley, G. E., Parkhill, J., and Flint, H. J., 2011. Dominant and diet-responsive groups of bacteria within the human colonic microbiota. *The ISME Journal*, 5 (2), 220–230.

Walton, K. L. W., He, J., Kelsall, B. L., Sartor, R. B., and Fisher, N. C., 2006. Dendritic cells in germ-free and specific pathogen-free mice have similar phenotypes and *in vitro* antigen presenting function. *Immunology Letters*, 102 (1), 16–24.

Wang, J., Gusti, V., Saraswati, A., and Lo, D. D., 2011. Convergent and divergent development among M cell lineages in mouse mucosal epithelium. *Journal of Immunology*, 187 (10), 5277–5285.

Wang, M., Saxon, A., and Diaz-Sanchez, D., 1999. Early IL-4 production driving Th2 differentiation in a human *in vivo* allergic model is mast cell derived. *Clinical Immunology*, 90 (1), 47–54.

Waskow, C., Liu, K., Darrasse-Jeze, G., Guermonprez, P., Ginhoux, F., Merad, M., Shengelia, T., Yao, K., and Nussenzweig, M., 2008. The receptor tyrosine kinase Flt3 is required for dendritic cell development in peripheral lymphoid tissues. *Nature Immunology*, 9 (6), 676–683.

Watchmaker, P. B., Lahl, K., Lee, M., Baumjohann, D., Morton, J., Kim, S. J., Zeng, R., Dent, A., Ansel, K. M., Diamond, B., Hadeiba, H., and Butcher, E. C., 2014. Comparative transcriptional and functional profiling defines conserved programs of intestinal DC differentiation in humans and mice. *Nature Immunology*, 15 (1), 98–108.

Welty, N. E., Staley, C., Ghilardi, N., Sadowsky, M. J., Igyarto, B. Z., and Kaplan, D. H., 2013. Intestinal lamina propria dendritic cells maintain T cell homeostasis but do not affect commensalism. *Journal of Experimental Medicine*, 210 (10), 2011–2024.

Wendland, M., Czeloth, N., Mach, N., Malissen, B., Kremmer, E., Pabst, O., and Förster, R., 2007. CCR9 is a homing receptor for plasmacytoid dendritic cells to the small intestine. *Proceedings of the National Academy of Sciences*, 104 (15), 6347–6352.

Wiles, S., Clare, S., Harker, J., Huett, A., Young, D., Dougan, G., and Frankel, G., 2004. Organ specificity, colonization and clearance dynamics *in vivo* following oral challenges with the murine pathogen *Citrobacter rodentium*. *Cellular Microbiology*, 6 (10), 963–972.

Wiles, S., Pickard, K. M., Peng, K., MacDonald, T. T., and Frankel, G., 2006. *In vivo* bioluminescence imaging of the murine pathogen *Citrobacter rodentium*. *Infection and Immunity*, 74 (9), 5391–5396.

Wilker, P. R., Sedy, J. R., Grigura, V., Murphy, T. L., and Murphy, K. M., 2007. Evidence for carbohydrate recognition and homotypic and heterotypic binding by the TIM family. *International Immunology*, 19 (6), 763–773.

Winter, S. E., Winter, M. G., Xavier, M. N., Thiennimitr, P., Poon, V., Keestra, A. M., Laughlin, R. C., Gomez, G., Wu, J., Lawhon, S. D., Popova, I. E., Parikh, S. J., Adams, L. G., Tsolis, R. M., Stewart, V. J., and Bäumler, A. J., 2013. Host-derived nitrate boosts growth of *E. coli* in the inflamed gut. *Science*, 339 (6120), 708–711.

Wong, K., Valdez, P. A., Tan, C., Yeh, S., Hongo, J.-A., and Ouyang, W., 2010. Phosphatidylserine receptor Tim-4 is essential for the maintenance of the homeostatic state of resident peritoneal macrophages. *Proceedings of the National Academy of Sciences*, 107 (19), 8712–8717.

Worbs, T., Bode, U., Yan, S., Hoffmann, M. W., Hintzen, G., Bernhardt, G., Förster, R., and Pabst, O., 2006. Oral tolerance originates in the intestinal immune system and relies on antigen carriage by dendritic cells. *Journal of Experimental Medicine*, 203 (3), 519–527.

Worthington, J. J., Czajkowska, B. I., Melton, A. C., and Travis, M. A., 2011. Intestinal dendritic cells specialize to activate transforming growth factor-beta and induce Foxp3+ regulatory T cells via integrin alphavbeta8. *Gastroenterology*, 141 (5), 1802–1812.

Wright, R. D. and Cooper, D., 2014. Glycobiology of leukocyte trafficking in inflammation. *Glycobiology*, 24 (12), 1242–1251.

Wu, W., Liu, H.-P., Chen, F., Liu, H., Cao, A. T., Yao, S., Sun, M., Evans-Marin, H. L., Zhao, Y., Zhao, Q., Duck, L. W., Elson, C. O., Liu, Z., and Cong, Y., 2016. Commensal A4 bacteria inhibit intestinal Th2-cell responses through induction of dendritic cell TGFβ production. *European Journal of Immunology*, 46, 1162–1167.

Wurbel, M.-A., McIntire, M. G., Dwyer, P., and Fiebiger, E., 2011. CCL25/CCR9 interactions regulate large intestinal inflammation in a murine model of acute colitis. *PLoS ONE*, 6 (1), e16442–e16442.

Xiao, S., Najafian, N., Reddy, J., Albin, M., Zhu, C., Jensen, E., Imitola, J., Korn, T., Anderson, A. C., Zhang, Z., Gutierrez, C., Moll, T., Sobel, R. A., Umetsu, D. T., Yagita, H., Akiba, H., Strom, T., Sayegh, M. H., Dekruyff, R. H., Khoury, S. J., and Kuchroo, V. K., 2007. Differential engagement of Tim-1 during activation can positively or negatively costimulate T cell expansion and effector function. *Journal of Experimental Medicine*, 204 (7), 1691–1702.

Xu, L., Zhang, M., Ma, W., Jin, S., Song, W., and He, S., 2013. Cockroach allergen Bla g 7 promotes TIM4 expression in dendritic cells leading to Th2 polarization. *Mediators of Inflammation*, 2013, 983149.

Xu, L., Zhao, P., Xu, Y., Gao, L., Wang, H., Jia, X., Ma, H., Liang, X., Ma, C., and Gao, L., 2016. Tim-4 protects mice against lipopolysaccharide-induced endotoxic shock by suppressing the NF-κB signaling pathway. *Laboratory Investigation*, 96, 1189-1197.

Yang, B., Li, L.-J., Xu, L.-Z., Liu, J.-Q., Zhang, H.-P., Geng, X.-R., Liu, Z.-G., and Yang, P.-C., 2016. Histone acetyltransferease p300 modulates TIM4 expression in dendritic cells. *Scientific Reports*, 6, 21336.

Yang, P.-C., Xing, Z., Berin, C. M., Söderholm, J. D., Feng, B.-S., Wu, L., and Yeh, C., 2007. TIM-4 expressed by mucosal dendritic cells plays a critical role in food antigen–specific Th2 differentiation and intestinal allergy. *Gastroenterology*, 133 (5), 1522–1533.

Yarovinsky, F., Kanzler, H., Hieny, S., Coffman, R. L., and Sher, A., 2006. Toll-like receptor recognition regulates immunodominance in an antimicrobial CD4+ T cell response. *Immunity*, 25 (4), 655–664.

Ye, P., Rodriguez, F. H., Kanaly, S., Stocking, K. L., Schurr, J., Schwarzenberger, P., Oliver, P., Huang, W., Zhang, P., Zhang, J., Shellito, J. E., Bagby, G. J., Nelson, S., Charrier, K., Peschon, J. J., and Kolls, J. K., 2001. Requirement of interleukin 17 receptor signaling for lung CXC chemokine and granulocyte colony-stimulating factor expression, neutrophil recruitment, and host defense. *Journal of Experimental Medicine*, 194 (4), 519–527.

Yeung, M. Y., Ding, Q., Brooks, C. R., Xiao, S., Workman, C. J., Vignali, D. A. A., Ueno, T., Padera, R. F., Kuchroo, V. K., Najafian, N., and Rothstein, D. M., 2015. TIM-1 signaling is required for maintenance and induction of regulatory B cells. *American Journal of Transplantation*, 15 (4), 942–953.

Yeung, M. Y., McGrath, M. M., Nakayama, M., Shimizu, T., Boenisch, O., Magee, C. N., Abdoli, R., Akiba, H., Ueno, T., Turka, L. A., and Najafian, N., 2013. Interruption of dendritic cell–mediated TIM-4 signaling induces regulatory T cells and promotes skin allograft survival. *The Journal of Immunology*, 191 (8), 4447–4455.

Yona, S., Kim, K.-W., Wolf, Y., Mildner, A., Varol, D., Breker, M., Strauss-Ayali, D., Viukov, S., Guilliams, M., Misharin, A., Hume, D. A., Perlman, H., Malissen, B., Zelzer, E., and Jung, S., 2013. Fate mapping reveals origins and dynamics of monocytes and tissue macrophages under homeostasis. *Immunity*, 38 (1), 79–91.

Yoshida, K., Matsuoka, M., Usuda, S., Mori, A., Ishizaka, K., and Sakano, H., 1990. Immunoglobulin switch circular DNA in the mouse infected with *Nippostrongylus brasiliensis*: evidence for successive class switching from mu to epsilon via gamma 1. *Proceedings of the National Academy of Sciences*, 87 (20), 7829–7833.

Yoshida, Y., Yoshimi, R., Yoshii, H., Kim, D., Dey, A., Xiong, H., Munasinghe, J., Yazawa, I., O'Donovan, M. J., Maximova, O. A., Sharma, S., Zhu, J., Wang, H., Morse, H. C. 3., and Ozato, K., 2014. The transcription factor IRF8 activates integrin-mediated TGFbeta signaling and promotes neuroinflammation. *Immunity*, 40 (2), 187–198.

Yrlid, U., Cerovic, V., Milling, S., Jenkins, C. D., Klavinskis, L. S., and MacPherson, G. G., 2006a. A distinct subset of intestinal dendritic cells responds selectively to oral TLR7/8 stimulation. *European Journal of Immunology*, 36 (10), 2639–2648.

Yrlid, U., Cerovic, V., Milling, S., Jenkins, C. D., Zhang, J., Crocker, P. R., Klavinskis, L. S., and MacPherson, G. G., 2006b. Plasmacytoid dendritic cells do not migrate in intestinal or hepatic lymph. *Journal of Immunology*, 177 (9), 6115–6121.

Yrlid, U., Milling, S. W. F., Miller, J. L., Cartland, S., Jenkins, C. D., and MacPherson, G. G., 2006c. Regulation of intestinal dendritic cell migration and activation by plasmacytoid dendritic cells, TNF-alpha and type 1 IFNs after feeding a TLR7/8 ligand. *Journal of Immunology*, 176 (9), 5205–5212.

Yurkovetskiy, L., Burrows, M., Khan, A. A., Graham, L., Volchkov, P., Becker, L., Antonopoulos, D., Umesaki, Y., and Chervonsky, A. V., 2013. Gender bias in autoimmunity is influenced by microbiota. *Immunity*, 39 (2), 400–412.

Zambell, K. L., Fitch, M. D., and Fleming, S. E., 2003. Acetate and butyrate are the major substrates for *de novo* lipogenesis in rat colonic epithelial cells. *The Journal of Nutrition*, 133 (11), 3509–3515.

Zeissig, S., 2004. Downregulation of epithelial apoptosis and barrier repair in active Crohn's disease by tumour necrosis factor alpha antibody treatment. *Gut*, 53 (9), 1295–1302.

Zelante, T., Iannitti, R. G., Cunha, C., De Luca, A., Giovannini, G., Pieraccini, G., Zecchi, R., D'Angelo, C., Massi-Benedetti, C., Fallarino, F., Carvalho, A., Puccetti, P., and Romani, L., 2013. Tryptophan catabolites from microbiota engage aryl hydrocarbon receptor and balance mucosal reactivity via interleukin-22. *Immunity*, 39 (2), 372–385.

Zhang, J.-G., Czabotar, P. E., Policheni, A. N., Caminschi, I., Wan, S. S., Kitsoulis, S., Tullett, K. M., Robin, A. Y., Brammananth, R., van Delft, M. F., Lu, J., O'Reilly, L. A., Josefsson, E. C., Kile, B. T., Chin, W. J., Mintern, J. D., Olshina, M. A., Wong, W., Baum, J., Wright, M. D., et al., 2012. The dendritic cell receptor Clec9A binds damaged cells via exposed actin filaments. *Immunity*, 36 (4), 646–657.

Zhang, L., Zhang, Y., and Hagen, K. G. T., 2008. A mucin-type O-glycosyltransferase modulates cell adhesion during *Drosophila* development. *Journal of Biological Chemistry*, 283 (49), 34076–34086.

Zhang, S., Santos, R. L., Tsolis, R. M., Stender, S., Hardt, W.-D., Bäumler, A. J., and Adams, L. G., 2002. The *Salmonella enterica* serotype Typhimurium effector proteins SipA, SopA, SopB, SopD, and SopE2 act in concert to induce diarrhea in calves. *Infection and Immunity*, 70 (7), 3843–3855.

Zhang, X., Liu, Q., Wang, J., Li, G., Weiland, M., Yu, F.-S., Mi, Q.-S., Gu, J., and Zhou, L., 2016. TIM-4 is differentially expressed in the distinct subsets of dendritic cells in skin and skin-draining lymph nodes and controls skin Langerhans cell homeostasis. *Oncotarget; Advance Online Publications*.

Zhao, B., Abdelmoudjib, G., Li, J., Li, H., Wei, C., Gong, Y., and Liu, Q., 2011. Two polymorphisms in the TIM-4 gene are associated with asthma in a Chinese Han population. *International Journal of Immunogenetics*, 38 (1), 31–35.

Zhao, S., Zhou, Y., Wang, C., Yang, Y., Wu, X., Wei, Y., Zhu, L., Zhao, W., Zhang, Q., and Wan, C., 2013. The N-terminal domain of EspF induces host cell apoptosis after infection with enterohaemorrhagic *Escherichia coli* O157:H7. *PLoS ONE*, 8 (1), e55164–e55164.

Zheng, Y., Valdez, P. A., Danilenko, D. M., Hu, Y., Sa, S. M., Gong, Q., Abbas, A. R., Modrusan, Z., Ghilardi, N., de Sauvage, F. J., and Ouyang, W., 2008. Interleukin-22 mediates early host defense against attaching and effacing bacterial pathogens. *Nature Medicine*, 14 (3), 282–289.

Zoetendal, E. G., Raes, J., van den Bogert, B., Arumugam, M., Booijink, C. C. G. M., Troost, F. J., Bork, P., Wels, M., de Vos, W. M., and Kleerebezem, M., 2012. The human small intestinal microbiota is driven by rapid uptake and conversion of simple carbohydrates. *The ISME Journal*, 6 (7), 1415–1426.

Zychlinsky, A., Thirumalai, K., Arondel, J., Cantey, J. R., Aliprantis, A. O., and Sansonetti, P. J., 1996. *In vivo* apoptosis in *Shigella flexneri* infections. *Infection and Immunity*, 64 (12), 5357–5365.